UNIVERSITY OF SOUTHAMPTON

Faculty of Natural and Environmental Sciences

# Nitric oxide mediates the neuroproliferative effect of Neuropeptide Y

By

Angela Cheung

A thesis submitted for the degree of PhD

May 2012

UNIVERSITY OF SOUTHAMPTON

ABSTRACT

FACULTY OF NATURAL AND ENVIRONMENTAL SCIENCES

Centre for Biological Sciences

Doctor of Philosophy

# NITRIC OXIDE MEDIATES THE NEUROPROLIFERATIVE EFFECT OF NPY

By Angela Cheung

Neuropeptide Y (NPY) is widely expressed in both the central and peripheral nervous system and has an important role in the regulation of adult hippocampal neurogenesis by mediating the proliferation of neural precursor cells in both health and disease. The mechanisms underlying this neuroproliferative effect of NPY, however, are unknown. The aim of this project was to investigate these cellular pathways and the possible involvement of nitric oxide (NO) in NPY-mediated neuroproliferation using postnatal rat hippocampal cultures *in vitro*.

NPY was found to have a purely proliferative effect on hippocampal neural precursor cells. The role of NO was explored by inhibiting the NO synthesising enzyme, nitric oxide synthase (NOS), which abolished the proliferative effect of NPY and supported the involvement of NO in NPY-mediated proliferation. Pharmacological analyses using subtype-selective inhibitors suggested that the neuronal isoform of NOS is the sole NOS subtype involved, which was expressed by both nestin$^+$ precursors and class III β-tubulin$^+$ neurons, the cell types previously shown to be responsive to NPY. The involvement of NO was further verified through loading hippocampal cells with an NO indicator, diaminofluorescein diacetate, where an increase in $NO/N_2O_3$ production was observed in nestin$^+$ precursors and class III β-tubulin$^+$ neurons in response to NPY treatment.

The downstream signalling pathways coupling NPY-mediated NO synthesis to cell proliferation were identified, through the use of selective pharmacological agonists and antagonists, as soluble guanylate cyclase, cGMP-dependent protein kinase (PKG) and the extracellular signal-regulated kinases (ERK) 1/2. By assessing levels of NPY-mediated ERK 1/2 phosphorylation in response to NOS inhibition, it was found that ERK 1/2 activation was mediated only via NOS/NO mechanisms. This proliferative cGMP-PKG-ERK 1/2 signalling cascade appears to be mediated by intracellularly released NO, while on the other hand, the addition of extracellular NO through the application of NO donors exerted an inhibitory effect on neural precursor cell proliferation. In addition to demonstrating the dual nature of NO, this is the first time that the signalling mechanisms underlying the proliferative effect of NPY on neural precursor cells have been described. Understanding the mechanisms underlying the proliferation of neural precursor cells will ultimately be beneficial by allowing the development of novel therapeutic interventions for promoting hippocampal neurogenesis.

To analyse the role of NO in the NPY-mediated neuroproliferation of hippocampal cells in three-dimensional (3D) cultures, Laponite, a novel synthetic silica hydrogel, was used. Culture medium-based Laponite hydrogels were developed before cell viability within the hydrogels were assessed by culturing hippocampal monolayers under gel cover. Hydrogel cover, however, resulted in cell behaviour reminiscent of preservation/fixation as monolayers showed no spatial or morphological changes over time, with one possible explanation being the high gel osmolarity. Although attempts at cell seeding showed more positive results, with cells adhering to a low heavy metal content variation of the hydrogel, determination of cell viability remained a problem due to prominent dye-gel binding. Although the rheological properties of Laponite make its use attractive, the biocompatibility of the hydrogels with hippocampal cells still require further optimisation if they are to be used as cell culture matrices.

# Table of Contents

# List of Figures

# List of Tables

## Declaration of Authorship

I, Angela Cheung, declare that the thesis entitled 'Nitric oxide mediates the neuroproliferative effect of Neuropeptide Y' and the work presented in the thesis are both my own, and have been generated by me as the result of my own original research. I confirm that:

- this work was done wholly or mainly while in candidature for a research degree at the University of Southampton;
- where any part of this thesis has previously been submitted for a degree or any other qualification at this University or any other institution, this has been clearly stated;
- where I have consulted the published work of others, this is always clearly attributed;
- where I have quoted from the work of others, the source is always given. With the exception of such quotations, this thesis is entirely my own work;
- I have acknowledged all main sources of help;
- where the thesis is based on work done by myself jointly with others, I have made clear exactly what was done by others and what I have contributed myself;
- none of this work has been published before submission,

**Signed:** …Angela Cheung……

**Date:**……03/05/2012……

**Acknowledgements**

I am very grateful to the Gerald Kerkut Charitable Trust for financially supporting my studies and my supervisors, Professor William P. Gray, Professor Philip L. Newland and Professor George Attard, for all their constructive advice, guidance and support during my PhD. I would also like to thank Dr Hansjürgen Schuppe and Dr Andreas Wyttenbach for their assistance and advice on diaminofluorescein diacetate imaging, Professor Dr Annette G. Beck-Sickinger for her contribution of the $Y_1$ agonist, and finally, Professor John Garthwaite for acting as my external PhD examiner and helping to significantly improve my thesis.

## Abbreviations

| | |
|---|---|
| ANOVA | Analysis of variance |
| APS | Ammonium persulphate |
| ATP | Adenosine-5'-triphosphate |
| BrdU | Bromodeoxyuridine |
| CaM | Calmodulin |
| DAF FM DA | Diaminofluorescein FM diacetate |
| DAPI | 4',6-diamidino-2-phenylindole |
| DCX | Doublecortin |
| DIV | Days *in vitro* |
| EDTA | Ethylenediaminetetraacetic acid |
| GABA | γ-Aminobutyric acid |
| GAPDH | Glyceraldehyde-3-phosphate dehydrogenase |
| GCL | Granule cell layer |
| GFAP | Glial fibrillary acidic protein |
| GPCR | G-protein-coupled receptor |
| GTP | Guanosine-5'-triphosphate |
| HEPES | 4-(2-hydroxyethyl)-1-piperazineethanesulfonic acid |
| HRP | Horseradish peroxidase |
| MAPK | Mitogen-activated protein kinase |
| MEK | MAPK/ERK kinase |
| NADPH | Nicotinamide adenine dinucleotide phosphate |
| NMDA | N-Methyl-D-aspartate |
| PFA | Paraformaldehyde |
| PI | Propidium iodide |
| PKC | Protein kinase C |
| PSA-NCAM | Polysialic acid-neural cell adhesion molecule |
| SGZ | Subgranular zone |
| SVZ | Subventricular zone |
| TEMED | Tetramethylethylenediamine |

# Chapter 1

## Chapter 1 - General Introduction

### 1.1 Adult hippocampal neurogenesis

Neurogenesis is the process by which new neurons are generated (Altman & Das, 1965). Prominent during embryonic development, neurogenesis had long been considered as restricted to neural development during the pre-natal period. The early theory of a fixed nervous system with "no new nerve cells after birth" and limited capacity for regeneration in the adult mammalian brain was well regarded by early neuroanatomists such as Ramón y Cajal (1928). This theory was widely accepted by the scientific community until around 50 years ago when the first evidence for neurogenesis in the adult mammalian brain was published in the 1960's by Altman and Das (1962, 1965). Since then, the existence of adult neurogenesis has been confirmed by countless studies and although initially met with scepticism, is now a well-accepted phenomenon (Ehninger & Kempermann, 2008; Andersen et al., 2007).

Neurogenesis in adults has been confirmed in two regions of the brain, the subgranular zone (SGZ) of the dentate gyrus of the hippocampus (Altman & Das, 1965), and the subventricular zone (SVZ) of the anterior lateral ventricles (Altman, 1969). The SGZ consists of a thin 2-3 cell layer which runs between the granule cell layer (GCL) and hilus of the hippocampus, while the new cells of the SVZ migrate via the Rostral migratory stream to the olfactory bulb (Altman & Das, 1965; Altman, 1969). These two regions (SGZ and SVZ) are described as 'neurogenic' or permitting adult neurogenesis (Fig. 1.1).

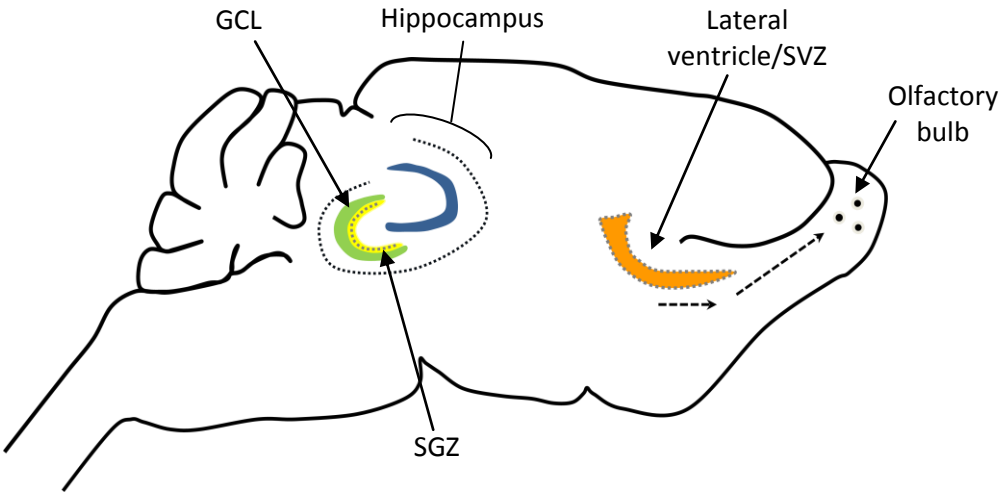


Figure 1.1 Neurogenic regions of the rat brain. The subgranular zone (SGZ; yellow with black dotted line) of the dentate gyrus of the hippocampus which populates the granule cell layer (GCL; green), and the forebrain subventricular zone (SVZ) which lines the anterior lateral ventricles

(orange) and provides new neurons for the olfactory bulb, are areas where adult neurogenesis have been confirmed.

### 1.2 Process of adult hippocampal neurogenesis

Adult hippocampal neurogenesis differs remarkably, in precursor cells, mechanism and regulation, from adult neurogenesis in the SVZ/olfactory system (Abrous et al., 2005). Neural stem cells within the SGZ of the dentate gyrus of the hippocampus give rise to new granule cell neurons that populate the GCL. Unlike embryonic neurogenesis, adult neurogenesis does not occur in the manner of an orchestrated homogenous population event. Instead, adult neurogenesis is highly individualistic, heterogeneous and parallel neuronal cells can be found at all developmental stages at any one time point. Adult neurogenesis is a highly complex, dynamic and ongoing process in the brain which is interspersed with a range of other processes such as gliogenesis (Steiner et al., 2004).

Gerd Kempermann et al. (2004) proposed a model of the sequence of cellular differentiation during adult hippocampal neurogenesis based on cell morphology and the expression of key cell markers. This model is divided into six main stages of neuronal development (stages 1 to 6) and begins at stage 1 with the mitotic division of a neural stem cell (also called a type-1 cell). Type-1 cells have a radial-glia-like morphology with a roughly triangular soma and a strong lengthy apical process, which extends into the granule cell layer, and although abundant in the SGZ, they rarely divide. Intermediate filament nestin and the astrocytic marker GFAP (glial fibrillary acidic protein) are both expressed by type-1 cells (Filippov et al., 2003). The asymmetric division of a type-1 stem cell results in one identical type-1 cell and a daughter progenitor cell (Fukuda et al., 2003), whereby neuronal development then progresses over three stages (2 to 4) which are characterised by three distinct types of highly proliferative progenitor cells called type-2a, type-2b and type-3. The type-2 transiently amplifying progenitor cells are morphologically distinct from type-1 cells and do not express GFAP (Kronenberg et al., 2003). The two subtypes of type-2 cells are both positive for nestin, but while one, type-2a, is negative for doublecortin (DCX, an immature neuronal marker), type-2b is $DCX^+$ (Brown et al., 2003). Type-2 cells exhibit short tangentially orientated processes, a small soma and the nuclei are irregularly shaped (Kronenberg et al., 2003). On the other hand, type-3 cells are more advanced with regards to the expression of neuronal markers and are nestin negative, $DCX^+$, and express PSA-NCAM (polysialated form of neural cell adhesion molecule)

(Filippov et al., 2003). Type-3 cells have a more variable morphology, generally with a rounder nucleus and soma, and a complex array of processes with various lengths (Ehninger & Kempermann, 2008). The radial migration of the type-3 cells into the GCL also occur at this stage (Kempermann et al., 2004). In the fifth stage of neurogenesis, the first postmitotic stage, cells are characterised by DCX, calcium binding protein calretinin and the mature neuron marker NeuN expression (Brandt et al., 2003). Similar to the late type-3 cells, the immature granule cell neurons have a rounded nucleus and vertical morphology with an apical dendrite. The immature granule cells at this stage will be subject to a selection process in which they are either recruited into long-term function or disposed of (where the majority of the new cells die by apoptosis) (Biebl et al., 2000; Kempermann et al., 2003). The final stage of adult hippocampal neurogenesis, stage 6, is where new granule cells integrate into the surrounding hippocampal network and circuitry and mature neuronally (Jessberger & Kempermann, 2003). Cells at this stage change expression from calretinin to calbindin (Brandt et al., 2003) and have the morphology of neurons (Fig. 1.2).

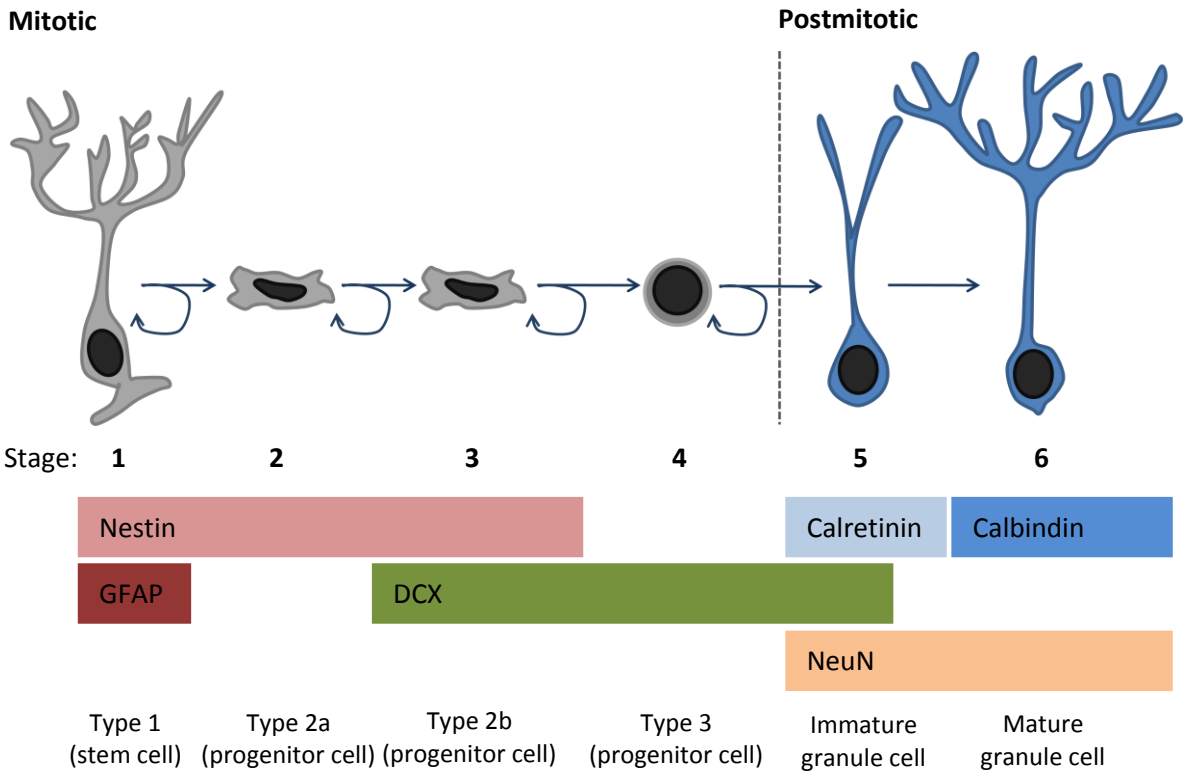


Figure 1.2 Sequence of cellular differentiation during adult hippocampal neurogenesis. The six stages of neurogenesis are distinguished by the cellular morphology and expression of key markers nestin, GFAP (glial fibrillary acidic protein), DCX (doublecortin), calretinin, calbindin and NeuN. During stage 1, a type-1 stem cell divides to give rise to three consecutive stages (stages 2-4) of

transiently amplifying progenitor cells (type 2a, 2b and 3) which have different profiles of neuronal differentiation and proliferative potential. After the mitotic stages 1-4, stage 5 is a transient postmitotic stage characterised by selection for long-term survival and establishment of network connections. Cells which survive the selection process develop into terminally differentiated, mature granule cells constituting the final stage of adult neurogenesis, stage 6 (redrawn from Kempermann et al., 2004).

It takes around 3 days for cells to develop from stage 1 through to stage 5 of the proposed model, whereby cell numbers would have expanded by four or five times (Kempermann et al., 2003). Two-thirds of the new cell population express post-mitotic markers on the third day. During stage 5, the numbers of new cells decrease dramatically as result of the post-mitotic selection process and 2 to 3 weeks is required for the maturation of immature granule cells to mature granule cell neurons in stage 6 (Kempermann et al., 2003). Four to seven weeks is needed for functional integration of the new granule cells into the surrounding hippocampal environment, when they then become indistinguishable from older granule cells (Jessberger & Kempermann, 2003, van Praag et al., 2002). Approximately 9000 new granule cells are generated per day within the SGZ (Cameron & McKay, 2001), although most of these cells die (Biebl et al., 2001), leaving approximately ½ to 1/3 of new granule cells functionally integrated into the hippocampal environment after four weeks (Kempermann et al., 2003).

### 1.3 Adult Neurogenesis in humans

Adult hippocampal neurogenesis is well established in mammalian brains, including humans, and rodents in particular show significant amounts of adult hippocampal neurogenesis (Andersen et al., 2007; Gould et al., 1999; Altman & Das, 1965). In the seminal study by Eriksson et al. (1998), adult human hippocampal neurogenesis was demonstrated in post-mortem brain tissue from cancer patients who had been treated, when they were alive, with the mitotic (S-phase) marker, bromodeoxyuridine (BrdU) (to assess the proliferative activity of tumour cells). Using immunohistochemistry, the presence of $BrdU^+$ cells was verified in both the dentate gyrus and the SVZ, and using double immunostaining for BrdU and the neuronal markers NeuN or Calbindin, confirmed the generation of new neurons from dividing progenitor cells in the dentate gyrus of the adult human hippocampus (Eriksson et al., 1998). A different study has also shown that, similar to the course of adult hippocampal neurogenesis observed in rodents (Seki & Arai, 1995; Kuhn et al., 1996), there is a decrease in the generation of immature neurons in the dentate

gyrus of the human brain, as demonstrated through assessing post-mortem human brain tissue ranging in age from fetal to 100 years for markers of cell proliferation and adult hippocampal neurogenesis (Knoth et al., 2010).

### 1.4 Functional relevance of adult hippocampal neurogenesis

The hippocampus plays important roles in the consolidation of memory and spatial navigation (Squire & Cave, 1991). The functional integration of newly born cells into the hippocampal circuitry during adult hippocampal neurogenesis (van Praag et al., 2002) has lead to the proposition that hippocampal neurogenesis may be important in learning processes and the formation of hippocampal-dependent memories (Gould et al., 1999; Snyder et al., 2001). Learning has been shown to promote adult hippocampal neurogenesis, which Gould et al. (1999) suggests is directly involved in the transient (temporary) storage of hippocampus-dependent memories. Importantly, the ablation of adult hippocampal neurogenesis through pharmacological, genetic or radiological procedures has been linked to the failure of certain hippocampal-dependent tasks (Ehninger & Kempermann, 2008). For example, Shors et al. (2001) ablated hippocampal precursor cells with the methylating agent methylazoxymethanol acetate (MAM) and found an impairment of a hippocampal-dependent eye-blink task but not a hippocampal-independent version of the task. Other hippocampal-dependent tasks, however, were not affected by MAM treatment, suggesting that adult hippocampal neurogenesis is functionally required for only some forms of hippocampal-dependent learning and memory (Shors et al., 2001, 2002). Although our knowledge of the mechanisms are incomplete, adult hippocampal neurogenesis fluctuates in response to a plethora of extrinsic and intrinsic regulators including exercise (van Praag et al., 1999), age (Seki & Arai, 1995; Kuhn et al., 1996), stress (Gould & Tanapat, 1999), antidepressants (Malberg et al., 2000; Santarelli et al., 2003), neurodegenerative diseases (Thompson et al., 2008), brain injury including seizures (Bengzon et al., 1997; Parent et al., 1997; Gray and Sundstrom, 1998), traumatic brain injury (Dash et al., 2001) and stroke (Liu et al., 1998a), hormones (Gould et al., 2000) and growth factors (Cameron et al., 1998), to name but a few. Although increased hippocampal neurogenesis does not necessarily equate to enhanced hippocampal function, the possibility of manipulating adult neurogenesis is attractive for the development of potential therapeutic treatments, for example, by activating endogenous stem cells from within to promote repair *in vivo* (Shihabuddin et al., 1999). Neuropeptides, in particular, are emerging as significant modulators of adult neurogenesis, especially neuropeptide Y (NPY).

### 1.5 Neuropeptide Y

Following its isolation from the porcine hypothalamus (Tatemoto et al., 1982), determination of its amino acid sequence (Tatemoto, 1982) and distribution in the rat brain (Allen et al., 1983), NPY, a 36 amino acid polypeptide, has been implicated in the regulation of a range of physiological processes, including circadian rhythm (Albers & Ferris, 1984), feeding behaviour (Flood & Morley, 1989), memory processing (Redrobe et al., 1999), affective disorders (Heilig, 2004) and seizure control (Erickson et al., 1996; Vezzani et al., 1999). In the hippocampus, NPY is expressed by GABA(γ-aminobutyric acid)ergic interneurons of the dentate hilus and hippocampus proper (Kohler et al., 1986; Freund & Buzsaki, 1996), and acts on G-protein coupled receptors (GPCR) in the rhodopsin-like GPCR family. Out of the five subtypes identified in mammals (NPY $Y_1$, $Y_2$, $Y_4$,$Y_5$ and $Y_6$), four ($Y_1$, $Y_2$, $Y_4$ and $Y_5$) are functional in humans (Michel et al., 1998), and show tissue-specific expression patterns (Mullins et al., 2002). Although all five NPY Y receptors appear to use similar intracellular signalling pathways, no one Y receptor is consistently linked with any one distinct pathway (Michel et al., 1998). The signalling mechanisms through which NPY exerts its diverse range of effects have not yet been fully characterised or understood (Mullins et al., 2002), however, what is known is that the Y receptors show preferential coupling to G-proteins of the $G_i$ and $G_o$ family (or the pertussis toxin-sensitive G-proteins) (Limbird, 1988).

### 1.6 NPY and neurogenesis

Hansel et al. (2001) first demonstrated the proliferative effects of NPY on neuronal precursor cells derived from the postnatal rat olfactory epithelium, which appear to be mediated via the NPY $Y_1$ receptor. Since then, NPY has been shown to be able to stimulate the proliferation of a range of cell types including neuronal precursor cells from the hippocampal SGZ (Howell et al., 2003), retinal glial (Muller) cells (Milenkovic et al., 2004), endothelial cells (Movafagh et al., 2006) and precursor cells from the SVZ (Agasse et al., 2008). Indeed, NPY plays a key role in regulating adult hippocampal neurogenesis under both normal and pathological conditions (Howell et al., 2005, 2007) and it has been proposed that NPY-releasing interneurons in the dentate hilus release NPY onto progenitors within the SGZ to regulate their proliferation and adult hippocampal neurogenesis (Gray, 2008). The neuroproliferative effect of NPY on SGZ precursor cells was shown to be $Y_1$ receptor mediated (Howell et al., 2003) and adult NPY $Y_1^{-/-}$ receptor knock-out mice had significantly reduced cell proliferation and reduced numbers of

immature $DCX^+$ neurons in the dentate (Howell et al., 2003). This correlates well with the predominant localisation of $Y_1$ receptors to the dentate and SGZ (Kopp et al., 2002). The signalling mechanisms underlying the proliferative effect of NPY, however, are not yet fully understood.

### 1.7 Nitric oxide

Nitric oxide (NO) is a ubiquitous gaseous signalling molecule involved in mediating a vast range of intra- and intercellular signalling cascades and regulation of physiological processes (Garthwaite, 1991). Also known as endothelium-derived relaxing factor (EDRF) for its roles in mediating vasodilation (Furchgott & Zawadzki, 1980; Ignarro et al., 1987; Palmer et al., 1987), NO is synthesised by the enzyme nitric oxide synthase (NOS), which converts the amino acid L-arginine into NO and citrulline through sequential oxygenation reactions (Villalobo, 2006). In mammals there are three isoforms of NOS, neuronal NOS (nNOS or NOS-I), inducible NOS (iNOS or NOS-II) and endothelial NOS (eNOS or NOS-III) (Alderton et al., 2001). The lipophilic and non-polar nature of NO allows it to diffuse rapidly and freely through barriers and lends to its wide ranging physiological effects (Philippides et al., 2000). Early ideas regarding the predicted physiological sphere of influence of an NO source, initially thought to be up to ~200 µm for a single source of NO that emits for 1 - 10 s (Wood & Garthwaite, 1994), have now been substantially revised. Simulating a 7 x 7 array of simultaneously active nNOS molecules generating NO at the highest achievable rate (Santolini et al., 2001), the NO concentration is predicted to reach only 1 nM and 250 pM, 60 nm and 1 µm away from the central source, respectively, a sphere of influence much smaller than initially predicted (Hall & Garthwaite, 2009).

The apparent half-life of NO varies across tissues and is highly dependent on its physiological environment and the presence of NO consuming pathways or enzymatic processes (Hall & Garthwaite, 2009). In the blood, for example, where the reaction of NO with oxyhaemoglobin to form methaemoglobin and nitrate in the blood is rapid (Liu et al., 1998b; Tsoukias, 2008), NO has a half life of ~0.1 - 2 ms (Hall & Garthwaite, 2009). In contrast, NO consumption is slower in brain tissue (cerebellum), with a half life of ~6 - 60 ms (Hall & Garthwaite, 2006; Hall & Attwell, 2008). As well as enzymatic NO consumption, NO has also been shown to chemically react with radicals such as superoxide or lipid peroxyl (Kissner et al., 1997; Padmaja & Huie, 1993), and in the presence of molecular oxygen, give rise to a variety of nitrogen oxides including $NO_2$ (nitrogen

dioxide), $N_2O_3$ (dinitrogen trioxide), $NO_2^-$ (nitrite), $NO_3^-$ (nitrate) and $ONOO^-$ (peroxynitrite anion), depending on the concentration (Conner et al., 1996; Robbins & Grisham, 1997).

A key target of NO is the hemoprotein soluble guanylate cyclase (sGC) that mediates one of the main transduction mechanisms through which NO exerts its physiological effects (Waldman & Murad, 1988). sGC catalyses the conversion of guanosine 5'-triphosphate (GTP) to the second messenger guanosine 3', 5'-monophosphate (cyclic GMP; cGMP), and the reaction between NO and the heme group of sGC increases this catalytic activity by 50 to 200-fold (Ignarro, 1990; Derbyshire & Marletta, 2009). In turn, signal transduction is transferred by cGMP onto three main effectors, including cGMP-dependent protein kinases, cGMP-gated cation channels and phosphodiesterases (Garthwaite & Boulton, 1995). cGMP-dependent protein kinases (PKG), of which there are two isoforms (PKG-I and PKG-II), are major cGMP effectors (Fiscus et al., 1983) and further mediate signalling transduction mechanisms through the phosphorylation of a variety of protein targets (Francis & Corbin, 1994). On the other hand, cGMP-gated cation channels have been shown to play a central role in visual (Yau & Baylor, 1989) and olfactory (Zufall et al., 1994) signal transduction, while cyclic nucleotide phosphodiesterases (PDEs) may be activated or inhibited in response to cGMP depending on the subtype (Garthwaite & Boulton, 1995) (Fig. 1.3). NO itself is also able to directly influence the activity of a range of enzymes through interaction with iron-sulphur enzymatic centres (Nathan, 1992).

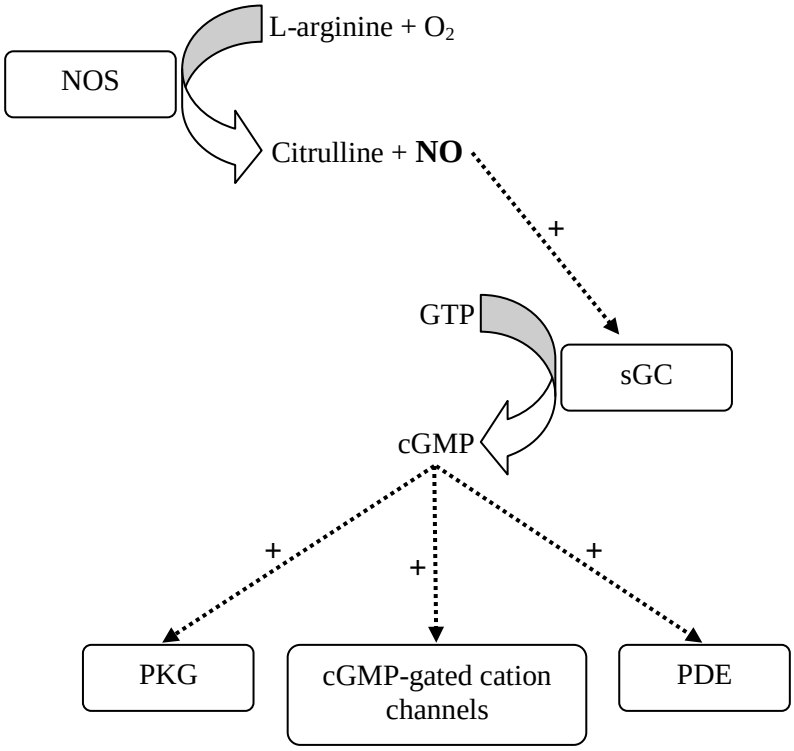


Figure 1.3 The NO-cGMP signalling pathway. NO generated by nitric oxide synthase (NOS) from the amino acid L-arginine acts on soluble guanylate cyclase (sGC) to increase its production of the second messenger cGMP. The three main effectors of cGMP are cGMP-dependent protein kinases (PKG), cGMP-gated cation channels and phosphodiesterases (PDE).

NO has been implicated particularly, among others, in the regulation of cardiovascular, immunological and neurological processes. As well as being a primary mediator of vasodilatory actions, which are important in the regulation of blood flow and blood pressure (Palmer et al., 1987), in penile erection for example (Burnett et al., 1992), NO is an important regulator of cardiac function and contractility (Kelly et al., 1996; Massion et al., 2003). In the immune system, NO production by iNOS acts as a cytotoxic mediator of macrophages (Hibbs et al., 1988) and may be a significant modulator of acute and chronic inflammatory processes (Moncada & Higgs, 1993). The role of NO as a neurotransmitter/neuromodulator has been extensively investigated since it was first implicated as an intercellular messenger in the central nervous system (Garthwaite et al., 1988). NO mediates the action of glutamate on N-Methyl-D-aspartate (NMDA) receptors in the brain (Garthwaite et al., 1988) and contributes to the maintenance of synaptic plasticity, including cerebellar long-term depression (Daniel et al., 1998) and hippocampal long-term potentiation (Hawkins et al., 1998). NO, however, is often described as a Janus-

faced molecule (Snyder, 1993) for its role in mediating both neuroprotective and neuropathological events.

### 1.8 NO and neurogenesis

NO has been directly implicated in the mechanisms underlying both the early stages (neurogenesis) and advanced stages (synaptogenesis and neural map formation) of neuronal differentiation and may also play an important role in developmental neurogenesis (Contestabile & Ciani, 2004). Indeed, NO exerts a dual role in cell proliferation by mediating both proliferative and antiproliferative effects (Villalobo, 2006). While NO exerts an antiproliferative effect on cells such as vascular smooth muscle cells (Garg & Hassid, 1989) and endothelial cells (RayChaudhury et al., 1996), it mediates a proliferative effect on fibroblasts (Du et al., 1997) and myoblasts (Ulibarri et al., 1999). Similarly, NO mediates both neuroinhibitory and neuroproliferative effects in adult neurogenesis and observations have shown NOS localisation to neurogenic sites in the dentate gyrus of the hippocampus and SGZ (Islam et al., 2003), and the SVZ, olfactory and rostral migratory stream (Moreno-Lopez et al., 2000). *In vivo* investigations by Packer et al. (2003) showed that the chronic inhibition of NOS with L-NAME increased proliferation in neurogenic zones such as the SGZ and SVZ in rats. Similarly, there was an increase in proliferating cells in response to systemic administration of a different NOS inhibitor, 7-nitroindazole, in mice, although this was observed only in the SVZ and not the SGZ (Moreno-Lopez et al., 2004). This disparity in region responses is probably due to the presence of specific cell types or sensitivity differences (Matarredona et al., 2005). These studies all support the idea that NO acts as a negative regulator of adult neurogenesis, although it must be noted that both L-NAME and 7-nitroindazole are relatively non-selective NOS inhibitors (Moore & Handy, 1997; Reiner & Zagvazdin, 1998).

Conversely, others have described NO as a positive regulator of adult neurogenesis. The administration of the NO donor, DETA/NONOate, increased cell proliferation in the SGZ and SVZ under both normal conditions and in response to stroke in young adult rats (Zhang et al., 2001). Likewise, the prior administration of 7-nitroindazole and the iNOS inhibitor aminoguanidine significantly reduced the number of proliferating cells in the dentate gyrus after pentylenetrazol-induced seizures in rats (Jiang et al., 2004), supporting a role for NO in brain repair after brain injury or seizures. DETA/NONOate has also been shown to produce antidepressant effects by promoting hippocampal neurogenesis in young

adult mice (Hua et al., 2008). The explanation for these paradoxical effects of NO may lie in the differential effects of the NOS isoforms (Cardenas et al., 2005) and/or the opposing effects of intracellular and extracellular NO signalling (Luo et al., 2010).

### 1.9 The aims of this project

A decline in adult hippocampal neurogenesis and cell loss has been linked with stress (Gould & Tanapat, 1999), depression (Malberg et al., 2000; Santarelli et al., 2003; Duman, 2004) and neurodegenerative diseases such as Alzheimer's disease (Haughey et al., 2002). It is only through furthering our understanding of the mechanisms controlling the proliferation of endogenous neural stem/precursor cells that new and more specific pharmacological targets can be identified for promoting hippocampal neurogenesis, neuronal regeneration and structural repair in the CNS in an attempt to alleviate these pathological conditions.

NPY is emerging as an important regulator of adult hippocampal neurogenesis although the mechanisms underlying this effect are unknown. Given the bifunctional effects of NO on neurogenesis and the localisation of NOS to NPY-responsive neurogenic areas, a key question to address is whether NO could be a mediator of NPY signalling. Indeed, a connection between NO and the physiological effects of NPY was previously described by Morley et al. (1991, 1999), who showed that a low dose of NPY was able to significantly increase NOS expression in the hypothalamus and that an NPY-induced increase in food intake was mediated via NOS. More recently, Alvaro et al. (2008) showed that NOS was involved in mediating the NPY-induced proliferation of retinal neural cells, further supporting this hypothesis.

The aim of this study was to investigate the involvement of NO in mediating the neuroproliferative effect of NPY. This was carried out using an established *in vitro* monolayer hippocampal cell culture system (Howell et al., 2003) upon which the survival, proliferation and differentiation of precursor and neuronal cells could be easily quantified. After confirming the neuroproliferative effects of NPY, the involvement of NO mechanisms and the key mediators of the signalling pathway involved in coupling NPY to cell, particularly nestin$^{+}$ stem/precursor cell, proliferation were investigated. Of particular interest was identifying the NOS subtype involved and the effects of intracellular or

extracellular NO, both of which are factors involved in determining the dual proliferative effects of NO.

# Chapter 2

## Chapter 2 - Neuropeptide Y promotes the proliferation of hippocampal precursor cells in culture

### 2.1 Introduction

NPY, named due to the many tyrosine (Y) residues within its structure (Tatemoto, 1982), has been implicated in the regulation of a series of physiological processes including memory processing, depression and seizures. In turn, these processes have been shown to influence, or be influenced by, fluctuations in levels of adult mammalian hippocampal neurogenesis. These initial observations suggest a role for NPY in the regulation of adult hippocampal neurogenesis. Using an *in vitro* primary cell culture system of hippocampal cells, first described by Brewer (1997) and adapted by Howell et al. (2003), the physiological effects of NPY on cell proliferation, phenotype and survival were investigated.

#### 2.1.1 Neuropeptide Y

In the peripheral nervous system, high levels of NPY-immunoreactivity are found in the sympathetic ganglia and in tissues innervated by the sympathetic system, including the heart, blood vessels, spleen and visceral smooth muscle (Lundberg et al., 1982, 1984a, 1988). NPY is released by sympathetic nerves, the adrenal glands (Briand et al., 1990) and platelets (Myers et al., 1988), and is also co-released with catecholamines such as noradrenalin into the blood in response to strong sympathetic activation such as exercise or shock (Lundberg et al., 1984b, 1985; Pernow et al., 1986). In the central nervous system, NPY-immunoreactivity is abundant, with the highest concentrations found in the paraventricular hypothalamic nucleus and hypothalamic arcuate nucleus (Chronwall et al. 1985). In addition, NPY-immunoreactivity has been shown colocalised to catecholamine neurons in the medulla oblongata and with a range of other neuropeptides and neurotransmitters (Hökfelt et al., 1983, Everitt & Hökfelt, 1989, Lundberg et al., 1990). The abundant and widespread distribution of NPY, as well as its coexistence with other neurotransmitter systems, supports its role as a central and complex signaling agent which interacts with other transmitter systems.

In the hippocampus, NPY is largely localised within a subset of gamma-aminobutyric acid (GABA)-ergic interneurons in the dentate hilus (Kohler et al., 1986; Freund & Buzsaki, 1996), and similar to other secreted neuropeptides, is synthesised as an inactive pre-pro-peptide (von Hörsten et al., 2004). The signal peptide of the pre-pro-NPY is

removed in the endoplasmic reticulum before pro-NPY is cleaved further by consecutive enzymes to generate the active amidated NPY which is released from cells via exocytosis (Silva et al., 2005). NPY also shares close homology to two other 36 amino-acid polypeptides, pancreatic polypeptide (PP) and Peptide YY (PYY) (Michel et al., 1998).

### 2.1.2 Neuropeptide Y receptors

There are five NPY receptor subtypes ($Y_1$, $Y_2$, $Y_4$, $Y_5$ and $Y_6$) which mediate the effects of NPY peptide. Activation of the GPCRs leads to the activation of intracellular signalling cascades (Michel et al., 1998). Following NPY binding and receptor phosphorylation, the $Y_1$ receptor is internalised by endocytosis as part of the desensitisation process (Pheng et al., 2003). Significant differences in the expression and distribution of the neuropeptide Y receptors in the brain are observed across species (rodents, guinea pig and primates) (Dumont et al., 1998), although regional differences are less pronounced. Within the hippocampus, high levels of the $Y_1$ receptor are localised within the molecular layer of the dentate gyrus (Kopp et al., 2002), while $Y_2$ is distributed predominantly in the CA3 region (Gustafson et al., 1997). One function of the $Y_1$ receptor is to mediate the neuroproliferative effects of NPY on selected cell types (Hansel et al., 2001; Howell et al., 2003). $Y_4$, which shows higher affinity for PP and PYY, is expressed at very low levels in the hippocampus (Dumont et al., 1998) while low levels of $Y_5$, which is implicated in feeding behaviour and obesity, is expressed in the Ammon's horn of the ventral hippocampus and molecular layer of the dentate gyrus (Wolak et al., 2003). As well as being highly distributed within the brain, NPY receptors are also widely distributed throughout the body due to its diverse physiological functions.

### 2.1.3 The neuroproliferative effect of NPY

Hansel et al. (2001) were one of the first to demonstrate the proliferative effects of NPY on neuronal precursor cells derived from the postnatal rat olfactory epithelium. NPY at concentrations as low as 10 nM were sufficient to promote the proliferation of precursor cells and neuroproliferation increased in a dose-dependent manner (Hansel et al., 2001). NPY is able to stimulate the proliferation of a range of cell types including neuronal precursor cells from the hippocampal SGZ (Howell et al., 2003), retinal glial (Muller) cells (Milenkovic et al., 2004), endothelial cells (Movafagh et al., 2006) and precursor cells from the SVZ (Agasse et al., 2008), while inhibiting the proliferation of human retinal pigment epithelial cells (Troger et al., 2003).

Studies by Howell et al. (2003) have shown that NPY acts exclusively to increase the proliferation of nestin$^+$ precursor cells and class III β-tubulin$^+$ neuroblasts in post-natal *in vitro* rat hippocampal cultures. NPY was proliferative for nestin$^+$ precursor cells from both the dentate gyrus and the rest of the hippocampus, but only for class III β-tubulin$^+$ neuroblasts from the dentate gyrus, suggesting regional specificities in proliferative responses to NPY in the hippocampal region (Howell at al., 2005; Gray, 2008). The small unipolar or bipolar nestin$^+$ proliferating precursor cells increased exponentially over time in response to NPY treatment, as shown by increases in total cell number, BrdU incorporation and nestin staining (Howell et al., 2003). These increases, which were mediated via the $Y_1$ receptor, were purely neuroproliferative, as opposed to neurotrophic, as there was no difference in cell death between control and NPY-treated cultures (Howell et al., 2003). Furthermore, to assess the effects of NPY on neural stem cells, neurospheres (free-floating stem cell aggregates) were exposed to NPY in culture (Howell et al., 2007). NPY had a specific proliferative effect on neurosphere cultures, increasing both sphere size and number, while the phenotype of cells within the spheres remained unchanged in comparison to control (Howell et al., 2007). When plated and cultured under differentiating conditions, the neurospheres gave rise to neurones, astrocytes and oligodendrocytes (Howell et al., 2003). The proliferative effect of NPY has also been demonstrated *in vivo*, where $Y_1^{-/-}$ receptor knock-out mice show significantly reduced cell proliferation and decreased levels of DCX$^+$ immature neurons in the dentate gyrus (Howell et al., 2005).

In the dentate gyrus, NPY is present in a least four types of GABAergic interneuron (Sperk et al., 2007). These NPY-releasing interneurons receive numerous inputs (Miettinen & Freund, 1992), control the output of a number of excitatory pyramidal neurons, and innervate the dentate outer molecular layer (Knowles & Schwartzkroin, 1981; Sperk et al., 2007). The hypothesis that GABAergic interneurons in the dentate hilus release NPY onto progenitors within the SGZ to control their proliferation (Gray, 2008) (Fig. 2.1.1) is further supported by studies showing that $Y_1$ receptors, that are involved in mediating the neuroproliferative effects of NPY, densely populate the SGZ of the dentate gyrus (Kopp et al., 2002).

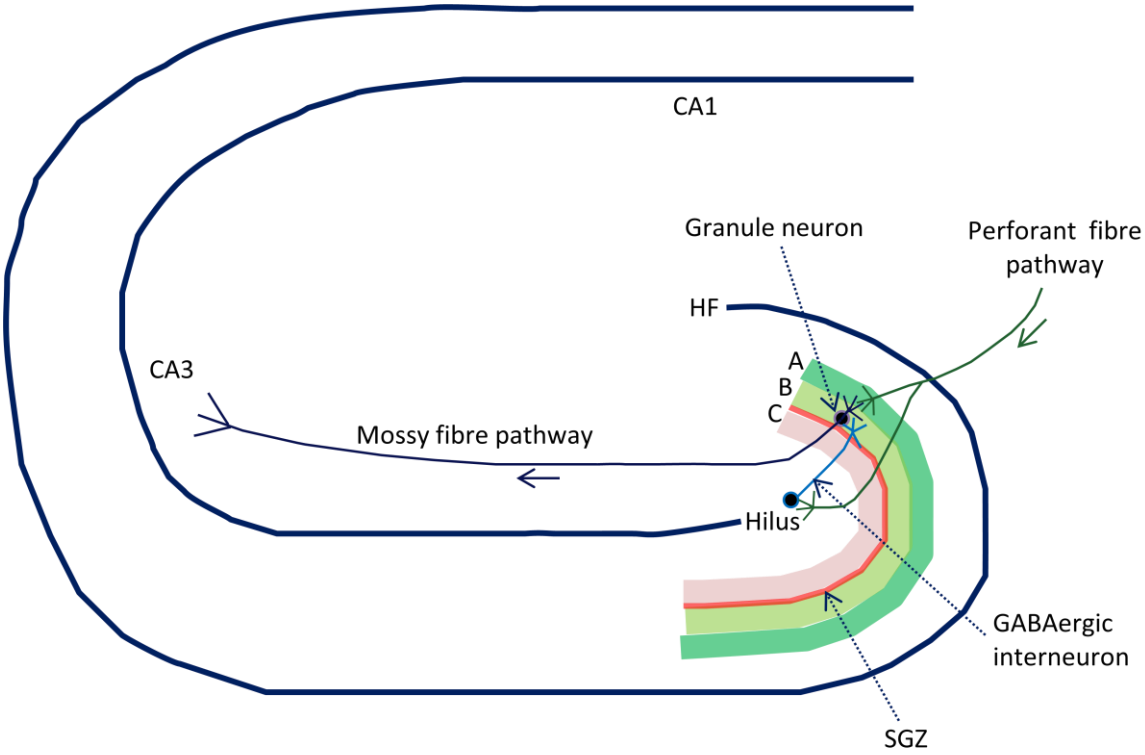


Figure 2.1.1 Schematic diagram of a cross-section of adult hippocampus showing GABAergic NPY-releasing interneurons in the dentate gyrus. The dentate gyrus is made up of three main layers, the (A) molecular layer, (B) granular layer and (C) polymorphic layer. The subgranular zone (SGZ) runs between the granular and polymorphic layers. GABAergic interneurons in the dentate hilus modulate granule cell neuron excitability through feedback circuits from mossy fibre collaterals/CA3 region and feed forward circuits from the entorhinal cortex (perforant fibre pathway) and contralateral hippocampus (Freund & Buzsaki, 1996). Through sampling neuronal activity, GABAergic interneurons may release NPY onto progenitors within the SGZ to control their proliferation (Gray, 2008). HF, hippocampal fissure.

### 2.1.4 The aims of this chapter

The aims of this chapter were to confirm the findings of Howell et al. (2003, 2005) regarding the neuroproliferative effects of NPY on primary hippocampal cultures derived from the postnatal rat hippocampus. The effects of NPY on cell proliferation, phenotype and survival were analysed.

## 2.2 Methods

### Methodology and experimental aim

The neuroproliferative effects of NPY on the proliferation, phenotype and survival of rat postnatal hippocampal cultures (Howell et al., 2003, 2005) were assessed using NPY peptide, the S-phase marker bromodeoxyuridine (BrdU), cell death markers and immunocytochemistry for a range of cell type-specific markers.

### 2.2.1 Primary hippocampal neuronal culture generation

Primary hippocampal neuronal culture generation is a multi-step procedure consisting of hippocampi dissection, enzymatic dissociation, gradient isolation of cells and cell plating as described previously by Howell et al. (2003) and adapted from Brewer (1997). Cultures were generated from early post-natal rats because the granule cell layer is formed predominantly between post-natal days 5 and 20 (Altman & Bayer, 1990), thus allowing for the greatest yield of precursor cells in culture for studying effects on neuroproliferation.

#### 2.2.1.1 Hippocampi dissection

Two sets of four (8 in total) Wistar rats of 7 to 10 post-natal day age were sacrificed by atlantoaxial dislocation followed by quick decapitation (Schedule I under the Animals Scientific Procedures Act 1986). Scissors were used to cut the skin and the skull, and forceps were used to remove the meninges. The whole brain was quickly transferred to a petri dish. Under sterile procedures, the hippocampi (two from each brain) were dissected and transferred onto a sterilised melinex strip on the stage of a MacIlwain tissue chopper with a small quantity of Gey's balanced salt solution (Life Technologies, Paisley, UK) supplemented with 4.5 mg $ml^{-1}$ glucose to prevent the tissue from drying out. The hippocampi were cut perpendicular to the long axis into slices of 400 µm thickness followed by rapid transfer into a petri dish containing 4 mls of Gey's solution supplemented with 4.5 mg $ml^{-1}$ glucose. The hippocampi were stored at 4°C for 5 min while the second set of hippocampi were dissected and cut.

#### 2.2.1.2 Enzymatic dissociation and cell release

The Gey's solution was aspirated and replaced with pre-warmed Neurobasal A (NBA-A) medium (Life Technologies, UK) supplemented with 2% B27 (Life Technologies) and 0.5 mM Glutamine (Glu; Sigma Aldrich, UK) for 5 min at 37°C. Papain (22.0 U/mg; Sigma Aldrich, UK) at 2 mg/ml in NBA-A/B27/Glu was prepared at least 30 min before and pre-warmed (37°C) before filter sterilisation through a 0.2 µm filter (0.22 µm pore, Millex-

GV, Millipore, USA). The filter sterilised pre-warmed papain solution was applied directly onto hippocampal slices for 30 min at 37°C to initiate enzymatic dissociation and cell release from hippocampal slices. After 30 min, the papain solution was aspirated and replaced with 4 ml of pre-warmed NBA-A/B27/Glu and further cell release was initiated by trituration. After trituration for about 10 times, the suspension was transferred into a 15 ml centrifuge tube, further triturated if necessary and allowed to settle for about 1 min, after which a volume constituting half of the suspension (i.e. 2 ml from an original 4 ml) was removed from the top. The remaining sediment (2 ml) was further suspended in 2 ml of fresh pre-warmed NBA-A/B27/Glu for further trituration. After full dissociation by trituration, a cloudy cell suspension in 6 mls NBA-A/B27/Glu per four animals was obtained.

#### 2.2.1.3 Gradient isolation and enrichment of cells

To purify cells from debris, the cell suspension was applied carefully onto the top of a two-step density Optiprep (sterile solution of Iodixanol) gradient before centrifugation for 15 min at 1900 rpm at room temperature. The Optiprep gradient was prepared by adding 2 ml 10% Optiprep (Sigma Aldrich, UK) in NBA-A/B27/Glu gently on top of 2 ml 20% Optiprep in NBA-A/B27/Glu. After centrifugation, the fraction containing the cells was collected using a pipette and re-suspended into 2 ml of NBA-A/B27/Glu and centrifuged a second time for 2 min at 1100 rpm at room temperature to remove the Optiprep. After centrifugation, the supernatant was aspirated and the cell pellet re-suspended in 8 ml (1 ml/animal) NBA-A/B27/Glu.

To determine the number of viable cells, 30 µl of cell suspension was mixed with 50 µl Trypan blue (Sigma Aldrich, UK), transferred onto a haemocytometer slide and live (dye-excluding) cells counted. Cell suspension was typically diluted to a cell density of 100,000 viable cells per ml for use.

#### 2.2.1.4 Cell plating

Cells were plated onto 24 and 6 well polystyrene multiwell plates (Fisher Scientific, UK) which were pre-coated with poly-L-lysine. The coating of both 24 and 6 well multiwell plates involved the application of 250 µl and 800 µl of 50 µg/ml poly-L-lysine (Sigma Aldrich, UK) respectively, followed by incubation at room temperature for about 1 h, after which the poly-L-lysine was aspirated, allowed to dry, then rinsed with NBA-A/sterile distilled water to wash off any excess coating and warmed at 37°C before cell transfer.

Viable cells were plated at a density of 100,000 cells/ml in NBA-A/B27/Glu at 500 µl/well in 24 well plates (260 cells/mm$^2$) and 1000 µl/well in 6 well plates (105 cells/mm$^2$). Cells were incubated under 5% $CO_2$, 95% air (~20% $O_2$), 37°C and 100% humidity incubator conditions.

2 h after plating, the medium in the wells were aspirated to remove any non-adherent cells or debris, rinsed with pre-warmed NBA-A/B27/Glu and replaced with fresh NBA/B27/Glu medium supplemented with 1% antibiotic/antimycotic (Pen/Strep and Fungizone, Life Technologies, USA) under control conditions. Pharmacological agents under study were also added at this time, for example, NPY (1 µM) (Sigma Aldrich, UK). Two-thirds of the growth media was replaced every three days for cultures longer than three days.

#### 2.2.1.5 Plating on coverslips

Glass coverslips (13 mm radius borosilicate glass, VWR International, UK) were transferred into 24 well polystyrene multiwell plates and coated with 300 µl of 50 µg/ml poly-L-lysine. After 1 h incubation at room temperature, the poly-L-lysine was aspirated, allowed to dry, rinsed with NBA-A/sterile distilled water and warmed at 37°C. Viable cells were plated at a density of 100,000 cells/ml NBA-A/B27/Glu at 500 µl/well (260 cells/mm$^2$). Cells were incubated under 5% $CO_2$, 95% air (~20% $O_2$), 37°C and 100% humidity incubator conditions.

2 h after plating, the medium in the wells was aspirated to remove any non-adherent cells or debris, rinsed with pre-warmed NBA-A/B27/Glu and replaced with fresh NBA/B27/Glu medium supplemented with 1% antibiotic/antimycotic (Pen/Strep and Fungizone, Life Technologies, USA) under control conditions. Pharmacological agents under study were also added at this time.

### 2.2.2 Measuring cell proliferation by incorporation of bromodeoxyuridine

Proliferation in cultures was measured by the incorporation of bromodeoxyuridine (BrdU) (Sigma Aldrich, UK), a thymidine analogue, into dividing cells during the S-phase of the cell cycle (Cameron & McKay, 2001). Stocks of BrdU (1 mM in sterile water) were added directly to wells at a final concentration of 20 µM for 6 h before cell fixation. A 6 h exposure to BrdU was chosen because the S-phase is equal to a third to half of the total length of the cell cycle (12-14 h in progenitor cells (Hayes & Nowakowski, 2000)). During

cell fixation, the growth media was aspirated and cells rinsed once in 0.1 M phosphate buffered saline (PBS) for 3 min (Sigma Aldrich, pH 7.4) before fixation in 4% paraformaldehyde (PFA) for 20 to 30 min at 4ºC. Immunocytochemistry was used to label incorporated BrdU and was combined with 4', 6-diamidino-2-phenylindole (DAPI) (Sigma Aldrich, UK) staining to derive the proliferation status of the cell population (number of $BrdU^+$ cells divided by the total cell count (DAPI)), otherwise known as the mitotic index. DAPI is a blue nuclear stain which binds to the double-stranded DNA of both healthy and dying cells. The combination of double staining with BrdU and cell phenotype specific markers (e.g. nestin for precursor cells) reveals the effect of treatments on the proliferating status of a specific cell type.

### 2.2.3 Immunocytochemistry

The fixed cultures were first washed in 0.1 M PBS 3 times to remove PFA. Cultures treated with BrdU underwent an additional step which included incubation with 2 M hydrochloric acid (HCL) (Sigma Aldrich, UK) for 30 min at 37ºC. The HCL disrupts the nuclear envelope and unfolds the double stranded DNA to aid antibody binding to the nuclear incorporated BrdU antigen (Howell et al., 2003). Cells were then washed in PBS 3 times before incubation in 5% donkey blocking serum (DBS) (Sigma Aldrich, UK) in 0.1 M PBS-0.1% Triton (PBS-T) for 30 min at 25°C (room temperature). Triton (X-100) (Sigma Aldrich, UK) is a non-ionic surfactant used to permeabilise eukaryotic cell membranes. Cells were then incubated in 5% DBS in PBS-T with dilutions of primary antibodies (Table 2.2.1) overnight at 4ºC. The next day, cells were washed once in PBS before incubation with PBS-T containing dilutions of secondary antibodies (Table 4.2.1) for 2 h at room temperature (maintained under dark conditions to avoid bleaching). Cells were then washed once in PBS before being counterstained with the nuclear stain DAPI (20 µg/ml DAPI in distilled water) for 6 min. Cells were rinsed once in distilled water, twice in PBS and maintained in distilled water for imaging.

Table 2.2.1 Primary and secondary antibody dilutions

| Primary antibodies | Company | Dilution |
|---|---|---|
| Rat anti-BrdU | AbD Serotec, UK | 1:500 |
| Mouse anti-rat nestin | BD Biosciences, UK | 1:200 |
| Mouse anti-TUJ1 | Cambridge Bioscience, UK | 1:500 |
| Rabbit anti-TUJ1 | Cambridge Bioscience, UK | 1:500 |
| Rabbit anti-GFAP | Dako, UK | 1:2000 |
| Isolectin B4 (IB4) AF555 conjugated | Invitrogen | 1:500 |
| Secondary antibodies | Company | Dilution |
| Alexa Fluor donkey anti-rat 488 | Molecular Probes, Invitrogen, UK | 1:1000 |
| Alexa Fluor donkey anti-mouse 555 | Molecular Probes, Invitrogen, UK | 1:500 |
| Alexa Fluor donkey anti-rabbit 555 | Molecular Probes, Invitrogen, UK | 1:500 |
| Alexa Fluor donkey anti-mouse 488 | Molecular Probes, Invitrogen, UK | 1:500 |
| Alexa Fluor donkey anti-rat 594 | Molecular Probes, Invitrogen UK | 1:500 |
| Cy5 donkey anti-rabbit | Millipore, UK | 1:500 |

Coverslips underwent an additional mounting step. Immunostained coverslips were transferred (cell side down) onto mounting medium Mowiol (Sigma Aldrich, UK) on glass microscope slides. After a 40 min drying step, mounted coverslips were sealed with clear nail varnish which was allowed to dry before imaging.

### 2.2.4 Cell counting and statistical analysis

An inverted Leica DM IRB microscope (Leica Microsystems UK Ltd., Milton Keynes, UK) was used to capture fluorescent images for cell counting. Cell quantification was performed on 6 random 20X fields per well using the Volocity image capturing system version 4.2.0 (Improvision Inc., Lexington, USA). The area of a 20X field was previously measured using a 255 μm graticule slide. Raw data counts were averaged and expressed as cells/mm² per well or percentage of control, and plotted with the standard error of the mean (SEM). Plots were based on the mean of a sample of at least 4 wells per condition per experiment from a minimum of three independent experiments ($n \geq 3$), with each experiment consisting of 16 hippocampi pooled from 8 animals. Data were plotted using GraphPad Prism data analysis software (GraphPad Software Inc., San Diego, CA, USA) and the appropriate statistical test (ANOVA with Dunnett's multiple comparison post-hoc

test, ANOVA with Bonferonni's post-hoc test or the Unpaired Students t-test) applied on the means.

### 2.2.5 Culture characterisation

The phenotypic characterisation of cells was carried out on rat primary hippocampal cultures. Hippocampal cells were cultured under control conditions (NBA-A/B27/Glu medium plus 1% antibiotic/antimycotic) or in the presence of 1 μM NPY for 3 days *in vitro* (DIV) (Howell et al., 2003; Howell et al., 2005). On day 3, cells were pulsed with 20 μM BrdU for 6 h before cell fixation in 4% PFA (Sigma Aldrich, UK). Fixed cultures were immunocytochemically stained for the S-phase marker BrdU, the stem/precursor cell marker nestin, the astrocytic marker GFAP, the neuronal marker class III β-tubulin, the microglial marker isolectin IB4 and DAPI before imaging, cell quantification and analysis.

### 2.2.6 Neuroproliferative effect of NPY on primary hippocampal neuronal cultures

NPY has previously been shown to increase the proliferation of nestin$^{+}$ precursor cells in primary hippocampal neuronal cultures (Howell et al., 2003). This study was repeated to confirm the neuroproliferative effects of NPY (Sigma Aldrich, UK) as a control for further investigations. Hippocampal cells were cultured under control conditions or in the presence of 1 μM NPY for 5 DIV (Howell et al., 2003; Howell et al., 2005). Two-thirds of the growth media was replaced on day 3. On day 5, cells were pulsed with 20 μM BrdU for 6 h before cell fixation in 4% PFA. Fixed cultures were immunocytochemically stained for the S-phase marker BrdU, the stem/precursor cell marker nestin and DAPI before imaging, cell quantification and analysis.

### 2.2.7 The acute neuroproliferative effect of NPY

To assess the acute neuroproliferative effects of NPY, cells were grown under control conditions for 3 DIV before being pulsed with BrdU (20 μM) and either control medium or NPY (1 μM) for 6 h. Cells were fixed and cultures immunocytochemically stained for BrdU and nestin before cell imaging, quantification and analysis.

### 2.2.8 Neurotrophic effect of NPY

The neuroproliferative effects of NPY have been well demonstrated at a range of NPY concentrations (1 nM to 1 μM) (Howell et al., 2003). Howell et al. (2003) also showed that NPY was not neurotrophic and did not affect cell survival at 1 μM concentration using chromatin condensation as an assessment of cell death (Howell et al., 2003). To determine whether NPY has neurotrophic effects at lower concentrations, cell death was quantified in

primary hippocampal cultures in the presence of lower concentrations of NPY. Hippocampal cells were cultured for 5 DIV in the absence of NPY (control) or in the presence of 1 pM, 1 nM or 1 μM NPY. On the fifth day, cell death in culture was quantified using the cell death marker Propidium Iodide (PI) and nuclear stain DAPI. PI, which is usually excluded from healthy cells with an intact membrane, binds to nucleic acids in dead or dying cells with a leaky membrane, emitting a fluorescence of about 590 nm wavelength. PI (Sigma Aldrich, UK) was added directly to live cultures at a concentration of 5 μg/ml (Eyupoglu et al., 2003) for 40 min at 37°C. The PI-containing medium was then aspirated and replaced with medium (NBA-A/B27/Glu) containing DAPI (20 μg/ml) for 40 min before aspiration, and replaced with fresh medium for imaging. The relative proportion of dead cells ($PI^+$) to total cell count (DAPI) was quantified.

## 2.3 Results

### 2.3.1 Culture characterisation

Primary hippocampal cultures generated from postnatal rats resulted in mixed cultures containing a variety of cell types. The cell types and proportions within the cultures were characterised using immunocytochemistry to cell type specific markers, as well as to the S-phase marker BrdU, after 3 days in culture (Fig. 2.3.1A). There were cells immunopositive for the precursor cell marker nestin (Fig. 2.3.1B), the neuronal marker class III β-tubulin (Fig. 2.3.1C), the astrocytic marker GFAP (Fig. 2.3.1D) and the microglial marker isolectin IB4 (Fig. 2.3.1E).

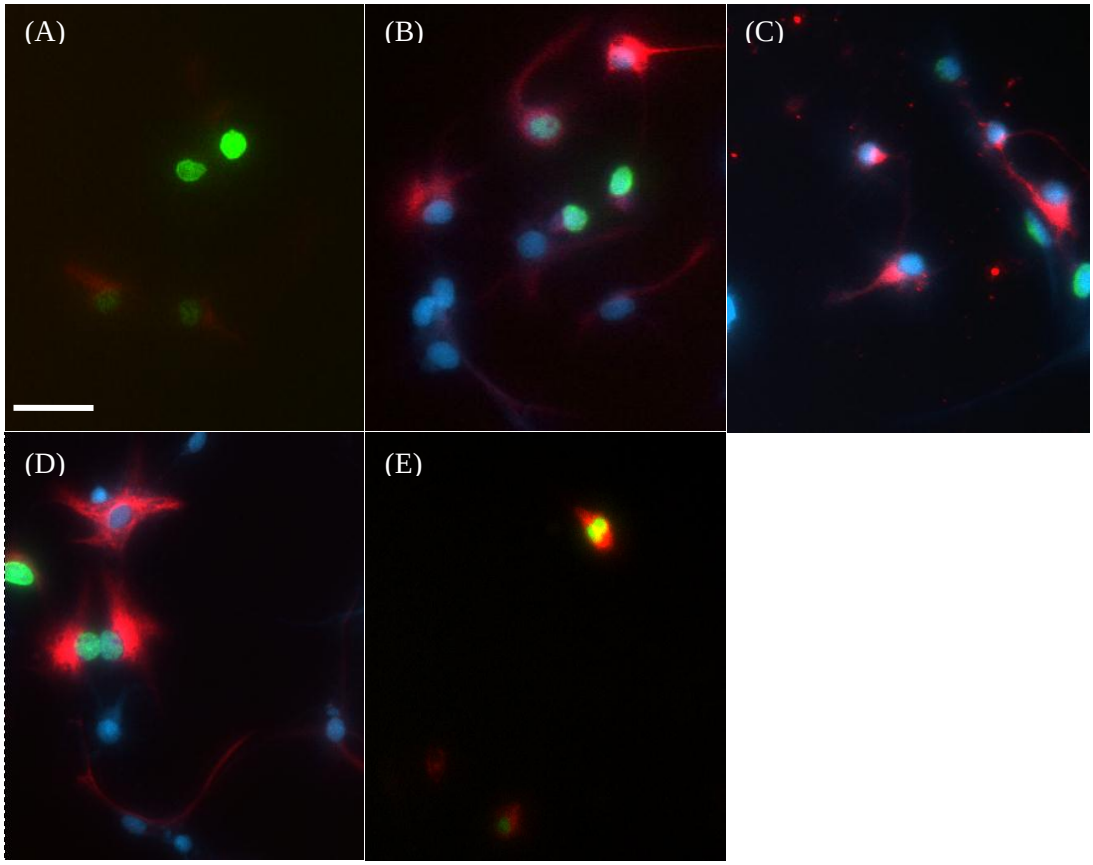


Figure 2.3.1 Culture characterisation. Primary hippocampal cultures were stained for (A) the S-phase cell marker BrdU (green), and a range of cell type-specific markers against (B) the precursor cell marker nestin (red), (C) the neuronal marker class III β-tubulin (red), (D) the astrocytic marker GFAP (red), and (E) the microglial marker isolectin IB4 (red). The cell nuclei were stained with DAPI (blue). Scale bar, 50 μm.

As well as uniform BrdU staining, speckled BrdU staining of cells was also observed (Fig. 2.3.1A bottom two cells). This speckled characteristic is representative of cells which

have entered the S-phase later or when a labelled cell undergoes cell division, which dilutes the amount of BrdU present (Raza et al., 1985).

The proportions of nestin$^+$, class III β-tubulin$^+$, GFAP$^+$ and IB4$^+$ cells were assessed in 3-day-old cultures. Nestin$^+$ and GFAP$^+$ cells were the most abundant cell phenotypes observed, with 40% and 41% proportions respectively, while just under a quarter of cells (24%) were class III β-tubulin$^+$. IB4$^+$ cells were in the minority (12%) (Table 2.3.1).

Table 2.3.1 Proportions of specific cell phenotypes and BrdU incorporation in hippocampal cultures after 3 d growth under control (NBA-A/B27/Glu medium plus 1% antibiotic/antimycotic) conditions*. The cultures were exposed to the S-phase marker BrdU for the final 6 h of the experiment. *n*, number of wells sampled from at least 2 separate experiments.

| | BrdU (%) | Nestin (%) | B-tubulin (%) | GFAP (%) | IB4 (%) |
|---|---|---|---|---|---|
| Mean | 10 | 40 | 24 | 41 | 12 |
| SEM | 0.5 | 1.5 | 2.6 | 1.4 | 1.6 |
| *n* | 48 | 29 | 6 | 6 | 5 |

*The expression of cell markers overlap.

### 2.3.2 NPY is neuroproliferative for hippocampal precursor cells

To confirm that NPY is neuroproliferative for hippocampal precursor cells, 1 μM NPY was added to cultures over 5 DIV. Observations showed that NPY increased cell numbers as well as the number of BrdU$^+$ cells (Fig. 2.3.2). In response to NPY exposure, there were significant increases in the total cell count (DAPI) (196.3 ± 8.8 cells/mm$^2$ in control condition compared to 255.5 ± 11.2 cells/mm$^2$ in NPY condition; Students unpaired t-test, p=0.0003, t=4.075, d.f.=30 and F=1.824) (Fig. 2.3.3A), BrdU$^+$ cell number (19.7 ± 1.5 cells/mm$^2$ in control condition compared to 50.5 ± 9.3 cells/mm$^2$ in NPY condition; Students unpaired t-test, p=0.0044, t=3.084, d.f.=30 and F=42.64) (Fig. 2.3.3B) and the mitotic index (9.7 ± 2.5% in control condition compared to 20.7 ± 3.9% in NPY condition; Students unpaired t-test, p=0.0154, t=2.571, d.f.=30 and F=41.52) (Fig. 2.3.3E) of cultures. In addition, NPY also increased the numbers of nestin$^+$ precursor cells (95.4 ± 5.0 cells/mm$^2$ in control condition compared to 121.0 ± 20.5 cells/mm$^2$ in NPY condition; Students unpaired t-test, p=0.0011, t=3.606, d.f.=30 and F=1.101) (Fig. 2.3.3C) and nestin$^+$ BrdU$^+$ precursor cells (12.1 ± 1.2 cells/mm$^2$ in control condition compared to 34.0 ± 5.7 cells/mm$^2$ in NPY condition; Students unpaired t-test, p=0.0013, t=3.534, d.f.=30 and

F=25.15) (Fig. 2.3.3D) as well as the mitotic index of the nestin$^+$ precursor cell population (12.3 ± 1.1% in control condition compared to 28.9 ± 4.7% in NPY condition; Students unpaired t-test, p=0.0030, t=3.225, d.f.=30 and F=18.70) (Fig. 2.3.3F).

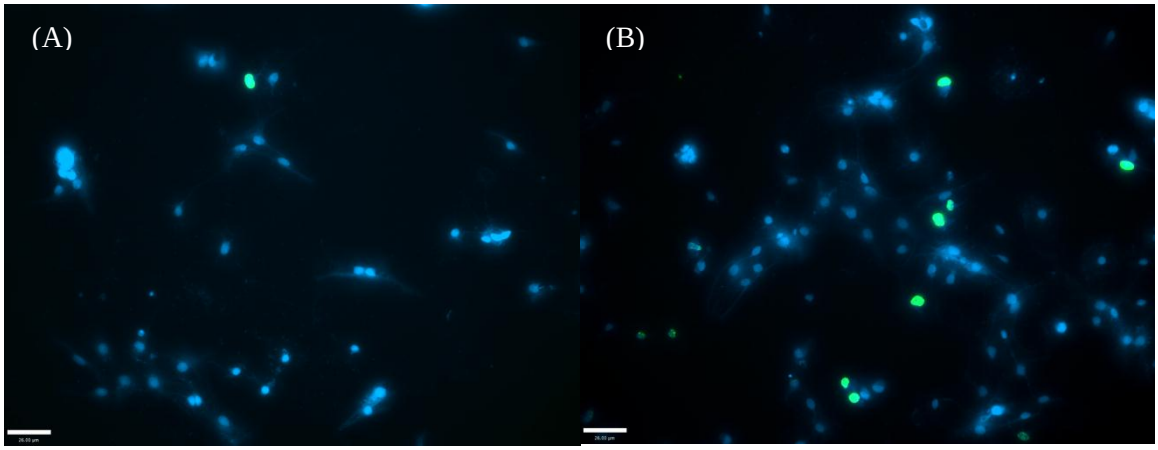


Figure 2.3.2 Exposure to NPY increased total cell counts. Hippocampal cultures treated under (A) control conditions (Neurobasal A/B27/glutamine) or (B) with NPY (1µM) at 5 DIV. The cultures were exposed to the S-phase marker BrdU for the final 6 h before fixation and immunocytochemistry for BrdU (green). The cell nuclei were stained with DAPI (blue). Scale bar, 50 µm.

### 2.3.4 NPY has an acute proliferative effect

Hippocampal cultures (3 DIV) were exposed to a short 6 h pulse of 1 µM NPY to assess its acute neuroproliferative effects. The proliferation of the cultures increased over 6 h in response to NPY treatment. The total number of BrdU$^+$ cells was significantly increased (Students unpaired t-test, p=0.0026, t=3.339, d.f.=25 and F=1.399) (Fig. 2.3.4A), while the mitotic index of nestin$^+$ BrdU$^+$ precursors was also significantly enhanced by the presence of NPY (Students unpaired t-test, p=0.0016, t=3.548, d.f.=25 and F=1.054) (Fig. 2.3.4B).

### 2.3.5 The effect of NPY on cultures is purely proliferative and not neurotrophic

The increase in cell number in response to NPY treatment may be as a result of either proliferative or trophic effects. To clarify the effects of NPY on cell number, the effect of NPY concentration on cell survival was investigated. Hippocampal cultures were exposed to none (control), 1 pM, 1 nM or 1 µM NPY over 5 DIV before assessment of cell death by DAPI and PI staining. An increase in NPY concentration increased the total cell count, with a significant increase in response to 1 µM NPY (One-way ANOVA with Dunnett's post-hoc test, $p<0.05$, F=10.00 and d.f.=51) (Fig. 2.3.5A). On the other hand, increasing concentrations of NPY had no significant effect on the percentage cell death (PI$^+$ cells/total

cell count) of cultures (One-way ANOVA with Dunnett's post-hoc test, $p>0.05$, $F=1.366$ and d.f.=50) (Fig. 2.3.5B). If NPY had a neurotrophic effect, the percentage of dead or dying cells compared to control would be significantly decreased. It can be concluded from the results that the effect of NPY was purely proliferative and not neurotrophic.

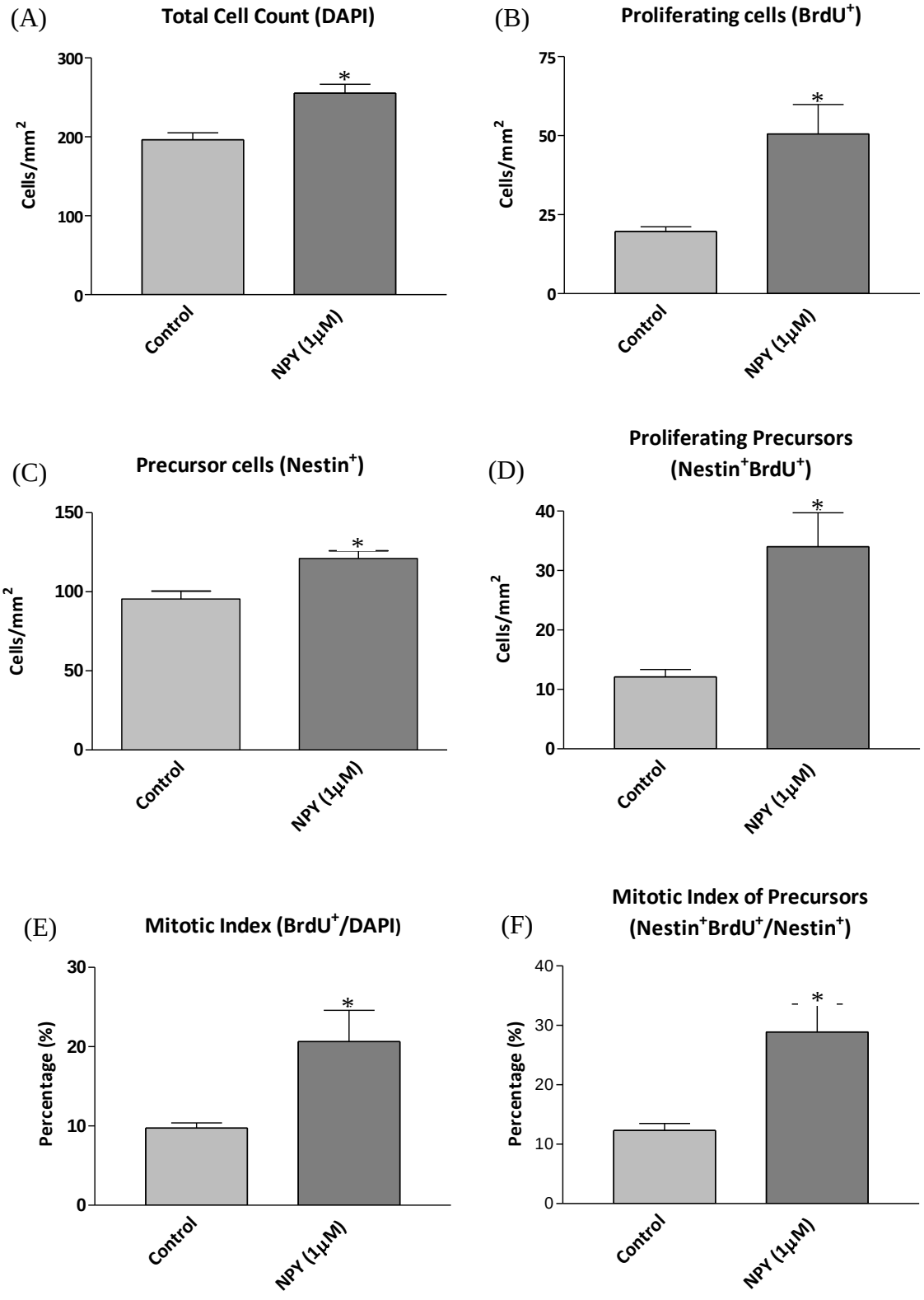


Figure 2.3.3 NPY was neuroproliferative for nestin$^+$ hippocampal precursor cells. Cells were cultured under control conditions (Neurobasal A/B27/glutamine) or in the presence of 1 µM NPY for 5 DIV. BrdU was added for the final 6 h. (A) Total cell counts increased significantly with NPY treatment. (B) BrdU$^+$ cells, (C) nestin$^+$ precursor cells and (D) BrdU$^+$ precursor cells also increased significantly in response to NPY. The proliferation status or mitotic index of both (E) total cells

and (F) precursor cells was enhanced in the presence of NPY. Data represent mean ± SEM based on a sample that represents at least 15-17 wells per condition from three separate experiments. Students t-test *p < 0.05.

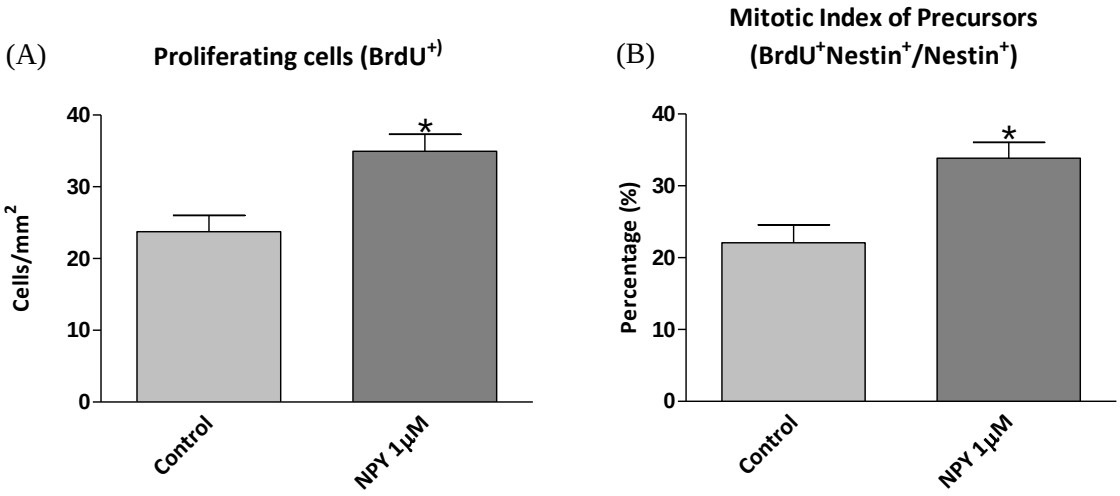


Figure 2.3.4 NPY had an acute proliferative effect on hippocampal cultures. Cells were cultured under control conditions (Neurobasal A/B27/glutamine) for 3 DIV before 20 µM BrdU and/or 1 µM NPY was added for the final 6 h. (A) NPY significantly increased the number of $BrdU^+$ cells as well as (B) the mitotic index (proliferation status) of $nestin^+$ hippocampal precursor cells. Data represent mean ± SEM based on a sample that represents at least 12 wells per condition from three separate experiments. Students t-test *p < 0.05.

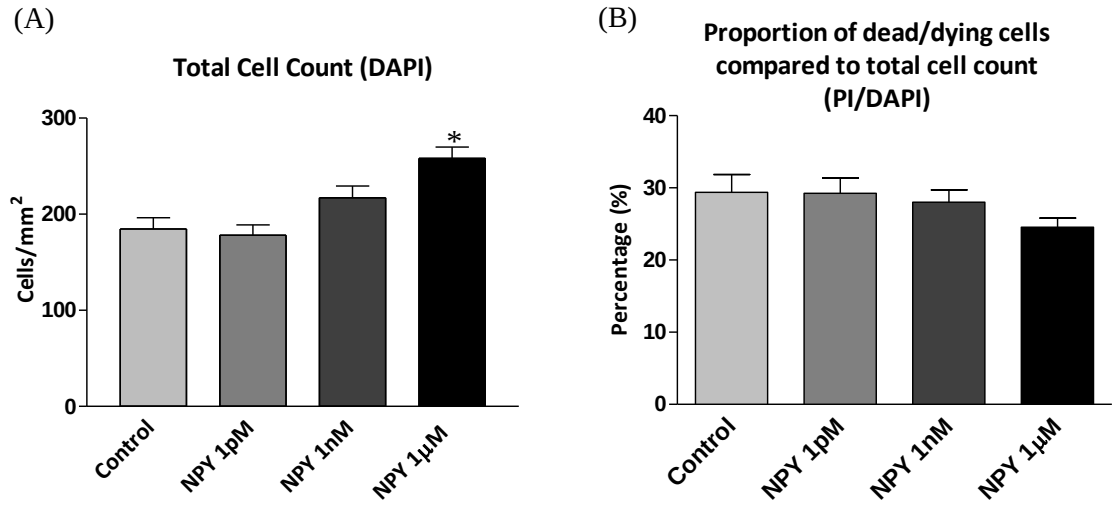


Figure 2.3.5 The effect of NPY was purely proliferative and not neurotrophic. Cells were cultured under control conditions (Neurobasal A/B27/glutamine) or in the presence of 1 pM, 1 nM or 1 µM NPY for 5 DIV. On day 5, cell death was assessed by PI and DAPI staining. (A) Total cell counts

were increased by increasing concentrations of NPY. The increase in total cell count was significant for 1 μM NPY. (B) Increasing NPY concentration had no significant effect of the proportion of dead or dying cells. Data represent mean ± SEM based on a sample that represents at least 13 wells per condition from three separate experiments. One-way ANOVA with Dunnett's multiple comparison test *$p < 0.05$.

## 2.4 Discussion

The neuroproliferative effect of NPY, first observed by Hansel et al. (2001) on postnatal precursor cells derived from the olfactory epithelium, and by Howell et al. (2003) on postnatal hippocampal cultures, was also observed on primary hippocampal cultures in this study. It was important to verify these previous findings due to several reasons. Firstly, cell culturing techniques (adapted from Howell et al., 2003) often fluctuate between studies, so repetition allows for any major disparity to be identified, and secondly, it was important to validate these initial findings before carrying out further investigations into the actions of NPY.

### 2.4.1 Culture characterisation

The relative proportions of different cell phenotypes within cultures were assessed by immunocytochemistry. There were cells immunopositive for the precursor cell marker nestin, the astrocytic marker GFAP, the neuronal marker class III β-tubulin and the microglial marker isolectin IB4. These results can be compared to a similar study by Howell et al (2003) who investigated the relative proportions of cell phenotype present in rat hippocampal cultures after 5 DIV (Table 2.4.1).

Table 2.4.1 Cell phenotype after 5 DIV under control conditions (Howell et al., 2003). Proportions of specific cell phenotypes and BrdU incorporation in hippocampal cultures after 5 days growth under control (NBA-A/B27/Glu medium plus 1% antibiotic/antimycotic) conditions[*]. The cultures were exposed to the S-phase marker BrdU for the final 24 h of the experiment. *n*, number of wells sampled from at least 4 separate experiments. For comparison, the mean values found in this present study (from Table 2.3.1) are shown in parentheses.

| | BrdU (%) | Nestin (%) | B-tubulin (%) | GFAP (%) |
|---|---|---|---|---|
| Mean | 45.6 | 37.3 | 25.1 | 28.4 |
| | (10[†]) | (40) | (24) | (41) |
| SEM | 1.9 | 3.4 | 2.4 | 3.8 |
| *n* | 54 | 22 | 29 | 14 |

[*]The expression of cell markers overlap.

[†]Cultures were exposed to BrdU for 6 h (instead of 24 h) in this study.

The relative proportions of nestin$^+$ cells (37.3%) and class III β-tubulin$^+$ cells (25.1%) obtained in Howell et al's study were similar to the proportions found here (40% and 24%, respectively), although Howell et al (2003) found the proportion of GFAP$^+$ cells to be

slightly lower (around 10% lower). There was also a significantly higher proportion of proliferating cells ($BrdU^+$) observed by Howell et al. (2003), which is likely due to the 24 h (instead of 6 h) exposure to BrdU.

### 2.4.2 The neuroproliferative effect of NPY

As demonstrated by previous studies, NPY has a key role in modulating the proliferation of a range of cell types. Howell et al. (2003) have shown that the neuroproliferative effect of NPY on hippocampal neuronal cultures was primarily on $nestin^+$ hippocampal precursor cells and $\beta$-$tubulin^+$ neuroblasts. Similarly, my results confirm the proliferative effect of NPY (1 μM) on postnatal rat hippocampal neuronal cultures, as indicated by significant increases in total cell count, numbers of proliferating cells and mitotic indices (indicative of proliferating status). The neuroproliferation of $nestin^+$ precursor cells also increased significantly in response to 1 μM NPY treatment over 5 DIV. Indeed, previous studies have shown that even concentrations as low as 1 nM are proliferative for rat hippocampal cultures, and this proliferative effect was enhanced with an increase in peptide concentration (Howell et al., 2003). With regards to whether the pharmacological concentrations used *in vitro* are representative of *in vivo* levels, a study by Nam et al. (2001) showed that the average concentration of NPY in the cerebrospinal fluid of normal weight individuals was ~130 pg/ml, equivalent to about 30 nM free NPY. These concentrations are likely to be much higher at the site of NPY release *in vivo* and are reflective of levels at which NPY was used in pharmacological studies. 1 μM NPY was chosen for further studies into the underlying mechanisms because of its potent proliferative effects and was the concentration most frequently used in other studies (Howell et al., 2003, 2005; Alvaro et al., 2008), thus allowing comparison between data sets. In addition to having a general proliferative effect on hippocampal cultures, a significant increase in proliferation was observed in response to an acute pulse of NPY for 6 h. This acute effect of NPY had also been shown to be effective in response to a 4 h exposure (Howell et al., 2003). Results confirm that the proliferative effect of NPY was purely proliferative and not as a result of trophic mechanisms. Through an assessment of total cell count and cell death in response to increasing levels of peptide (1 pM, 1 nM and 1 μM), no significant trophic effects were observed. Although there seemed to be a minor downward trend in cell death with increasing peptide concentration, this observation was not significant. In similar studies which used nuclear condensation (pyknotic nuclei) (Howell et al., 2003) or the TUNEL apoptosis assay (Hansel et al., 2001) as a marker of

cell death, the effect of NPY was also confirmed to be purely proliferative as levels of cell death were comparable between control and NPY treated cultures. Results show that total cell counts increased in response to increasing concentrations of NPY, an observation previously confirmed by Howell et al. (2003). However, in comparison to that study, although there was an increase in total cell counts at 1 nM NPY exposure compared to control (Fig. 2.3.5); current results did not show a significant proliferative effect at that low a concentration. One explanation may be a difference in the source of the NPY peptide.

### 2.4.3 NPY in learning and memory

Adult hippocampal neurogenesis is functionally required and important for some forms of hippocampal-dependent learning and memory (Shors et al., 2001; Shors et al., 2002). Research has shown that NPY may play an important role in the modulation of learning and memory processes. Flood et al (1987) have shown that intracerebroventricular injections of porcine NPY fragments enhanced memory retention after training in mice and also alleviated amnesia induced by anisomycin (protein synthesis inhibitor) and scopolamine (anticholinergic). Furthermore, NPY over-expressing transgenic mice show selective impairment of spatial memory acquisition in Morris water maze trials, which was associated with decreased hippocampal NPY-$Y_1$ receptor binding in response to elevated NPY levels (Thorsell et al., 2000). The $Y_2$ receptor subtype had also been implicated in cognitive processing. NPY $Y_2$ receptor-negative mice (NPY $Y_2^{-/-}$) display deficits in Morris water maze tasks and exhibit significant deterioration in object memory tests, supporting the possible involvement of NPY action on $Y_1$ and $Y_2$ receptors as a modulator of learning and memory (Redrobe et al., 2004).

### 2.4.4 The role of NPY in depression

Adult hippocampal neurogenesis is frequently linked to the pathogenesis of depression. Stress, a common prerequisite for depression, has been shown to decrease hippocampal neurogenesis (Gould et al., 1997), while hippocampal neurogenesis was increased in rats following the chronic administration of antidepressants (Malberg et al., 2000). This increase in dividing hippocampal neural progenitor cells in response to antidepressant treatment has also been observed post-mortem in the dentate gyrus of patients with major depressive disorder (Boldrini et al., 2009). There have been a range of animal and human studies implicating NPY in depression (Redrobe et al., 2002a). Electroconvulsive therapy (ECT) is a well established psychiatric therapy for depression and studies have shown that electroconvulsive shock stimulation (ECS), an animal model of ECT, increases NPY gene

expression and NPY immunoreactivity in hippocampal and cortical homogenates (Stenfors et al., 1995). Moreover, decreased levels of NPY have been detected in the cerebrospinal fluid (CSF) of depressed patient compared to healthy controls (Widerlov et al., 1988). The action of NPY in regulating hippocampal neurogenesis has also been implicated in the mechanism of action of many antidepressant drugs (Redrobe et al., 2002a). Lithium treatment, which was often used in the management of bipolar disorder, had been shown to increase mRNA and peptide levels of NPY (Husum et al., 2000), while chronic antidepressant treatment with antidepressant drugs such as fluoxetine and imipramine increase mRNA levels of NPY peptide and NPY $Y_1$ receptor (Caberlotto et al., 1998). In animal forced swimming tests, which are widely used for the screening of prospective antidepressant drugs, intracerebroventricular NPY and [$Leu^{31}Pro^{34}$]PYY (selective $Y_1/Y_5$ agonist) administration significantly reduced the immobility time (time in which animal spends without moving). The immobility time tends to be decreased with antidepressants. Meanwhile, selective $Y_1$ antagonists such as BIBP3226 blocked the anti-immobility effects of NPY, suggesting the possible involvement of the $Y_1$ receptor in the pathogenesis of depression (Redrobe et al., 2002a). With further understanding of the mechanisms underlying the mediation of depression, novel pharmacotherapeutic treatments for depressive disorders, such as synthetic NPY $Y_1$ agonists, may be developed (Redrobe et al., 2002b).

### 2.4.5 NPY and temporal lobe epilepsy

Seizures have been shown to increase neurogenesis in both the SGZ and SVZ (Parent et al., 1997; Bengzon et al., 1997; Parent et al., 2002), while NPY levels in the dentate gyrus and hippocampus have been shown to increase significantly in response to seizure activity (Marksteiner et al., 1989). A study by Howell et al (2007) has demonstrated the link between NPY and seizure-induced precursor cell proliferation in the hippocampus using $NPY^{-/-}$ mice. Using BrdU as a marker of dividing cells in kainate-induced seizures, $NPY^{-/-}$ mice exhibited a 41% reduction in BrdU-immunopositive cells within the SGZ in comparison to control animals. The results suggested that NPY was an important modulator of precursor cell proliferation under both normal conditions and in response to seizure activity (Howell et al., 2007).

In conclusion, the neuroproliferative effects of NPY first observed by Hansel et al. (2001) and Howell et al. (2003) have been verified by this study. The effect of NPY was

purely proliferative with no trophic effects on hippocampal cultures. This confirmation now allows us to further investigate this proliferative effect and the possible intracellular signalling mechanisms involved.

# Chapter 3

## Chapter 3 – The proliferative effect of NPY is mediated via NOS and NO

### 3.1 Introduction

NPY exerts a purely proliferative effect on postnatal hippocampal cultures which is mediated via its NPY $Y_1$ receptor. The cellular mechanisms underlying this proliferative effect are not fully understood, although NOS and NO may be implicated.

#### 3.1.1 Nitric oxide synthase

The three isoforms of NOS, nNOS, eNOS and iNOS, first identified in 1989, are individually encoded by distinct genes and have differential regulatory, catalytic and inhibitory properties and localisation profiles (Knowles et al., 1989; Knowles & Moncada, 1994; Cardenas et al., 2005). nNOS was the first NOS isoform identified and predominates in neuronal tissue (Bredt & Snyder, 1990), while iNOS is named due to its inducible expression in a range of tissues and cells (Stuehr & Griffith, 1992). eNOS, on the other hand, was first identified in vascular endothelial cells (Pollock et al., 1991). Generally, the isoforms are further categorised based on their constitutive (nNOS and eNOS) versus inducible (iNOS) expression, and calcium-dependence (nNOS and eNOS) or -independence (iNOS) (Bredt & Snyder, 1990; Yui et al., 1991). There is a 51-57% homology between the NOS isoforms in humans (Alderton et al., 2001). Simply put, NOS catalyses a reaction between the substrates L-arginine, NADPH and oxygen to the reaction products citrulline, NADP and a free radical NO (Knowles et al., 1989; Knowles et al., 1990). As well as the presence of calmodulin (CaM), other coenzymes or cofactors are also required, including iron protoporphyrin IX (haem), FAD, FMN and $BH_4$, which are all relatively tightly-bound (Knowles & Moncada, 1994). Structurally, the NOSs have a bidomain structure, consisting of an N-terminal oxygenase domain which is interconnected to the C-terminal reductase domain through a CaM-recognition site (Ghosh & Stuehr, 1995; Sheta et al., 1994). The oxygenase domain contains binding sites for haem, $BH_4$ and L-arginine, while the reductase domain binds FMN, FAD and NADPH (Ghosh & Stuehr, 1995) (Fig. 3.1.1).

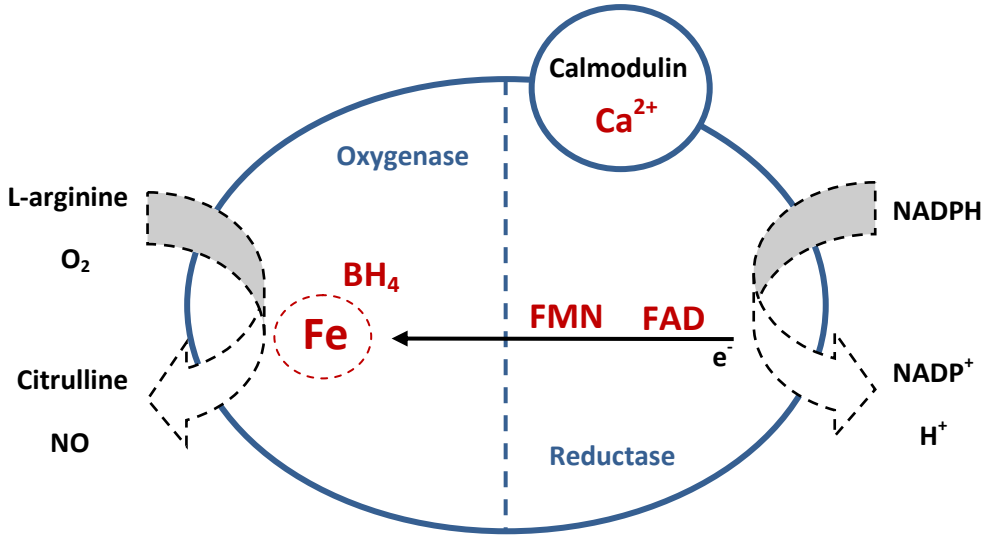


Figure 3.1.1 The bidomain structure of NOS. NADPH donates electrons ($e^-$) to the reductase domain which flows through FAD and FMN before reaching the oxygenase domain and interacting with the haem iron and $BH_4$. This active site then catalyses the reaction of L-arginine with oxygen, generating the reaction products citrulline and NO. Bound $Ca^{2+}$/CaM is required for electron flow (adapted from Alderton et al., 2001).

Subtype specific variances at the primary, secondary, tertiary and even quaternary structural level account for their distinct properties. In their active form, two monomers of NOS (dimeric form) associate with two CaMs, resulting in a tetrameric complex (Alderton et al., 2001).

### 3.1.2 Regulation of NOS activity

NO is important in mediating a variety of physiological roles, influenced in part by the localisation of the NOS subtypes to specific cells and tissues through transcriptional regulation and the regulation of NOS activity by phosphorylation or proteins such as CaM (Gachhui et al., 1998), protein inhibitor of nNOS (PIN) (Jaffrey & Snyder, 1996), nitric oxide synthase interacting protein (NOSIP) (Dreyer et al., 2004) or heat-shock protein 90 (Hsp90) (Garcia-Cardena et al., 1998), to name a few. Phosphorylation of NOS results in either an increase or decrease in NOS activity depending on the phosphorylation site and the NOS subtype. For example, while the NO production activity of eNOS is increased in response to the phosphorylation of $Ser^{1179}$ by protein kinase Akt (Dimmeler et al., 1999), nNOS activity is decreased in response to $Ser^{847}$ phosphorylation by CaM-dependent kinases (Komeima et al., 2000) but increased in response to $Ser^{1412}$ phosphorylation (Adak et al., 2001). The dephosphorylation of nNOS by protein phosphatase 1 at sites such as

$Ser^{847}$ also increases nNOS activity, acting as a means by which to control nNOS activity (Rameau et al., 2004; Zhou & Zhu, 2009). Protein-protein interactions involving CaM are essential for the NOS activity of all three isoforms, although the $Ca^{2+}$ dependence may be different, and facilitates the electron flow from NADPH to the reductase domain (Gachhui et al., 1998). The proteins PIN and NOSIP have been shown to inhibit nNOS activity (Jaffrey & Snyder, 1996; Dreyer et al., 2004; Zhou & Zhu, 2009), while the heat-shock protein, Hsp90, is also a regulator of NOS, specifically eNOS, activity (Garcia-Cardena et al., 1998). Garcia-Cardena et al. (1998) showed that agonists, such as vascular endothelial growth factor, histamine and fluid shear stress, which stimulate NO production, increase the interaction between eNOS and Hsp90 and enhance eNOS activity.

### 3.1.3 Galanin

Galanin is a widely expressed 29-30 amino acid neuropeptide whose effects are mediated via its three known receptors (GalR1, 2 and 3) which are also a part of the GPCR superfamily of receptors. Like NPY, galanin has been implicated in the control of physiological processes such as feeding behaviour, seizure activity, cognitive processes (learning and memory) and mood (Lundström et al., 2005; Hobson et al., 2008). Similarly, galanin has been shown to promote neurogenesis and is neuroprotective by acting through its GalR2/3 receptor (Hobson et al., 2008, Abbosh et al., 2011). During development and adulthood there are high levels of galanin peptide and GalR1/2 in the SVZ and SGZ (Shen et al., 2005) and, like NPY, galanin is proliferative for postnatal hippocampal precursor cells (Abbosh et al., 2011) and neurospheres derived from hippocampal precursor cells (Hawes et al., 2006).

### 3.1.4 The aims of this chapter

The aims of this chapter were to determine the involvement of NOS and NO in mediating the neuroproliferative effect of NPY on postnatal hippocampal cultures, which was explored through the use of NOS and NO selective pharmacological agonists and antagonists, fluorescent NO indicators and immunocytochemistry. The widespread physiological effects of NO can be attributable, in part, to the existence of the NOS isoforms, prompting further investigations into the NOS subtype involved. To determine whether NOS and NO signalling is common in the proliferative action of other neuropeptides, the signalling pathway involving the neuropeptide galanin was also analysed.

## 3.2 Methods

### Methodology and experimental aim

The NOS and NO mechanisms underlying NPY-mediated neuroproliferation were investigated in an *in vitro* rat hippocampal cell culture system. A detailed description of primary hippocampal cell culture generation, cell plating, the assessment of cell proliferation with BrdU, immunocytochemistry and cell quantification and statistical analysis is provided in Chapter 2. Unless otherwise stated, a one-way ANOVA with Dunnett's multiple comparison test was applied to the raw data to determine significance levels compared to control conditions ($p = <0.05$). The concentration of pharmacological agonists or antagonists were chosen based on published literature (Table 3.2.1).

Table 3.2.1 Agonists and antagonists

| Agonists | Company | Concentration |
|---|---|---|
| $Y_1$ agonist [F7, P34]NPY | Prof. Dr A.G. Beck-Sickinger, Universität Leipzig, Germany | 1 µM (Howell et al., 2003) |
| L-arginine | Sigma Aldrich, UK | 500 µM (Nakamura et al., 2006) |
| Galanin 2-11 | Sigma Aldrich, UK | 100 nM (Abbosh et al., 2011) |
| Antagonists | Company | Concentration |
| N(ω)-Nitro-L-arginine methyl ester (L-NAME) | Sigma Aldrich, UK | 500 µM (Alvaro et al., 2008) |
| N(ω)-Nitro-D-arginine methyl ester (D-NAME) | Sigma Aldrich, UK | 500 µM (used same concentration as active enantiomer L-NAME) |
| 3-Bromo7-nitroindazole (3B7N) | Tocris Bioscience, UK | 100 nM (Bland-Ward & Moore, 1995) |
| EIT hydrobromide (EITH) | Tocris Bioscience, UK | 100 nM (Nakane et al., 1995) |
| N-(4S)-4-amino-5-[aminoethyl]aminopentyl-N′-nitroguanidine (AAAN) | Sigma Aldrich, UK | 200 nM (Hah et al., 2001) |

### 3.2.1 Effect of L-NAME on NPY-mediated neuroproliferation

N(ω)-Nitro-L-arginine methyl ester (L-NAME) (Sigma Aldrich, UK) was used to study the involvement of NO in NPY-mediated neuroproliferation. L-NAME, a non-subtype selective inhibitor of NOS, is frequently used in the study of NO signalling. N(ω)-Nitro-D-arginine methyl ester (D-NAME) (Sigma Aldrich, UK), an inactive enantiomer of L-NAME was used as a control and to test the specificity of L-NAME. Primary hippocampal cells were cultured under control conditions (NBA-A/B27/Glu medium plus 1% antibiotic/antimycotic) and in the presence of NPY (1 µM) and 500 µM L-NAME or D-NAME (Alvaro et al., 2008) for 3 DIV. On day 3, cultures were pulsed with 20 µM BrdU

for 6 h before cell fixation with 4% paraformaldehyde (PFA), immunocytochemistry for BrdU and nestin, cell imaging, quantification and analysis.

The proliferative effect of NPY on hippocampal cultures is mediated via the $Y_1$ receptor (Howell et al., 2003). To assess the involvement of NO in $Y_1$-mediated proliferative effects, the $Y_1$ agonist [F7, P34]NPY (courtesy of Prof. Dr A.G. Beck-Sickinger, Universität Leipzig, Germany) was used in the presence of L-NAME and D-NAME. Primary hippocampal cells were cultured under control and in the presence of [F7, P34]NPY (1 μM) and/or 500 μM L-NAME or D-NAME for 3 DIV. On day 3, cultures were pulsed with 20 μM BrdU for 6 h before cell fixation, immunocytochemistry for BrdU and nestin, cell imaging, quantification and analysis.

### 3.2.2 L-arginine effects on hippocampal cultures

The amino acid L-arginine is a substrate used by NOS in the production of NO. L-arginine was added to cultures as a way of increasing the endogenous production of NO to assess the involvement of NO in cell proliferation. D-arginine, an inactive enantiomer of L-arginine was used as a control. Hippocampal cells were cultured under control conditions and in the presence of 500 μM L-arginine or D-arginine (Sigma Aldrich, UK) for 3 DIV. On the third day, cultures were pulsed with 20 μM BrdU for 6 h before cell fixation. The cultures were then stained immunocytochemically for BrdU and nestin, imaged, quantified and analysed.

### 3.2.3 Selective inhibition of NOS isoforms *in vitro*

Subtype-selective antagonists were used to identify the NOS subtype involved in mediating the neuroproliferative effect of NPY. Potent and selective inhibitors of eNOS were not commercially available, so investigations were focused on either selective nNOS or iNOS inhibition. The subtype-selectivity of NOS inhibitors, however, is sometimes debated (Moore & Handy, 1997). 7-nitroindazole, for example, which is often used as a selective inhibitor of nNOS in a range of studies, and was originally thought to be very selective, especially *in vivo* (Moore et al., 1993), has now been demonstrated to be relatively non-selective (Cholet et al., 1996; Zagvazdin et al., 1996). Indeed, the highly conserved active site of NOS makes the design of selective NOS inhibitors difficult (Garcin et al., 2008), the choice of inhibitors is often limited, and perfect inhibitors do not exist. Instead, caution must be made when interpreting the results of NOS inhibition when using any 'subtype-selective' inhibitors.

Hippocampal cells were exposed to control (NBA/B27/Glu and 1% antibiotic/antimycotic), 1 µM NPY and/or 100 nM 3-Bromo7-nitroindazole (3B7N, Tocris Bioscience) or 100 nM EIT hydrobromide (EITH, Tocris Bioscience) for 3 DIV before a 6 h 20 µM BrdU pulse and cell fixation. 3B7N is a nNOS and partial iNOS inhibitor (Bland-Ward et al., 1994), while EITH is a selective iNOS inhibitor (Nakane et al., 1995). To further confirm the involvement of the nNOS isoform in mediating the effects of NPY, hippocampal cells cultured for 3 DIV were exposed to 1 µM NPY and/or N-(4S)-4-amino-5-[aminoethyl]aminopentyl-N′-nitroguanidine (AAAN, 200 nM; Sigma Aldrich) and 20 µM BrdU for 6 h on the final day before cell fixation. AAAN is a selective inhibitor of the nNOS isoform, supposedly showing 2500- and 320-fold selectivity for nNOS over eNOS and iNOS, respectively (Hah et al., 2001). The cultures were stained immunocytochemically for BrdU, before they were imaged, quantified and analysed.

### 3.2.4 Immunocytochemistry for nNOS and eNOS

Hippocampal cells were cultured on poly-L-lysine-coated glass coverslips (13 mm radius borosilicate glass, VWR International, UK) under control or 1 µM NPY for 3 DIV before cell fixation. Chapter 2, section 2.2.3 outlines the detailed immunocytochemistry method. Immunocytochemistry was carried out using PBS-0.3% Triton (PBS-T) for better antibody permeability. The antibodies used and their dilutions are listed in Table 3.2.2.

Table 3.2.2 Primary and secondary antibody dilutions

| Primary antibodies | Company | Dilution |
|---|---|---|
| Rabbit anti-nNOS | Millipore, UK | 1:250, 1:500, 1:1000 |
| Rabbit anti-eNOS | BD Transduction Laboratories, UK | 1:250, 1:500, 1:1000 |
| Mouse anti-eNOS | BD Transduction Laboratories, UK | 1:500 |
| Secondary antibodies | Company | Dilution |
| Alexa Fluor donkey anti-rabbit 488 | Molecular Probes, Invitrogen, UK | 1:500 |
| Alexa Fluor donkey anti-mouse 555 | Molecular Probes, Invitrogen, UK | 1:500 |
| Alexa Fluor donkey anti-rabbit 555 | Molecular Probes, Invitrogen, UK | 1:500 |
| Alexa Fluor donkey anti-mouse 488 | Molecular Probes, Invitrogen, UK | 1:500 |

Immunostained coverslips were transferred (cell side down) onto mounting medium Mowiol (Sigma Aldrich, UK) on glass microscope slides. After a 40 min drying step,

mounted coverslips were sealed with clear nail varnish which was allowed to dry before imaging. Confocal images were taken on a Nikon C1 Digital Eclipse Modular Confocal microscope system (Nikon UK Ltd., UK) using Nikon EZ-C1 Gold v3.70 software (Nikon Corporation, 2002). The appropriate immunocytochemical controls were used to ensure that there was no bleed-through (crossover or crosstalk) fluorescence and that any observed staining was real (Table 3.2.3).

Table 3.2.3 Immunocytochemical staining controls

| Immunocytochemical controls | Antibodies |
|---|---|
| Autofluorescence control | No primary or secondary |
| Control for primary antibody autofluorescence | Primary, no secondary |
| Control for secondary antibody | Secondary, no primary |
| Control for secondary antibody specificity during co-staining | One primary, both secondary's or both primaries, one secondary |

### 3.2.5 Western blotting for nNOS in cell lysate

Western blotting was used to verify nNOS protein expression in hippocampal cell lysate.

#### 3.2.5.1 Protein extraction

Cells derived from the hippocampus were plated at a density of $10^6$ cells/ml in 6 well plates and cultured for 3 DIV under control conditions (NBA-A/B27/Glu medium plus 1% antibiotic/antimycotic). On the final day, the cells were washed in ice-cold PBS for 1 min before they were lysed for ~5 min in 300 µl/well cold lysis buffer (25 mM NaCl, 2 mM EDTA, 0.5 mM dithiothreitol, 20 mM HEPES, 20 mM glycerophosphate, 50 mM NaF, 1 mM $NaVO_3$ and 0.1% Triton X-100) containing a phosphatase inhibitor cocktail at 10:1000 (phosphatase inhibitor cocktail 2, Sigma Aldrich, UK) and protease inhibitor mixture (1 tablet/10 ml) (Roche Diagnostics, Basel, Switzerland). During cell lysis, a cell scraper was used to scrape cells off of the well bottom and aid protein extraction. The buffer was collected from the wells into ependorfs and centrifuged (5000 rpm for 1 min) before the supernatant was collected and stored as frozen aliquots. Protein content of samples was determined using the Bradford assay protocol using Bradford reagent (Sigma Aldrich, UK) to ensure similar protein content across samples.

### 3.2.5.2 Gel electrophoresis

Glass electrophoresis plates were cleaned with distilled water and ethanol and secured into the casting stands before they were loaded with resolving gel (Table 3.2.4) and allowed to polymerise for ~30 min. After polymerisation of the resolving gel layer, the stacking gel layer (Table 3.2.4) was transferred over the top along with a 10 lane comb and allowed to polymerise for a further 30 min. The gel plates were then transferred into the running chamber and filled with electrophoresis buffer (25 mM Tris-HCl, 192 mM glycine, 0.1% sodium dodecyl sulphate (SDS), pH 8.3).

Table 3.2.4 Resolving and stacking gel formulations (Burnette, 1981).

| Resolving Gel (10 ml – 12% gel) | | Stacking Gel (5 ml – 3.75%) | |
|---|---|---|---|
| 1.5 M Tris HCl | 2.5 ml | 1 M Tris HCl | 1.25 ml |
| Acrylamide 30% | 4.0 ml | Acrylamide 30% | 625 µl |
| Distilled water | 3.29 ml | Distilled water | 2.825 ml |
| 10% SDS | 100 µl | 10% SDS | 50 µl |
| TEMED | 10 µl | TEMED | 3.75 µl |
| 10% APS* | 100 µl | 10% APS* | 250 µl |

*APS is always made up fresh before each experiment and added last during gel formation

Protein aliquots were defrosted and 15 µl of the sample mixed with 15 µl SDS sample loading buffer (62.5 mM Tris-HCl, 2% w/v SDS, 10% glycerol, 50 mM DTT, 0.01% w/v bromophenol blue, pH 6.8). Samples were heated for 10 min at 99°C, followed by loading (20 µl/well – 4 µg/well) into the acrylamide gel along with a lane of (Amersham) full-range rainbow molecular weight markers (5 µl; GE Healthcare Life Sciences, Bucks, UK) with the aid of fine pipette tips. The gel was run at 110 V at 25°C until the dye front reached the bottom of the gel (~1.5 h).

### 3.2.5.3 Gel transfer

After gel electrophoresis and protein separation, the proteins on the acrylamide gel were transferred to a polyvinylidene fluoride (PVDF) blotting membrane for easier handling. Blotting cassettes consisting of filter paper, the acrylamide gel, PVDF membrane and sponge pads were constructed and soaked in blotting buffer (1 L working solution of 25 mM Tris-HCl, 192 mM glycine, 0.02% SDS and 20% methanol at pH 8.3) before transfer into the blotting chamber. After the blotting cassettes were secured and ice block inserted, the chamber was filled with blotting buffer and run at 100 V at 25°C for 1 h.

### 3.2.5.4 Immunodetection of proteins

After transfer, the PVDF membrane was washed with tris-buffered saline (TBS; pH 7.6) for 5 min before incubation with blocking buffer (TBST (TBS with 0.1% Tween-20) with 5% w/v non-fat dry milk) for 1 h with gentle agitation. The membrane was then washed 3 x 5 min with TBST before it was incubated with the primary antibody, rabbit anti-nNOS (1:5000 in TBS-T 5% w/v non-fat dry milk; Millipore, UK), overnight at 4°C with gentle agitation. After overnight incubation, the primary antibody solution was discarded and the membrane washed for 3 x 5 min in TBST. The membrane was then incubated with the secondary antibody, anti-rabbit IgG horseradish peroxidase (HRP)-linked (1:2000 in TBS-T 5% w/v non-fat dry milk; Cell Signaling Technology) in dilution buffer for 2 h at 25°C with gentle agitation. After incubation, the membrane was washed 3 x 5 min with TBST and 1 x 5 min with TBS.

### 3.2.5.5 Enhanced chemiluminescence (ECL)

The proteins on the membrane were detected via ECL, which relies on the conversion of the ECL substrate, i.e. luminol, into a sensitised reagent by the HRP-tethered onto the secondary antibody. This reagent is then further oxidised by hydrogen peroxide into an excited carbonyl which emits light when it decays. The membrane was exposed to a mixture of two ECL kit reagents, reagent A and reagent B (LumiGlo reagent and Peroxide; Cell Signaling Technology, New England Biolabs, UK) for 1 min before excess solution was drained and the membrane wrapped in cling film (ensuring all air bubbles were brushed out) and transferred into a film cassette. In a dark room, the membrane was exposed to photographic film for different time periods, until optimal bands were obtained (not under- or over-exposed), before the film was developed (1-2 min in developer followed by 5 min in fixative and a 15 min water rinse and then allowed to dry). The ladders on the membrane blot were recorded onto the film, the film scanned into the computer and the data analysed with ImageJ analysis software (National Institutes of Health).

### 3.2.5.6 Stripping of antibodies and re-probing of membrane

After ECL and film exposure, the membrane was washed 4 x 5 min in TBST before it was incubated with 50 ml stripping buffer (62.5 mM Tris-HCl at pH 6.8, 2% SDS and 100 mM 2-mercaptoethanol) for 30 min at 50°C. After incubation, the membrane was washed for 6 x 5 min in TBST before the membrane was re-blocked with blocking buffer and reprobed (refer back to 3.2.5.4). Probed Western blots were stripped of antibody, re-blocked, then

re-probed with rabbit anti-GAPDH (1:10000 in TBS-T 5% w/v non-fat dry milk; Abcam, UK) as a control for protein normalisation.

### 3.2.6 Visualising NO using the fluorescent probe: Diaminofluorescein diacetate

Diaminofluorescein diacetate (DAF-2 DA) is a cell permeable fluorescent indicator of NO first synthesised in 1998 (Kojima et al., 1998a). As one of the most widely utilised NO indicators, DAF-2 DA is frequently used to investigate NO levels in live cells (Kojima et al., 1998b) and many derivatives have been synthesised with selective properties. The non-fluorescent DAF-2 is converted into its green-fluorescent triazole derivative, DAF-2T, by an N-nitrosation reaction with oxidised NO ($N_2O_3$), and is thus, an indirect NO indicator (Espey et al., 2001) (Fig. 3.2.1).

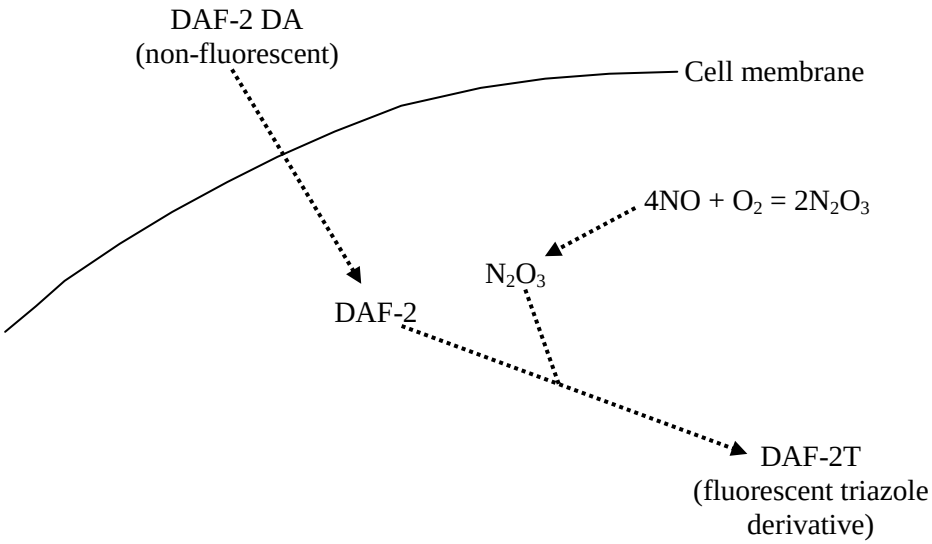


Fig. 3.2.1 Intracellular reactions of the indirect NO indicator, DAF-2 DA. The cell permeable DAF-2 DA traverses the cell membrane into the cell, whereby the diacetate groups are hydrolysed by intracellular esterases, releasing DAF-2. DAF-2 is converted into its fluorescent triazole derivative, DAF-2T, upon reaction with the oxidised form of NO, $N_2O_3$ (Kojima et al., 1998a). In this case, fluorescence intensity depends not only on the production of NO, but also the rate of NO oxidation, a reaction which requires oxygen.

DAF-2-DA is excited at 488 nm and emission is at 515 nm (fluorescein filter). DAF FM DA (Sigma Aldrich, UK), a more photo- and pH-stable variant of DAF-2 DA was used to investigate NO production in response to NPY. DAF FM DA is a more sensitive indicator than the conventional DAF-2 DA, with a NO/ $N_2O_3$ detection limit of 3 nM, compared to 5 nM. A range of DAF FM DA concentrations (0.1-10 µM) were tested and the loading protocol refined and optimised for primary hippocampal cultures.

$NO/N_2O_3$ production was investigated using DAF FM DA in two separate experimental paradigms. The first involved pre-treating cultures under control or NPY conditions for 3 DIV before loading with DAF FM DA and live imaging to determine cellular differences in DAF FM DA fluorescence due to NPY treatment, while in the second paradigm, cells were cultured under control conditions for 3 DIV before loading with DAF FM DA and use of time-lapse imaging to directly visualise the cellular response to a NPY pulse. For both paradigms, hippocampal cells were cultured on 23 x 23 mm photoetched coverslips (BellCo Glass, NJ, USA) in 6-well plates for 3 DIV under control conditions (NBA/B27/Glu and 1% antibiotic/antimycotic) or 1 µM NPY. Plates were loaded with DAF FM DA (5 µM) in phenol red free-NBA/B27 (Life Technologies) for 30 min at 37°C before the cells were rinsed 6 x with sterile PBS to remove the excess. All DAF FM DA loaded cells were imaged in 900 µl PBS under dimmed light conditions to avoid sample bleaching. Imaging was conducted on a Nikon Eclipse E800 Microscope (Nikon UK Ltd., UK) with a 40x water-dipping objective using MetaMorph® analysis software (v6.2; Universal Imaging Corporation, Molecular Devices, USA). In the pre-treated investigation, the NPY group was exposed to 1 µM NPY throughout the whole loading and imaging process to ensure consistency. Pre-treated wells were imaged on a rota of 3 grids/condition until there were at least 12 grids/condition/experiment. Experimental settings and conditions were replicated across 4 independent experiments (Fig. 3.2.2A). The time-lapse investigation involved imaging select cells in DAF FM DA loaded cultures (cultured under control conditions) every 15 s over a time period of 20 min. The first 2 min served as a control period before 100 µl of sterile PBS or 10 µM NPY (final concentration in well) was added. Experimental settings were replicated across 4-5 independent experiments per condition (Fig. 3.2.2B).

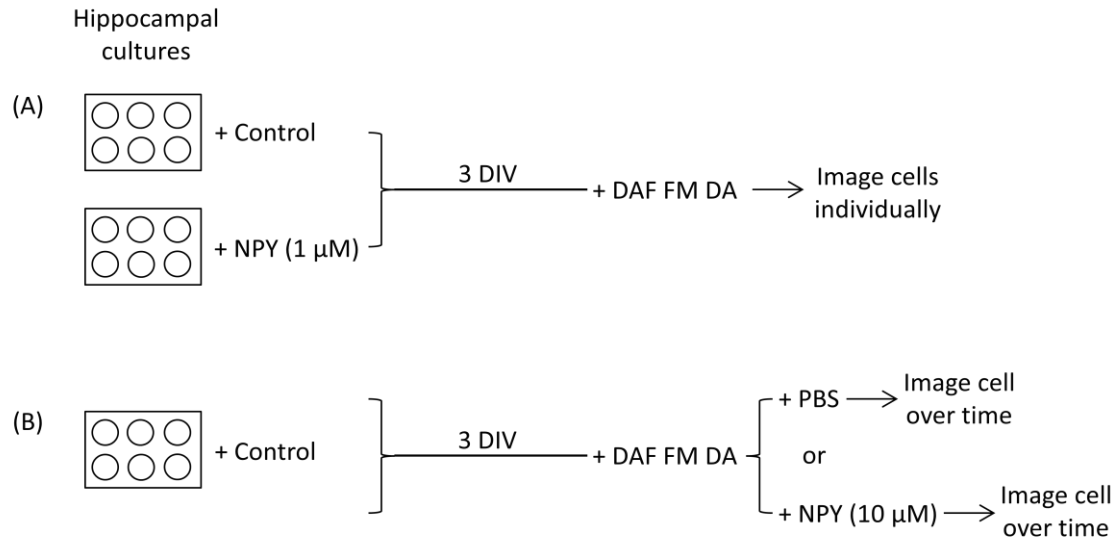


Figure 3.2.2 Visualising $NO/N_2O_3$ in hippocampal cells using diaminofluorescein diacetate (DAF-FM DA). (A) In the first experimental paradigm, cells were pre-treated under control (Neurobasal A/B27/glutamine) or NPY conditions for 3 DIV before loading with DAF FM DA and the imaging of individual cells within each group. (B) In the second experimental paradigm, cells were cultured under control conditions for 3 DIV before loading with DAF FM DA and the use of time-lapse imaging to directly visualise the cellular $NO/N_2O_3$ response to a PBS or NPY pulse.

The short-term NO donor (S)-Nitroso-N-acetylpenicillamine (SNAP; Tocris Bioscience) was used as a positive control for DAF FM DA fluorescence. Imaged cells were fixed in 4% PFA and the cell phenotype ($nestin^+$ or class III $\beta$-$tubulin^+$) identified via immunocytochemistry. The fluorescence intensity of cells was analysed using ImageJ analysis software whereby the average background intensity was subtracted from the cell intensity within each image. Time-lapse data of individual time points was normalised across experiments by plotting data relative to the cell intensity at time point 0 (T0). Linear regression analysis was used to test significance.

### 3.2.7 Galanin-mediated neuroproliferation and NO

To determine whether the proliferative effect of galanin was also mediated through NOS, hippocampal cultures were exposed to control conditions or 100 nM galanin 2-11 (GALR2/3 agonist) (Sigma Aldrich, UK) in the presence of the NOS inhibitor L-NAME (500 µM) or its inactive enantiomer, D-NAME (500 µM). Cultures were exposed for 3 DIV before cell proliferation was assessed on the final day with a 20 µM pulse of BrdU for 6 h before cell fixation, immunocytochemistry, cell imaging, quantification and analysis.

## 3.3 Results

The involvement of NOS and NO mechanisms in mediating the proliferative effect of NPY in postnatal hippocampal cultures were investigated.

### 3.3.1 L-NAME inhibits NPY-mediated neuroproliferation

To investigate the role of NOS and NO in NPY-mediated proliferation, hippocampal cultures were exposed for 3 DIV to 1 μM NPY and 500 μM of the (non subtype-selective) nitric oxide synthase inhibitor L-NAME or inactive enantiomer D-NAME. As expected from previous studies (Chapter 2), NPY induced a significant increase in total cell count ($p<0.05$, $F=16.61$ and $d.f.=83$) (Fig. 3.3.1A), the number of $BrdU^+$ cells ($p<0.05$, $F=14.07$ and $d.f.=83$) (Fig. 3.3.1B), $nestin^+$ precursor cells ($p<0.05$, $F=3.578$ and $d.f.=56$) (Fig. 3.3.1C) and $BrdU^+$ precursor cells ($p<0.05$, $F=11.16$ and $d.f.=56$) (Fig. 3.3.1D). In addition, the proliferation status (mitotic index) of the overall cell population ($p<0.05$, $F=5.754$ and $d.f.=80$) (Fig. 3.3.1E) as well as the mitotic index of the $nestin^+$ precursor cell population ($p<0.05$, $F=2.446$ and $d.f.=56$) (Fig. 3.3.1F) was significantly enhanced by the presence of NPY.

On the other hand, the addition of NPY in the presence of L-NAME reduced the neuroproliferative effects of NPY back down to control levels. Total cell counts were comparable to control levels in the presence of L-NAME ($p>0.05$, $F=16.61$ and $d.f.=83$) (Fig. 3.3.1A), which was also reflected in the number of $BrdU^+$ cells ($p>0.05$, $F=14.07$ and $d.f.=83$) (Fig. 3.3.1B), $nestin^+$ precursor cells ($p>0.05$, $F=3.578$ and $d.f.=56$) (Fig. 3.3.1C) and $BrdU^+$ precursor cells ($p>0.05$, $F=11.16$ and $d.f.=56$) (Fig. 3.3.1D). The mitotic index of both the overall cell population ($p>0.05$, $F=5.754$ and $d.f.=80$) (Fig. 3.3.1E) and of the precursor cell population ($p>0.05$, $F=2.446$ and $d.f.=56$) (Fig. 3.3.1F) was also similarly reduced to control levels. With regards to combined NPY and D-NAME treatment, a significant increase was observed in the total cell count ($p<0.05$, $F=16.61$ and $d.f.=83$) (Fig. 3.3.1A), number of $BrdU^+$ cells ($p<0.05$, $F=14.07$ and $d.f.=83$) (Fig. 3.3.1B) and number of $BrdU^+$ precursor cells ($p<0.05$, $F=11.16$ and $d.f.=56$) (Fig. 3.3.1D), which suggested that the inactive enantiomer had no inhibitory effect on NPY action, thus confirming the specificity of L-NAME in NOS inhibition. The presence of D-NAME, however, reduced the effects of NPY back down to control levels with regards to the number of precursor cells in culture ($p>0.05$, $F=3.578$ and $d.f.=56$) (Fig. 3.3.1C), as well as the mitotic indices of both the overall cell population ($p>0.05$, $F=5.754$ and $d.f.=80$) (Fig.

3.3.1E) and precursor cell population ($p>0.05$, $F=2.446$ and $d.f.=56$) (Fig. 3.3.1F). This suggests that, under certain conditions, D-NAME exerted an inhibitory effect on the enzyme NOS.

### 3.3.2 L-NAME inhibits $Y_1$ receptor-mediated proliferation

The proliferative effect of NPY is mediated via its $Y_1$ receptor (Howell et al., 2003). To confirm the involvement of NOS in mediating the proliferative effect of NPY through the $Y_1$ receptor, primary hippocampal cells were cultured under control and in the presence of the $Y_1$ agonist [F7, P34]NPY (1 μM) and/or 500 μM L-NAME or D-NAME for 3 DIV. The addition of a $Y_1$ agonist significantly increased the total cell count ($p<0.05$, $F=44.74$ and $d.f.=87$) and number of $BrdU^+$ cells ($p<0.05$, $F=21.08$ and $d.f.=86$), which was reduced back down to control levels by the presence of the NOS inhibitor L-NAME (Fig. 3.3.2A and Fig. 3.3.2B, respectively). The inactive enantiomer D-NAME had no inhibitory effect on the significant increase observed on the total cell count ($p<0.05$, $F=44.74$ and $d.f.=87$) and the number of $BrdU^+$ cells ($p<0.05$, $F=21.08$ and $d.f.=86$) in response to NPY treatment (Fig. 3.3.2A and Fig. 3.3.2B, respectively). Similarly, the NPY-mediated increase in the mitotic index of the cell population ($p<0.05$, $F=4.172$ and $d.f.=86$) was reduced to control levels in the presence of L-NAME, while D-NAME had no inhibitory effect on NPY action and the proliferation status remained high ($p<0.05$, $F=4.172$ and $d.f.=86$) (Fig. 3.3.2C). To determine the specificity of effects observed in response to L-NAME and D-NAME treatment in the inhibition of NPY, both compounds were also exposed to cultures individually. L-NAME and D-NAME had no significant effect on basal proliferation rates on their own ($p>0.05$, $F=4.172$ and $d.f.=86$) (Fig. 3.3.2).

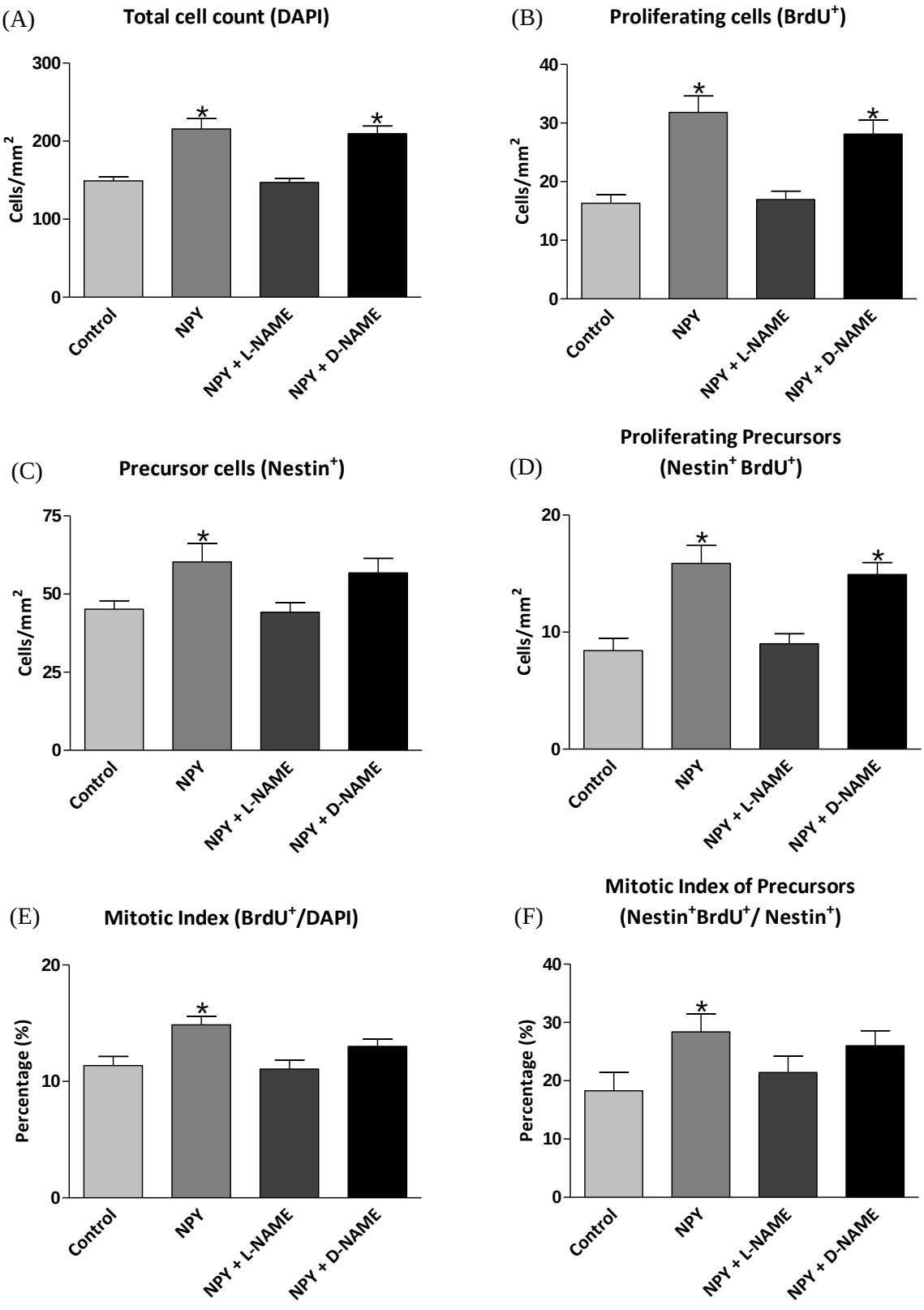


Figure 3.3.1 The neuroproliferative effect of NPY was reduced by L-NAME. Cells were grown under control conditions (NBA-A/B27/glutamine) or 1 μM NPY and 500 μM L-NAME or D-NAME for 3 DIV. BrdU was added for the final 6 h. NPY induced a significant increase in (A) total cell count, (B) $BrdU^+$ cells, (C) $nestin^+$ precursor cells, (D) $BrdU^+$ precursors, (E) overall mitotic index and (F) mitotic index of precursor cells, which was reduced by L-NAME back down

to control levels, but unaffected by the inactive enantiomer D-NAME. Data represent mean ± SEM based on a sample that represents at least 15 wells per condition from three separate experiments. One-way ANOVA with Dunnett's multiple comparison test, compared to control condition. *p < 0.05.

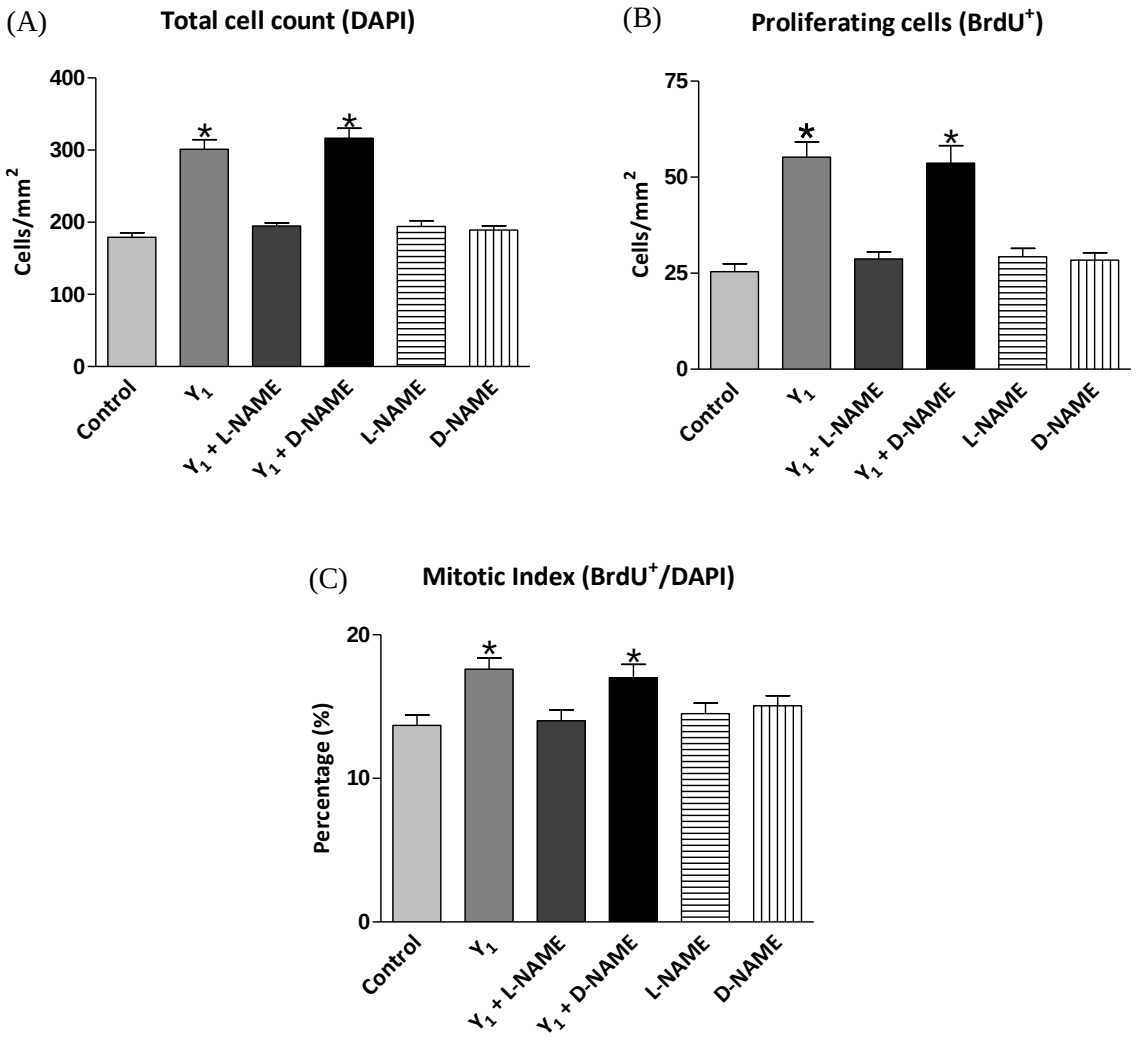


Figure 3.3.2 L-NAME reduced the proliferative effects of the $Y_1$ receptor agonist [F7, P34]NPY. Cells were grown under control conditions (NBA-A/B27/glutamine) or 1 μM [F7, P34]NPY and/or 500 μM L-NAME or D-NAME for 3 DIV. BrdU was added for the final 6 h. The $Y_1$ agonist significantly increased (A) the total cell count, (B) $BrdU^+$ cells and (C) the mitotic index. The addition of L-NAME completely abolished the proliferative effects of the $Y_1$ agonist, while the inactive enantiomer D-NAME had no effect on $Y_1$ agonist action. L-NAME and D-NAME had no effects on basal proliferation rates on their own. Data represent mean ± SEM based on a sample that represents at least 13 wells per condition from four separate experiments. One-way ANOVA with Dunnett's multiple comparison test, compared to control condition. *p < 0.05.

### 3.3.3 L-arginine is proliferative for hippocampal cultures

To analyse the role of endogenous NO in NPY-mediated proliferation, the amino acid L-arginine, which is the substrate for NOS in the synthesis of NO, was exposed to cultures. A significant increase in the total cell count ($p<0.05$, $F=12.09$ and $d.f.=49$) and number of $BrdU^+$ cells ($p<0.05$, $F=32.94$ and $d.f.=49$) was observed in response to L-arginine treatment, while treatment with the inactive enantiomer, D-arginine, had no effect on basal proliferation rates and levels were comparable to control (Fig. 3.3.3A and Fig. 3.3.3B, respectively). Similarly, L-arginine treatment significantly enhanced the mitotic index of the overall cell population compared to control ($p<0.05$, $F=5.622$ and $d.f.=49$) while D-arginine had no effect (Fig. 3.3.3C).

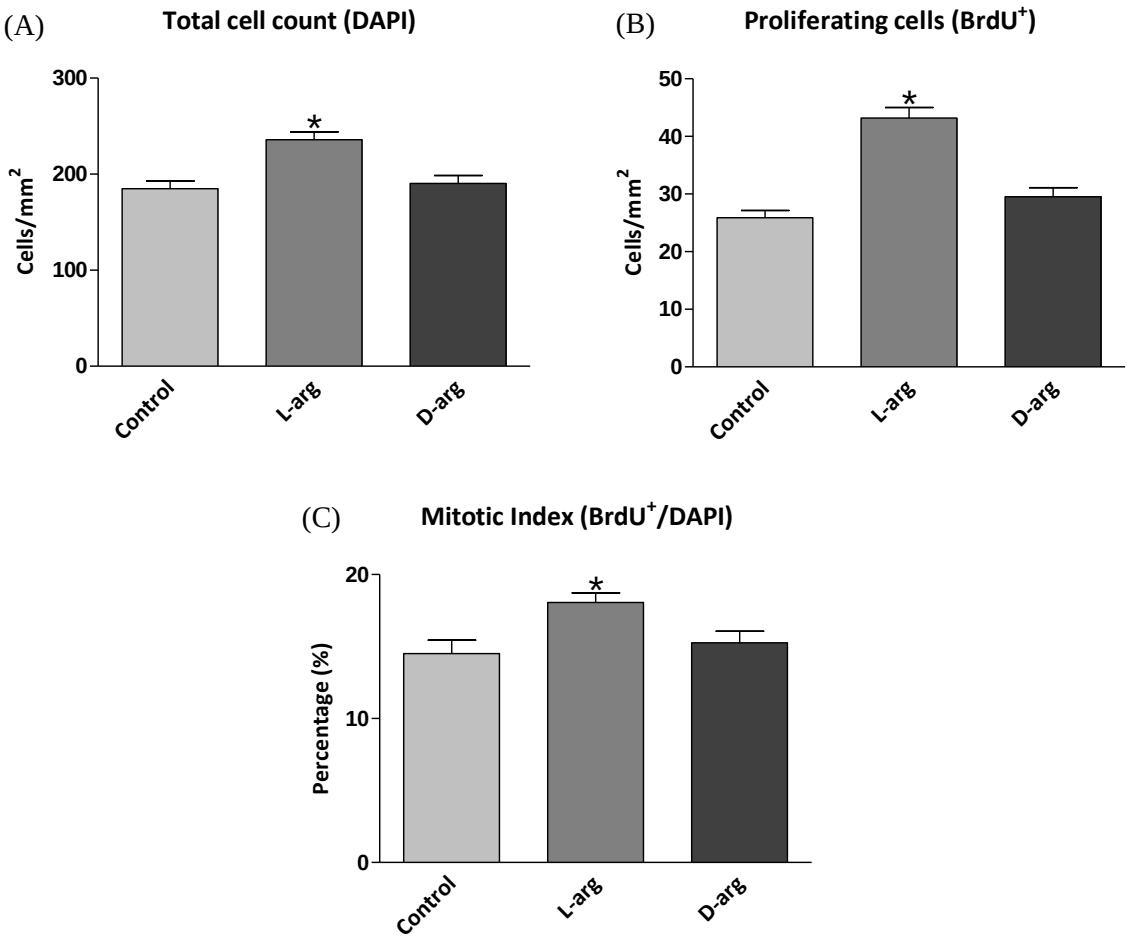


Figure 3.3.3 L-arginine significantly increased the proliferation status of hippocampal cultures. Cells were grown under control conditions (NBA-A/B27/glutamine), 500 μM L-arginine and 500 μM D-arginine for 3 DIV. BrdU was added for the final 6 h. L-arginine significantly increased the (A) total cell count, (B) numbers of $BrdU^+$ proliferating cells and (C) the mitotic index. The inactive enantiomer D-arginine had no effect on total cell count, numbers of $BrdU^+$ cells or basal

proliferation rates. Data represent mean ± SEM based on a sample that represents at least 16 wells per condition from five separate experiments. One-way ANOVA with Dunnett's multiple comparison test, compared to control. *$p < 0.05$.

### 3.3.4 iNOS is not likely involved in mediating the proliferative effect of NPY

Although NOS has previously been shown to mediate the effects of NPY on feeding behaviour (Morley et al, 1999) and retinal neural cell proliferation (Alvaro et al., 2008), no attempts have yet been made to identify the subtype of NOS involved. The proliferation of hippocampal cultures in response to NPY was investigated in the presence of the selective iNOS inhibitor, EITH, and the partial iNOS/nNOS inhibitor, 3B7N. Over three days in culture, the presence of NPY significantly enhanced the total cell count ($p<0.05$, $F=6.138$ and $d.f.=80$) (Fig. 3.3.4A), number of $BrdU^+$ cells ($p<0.05$, $F=10.53$ and $d.f.=80$) (Fig. 3.3.4B) and mitotic index ($p<0.05$, $F=8.054$ and $d.f.=80$) (Fig. 3.3.4C). Similarly, NPY in the presence of EITH also produced a significant increase in the total cell count ($p<0.05$, $F=6.138$ and $d.f.=80$) (Fig. 3.3.4A), number of $BrdU^+$ cells ($p<0.05$, $F=10.53$ and $d.f.=80$) (Fig. 3.3.4B) and mitotic index ($p<0.05$, $F=8.054$ and $d.f.=80$) (Fig. 3.3.4C), reflective of levels induced by NPY alone. EITH did not affect levels of NPY-mediated proliferation, suggesting iNOS was not involved in the signalling process. On the other hand, 3B7N reduced the proliferation mediated by NPY. The total cell count ($p>0.05$, $F=6.138$ and $d.f.=80$) (Fig. 3.3.4A), number of $BrdU^+$ cells ($p>0.05$, $F=10.53$ and $d.f.=80$) (Fig. 3.3.4B) and mitotic index ($p>0.05$, $F=8.054$ and $d.f.=80$) (Fig. 3.3.4C) were comparable to control levels in the presence of NPY and 3B7N. Since the application of EITH indicated that iNOS was probably not involved in the proliferative process, the reduction caused by the application of 3B7N could be attributable to its action on nNOS. On their own, EITH and 3B7N had no effect on basal proliferation rates (Fig. 3.3.4).

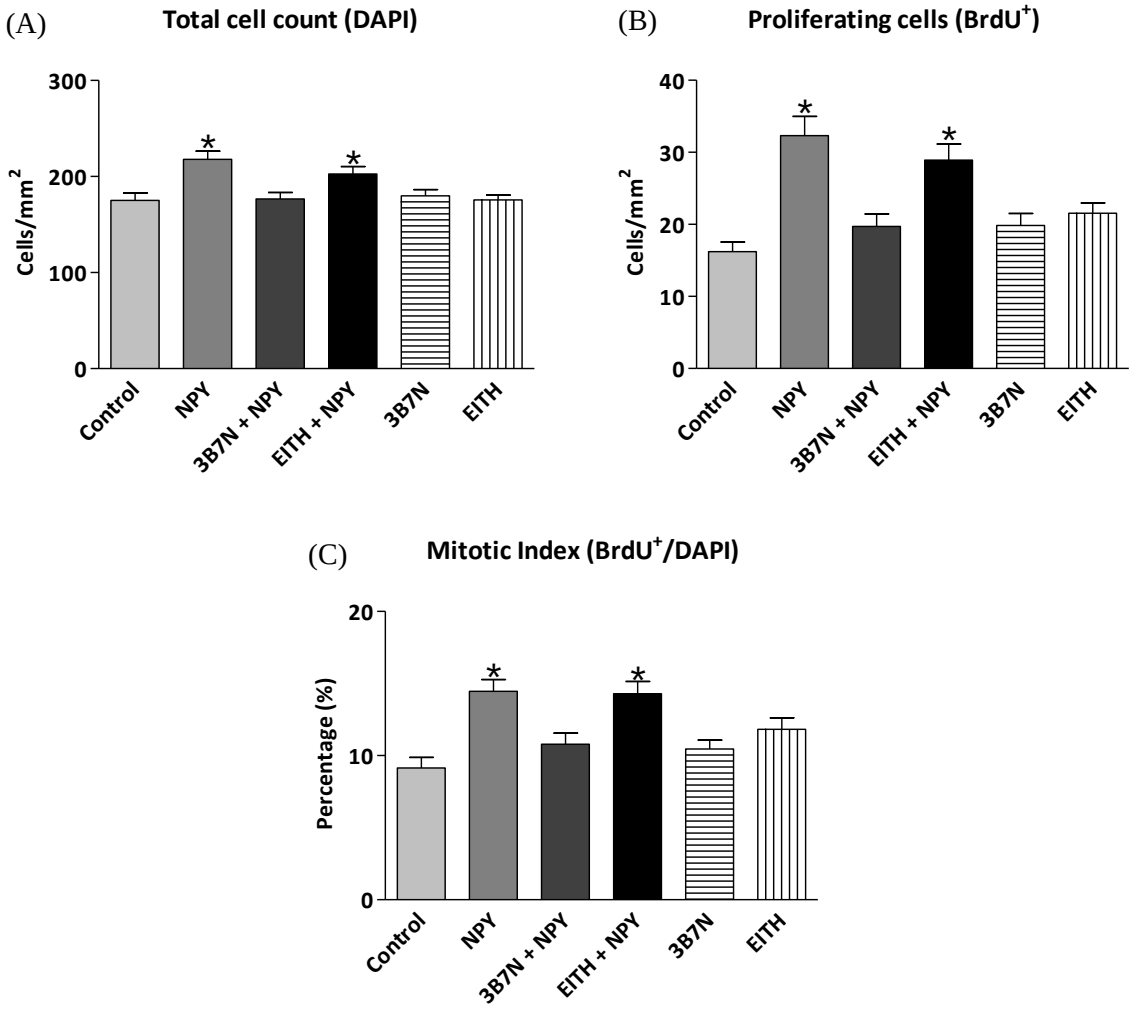


Figure 3.3.4 iNOS is not likely involved in mediating the proliferative effect of NPY. Hippocampal cultures were exposed to control (NBA-A/B27/glutamine), 1 μM NPY and/or 100 nM EITH (selective iNOS inhibitor) or 100 nM 3B7N (partial iNOS/nNOS inhibitor) for 3 DIV. BrdU was added for the final 6 h. NPY significantly increased (A) the total cell count, (B) $BrdU^+$ proliferating cells and (C) mitotic index. The addition of 3B7N reduced the proliferative effect of NPY, while EITH showed no inhibitory effect on NPY action, suggesting only nNOS involvement. EITH and 3B7N had no effects on basal proliferation rates on their own. Data represent mean ± SEM based on a sample that represents at least 13 wells per condition from three separate experiments. One-way ANOVA with Dunnett's multiple comparison test, compared to control condition. *$p < 0.05$.

### 3.3.5 nNOS most likely mediates the proliferative effect of NPY

To further verify the involvement of nNOS, a selective inhibitor of nNOS, AAAN, was added to hippocampal cultures for 6 h in the presence of NPY. NPY induced an increase in total cell count ($p<0.05$, $F=16.86$ and $d.f.=54$) (Fig. 3.3.5A), number of $BrdU^+$ cells ($p<0.05$, $F=14.52$ and $d.f.=54$) (Fig. 3.3.5B) and mitotic index ($p<0.05$, $F=3.404$ and $d.f.=54$) (Fig. 3.3.5C), which was as expected from previous investigations. The presence of AAAN, however, significantly reduced the proliferative effect of NPY. The total cell count ($p>0.05$, $F=16.86$ and $d.f.=54$) (Fig. 3.3.5A), number of $BrdU^+$ cells ($p>0.05$, $F=14.52$ and $d.f.=54$) (Fig. 3.3.5B) and mitotic index ($p>0.05$, $F=3.404$ and $d.f.=54$) (Fig. 3.3.5C) was reduced to levels comparable to control levels, while AAAN exerted no effect on basal proliferation rates on its own (Fig. 3.3.5).

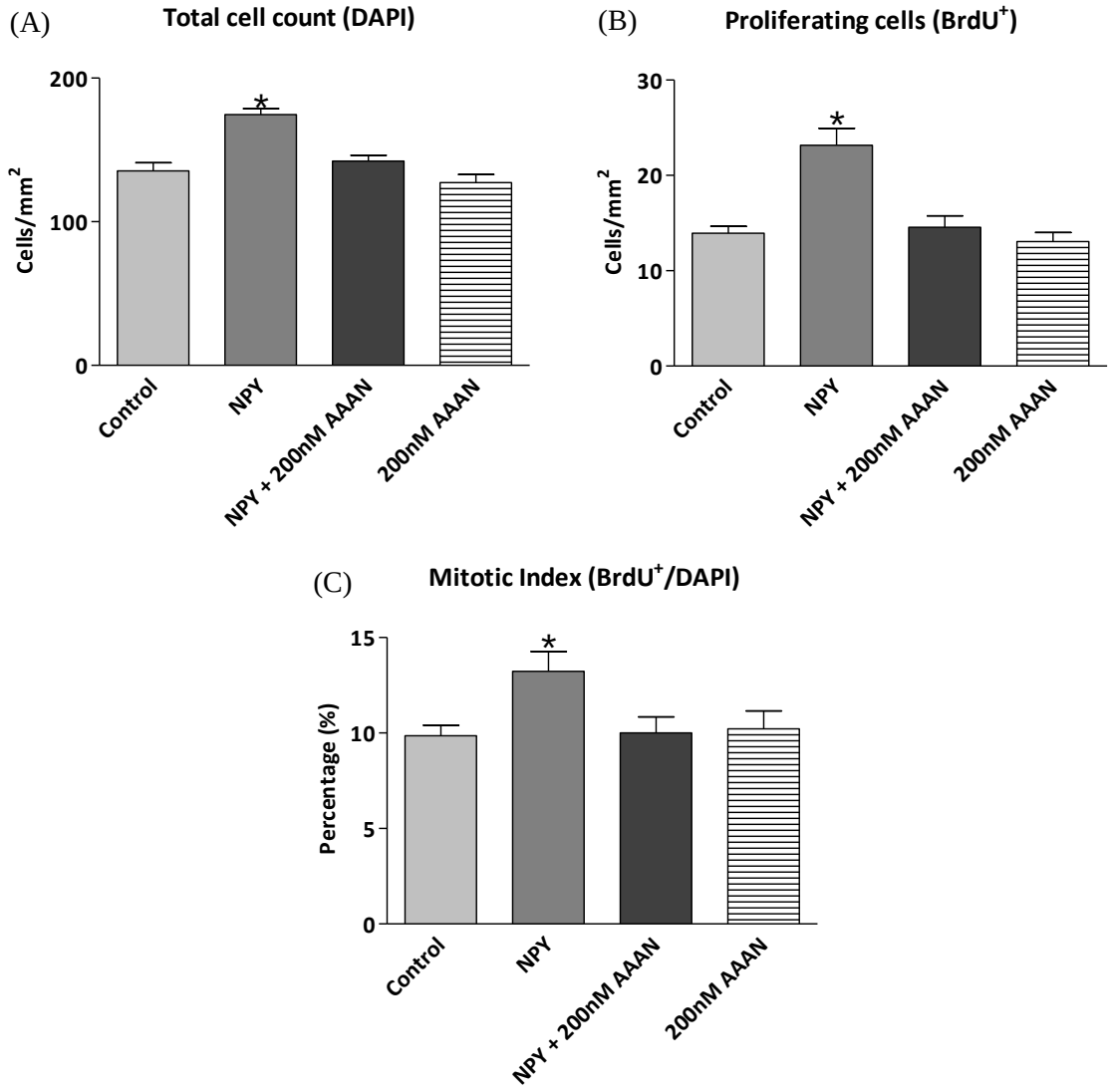


Figure 3.3.5 nNOS most likely mediates the proliferative effect of NPY on hippocampal cultures. Hippocampal cells were cultured under control conditions (NBA-A/B27/glutamine) for 3 DIV, before 1 μM NPY and/or 200 nM AAAN (selective nNOS inhibitor) and BrdU was added for the final 6 h. NPY significantly increased (A) the total cell count, (B) $BrdU^+$ proliferating cells and (C) the mitotic index, which was reduced to control levels by the presence of AAAN. Data represent mean ± SEM based on a sample that represents at least 13 wells per condition from three separate experiments. One-way ANOVA with Dunnett's multiple comparison test, compared to control condition. *$p < 0.05$.

### 3.3.6 nNOS and eNOS are both expressed by precursor cells and neurons

The proliferative effect of NPY is likely to be mediated principally through the nNOS subtype. In the CNS, nNOS expression was previously demonstrated in neurons (Bredt et al., 1990), astrocytes (Arbonés et al. 1996) and neural precursor cells (Wang et al., 1999a; Torroglosa et al., 2007; Luo et al., 2010). To further verify the involvement of nNOS in mediating the proliferative effect of NPY, immunocytochemistry was used to identify the cellular expression of nNOS in hippocampal cultures. Moreover, the involvement of eNOS was also assessed. Specifically, nNOS and eNOS expression was investigated in nestin$^+$ precursor cells and class III β-tubulin (TUJ1)$^+$ neurons, the cell phenotypes previously shown by Howell et al (2003) to be responsive to NPY. A range of nNOS and eNOS antibody dilutions were investigated to determine the optimal concentration for immunostaining. The ratio of immunostaining to background fluorescence was found to be best within the dilution ranges of 1:500-1:1000 for nNOS and 1:250-1:500 for eNOS. Respective immunocytochemical controls were carried out (Table 3.2.3) to ensure that there was no background/antibody autofluorescence or bleed-through, confirming the validity of any staining observed.

Both nNOS and eNOS were expressed in nestin$^+$ precursor cells and class III β-tubulin$^+$ neurons in hippocampal cultures (Fig. 3.3.6). All nestin$^+$ and class III β-tubulin$^+$ cells were immunopositive for nNOS and eNOS. In nestin$^+$ cells, nNOS immunoreactivity was generally evenly distributed across the whole cell, although in some cases, increased immunoreactivity was observed localised to the cell nucleus (Fig. 3.3.6A-C). Similarly, eNOS immunoreactivity in nestin$^+$ cells was mostly localised to the nucleus, while reactivity in the soma was comparatively low (Fig. 3.3.6G-I). nNOS immunoreactivity in class III β-tubulin$^+$ cells was also distributed across the cell, however, immunoreactivity varied, with some cells showing higher nNOS immunoreactivity in the nucleus, while in others nNOS was localised to the soma (Fig. 3.3.6D-F). Clear nNOS staining was also obtained using a 1:1000 dilution of the nNOS antibody. eNOS immunoreactivity in class III β-tubulin$^+$ cells, on the other hand, was distributed evenly across the whole cell (Fig. 3.3.6J-L).

nNOS and eNOS immunocytochemistry was carried out using NOS antibodies raised in rabbit, combined with mouse anti-nestin or mouse anti-TUJ1 antibodies for cell phenotyping. As all nestin$^+$ and class III β-tubulin$^+$ cells were immunopositive for both

nNOS and eNOS, this raised the question as to whether both subtypes were expressed together in the same cells or if this was as a result of non-specific NOS antibody binding to other subtypes. To answer this question a double immunostaining protocol with a rabbit anti-nNOS and mouse anti-eNOS was carried out to verify the expression profiles of each NOS subtype in the same sample. An nNOS and eNOS antibody dilution of 1:500, which is within the optimal immunostaining range of both antibodies, was chosen for consistency. Immunocytochemistry showed the expression of both subtypes in all the cells studied. All $nNOS^+$ cells were found to be also $eNOS^+$, and the distribution similar (Fig. 3.3.7). To further reinforce the immunocytochemical results showing the presence of nNOS in hippocampal cultures, a different method for quantifying protein expression, Western blotting, was used. nNOS expression was identified in all three samples of hippocampal cell lysate analysed (Fig. 3.3.8).

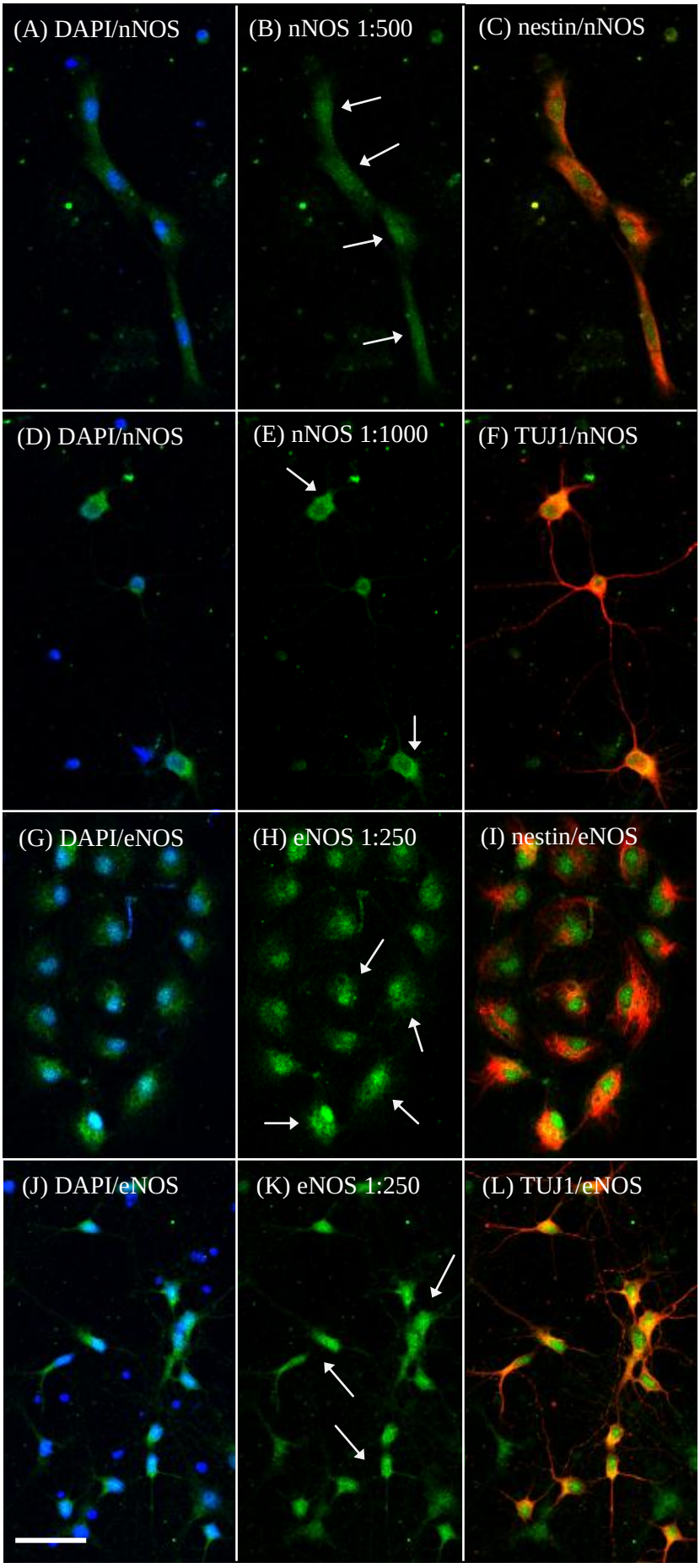
(A) DAPI/nNOS
(B) nNOS 1:500
(C) nestin/nNOS
(D) DAPI/nNOS
(E) nNOS 1:1000
(F) TUJ1/nNOS
(G) DAPI/eNOS
(H) eNOS 1:250
(I) nestin/eNOS
(J) DAPI/eNOS
(K) eNOS 1:250
(L) TUJ1/eNOS

Figure 3.3.6 Both nNOS and eNOS were expressed in nestin$^{+}$ precursor cells and class III β-tubulin (TUJ1)$^{+}$ neurons. nNOS/eNOS (green) and nestin/TUJ1 (red). All nestin$^{+}$ and TUJ1$^{+}$ cells were immunopositive for nNOS and eNOS, although not all cells were nNOS$^{+}$ or eNOS$^{+}$ (see DAPI (blue) staining for all cells). (A-C) nNOS immunoreactivity in nestin$^{+}$ cells was generally evenly distributed across cells, although in some cases increased localisation to the nucleus was observed (arrows). Similarly, (D-F) some TUJ1$^{+}$ cells showed increased nNOS immunoreactivity in the cytoplasm when compared to the nucleus (arrows). The optimal antibody dilution range for nNOS immunostaining was between 1:500-1:1000, as demonstrated in (B; 1:500) and (E; 1:1000), respectively. In the case of eNOS, immunoreactivity in (G-I) nestin$^{+}$ cells was largely localised to the nucleus (arrows), while in (J-L) TUJ1$^{+}$ cells, eNOS was evenly distributed throughout the cell (arrows). The optimal antibody dilution range for eNOS immunostaining was between 1:250-1:500. Scale bar, 25 µm.

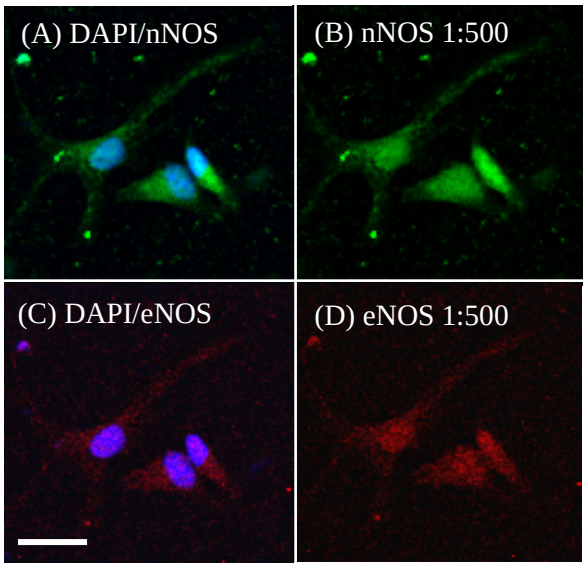


Figure 3.3.7 nNOS and eNOS was expressed within the same cells. A double immunostaining protocol was used to identify the expression profiles of nNOS and eNOS. All (A and B) nNOS$^{+}$ cells (green), were also (C and D) eNOS$^{+}$ (red). The cell nuclei were stained with DAPI (blue). The distribution of nNOS and eNOS was similar. Staining was specific as controls with the nNOS, but without the eNOS, antibody (and vice-versa) showed no staining or bleed-through. Scale bar, 10 µm.

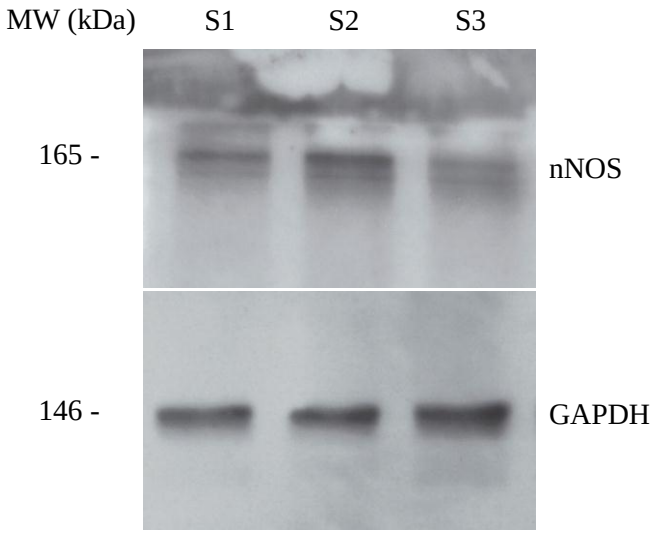


Figure 3.3.8 nNOS expression was identified in hippocampal cell lysate. 3 day old hippocampal cultures were treated with control media (NBA-A/B27/Glu) before cell lysis and Western blotting. Immunoblots were probed with antibodies against nNOS and GAPDH. All three samples (S) showed nNOS expression.

### 3.3.7 DAF FM DA fluorescence suggests increased NO production in response to NPY exposure

To show a correlation between NPY and NO production, the intracellular release of NO in response to NPY was investigated using the fluorescent $NO/N_2O_3$ probe, DAF FM DA, which was combined with live cell imaging. Although some issues have been associated with the commonly used incubation concentration of 10 µM DAF FM DA, which can lead to intracellular DAF accumulation and a high autofluorescence background, thus limiting detection sensitivity (Rodriguez et al., 2005), a range of DAF FM DA concentrations was initially tested in this study before 5 µM was determined as the optimal concentration. A lower concentration of DAF FM DA was suggested by Rodriguez et al. (2005) for reliable measurement of $NO/N_2O_3$. However, low DAF FM DA concentrations tested at 1 µM required a high fluorescence exposure, which increased the risk of bleaching, while no detectable fluorescence was achieved with 0.1 µM even at the highest exposure settings.

As a positive control, the short-term NO donor, SNAP, was exposed to DAF FM DA-loaded hippocampal cultures, whereby a significant increase in cell fluorescence intensity was observed, which continued to increase linearly over the exposure period of 10 min (Linear regression analysis *$p<0.0001$) (Fig. 3.3.9). Cultures were pre-treated under either control or NPY conditions before DAF FM DA fluorescence intensity in the nestin$^+$ and class III β-tubulin$^+$ cell populations was assessed. Hippocampal cells were cultured onto

photoetched glass coverslips so that after DAF FM DA imaging (Fig. 3.3.10A) the respective grid could be relocated after immunocytochemistry for identification of cell phenotypes (Fig. 3.3.10B,C). In both nestin$^+$ and class III β-tubulin$^+$ populations, the NPY pre-treated group showed significantly enhanced DAF FM DA fluorescence compared to the untreated control group (Student's *t*-test, p=0.0003 and p=0.0324 for nestin$^+$ and class III β-tubulin$^+$ cell populations, respectively) (Fig. 3.3.11A,B), indicative of increased $NO/N_2O_3$ production in response to NPY exposure. Similarly, in a second approach, a 10 µM NPY pulse significantly enhanced the DAF FM DA fluorescence intensity of nestin$^+$ and class III β-tubulin$^+$ cells compared to a control pulse of PBS (Linear regression analysis *p<0.0001) (Fig. 3.3.11C-F), which suggests the involvement of NO and its production within the intracellular signalling pathway of NPY. Although a significant linear increase in DAF FM DA fluorescence was also observed in PBS treated cultures in both nestin$^+$ and class III β-tubulin$^+$ cells (Linear regression analysis *p<0.0001) (Fig. 3.3.11C,D), probably as a result of basal $NO/N_2O_3$ generation, the fluorescence increase in NPY-treated cultures was more remarked and still significantly increased after subtracting the respective control traces (Linear regression analysis *p<0.0001) (Fig. 3.3.11E,F).

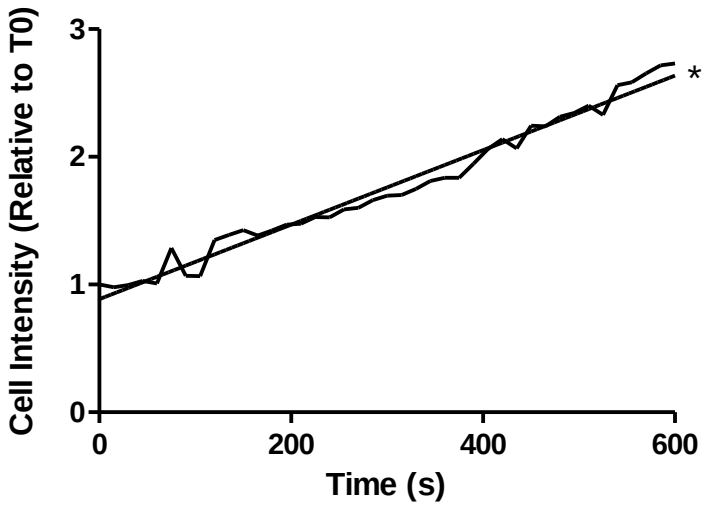


Figure 3.3.9 DAF FM DA fluorescence increased over time in response to the addition of a NO donor. Hippocampal cells were cultured for 3 DIV under control conditions (NBA-A/B27/glutamine) before they were loaded with 5 µM of the $NO/N_2O_3$ probe, DAF FM DA. The NO donor, SNAP, was added to the DAF loaded cells at T0 before imaging, which resulted in a significant linear increase in cell fluorescence intensity over time (Linear regression analysis *p<0.0001).

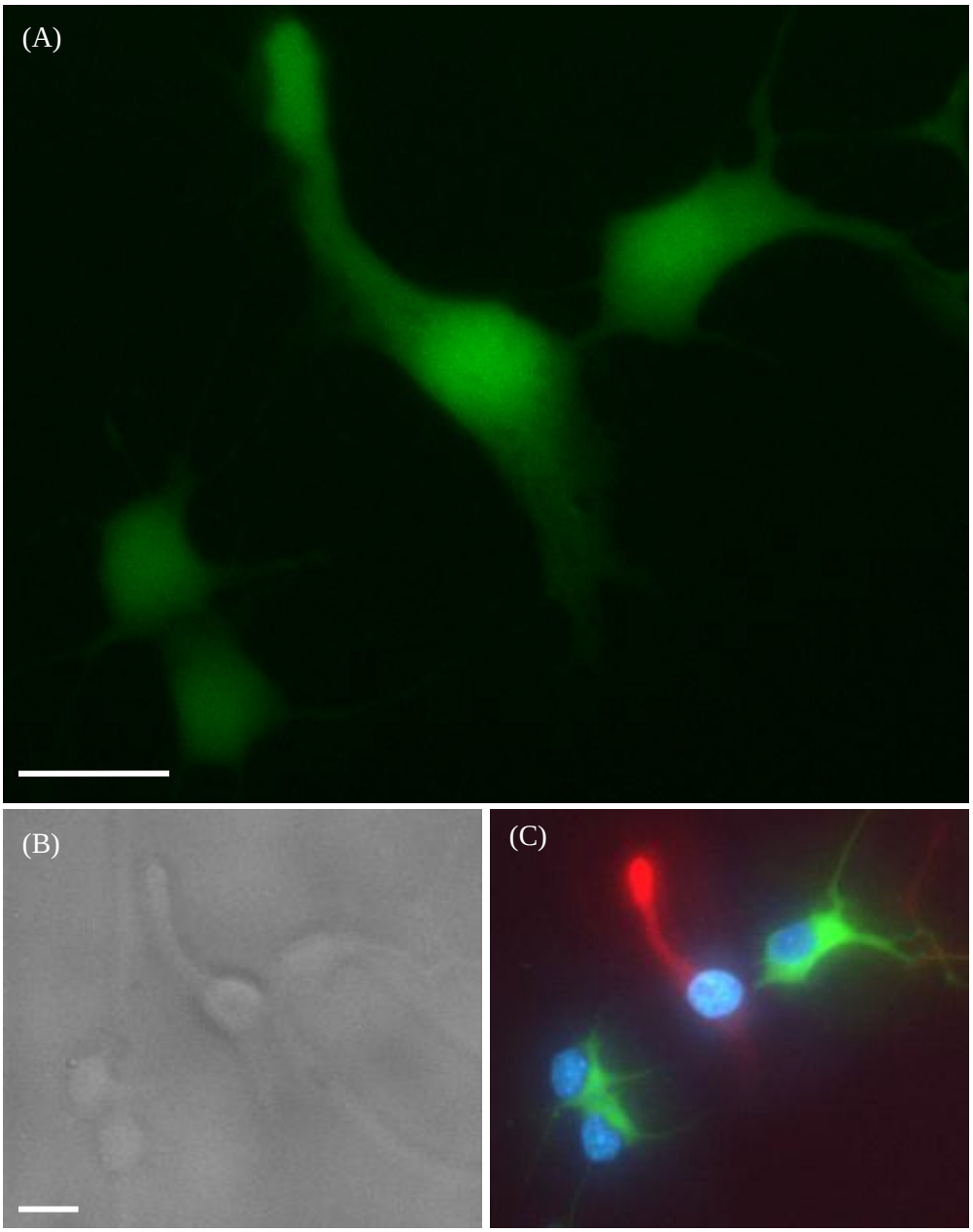


Figure 3.3.10 Identification of cell phenotype was attained through the use of photoetched coverslips. Hippocampal cells were cultured on photoetched glass coverslips so that after (A) DAF FM DA imaging, the cells could be relocated after immunocytochemistry via the photoetched grid under (B) phase imaging, before (C) phenotype identification. Immunocytochemistry was carried out against the precursor cell marker nestin (red), the neuronal marker class III β-tubulin (green) and the cell nuclei were stained with DAPI (blue). Scale bars, 10 μm.

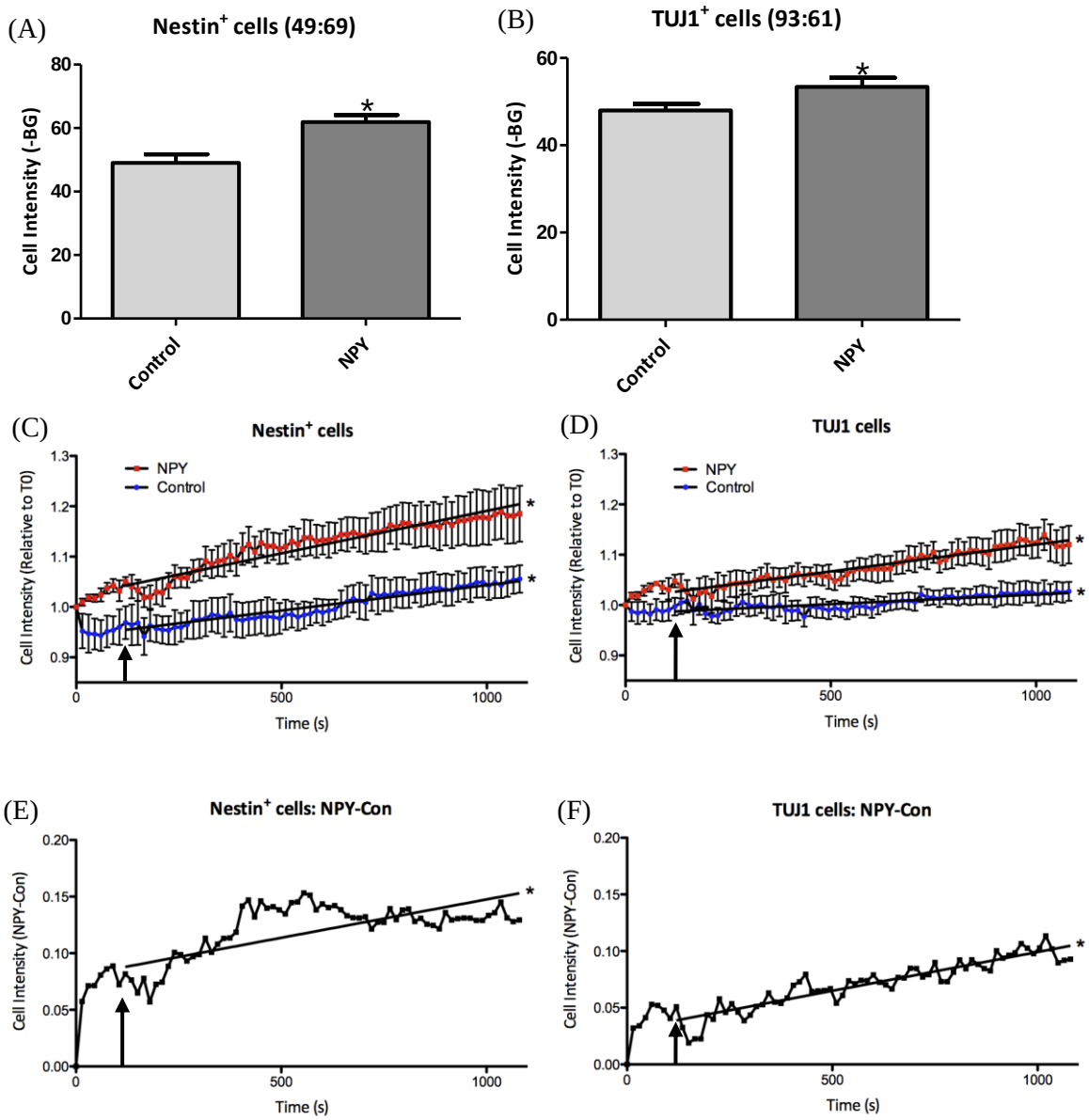


Figure 3.3.11 DAF FM DA fluorescence intensity in cells treated with NPY. Hippocampal cells were cultured under control conditions (NBA-A/B27/glutamine) or 1 μM NPY for 3 DIV before DAF FM DA loading and imaging. NPY pre-treated (A) nestin$^+$ and (B) class III β-tubulin$^+$ (TUJ1$^+$) cell populations showed significantly increased fluorescence intensity compared to control treated cell populations (Student's *t*-test, p=0.0003 and p=0.0324 for nestin$^+$ and class III β-tubulin$^+$ cell populations, respectively). Cultures exposed to a pulse (time point indicated with arrows) of NPY or PBS under time-lapse studies showed a linear increase in DAF FM DA fluorescence over time, irrespective of the treatment condition, in both (C) nestin$^+$ and (D) class III β-tubulin$^+$ cells (Linear regression analysis *p<0.0001). The NPY pulsed cells, however, showed a significantly higher cell fluorescence intensity compared to the control pulse in both cell types (Linear regression analysis, test for slope difference*p<0.0001). Subtraction of the control trace from the NPY trace for (E) nestin$^+$ and (F) class III β-tubulin$^+$ cells also showed a significant linear increase

in cell fluorescence in response to NPY treatment (Linear regression analysis *$p<0.0001$). Experimental settings and conditions were replicated across 4-5 independent experiments for both the pre-treated culture and the time-lapse investigations.

### 3.3.8 NOS is not required for mediating the proliferative effect of galanin

Is signalling through NO-dependent mechanisms specific to NPY or do other proliferative neuropeptides also act via a similar pathway? To clarify this question, galanin, a neuropeptide which elicits proliferative effects similar to that of NPY, was added to cultures and the role of the NOS inhibitor L-NAME and its inactive enantiomer D-NAME assessed. Galanin induced a significant increase in the total cell count ($p<0.05$, $F=9.792$ and $d.f.=59$) and $BrdU^+$ cell number ($p<0.05$, $F=6.180$ and $d.f.=59$), which was unaffected by the presence of L-NAME or D-NAME ($p>0.05$, $F=9.792$ and $d.f.=59$ for total cell counts and $p>0.05$, $F=6.180$ and $d.f.=59$ for $BrdU^+$ cells) (Fig. 3.3.12A and Fig. 3.3.12B, respectively). In the case of the mitotic index, a small but significant increase in the mitotic index was observed with respect to galanin treatment in the presence of L-NAME ($p<0.05$, $F=2.953$ and $d.f.=59$) (Fig. 3.3.12C). The inhibition of NOS had no effect on galanin action.

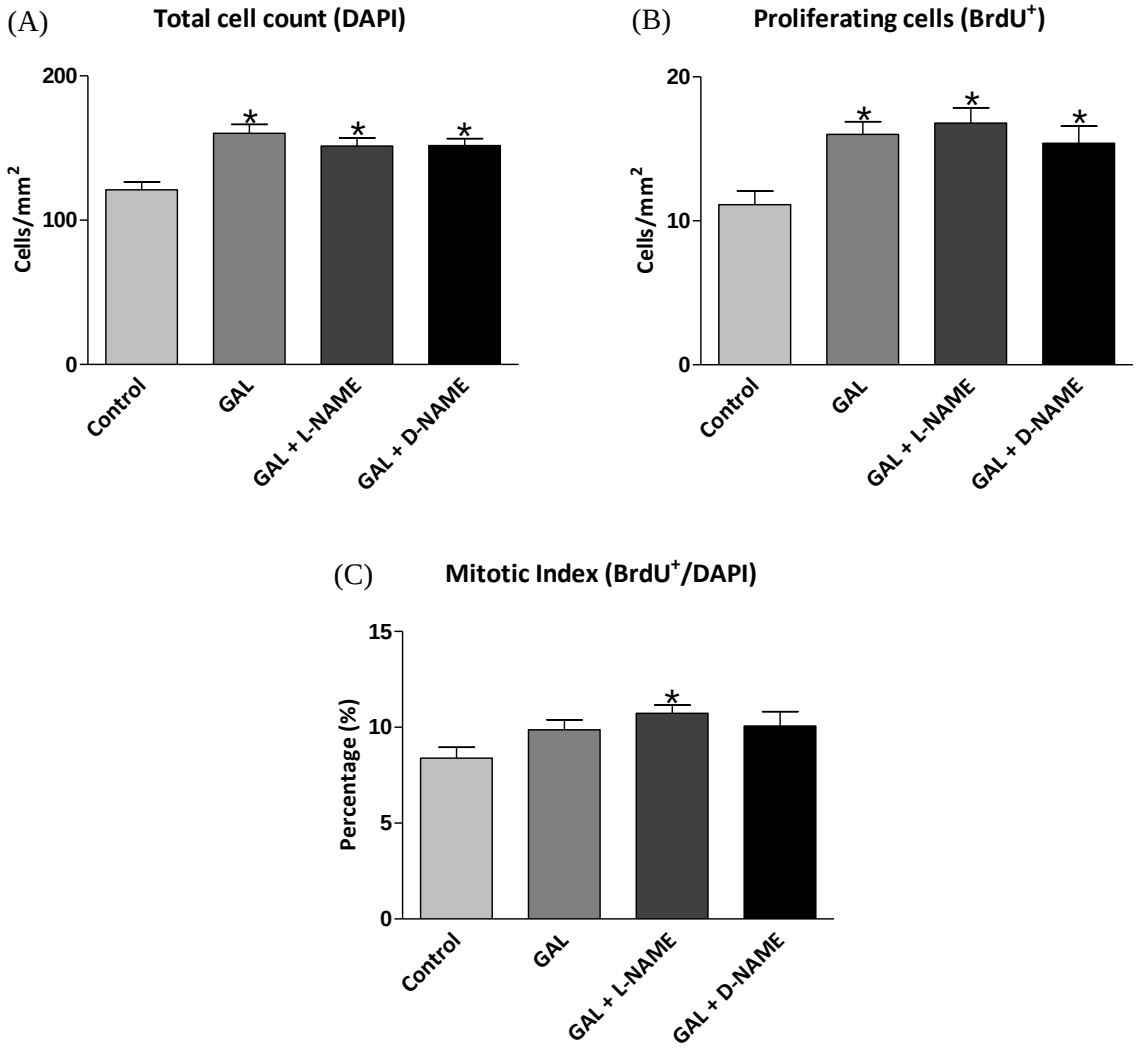


Figure 3.3.12 NOS is not required for mediating the proliferative effect of galanin. Cells were cultured under control conditions (NBA-A/B27/glutamine) or 100 nM galanin in the presence of 500 µM L-NAME or D-NAME for 3 DIV. BrdU was added for the final 6 h. Galanin increased (A) the total cell count and (B) the number of $BrdU^+$ cells, which were unaffected by the presence of L-NAME or D-NAME. Galanin induced a significant increase in (C) the mitotic index in the presence of L-NAME, but not on its own or in the presence of D-NAME. Data represent mean ± SEM based on a sample that represents at least 15 wells per condition from four separate experiments. One-way ANOVA with Dunnett's multiple comparison test, compared to control condition. *$p < 0.05$.

## 3.4 Discussion

The involvement of NOS and NO in the signalling pathway underlying the neuroproliferative effect of NPY was investigated using pharmacological, immunocytochemical and live cell imaging techniques. To my knowledge, this is the first time that these signalling mechanisms underlying the neuroproliferative effect of NPY on cultures from the postnatal rat hippocampus have been extensively explored.

### 3.4.1 The neuroproliferative effect of NPY is mediated via NO

Through the use of selective pharmacological agents, the involvement of NOS and NO in mediating the neuroproliferative effect of NPY was demonstrated in postnatal hippocampal cultures. NPY-mediated neuroproliferation was reduced to control levels through the inhibition of NOS, the NO-synthesising enzyme, using the inhibitor L-NAME. As well as an inhibition of the overall proliferation rates of the total cell population (mitotic index), the proliferation status of the nestin$^{+}$ precursor cell population was also reduced. On the other hand, the inactive enantiomer of L-NAME, D-NAME, had no significant inhibitory effect on proliferation rates and both compounds had no effects on basal proliferation rates on their own. In some instances, however, such as under combined NPY and D-NAME treatment, NPY-mediated proliferation could not reach NPY-only levels, suggesting D-NAME had a slight inhibitory effect. This observation could be explained by the presence of impure batches of the inactive D-NAME enantiomer, which may contain minute proportions of the active L-NAME analogue. The supplementation of cultures with the precursor for NO synthesis, the amino acid L-arginine, significantly enhanced proliferation rates, further suggesting the involvement of NOS and NO. The fact that the inactive enantiomer, D-arginine, had no effect on proliferation rates demonstrates the specificity of this system for L-arginine. What must be noted, however, is that Neurobasal A medium already contains around 398 µM L-arginine (Media Formulation, Life Technologies, UK), which means that, with an apparent $K_m$ value of ~8.4 µM of nNOS for L-arginine (Todoroki et al., 1998), nNOS activity should already be saturated in culture even without additional L-arginine supplementation. Even so, 500 µM L-arginine supplementation had a clear proliferative effect on hippocampal cultures, which may have been because the amount of L-arginine already present in the culture medium was not sufficient to support maximal nNOS activity over the full course of 3 days in culture without extra addition. For example, the relatively high hippocampal expression of the enzyme arginase, which metabolises L-arginine into L-ornithine and urea, may possibly contribute to the depletion

of L-arginine in culture (Liu et al., 2003). One way of clarifying this would be to quantify levels of L-arginine and/or L-ornithine in hippocampal culture over time, possibly via high-performance liquid chromatography (Volke et al., 2006).

The neuroproliferative effect of NPY is mediated via its $Y_1$ receptor (Howell et al., 2003, Alvaro et al., 2008). The link between $Y_1$ receptor activation and subsequent activation of NOS was confirmed by the inhibition of $Y_1$ receptor agonist, [F7, P34]NPY, -mediated proliferation of hippocampal cells by L-NAME. L-NAME significantly blocked the proliferative effects of the $Y_1$ agonist while D-NAME had no significant effect, thus confirming the relationship between the $Y_1$ receptor, NOS and proliferation.

### 3.4.2 The nNOS isoform of NOS most likely mediates the proliferative effect of NPY and is expressed in precursor cells and neurons

Through the use of subtype-selective antagonists, nNOS was identified as the most likely NOS subtype responsible for mediating the proliferative effect of NPY. Although earlier studies have demonstrated the importance of NOS in mediating NPY's effect (Morley et al., 1999; Alvaro et al., 2008), no study had attempted to identify the NOS subtype involved. It was important to identify the NOS subtype because the subtype and its localisation significantly influences the physiological effects of NO. While we knew nothing of the NOS subtype in the hippocampus, Cordelier et al. (1999) showed in Chinese hamster ovary (CHO) cells that nNOS plays a role in proliferation. They showed that the cholecystokinin A receptor, a GPCR similar to the NPY $Y_1$ receptor, activated nNOS via the G-protein $\beta\gamma$ subunit and the tyrosine phosphatase SHP-2 in the cholecystokinin-mediated proliferation of CHO cells. While Cordelier et al. (1999) demonstrated the importance of the nNOS subtype in mediating proliferative pathways, the proliferative agent and cell type studied were different. The present study is the first time that the NOS subtype responsible for mediating the proliferative effect of NPY on postnatal rat hippocampal cultures has been explored.

The possible role of nNOS in mediating proliferative effects was further investigated through immunocytochemistry. Although pharmacological studies eliminated the direct involvement of iNOS, the involvement of eNOS could not be ascertained due to a lack of selective inhibitors. Pharmacological studies, however, showed that the proliferative effect of NPY was completely reduced to control levels in the presence of the nNOS inhibitor,

AAAN, which suggests that only nNOS was involved. If eNOS was also involved, AAAN may not have been able to fully reduce NPY's effects. To provide evidence for the role of nNOS, as well as eNOS, immunocytochemistry was carried out to analyse their expression profiles. Both nNOS and eNOS were expressed in all nestin$^{+}$ and class III β-tubulin$^{+}$ cells. As Howell et al. (2003) demonstrated previously, NPY exerts its proliferative effect on nestin$^{+}$ and class III β-tubulin$^{+}$ cells in rat hippocampal cultures. In addition, my own study has also confirmed the proliferative effect of NPY on nestin$^{+}$ precursor cells and the importance of NOS in mediating this effect. The distribution of both nNOS and eNOS varied widely within cells, although double immunostaining showed that all nNOS$^{+}$ cells were also eNOS$^{+}$. As well as the same expression profile, the distribution of both nNOS and eNOS within cells were identical, which could be either as a result of co-expression, or more likely, lack of antibody specificity to a select NOS subtype. The antibodies supposedly react specifically to subtype selective immunogens, such as the N-terminus of nNOS in the case of the nNOS-selective antibody, and for the eNOS-selective antibody, the C-terminus of eNOS. Although eNOS expression had previously been shown in hippocampal pyramidal cells (Dinerman et al., 1994) and precursor cells (Wang et al., 1999a), it is mainly associated with the brain vasculature (Dinerman et al., 1994; Seidel et al., 1997) and it is unlikely that both nNOS and eNOS immunoreactivity would be exactly the same. Most probably, the 57% homology between the nNOS and eNOS isoforms (Alderton et al., 2001) resulted in some non-specific reactions of either the nNOS antibody with eNOS, the eNOS antibody with nNOS, or both. Although the involvement of eNOS could not be ruled out, the pharmacological results appear to support the contribution of nNOS in mediating the proliferative effect of NPY.

Using the same nNOS antibody, Luo et al. (2010) showed in their investigations that nNOS expression was localised to the nucleus in neural stem cells, while in neurons, nNOS was localised to the cytoplasm. This nNOS distribution pattern was also present in a number of cells in the immunocytochemistry carried out in this study and may be an important regulator of the effects of NO. I also demonstrated nNOS expression in hippocampal cultures using a different method for examining protein expression, Western blotting, but unfortunately, did not have time to repeat this using the eNOS antibody. Indeed, the demonstration by Islam et al. (2003) that nNOS was localised to sites of neuronal proliferation and migration in the hippocampal dentate gyrus provides a

morphological basis which supports the involvement of only nNOS in mediating the effect of NPY.

### 3.4.3 DAF FM DA fluorescence indicates increased NO production in response to NPY exposure

DAF FM DA-loaded nestin$^+$ precursor cells and class III β-tubulin$^+$ neurons, which had either been pre-treated with or exposed to a pulse of NPY, showed significantly enhanced DAF FM DA fluorescence intensity compared to control (PBS)-treated cells, suggesting a link between NPY and NO production. Although the hippocampal cells were already DAF FM DA fluorescent before the NPY or PBS pulse, indicative of basal NO/$N_2O_3$ production, it is unlikely that this background NO was involved in mediating proliferative processes as the pharmacological control investigations with only L-NAME had no effect on cell proliferation. This background NO is probably involved in mediating other cellular processes. Indeed, it would have been interesting to see whether DAF-FM DA fluorescence would be completely eliminated by the prior incubation of tissue samples with the NOS inhibitor L-NAME, but unfortunately, due to time constraints, I was unable to investigate this further.

A plethora of fluorescent NO indicators exist, ranging from the o-Phenylenediamines to metal-based and genetically encoded fluorescent indicators for NO (Ye et al., 2008). The probe used within this study, DAF FM DA, falls into the diaminofluorescein (DAF) subgroup of the o-Phenylenediamine NO indicators. The DAFs are extremely sensitive NO/$N_2O_3$ probes, with DAF FM DA having an NO/$N_2O_3$ detection limit of 3 nM (Ye et al., 2008). Although they do not react with NO directly, the use of fluorescence microscopy combined with fluorescent indicators such as DAF FM DA provides a relatively simple method for estimating levels of NO production in single cells (Schuppe et al., 2002). These probes, however, are not without their limitations. The formation of $N_2O_3$, for example, is simple in air-equilibrated culture media containing NO, however, due to the high reactivity of the $NO_2$ precursor with antioxidants, biological $N_2O_3$ formation is slow and inefficient, suggesting that the reaction of DAF FM DA with $N_2O_3$ is unlikely (Wardman, 2007). Instead, it is more probable that the fluorescent triazole derivative is formed as a result of a two stage reaction which first involves the oxidation of DAF to an intermediate DAF radical, before the subsequent addition of NO. This means that any event or reagent which interferes with DAF radical formation, such as oxidants,

antioxidants (ascorbate) (Zhang et al., 2002), and even exposure to light (Broillet et al., 2001), will ultimately affect DAF fluorescence, regardless of fluctuations in NO levels (Wardman, 2007). Although widely utilised for quantifying NO levels, the susceptibility of DAF probes to diverse environmental factors must be considered when interpreting experimental DAF fluorescence levels. Nevertheless, the quantification of NO in live cells is difficult, and even attempts at direct NO measurement using electrochemical microelectrodes (Shibuki, 1990) are not without their problems, with one being the huge variability in NO concentrations obtained by different groups (Hall & Garthwaite, 2009). Indeed, recent progress in the development of more sensitive techniques for the detection of NO levels has been the creation of NO detector cells expressing sGC and phosphodiesterase-5 (Wood et al., 2011). These NO detector cells were able to sensitively monitor NO release from brain tissue slices and detected NO concentrations down in the pM range. The further development of techniques such as these will allow more physiologically representative concentrations of NO to be detected and measured (Wood et al., 2011).

### 3.4.4 The proliferative effect of galanin is not mediated through NOS

Of the three galanin receptors (GALR1, GALR2 and GALR3), only GALR1 and GALR2 activate the MAPK pathway and GALR2/3 is responsible for the proliferative effect of galanin (Hobson et al., 2008; Abbosh et al., 2011). In the present study, galanin exerted a neuroproliferative effect similar to that of NPY, but did not require NOS to mediate its proliferative effect. The selective activation of the GALR2/3 receptor with the GALR2/3 agonist (galanin 2-11) significantly enhanced the proliferation of hippocampal cultures, which was not reduced through NOS inhibition. Other studies have shown that GALR2 activation leads to the stimulation of phospholipase C via $G_q/11$, resulting in calcium mobilisation, diacylglycerol formation and protein kinase C activation (Wang et al., 1998). The activation of NOS and NO mechanisms may not be a universal signalling mechanism in mediating the proliferative action of neuropeptides other than NPY, although, on another note, NOS/NO may be involved in mediating their other neurophysiological effects. For example, the binding of galanin to the N-methyl-D-aspartate receptor activates a NOS-NO-cGMP pathway in the ventral hippocampus *in vivo* which may be important in memory processes (Consolo et al., 1998).

### 3.4.5 The differential roles of NOS isoforms in adult neurogenesis

Pharmacological studies have shown that NO initiates both neuroinhibitory and neuroproliferative effects on adult neurogenesis (Cardenas et al., 2005). These contradictory effects of NO can be explained by the existence of the different NOS subtypes, which provided the basis for the subtype investigations covered in this chapter. To further evaluate the precise role in which NO and the subtypes of NOS confer on neurogenesis, the existing literature must be considered. *In vivo* studies using NOS isoform-specific knockout mice to identify the contributions by each NOS to adult neurogenesis offer higher specificity compared to using subtype-selective pharmacological inhibitors, which can be relatively non-specific, especially in the case of the eNOS inhibitors. In general, most studies suggest an inhibitory role for NO derived from nNOS, although the cellular mechanisms underlying this are not well understood. Packer et al. (2003), for example, showed that the number of $BrdU^+$ cells was significantly increased in the neurogenic regions (olfactory subependyma and dentate gyrus) of the adult nNOS knockout mouse brain, implying that the endogenous action of nNOS negatively regulates adult neurogenesis. Similarly, Sun et al. (2005) showed that nNOS knockout mice showed reduced infarct size in response to transient focal cerebral ischemia and increased neurogenesis under both basal and ischemia-induced conditions, while Zhou et al. (2007) found that nNOS-derived NO contributes to chronic stress-induced depression by suppressing levels of hippocampal neurogenesis. On the other hand, proliferative roles have been shown by the eNOS and iNOS isoforms, which seem to be involved in promoting adult neurogenesis under basal and ischemic conditions, respectively. eNOS-deficient mice show a significant reduction in basal neuronal progenitor cell proliferation in the dentate gyrus (Reif et al., 2004), while ischemia-induced, but not basal, neurogenesis was significantly reduced in iNOS knockout rodents (Zhu et al., 2003).

The present study has identified the nNOS isoform as the most probable mediator of the neuroproliferative effect of NPY, which, considering the inhibitory role of nNOS on neurogenesis suggested in the literature, is contradictory to the well-established proliferative effect of NPY on neurogenesis. NO mechanisms, however, are highly complex and still need further investigation. It would be simplistic to assume that nNOS-derived NO can only be inhibitory in adult neurogenesis. The cell type, cell source, reactive status, timing of synthesis and concentration are major determinants of NO's effects (Cardenas et al., 2005). As suggested by Cardenas et al. (2005), while low levels

and early synthesis of NO, such as by eNOS, may be beneficial through a local vasodilatatory effect, high and sustained levels of NO production by nNOS, for example, may be neurotoxic by contributing to oxidative stress. In fact, Park et al. (2003) also demonstrated that only chronic (15 days), and not acute, NOS inhibition had a stimulatory effect on neuronal stem cell proliferation.

### 3.4.6 Conclusion

I have shown, for the first time, that NOS and NO play an important role in mediating the proliferative effect of NPY on hippocampal cultures, especially on the nestin$^{+}$ precursor cell population. nNOS was identified as the most likely subtype involved, while live cell imaging using the NO/$N_2O_3$ indicator, DAF FM DA, suggests a link between NPY and increased NO production. Although NO mechanisms have been identified as a mediator of NPY, how do these processes translate to cell proliferation? The next chapter focuses on deciphering the NPY-mediated signalling mechanisms downstream of NOS leading to cell proliferation.

# Chapter 4

## Chapter 4 – Coupling NO mechanisms to cell proliferation

### 4.1 Introduction

I have shown that the proliferative effect of NPY is most likely mediated through the nNOS subtype and that $NO/N_2O_3$ production significantly increased in response to NPY addition in hippocampal cells. Although I have identified NOS and NO as mediators of the proliferative effect of NPY, our knowledge of the underlying signalling pathways are incomplete. To understand how NOS activation and NO synthesis may lead to an increase in cell proliferation, the signalling pathway of NPY was further investigated in hippocampal cultures.

#### 4.1.1 Signalling mechanisms of the NPY receptors

The expression patterns of the NPY Y receptors ($Y_1$, $Y_2$, $Y_4$, $Y_5$ and $Y_6$) are tissue-specific, unlike the ubiquitous expression of NPY, which probably accounts for its varied physiological effects (Gehlert, 2004). The Y receptors show preferential coupling to the G-proteins of the $G_i/G_o$ class (Michel et al., 1998), which are inhibited by pertussis toxin (PTX) and show their own distinct response patterns (Gilman, 1987). The $G_i$ pathway is mediated by its βγ-subunit and is dependent on phosphatidylinositol 3-kinase (PI3K) activity, while being independent of protein kinase C (PKC) (Wettschureck & Offermanns, 2005). A common target of the activated $G_i$ subunit is adenylate cyclase, which it inhibits from producing the second messenger cAMP from ATP (Limbird, 1988). On the other hand, the $G_o$ pathway is mediated by its α-subunit and is dependent on the activity of PKC (Wettschureck & Offermanns, 2005). After activation of the G-proteins by NPY, signalling responses are restricted to tissue and cell type, with targets ranging from the regulation of $Ca^{2+}$ or $K^+$ channels and $Ca^{2+}$ release from intracellular stores (Herzog et al., 1992), to the control of cell proliferation and differentiation (Michel et al., 1998).

#### 4.1.2 NPY coupling to the ERK 1/2

The ERK 1/2 are a group of mitogen-activated protein kinases (MAPK) which are activated via multistep protein kinase cascades by phosphorylation (Alvaro et al., 2008; Lopez-Ilasaca, 1998). In turn, the ERK 1/2 are involved in mediating intracellular signals which regulate the expression of genes controlling cell proliferation and differentiation (Cano & Mahadevan, 1995). Studies have shown that the neuroproliferative effect of NPY, acting through the NPY $Y_1$ receptor, is eliminated by the addition of an ERK 1/2 inhibitor, U0126. ERK 1/2 phosphorylation has been shown to be involved in the intracellular mechanisms underlying NPY-mediated neuroproliferation in neuroblasts from the

olfactory epithelium (Hansel et al., 2001), hippocampal precursor cells from the dentate gyrus (Howell et al., 2005), retinal neural cells (Alvaro et al., 2008) and SVZ stem cells (Agasse et al., 2008).

NPY receptor activation ($Y_1$, $Y_2$, $Y_4$ or $Y_5$) leads to the activation of ERK 1/2 by a PTX-sensitive mechanism i.e. through the involvement of the $G_i/G_o$ G proteins, in CHO cells (Mullins et al., 2002). However, while the NPY $Y_5$ receptor seems to rely on PI3K and PKC for signalling in CHO cells, $Y_1$, $Y_2$ and $Y_4$ act through a PKC- independent mechanism (Mullins et al., 2002). Mullins et al. (2002) suggest that the NPY $Y_5$ receptor couple to $G_i/G_o$ proteins, while $Y_1$, $Y_2$ and $Y_4$ use only $G_i$ proteins (dependent on PI3K), to mediate the phosphorylation of ERK. These differences in the signalling mechanisms used to phosphorylate ERK may be due to structural differences between the NPY receptor subtypes (Mullins et al., 2002; Nie & Selbie, 1998).

### 4.1.3 Coupling ERK 1/2 activation to proliferation

The ERK 1/2 are critical components of mitogenic signalling and growth pathways and the activation of ERK 1/2 in response to NPY binding helps to initiate downstream signals which coordinate proliferative processes (Gutkind, 1998). In the NPY-mediated proliferation of vascular smooth muscle cells (VSMC) through NPY $Y_1$ receptors, Pons et al. (2008) showed that the mitogenic effects were blocked by pertussis toxin and inhibitors of calcium/calmodulin-dependent kinase II (CaMKII), PKC and MEK (MAPK/ERK kinase) 1 and 2. This suggests that the proliferative effect of NPY on VSMCs is mediated via a PKC, $Ca^{2+}$ (through increased intracellular $Ca^{2+}$) and CaMKII-dependent pathway(s) which results in the phosphorylation (activation) of ERK 1/2 by MEK 1/2 (Pons et al., 2008).

NPY has been shown to regulate not only the proliferation of normal and healthy cells, but also cancerous cells (Ruscica et al., 2006). NPY regulates the proliferation of prostate cancer cells via the $Y_1$ receptor (Ruscica et al., 2006). Although the effects of NPY treatment varied across different strains of human prostate cancer cell lines, producing either inhibitory or proliferative effects, these responses were all inhibited by treatment with the $Y_1$ receptor antagonist, BIBP3226. This direct regulation of cancerous cell growth by NPY, which also appeared to be related to ERK1/2 activation, was either long-lasting, or rapid and transient, depending on the strain (Ruscica et al., 2006).

### 4.1.4 Intracellular and extracellular NO

NO itself is a highly diffusible signalling molecule (Lancaster, 1997; Wood & Garthwaite, 1994) which is able to mediate both intracellular and intercellular signalling pathways through intracellular and/or extracellular release. This raises the question over whether NO may be synthesised and released from one cell, before diffusing to and exerting its effects on another cell. Is the NO synthesised in response to NPY stimulation released within the same cell, whereby proliferative processes are mediated intracellularly, or is NO released extracellularly before acting on cells within its proximity? In fact, a previous study by Luo et al. (2010) found that the source of NO (intracellular or extracellular) was important in determining its cellular effects. nNOS-derived NO from neural stem cells acted intracellularly and promoted neural stem cell proliferation whereas nNOS-derived NO from neurons was released extracellularly into the media, where it exerted anti-proliferative effects on neural stem cell proliferation (Luo et al., 2010). In this case, could intracellularly released NO be involved in mediating proliferative effects, while extracellularly released NO be a negative regulator of cell proliferation in postnatal hippocampal cultures?

### 4.1.5 The aims of this chapter

NOS and NO mechanisms are significant players in mediating the proliferative effect of NPY on hippocampal cells, although how these mechanisms lead to an increase in cell proliferation is unknown. ERK 1/2 seem to be key mediators of proliferative pathways and have been shown to mediate the proliferative effect of NPY on a range of cell types (Howell et al., 2005; Agasse et al., 2008; Alvaro et al., 2008), which brings into question whether NPY-mediated NOS/NO production could be linked to ERK 1/2 mechanisms, and if it is, how? The aims of this chapter, therefore, were to further investigate the signalling pathway of NPY and how the activation of NOS could lead to proliferative processes. Does NO produced by NOS in response to NPY stimulation act intracellularly or extracellularly, and what are the consequences of the NO source? The most common mediators of NO processes, sGC and cGMP, were investigated, as well as the ERK 1/2 kinases, in addition to verifying the connectivity within the signalling pathway.

## 4.2 Methods

### Methodology and experimental aim

The NOS and NO signalling cascade underlying NPY-mediated cell proliferation was investigated in an *in vitro* rat hippocampal cell culture system. A detailed description of primary hippocampal cell culture generation, cell plating, the assessment of cell proliferation with BrdU, immunocytochemistry and cell quantification and statistical analysis is provided in Chapter 2. Unless otherwise stated, a one-way ANOVA with Dunnett's multiple comparison test was applied to the raw data to determine significance levels compared to control conditions ($p = <0.05$). The concentration of pharmacological agonists or antagonists were chosen based on either published literature (where the chosen concentrations have already been tested on neuronal cells in a similar context) and/or by testing a range of different concentrations (Table 4.2.1).

Table 4.2.1 Agonists and antagonists

| Agonists | Company | Concentration |
|---|---|---|
| 8-Bromo(Br)-cGMP | Tocris Bioscience, UK | 20 µM (dose response and Alvaro et al., 2008) |
| Antagonists | Company | |
| 1H-[1,2,4]oxadiazolo[4,3-a]quinoxalin-1-one (ODQ) | Ascent Scientific, UK | 50 µM (Alvaro et al., 2008) |
| U0126 | Ascent Scientific, UK | 1 µM (Howell et al., 2005) |
| KT5823 | Tocris Bioscience, UK | 1 µM (Reyes-Harde et al., 1999) |
| Carboxy-PTIO | Tocris Bioscience, UK | 10 µM (Luo et al., 2010) |
| DETA/NONOate (NOC-18) | Calbiochem, Merck Biosciences, UK | 50, 100, 200 µM (Luo et al., 2010) |

### 4.2.1 The effect of 8-Br-cGMP on hippocampal cultures

The enzyme sGC is a common target of NO (Denninger & Marletta, 1999) which converts GTP to cGMP. 8-Bromo(Br)-cGMP is a membrane-permeable analogue of cGMP. To assess the effects of the second messenger of NO, cGMP, on proliferation, cells were cultured under control conditions (NBA-A/B27/Glu medium plus 1% antibiotic/antimycotic) and/or in the presence of 1 µM NPY or 10 µM, 20 µM or 50 µM 8-Br-cGMP (Tocris Bioscience, UK) (Alvaro et al., 2008) for 3 DIV. Cells were pulsed with 20 µM BrdU for 6 h on day 3, followed by cell fixation, immunocytochemistry for BrdU and DAPI, imaging, quantification and analysis.

### 4.2.2 Inhibiting sGC on the neuroproliferative effect of NPY

As well as using the cGMP analogue 8-Br-cGMP to study the mechanisms underlying NPY-mediated neuroproliferation, the effect of sGC inhibition using 1H-[1,2,4]oxadiazolo[4,3-a]quinoxalin-1-one (ODQ) was also explored. ODQ is a highly selective and potent inhibitor of the nitric oxide sensitive sGC. To investigate the effect of sGC inhibition on proliferation, hippocampal cells were cultured under control conditions and 1 μM NPY, 20 μM 8-Br-cGMP and/or 50 μM ODQ (Ascent Scientific, UK) (Alvaro et al., 2008) for 3 DIV. Cells were pulsed with 20 μM BrdU for 6 h on day 3 before cell fixation. Fixed cells were immunocytochemically stained for BrdU and DAPI before imaging, quantification and analysis.

### 4.2.3 ERK 1/2 inhibition on NPY- and 8-Br-cGMP-mediated proliferation

The ERK 1/2 kinases are involved in mediating a range of intracellular signalling cascades which regulate cell proliferation and differentiation (Cano & Mahadevan, 1995). U0126 (Ascent Scientific, UK) is an inhibitor of MAP kinase kinase (MEK) 1/2, which are the upstream kinases involved in mediating the activation of ERK 1/2 by phosphorylation. Cells were cultured under control conditions and 1 μM NPY, 20 μM 8-Br-cGMP and/or 1 μM U0126 (Howell et al., 2005) for 3 DIV. Cultures were pulsed with 20 μM BrdU for 6 h on day 3 before cell fixation, immunocytochemistry, cell imaging, quantification and analysis.

### 4.2.4 The effects of ODQ and U0126 on the proliferative effect of L-arginine

The pharmacological inhibitors of sGC and ERK 1/2, ODQ (50 μM) and U0126 (1 μM), respectively, were applied individually to hippocampal cultures in the absence or presence of 500 μM L-arginine for 3 DIV. Cultures were pulsed with 20 μM BrdU for 6 h on day 3 before cell fixation, immunocytochemistry, cell imaging, quantification and analysis.

### 4.2.5 cGMP-dependent protein kinase (PKG) and the proliferative effect of NPY

PKGs are one of the most common targets of cGMP (Francis & Corbin, 1999). To assess the involvement of PKG in mediating the proliferative effect of NPY, the selective inhibitor of PKG, KT5823 (Tocris Biosciences, UK), was used. Hippocampal cultures were exposed to control conditions, 1 μM NPY or 20 μM 8-Br-cGMP in the absence or presence of 1 μM KT5823 for 3 DIV. Cultures were pulsed with 20 μM BrdU for 6 h on day 3 before cell fixation, immunocytochemistry, cell imaging, quantification and analysis.

### 4.2.6 Western blotting for ERK 1/2 activation

Western blotting was used to determine the activation (phosphorylation) status of ERK 1/2 in response to NPY (1 µM) treatment in the absence or presence of the NOS inhibitor L-NAME and its inactive enantiomer D-NAME. Cells derived from the hippocampus were plated at a density of $10^6$ cells/ml in 6 well plates and cultured for 3 DIV under control conditions (NBA-A/B27/Glu medium plus 1% antibiotic/antimycotic) before treatment. The treatment conditions were control, 1 µM NPY, 1 µM NPY and 500 µM L-NAME, 1 µM NPY and 500 µM D-NAME, and 500 µM L-NAME or 500 µM D-NAME, for 8 min at 37°C. The wells that were treated with NAME were pre-treated with 1 mM L-NAME or D-NAME for 10 min in order to ensure adequate NOS inhibition (El Mabrouk et al., 2000). Treated cells were immediately washed in ice-cold PBS before cell lysis and protein extraction. The protocol for protein extraction and Western blotting is described in Chapter 3, section 3.2.5. Immunodetection of protein was carried out with the aid of PhosphoPlus p44/42 MAP kinase (Thr202/Tyr204) antibody kit (Cell Signaling Technology, New England Biolabs Ltd., Hertfordshire, UK) containing primary antibodies against phosphorylated ERK 1/2 and total ERK 1/2, and horseradish peroxidase (HRP)-linked secondary antibodies (Table 4.2.2).

Table 4.2.2 Primary and secondary antibodies used during Western blotting for assessing ERK 1/2 activation (phosphorylation).

| Primary antibodies | Host | Company | Dilution | Dilution buffer |
|---|---|---|---|---|
| Anti-phospho-p44/42 MAPK (Thr202/Tyr204) monoclonal | Rabbit | Cell Signaling Technology, New England Biolabs, UK | 1:2000 | TBST with 5% w/v bovine serum albumin (BSA) |
| Anti-p44/42 MAP Kinase (137F5) monoclonal | Rabbit | Cell Signaling Technology, New England Biolabs, UK | 1:1000 | TBST with 5% w/v BSA |
| Anti-α-tubulin monoclonal | Mouse | Sigma Aldrich, UK | 1:2000 | TBST with 5% w/v non-fat dry milk |
| Anti-GAPDH polyclonal | Rabbit | Abcam, UK | 1:10000 | TBST with 5% w/v non-fat dry milk |
| Secondary antibodies | Host | Company | Dilution | |
| Anti-rabbit IgG HRP-linked | Goat | Cell Signaling Technology, New England Biolabs, UK | 1:2000 | TBST with 5% w/v non-fat dry milk |
| Anti-mouse IgG HRP-linked | Goat | Cell Signaling Technology, New England Biolabs, UK | 1:2000 | TBST with 5% w/v non-fat dry milk |

The Western blots were analysed with ImageJ analysis software (National Institutes of Health) and because there are two distinct ERK kinases (1 and 2, or p44 and p42, respectively), each ERK kinase band was analysed separately to determine if the contribution by each ERK was different. At least three independent experiments were carried out before the data was plotted using GraphPad Prism data analysis software (GraphPad Software Inc., San Diego, CA, USA) and the unpaired Students t-test applied on the means.

### 4.2.7 NPY-mediated NO release

Hippocampal cultures were exposed to control conditions, 1 µM NPY and/or 10 µM Carboxy-PTIO (CPTIO; Tocris Bioscience), a cell membrane-impermeable NO scavenger, for 3 DIV. The NO scavenger inhibits any effects mediated by extracellularly released NO (Akaike et al., 1993). Cell proliferation was assessed via BrdU incorporation for 6 h on the final day. The cultures were fixed and stained immunocytochemically for BrdU and nestin before they were imaged, quantified and analysed.

### 4.2.8 The role of extracellular NO

To assess the effect of extracellular NO on cell proliferation, the NO donor, DETA/NONOate (NOC-18; Calbiochem, Merck Biosciences, UK), was added to cultures at 50, 100 or 200 µM (Luo et al., 2010) for 3 DIV. Cell proliferation was assessed via BrdU incorporation for 6 h on the final day. The cultures were fixed and stained immunocytochemically for BrdU and nestin before they were imaged, quantified and analysed.

## 4.3 Results

### 4.3.1 8-Br-cGMP mimics the proliferative effect of NPY

The effects of cGMP, a second messenger of NO, on hippocampal cell proliferation was investigated to determine its involvement in mediating the effect of NPY. The cGMP analogue, 8-Br-cGMP, was added to hippocampal cultures at concentrations of 10, 20 and 50 μM for 3 DIV to assess the dose-response relationship. 8-Br-cGMP induced a significant increase in total cell counts at all concentrations tested ($p<0.05$, $F=17.20$ and d.f.=21) (Fig. 4.3.1), exhibiting an effect similar to that of 1 μM NPY. There were no significant differences between the proliferative effects induced by 1 μM NPY or 10, 20 and 50 μM 8-Br-cGMP ($p>0.05$, $F=17.20$ and d.f.=21) (Fig. 4.3.1). 8-Br-cGMP at 20 μM concentration was chosen for further investigations into cGMP to allow comparison between other studies (Alvaro et al., 2008).

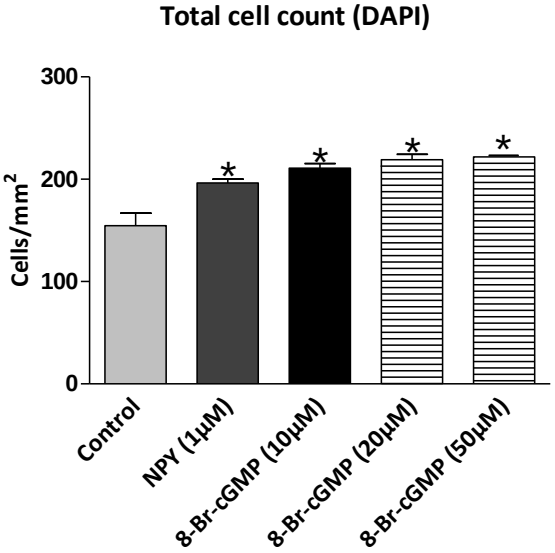


Figure 4.3.1 The c-GMP analogue 8-Br-cGMP induced a significant increase in total cell counts. Cells were grown under control conditions (NBA-A/B27/glutamine), 1 μM NPY or 10, 20 or 50 μM 8-Br-cGMP for 3 DIV. The increase in total cell count induced by 8-Br-cGMP was similar to that of NPY. There were no significant differences between the proliferative effects induced by NPY or 10, 20 and 50 μM 8-Br-cGMP. Data represent mean ± SEM based on a sample that represents at least 4 wells per condition. One-way ANOVA with Dunnett's multiple comparison test, compared against control condition. *$p < 0.05$.

### 4.3.2 ODQ inhibits the proliferative effect of NPY

The enzyme sGC, which converts GTP into cGMP, is one of the most common targets of NO and a potential target within the signalling pathway of NPY. To investigate the involvement of sGC, ODQ, a selective inhibitor of sGC, was added to cultures. As expected from previous studies (4.3.1), individual NPY or 8-Br-cGMP treatment induced a significant increase in the total cell counts ($p<0.05$, $F=31$ and $d.f.=86$) (Fig. 4.3.2A), number of $BrdU^+$ cells ($p<0.05$, $F=42.82$ and $d.f.=86$) (Fig. 4.3.2B) and the mitotic indices ($p<0.05$, $F=23.50$ and $d.f.=86$) (Fig. 4.3.2C). Both proliferative compounds exerted a similar magnitude of effect as the increases observed were not significantly different between NPY or 8-Br-cGMP conditions ($p>0.05$, $F=23.50$ and $d.f.=86$). Cultures were also simultaneously exposed to both NPY and 8-Br-cGMP to determine whether the combined treatment would result in a cumulative effect. Although combined treatment resulted in increased total cell count ($p<0.05$, $F=31$ and $d.f.=86$) (Fig. 4.3.2A), number of $BrdU^+$ cells ($p<0.05$, $F=42.82$ and $d.f.=86$) (Fig. 4.3.2B) and the mitotic index ($p<0.05$, $F=23.50$ and $d.f.=86$) (Fig. 4.3.2C), these increases were not significantly different to the levels observed with individual NPY or 8-Br-cGMP exposure, thus discounting any cumulative effects.

The addition of the sGC inhibitor, ODQ, significantly reduced the proliferative effect of NPY under all parameters investigated. The effect of NPY on total cell count was significantly reduced to control levels by the presence of ODQ (One-way ANOVA with Bonferroni's Multiple Comparison Test comparing NPY condition to NPY + ODQ condition, $p<0.05$, $F=31$ and $d.f.=86$), while the addition of ODQ on its own had no significant effect (Fig. 4.3.2A). Similarly, the increase in $BrdU^+$ cell number by NPY was significantly inhibited by the presence of ODQ (One-way ANOVA with Bonferroni's Multiple Comparison Test comparing NPY condition to NPY + ODQ condition, $p<0.05$, $F=42.82$ and $d.f.=86$), although in this instance, ODQ itself also seemed to have a negative effect when added on its own by significantly reducing $BrdU^+$ cell number to below control levels ($p<0.05$, $F=42.82$ and $d.f.=86$) (Fig. 4.3.2B). With regards to the mitotic index, the presence of ODQ, both in the presence and absence of NPY, exerted a negative effect which reduced the mitotic index to below control levels ($p<0.05$, $F=23.50$ and $d.f.=86$) (Fig. 4.3.2C). It was quite clear, however, that the proliferative effect of NPY on the mitotic index was significantly reduced by the presence of ODQ (One-way ANOVA

with Bonferroni's Multiple Comparison Test comparing NPY condition to NPY + ODQ condition, $p<0.05$, $F=23.50$ and d.f.=86) (Fig. 4.3.2C).

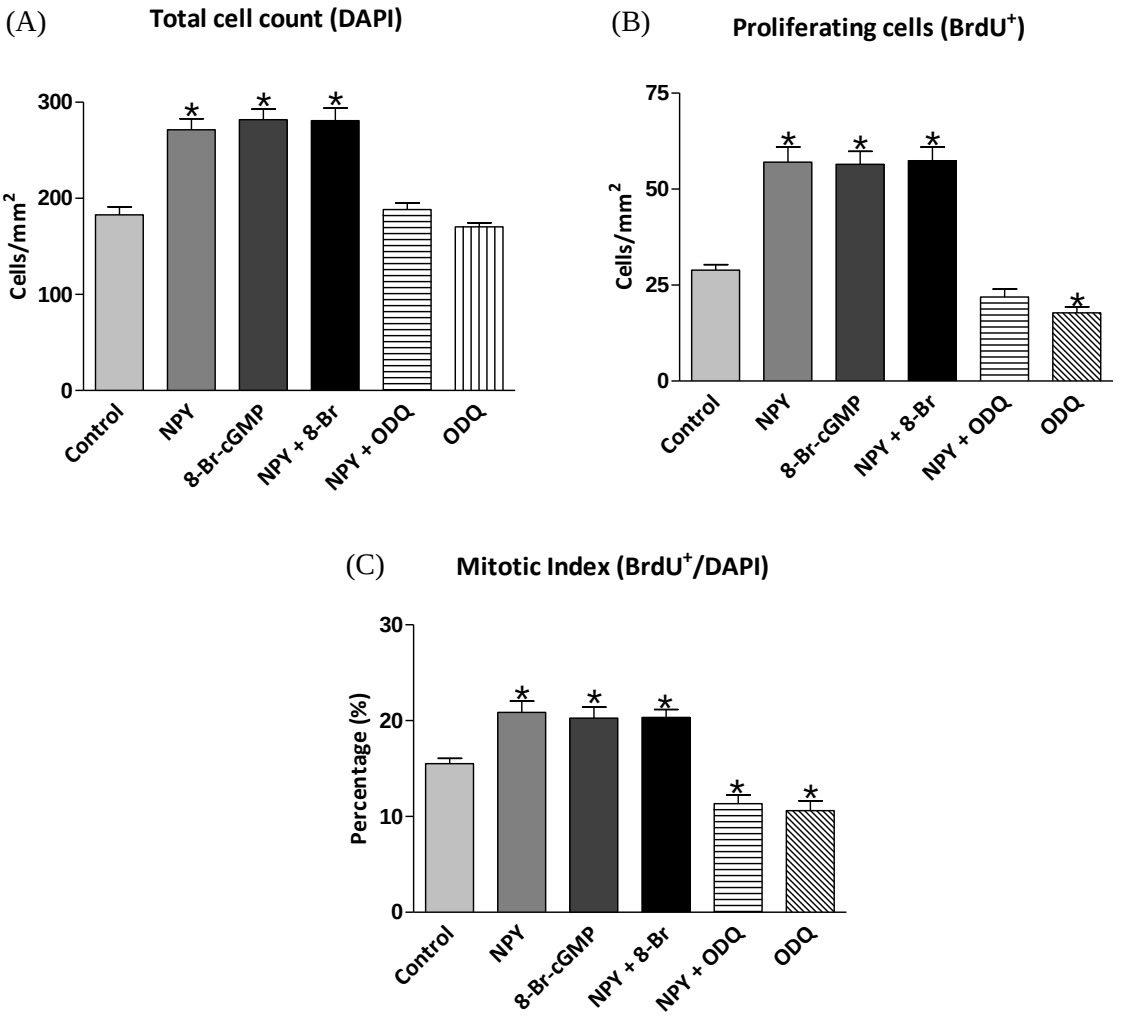


Figure 4.3.2 ODQ reduced the proliferative effect of NPY. Cells were grown under control conditions (NBA-A/B27/glutamine) and 1 μM NPY, 20 μM 8-Br-cGMP and/or 50 μM ODQ for 3 DIV. BrdU was added for the final 6 h. NPY or 8-Br-cGMP both induced a significant increase in (A) total cell count, (B) number of $BrdU^+$ cells and (C) the mitotic index. There were no cumulative effects from combined NPY and 8-Br-cGMP treatment. ODQ reduced the effect of NPY to control levels and also had negative effects on basal proliferation rates on its own. Data represent mean ± SEM based on a sample that represents at least 12 wells per condition from four separate experiments. One-way ANOVA with Dunnett's multiple comparison test, compared to control condition. *$p < 0.05$.

### 4.3.3 U0126 inhibits the proliferative effect of NPY and 8-Br-cGMP

The pharmacological compound U0126 is an inhibitor of the activation (phosphorylation) of ERK 1/2. The involvement of ERK 1/2 in mediating the effect of NPY had been shown by Hansel et al. (2001) and Howell et al. (2005) in postnatal precursor cells from the olfactory epithelium and hippocampus, respectively. The effects of U0126 on NPY and 8-Br-cGMP action was investigated to confirm ERK 1/2 involvement and further determine its role within the signalling cascade of NPY. As expected, the presence of NPY or 8-Br-cGMP induced a significant increase in total cell counts ($p<0.05$, $F=17.14$ and $d.f.=84$) (Fig. 4.3.3A), number of $BrdU^+$ cells ($p<0.05$, $F=33.59$ and $d.f.=84$) (Fig. 4.3.3B) and the mitotic indices ($p<0.05$, $F=20.48$ and $d.f.=84$) (Fig. 4.3.3C), reminiscent of previous studies. In the case of the total cell count and $BrdU^+$ cell numbers, the presence of U0126 completely reduced the effects of NPY or 8-Br-cGMP back down to control levels (One-way ANOVA with Bonferroni's Multiple Comparison Test comparing NPY condition to NPY + U0126 condition or 8-Br-cGMP condition to 8-Br-cGMP + U0126 condition. $p<0.05$, $F=17.14$ and $d.f.=84$ for total cell counts and $p<0.05$, $F=33.59$ and $d.f.=84$ for $BrdU^+$ cells) (Fig. 4.3.3A and Fig. 4.3.3B, respectively). This reduction was also observed in the mitotic index and its response to NPY or 8-Br-cGMP, whose proliferative effects were significantly inhibited by the presence of U0126 (One-way ANOVA with Bonferroni's Multiple Comparison Test comparing NPY condition to NPY + U0126 condition; and 8-Br-cGMP condition to 8-Br-cGMP + U0126 condition, respectively, $p<0.05$, $F=20.48$ and $d.f.=84$) (Fig. 4.3.3C). On its own, U0126 had no effects on the total cell count, number of $BrdU^+$ cells and the mitotic index.

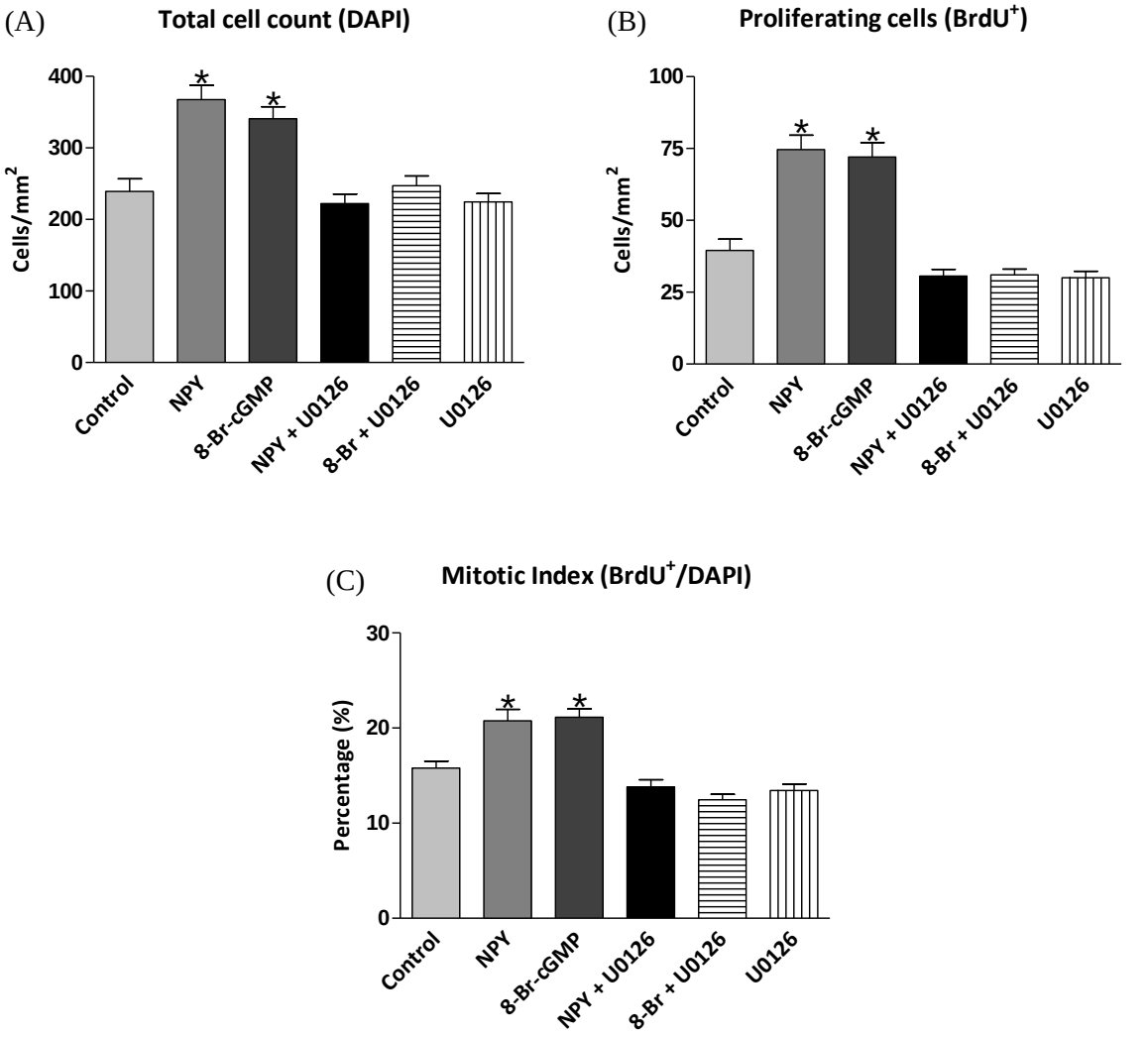


Figure 4.3.3 U0126 reduced the proliferative effect of NPY and 8-Br-cGMP. Cells were grown under control conditions (NBA-A/B27/glutamine) and 1 μM NPY, 20 μM 8-Br-cGMP and/or 1 μM U0126 for 3 DIV. BrdU was added for the final 6 h. NPY or 8-Br-cGMP both induced a significant increase in (A) total cell count, (B) number of $BrdU^+$ cells and (C) the mitotic index, which was reduced back down to control levels by U0126. On its own, U0126 had no effect on basal proliferation rates. Data represent mean ± SEM based on a sample that represents at least 9-13 wells per condition from four separate experiments. One-way ANOVA with Dunnett's multiple comparison test, compared to control condition. *$p < 0.05$.

### 4.3.4 ODQ and U0126 inhibit the proliferative effect of L-arginine

To further verify the interlinks within the NPY signalling pathway, cultures were supplemented with L-arginine to stimulate endogenous NO production while in the presence of inhibitors of identified downstream targets of NO, including sGC and ERK 1/2. Primary hippocampal cultures were grown under control conditions and in the presence of L-arginine and ODQ or U0126 for 3 DIV.

As expected from previous studies (Fig. 3.3.3), stimulating endogenous NO production with L-arginine induced a proliferative effect in cultures. In the case of sGC inhibition with ODQ, the increase in total cell count ($p<0.05$, $F=97.91$ and $d.f.=29$) (Fig. 4.3.4A), $BrdU^+$ cell number ($p<0.05$, $F=89.63$ and $d.f.=29$) (Fig. 4.3.4B) and mitotic index ($p<0.05$, $F=17.47$ and $d.f.=29$) (Fig. 4.3.4C) observed in response to L-arginine treatment was significantly reduced in the presence of ODQ (One-way ANOVA with Bonferroni's Multiple Comparison Test comparing L-arginine condition to L-arginine + ODQ condition, $p<0.05$, $F=97.91$ and $d.f.=29$ for total cell counts, $p<0.05$, $F=89.63$ and $d.f.=29$ for $BrdU^+$ cells, and $p<0.05$, $F=17.47$ and $d.f.=29$ for the mitotic index) (Fig. 4.3.4). Similar to the results observed previously (4.3.2), ODQ exerted an inhibitory effect which significantly reduced the number of $BrdU^+$ cells ($p<0.05$, $F=89.63$ and $d.f.=29$) and the mitotic index ($p<0.05$, $F=17.47$ and $d.f.=29$) to below control levels, even in the presence of L-arginine (Fig. 4.3.4B and C).

Similarly, with regards to ERK 1/2 inhibition with U0126, L-arginine induced a significant increase in the total cell count ($p<0.05$, $F=8.111$ and $d.f.=40$) (Fig. 4.3.5A), $BrdU^+$ cell number ($p<0.05$, $F=9.789$ and $d.f.=40$) (Fig. 4.3.5B) and mitotic index ($p<0.05$, $F=4.454$ and $d.f.=40$) (Fig. 4.3.5C). In the presence of U0126, however, the proliferative effect of L-arginine was reduced to levels comparable to control conditions (Fig. 4.3.5). The total cell count ($p>0.05$, $F=8.111$ and $d.f.=40$) (Fig. 4.3.5A), $BrdU^+$ cell number ($p>0.05$, $F=9.789$ and $d.f.=40$) (Fig. 4.3.5B) and mitotic index ($p>0.05$, $F=4.454$ and $d.f.=40$) (Fig. 4.3.5C) were not significantly different to control. In line with previous studies, U0126, on its own, had no effect on basal proliferation rates (Fig. 4.3.3).

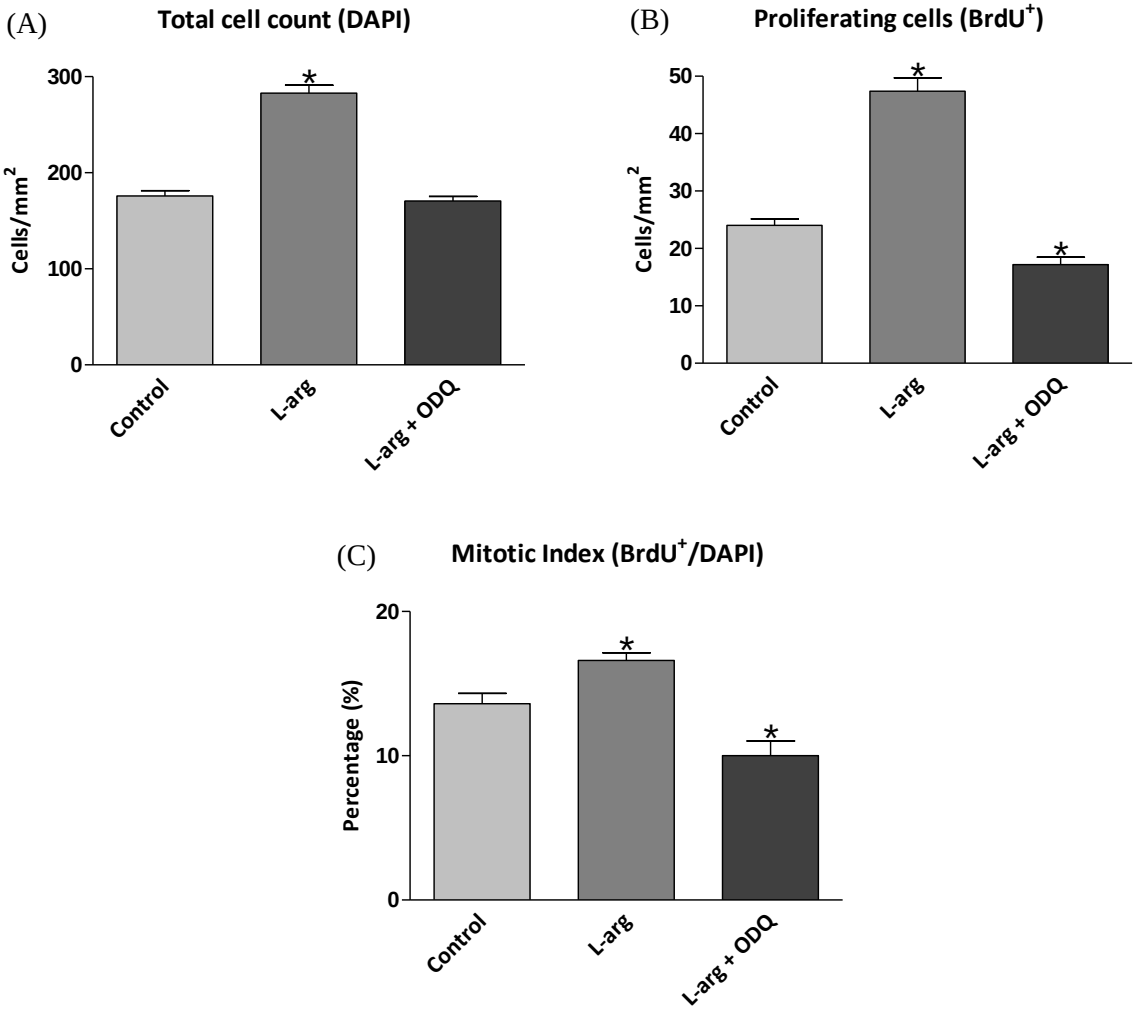


Figure 4.3.4 ODQ reduced the proliferative effect of L-arginine. Cells were grown under control conditions (NBA-A/B27/glutamine) and in the presence of 500 µM L-arginine or 500 µM L-arginine and 50 µM ODQ for 3 DIV. BrdU was added for the final 6 h. L-arginine induced proliferative effects which were reduced by the presence of ODQ. ODQ significantly reduced any increase in (A) total cell count, (B) number of $BrdU^+$ cells and (C) mitotic index mediated by L-arginine. In the presence of L-arginine, ODQ also significantly reduced the (B) number of $BrdU^+$ cells and (C) mitotic index to below control levels. Data represent mean ± SEM based on a sample that represents at least 10 wells per condition from three separate experiments. One-way ANOVA with Dunnett's multiple comparison test, compared to control condition. *$p < 0.05$.

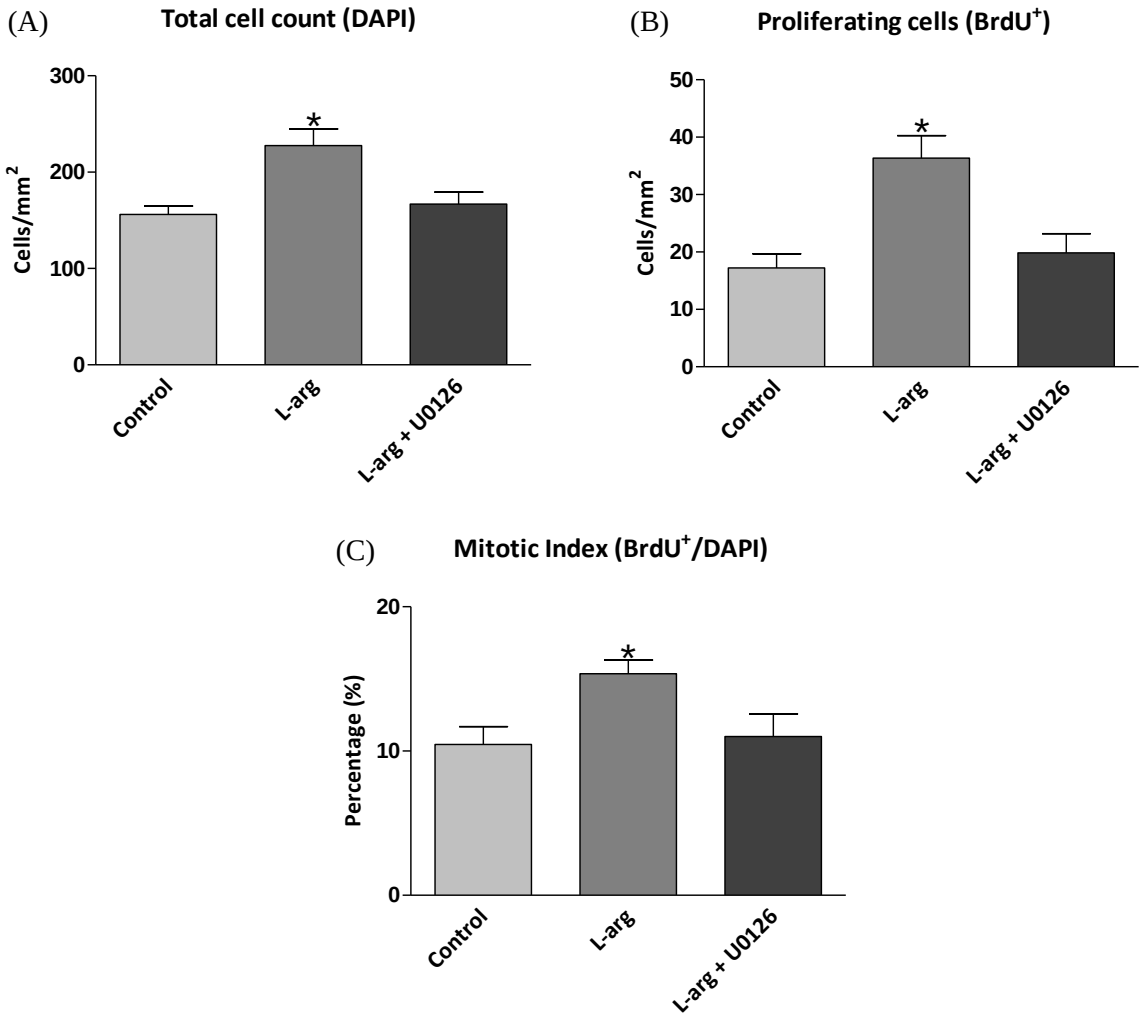


Figure 4.3.5 U0126 reduced the proliferative effect of L-arginine. Cells were cultured under control conditions (NBA-A/B27/glutamine) and in the presence of 500 µM L-arginine or 500 µM L-arginine and 1 µM U0126 for 3 DIV. BrdU was added for the final 6 h. The presence of L-arginine significantly increased (A) the total cell count, (B) number of $BrdU^+$ cells and (C) the mitotic index, which were all reduced to control levels by U0126. Data represent mean ± SEM based on a sample that represents at least 13 wells per condition from three separate experiments. One-way ANOVA with Dunnett's multiple comparison test, compared to control condition. *$p < 0.05$.

### 4.3.5 PKG is involved in mediating the effect of NPY

The kinase PKG was investigated to further explore the processes downstream of cGMP. A common target of cGMP, PKG is inhibited selectively by the compound KT5823 (Francis et al., 2010). Individually, NPY and 8-Br-cGMP exerted proliferative effects which increased total cell counts ($p<0.05$, $F=27.02$ and $d.f.=85$) (Fig. 4.3.6A), $BrdU^+$ cell numbers ($p<0.05$, $F=50.89$ and $d.f.=85$) (Fig. 4.3.6B) and the mitotic indices ($p<0.05$, $F=15.37$ and $d.f.=85$) (Fig. 4.3.6C). KT5823 significantly reduced the proliferative effects of NPY or 8-Br-cGMP on the total cell count and $BrdU^+$ cell number to control levels (One-way ANOVA with Bonferroni's Multiple Comparison Test comparing NPY condition to NPY + KT5823 condition or 8-Br-cGMP condition to 8-Br-cGMP + KT5823 condition. $p<0.05$, $F=27.02$ and $d.f.=85$ for total cell counts and $p<0.05$, $F=50.89$ and $d.f.=85$ for $BrdU^+$ cells) (Fig. 4.3.6A and Fig. 4.3.6B, respectively). On its own, KT5823 had no effect on either the total cell count or $BrdU^+$ cell number (Fig. 4.3.6A and Fig. 4.3.6B, respectively). The mitotic indices of both NPY and 8-Br-cGMP conditions were significantly reduced in the presence of KT5823 (One-way ANOVA with Bonferroni's Multiple Comparison Test comparing NPY condition to NPY + KT5823 condition or 8-Br-cGMP condition to 8-Br-cGMP + KT5823 condition. $p<0.05$, $F=15.37$ and $d.f.=85$) (Fig. 4.3.6C), while combined 8-Br-cGMP and KT5823 treatment, as well as KT5823 treatment on its own, significantly reduced the mitotic indices to below control levels ($p<0.05$, $F=15.37$ and $d.f.=85$) (Fig. 4.3.6C).

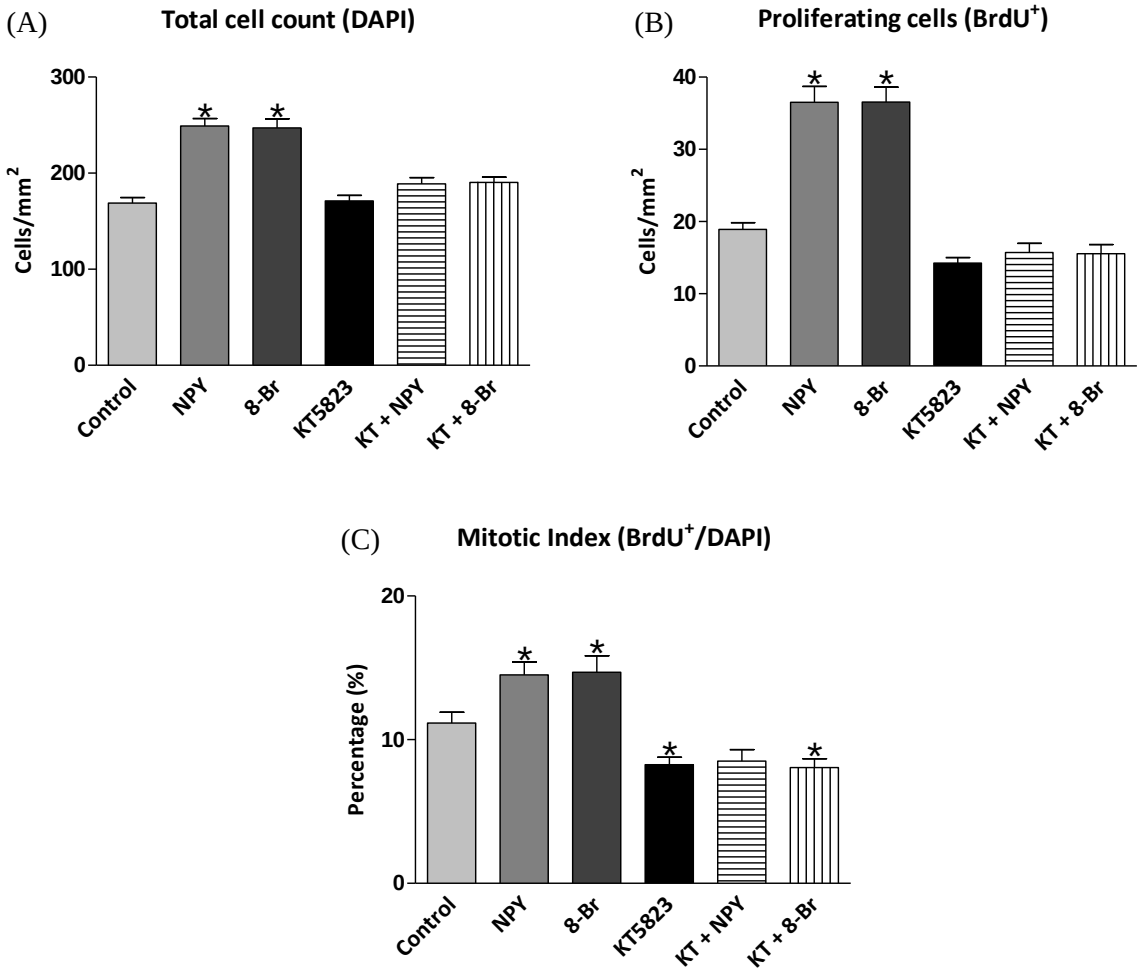


Figure 4.3.6 KT5823 reduced the proliferative effects of NPY and 8-Br-cGMP. Cells were grown under control conditions (NBA-A/B27/glutamine) and/or 1 µM NPY or 20 µM 8-Br-cGMP in the presence of 1 µM KT5823 for 3 DIV. BrdU was added for the final 6 h. The presence of NPY or 8-Br-cGMP induced an increase in (A) total cell counts, (B) number of $BrdU^+$ cells and (C) the mitotic indices, which were significantly reduced by KT5823. In the case of the mitotic indices, both treatment with KT5823 on its own and combined 8-Br-cGMP and KT5823 treatment resulted in a significant decrease to below control levels. Data represent mean ± SEM based on a sample that represents at least 13 wells per condition from four separate experiments. One-way ANOVA with Dunnett's multiple comparison test, compared to control condition. *$p < 0.05$.

### 4.3.6 ERK 1/2 activation by NPY is reduced by inhibiting NOS

The proliferative effect of NPY has been shown to require, and induce, ERK 1/2 activation (phosphorylation) (Hansel et al., 2001; Howell et al., 2005; Alvaro et al. 2008). To assess whether NPY mediates ERK activation through a NOS and upstream NO signalling pathway, ERK 1/2 phosphorylation was assessed via Western blotting in response to NPY treatment in the presence of the active inhibitor of NOS, L-NAME, or its inactive enantiomer, D-NAME. The Western blots showed two bands against ERK, an upper and lower band, which were representative of ERK 1 (p44) and 2 (p42), respectively. There was increased phosphorylation of ERK 1 (p44) and 2 (p42) in response to NPY treatment, detected as increased band intensity, which was reduced by the presence of L-NAME and D-NAME (Fig. 4.3.7). To account for variability in protein loading, α-tubulin or GAPDH were used as loading controls for normalisation of ERK bands.

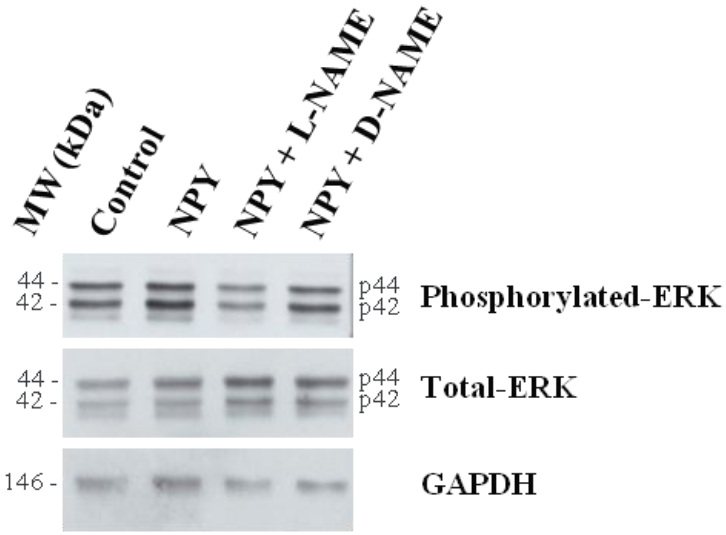


Figure 4.3.7 ERK 1/2 activation by NPY was reduced by inhibiting NOS. Western blots showing bands obtained in response to treatment of 3-d hippocampal cultures with control media (NBA-A/B27/glutamine), 1 µM NPY or 1 µM NPY in the presence of 500 µM L-NAME or D-NAME for 8 min. NAME treatment wells were pre-treated with 1 mM L-NAME or D-NAME for 10 min beforehand. Immunoblots were probed with antibodies against phosphorylated and total ERK, while GAPDH was used as a loading control. ERK 1 (p44) and 2 (p42) showed distinct bands. The addition of NPY increased the phosphorylation levels of ERK 1/2, while the presence of L-NAME reduced levels.

Treatment with NPY increased the phosphorylation levels of ERK 1 (p44) (Fig. 4.3.8A) which, in the case of ERK 2 (p42), showed a significant increase ($p<0.05$, $F=7.497$ and $d.f.=11$) (Fig. 4.3.8B). The increased phosphorylation levels of ERK 1/2 induced by NPY were significantly decreased by the presence of L-NAME and D-NAME ($p<0.05$, $F=9.077$ and $d.f.=11$, and $p<0.05$, $F=7.497$ and $d.f.=11$, for ERK p44 and p42, respectively) (Fig. 4.3.8A and B). L-NAME and D-NAME alone had no significant effect on ERK 1/2 phosphorylation levels ($p>0.05$, $F=0.2727$ and $d.f.=8$, and $p<0.05$, $F=0.3420$ and $d.f.=8$, for ERK p44 and p42, respectively) (Fig. 4.3.8C and D).

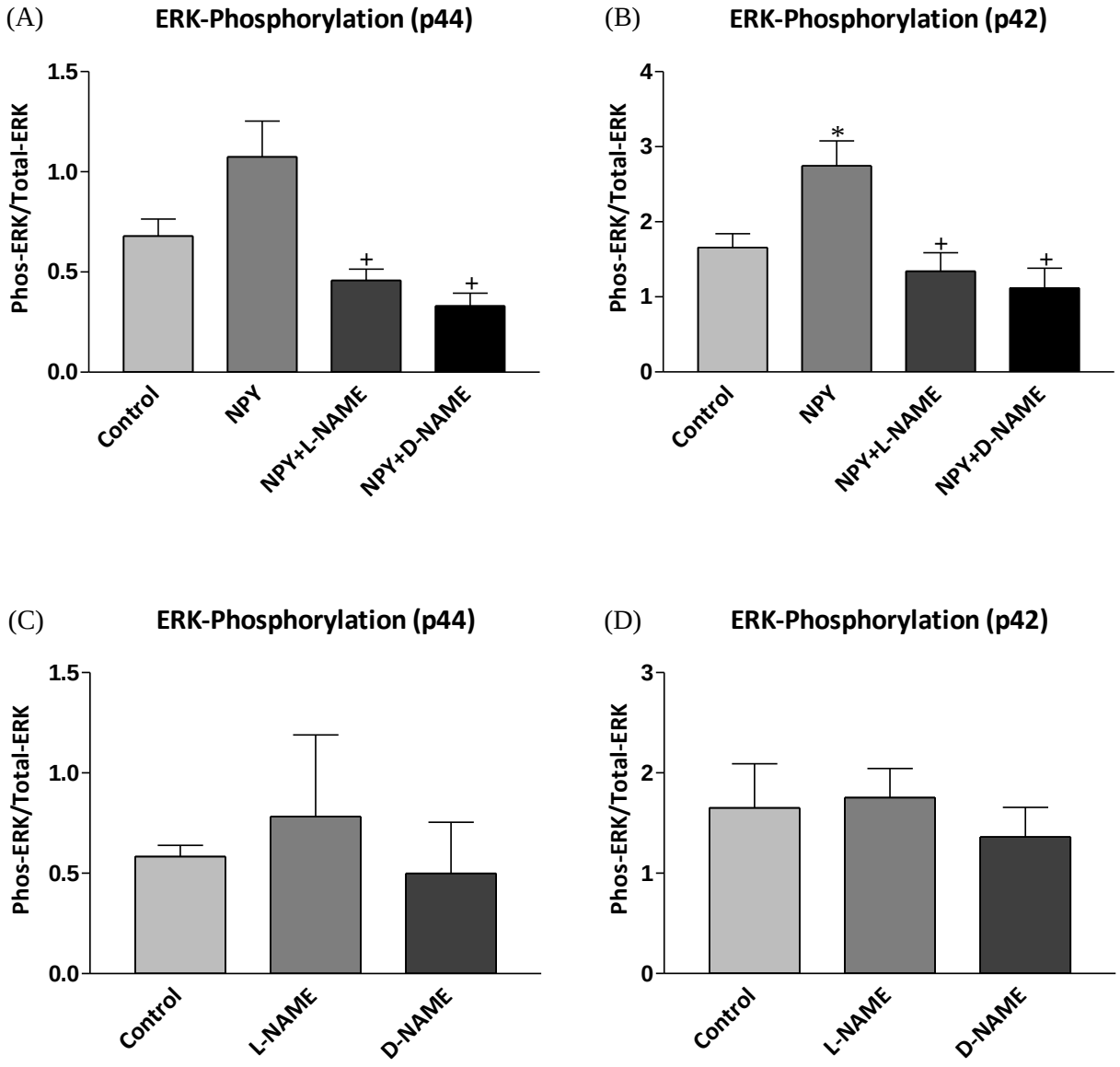


Figure 4.3.8 ERK 1 (p44) and 2 (p42) activation by NPY was reduced by inhibiting NOS. ERK 1/2 phosphorylation in response to NPY, L-NAME and D-NAME treatment. 3 d hippocampal cultures were treated with (A and B) control media (NBA-A/B27/glutamine), 1 µM NPY or 1 µM NPY in

the presence of 500 µM L-NAME or D-NAME, or (C and D) 500 µM L-NAME or D-NAME, for 8 min. NAME treatment wells were pre-treated with 1 mM L-NAME or D-NAME for 10 min beforehand. (A and B) ERK 1 (p44) and 2 (p42) showed an increase in phosphorylation levels in response to NPY treatment, which was significant with ERK 2 (*), while the presence of L-NAME and D-NAME significantly reduced ERK 1/2 phosphorylation levels compared to NPY treatment ($^{+}$). (C and D) L-NAME or D-NAME treatment alone did not affect ERK 1/2 phosphorylation levels. Data represent mean ± SEM based on three separate experiments. One-way ANOVA with Dunnett's (*) or Bonferroni's (+) multiple comparison test. *$p < 0.05$.

### 4.3.7 The proliferative effect of NPY is mediated via intracellular NO signalling and not by extracellular release and stimulation

To determine the precise NO signalling cascade (intracellular or extracellular) involved in mediating the proliferative effect of NPY, hippocampal cultures were exposed to NPY in the presence of the cell membrane-impermeable NO scavenger, CPTIO, for 3 DIV as a means to reduce any extracellularly released NPY.

On its own, NPY exerted a proliferative effect on cultures which significantly increased the total cell count ($p<0.05$, $F=20.84$ and $d.f.=46$) (Fig. 4.3.9A), number of $BrdU^{+}$ cells ($p<0.05$, $F=21.43$ and $d.f.=46$) (Fig. 4.3.9B) and the mitotic index ($p<0.05$, $F=8.659$ and $d.f.=46$) (Fig. 4.3.9E). Similarly, this effect was also observed with regards to the $nestin^{+}$ precursor cell population, with significantly enhanced $nestin^{+}$ cell ($p<0.05$, $F=8.999$ and $d.f.=47$) (Fig. 4.3.9C) and $nestin^{+}$ $BrdU^{+}$ cell numbers ($p<0.05$, $F=14.02$ and $d.f.=47$) (Fig. 4.3.9D) and mitotic index of $nestin^{+}$ precursor cells ($p<0.05$, $F=6.206$ and $d.f.=47$) (Fig. 4.3.9F). The proliferative effect of NPY was unaffected by the presence of the NO scavenger CPTIO, as demonstrated by the significantly increased total cell count ($p<0.05$, $F=20.84$ and $d.f.=46$) (Fig. 4.3.9A) and number of $BrdU^{+}$ cells ($p<0.05$, $F=21.43$ and $d.f.=46$) (Fig. 4.3.9B), $nestin^{+}$ cells ($p<0.05$, $F=8.999$ and $d.f.=47$) (Fig. 4.3.9C) and $nestin^{+}$ $BrdU^{+}$ cells ($p<0.05$, $F=14.02$ and $d.f.=47$) (Fig. 4.3.9D). Likewise, the increased proliferation status in response to NPY and CPTIO treatment was reflected in the mitotic indices of the overall cell population ($p<0.05$, $F=8.659$ and $d.f.=46$) (Fig. 4.3.9E) and the $nestin^{+}$ precursor cell population ($p<0.05$, $F=6.206$ and $d.f.=47$) (Fig. 4.3.9F), supporting the involvement of intracellular NO signalling pathways in mediating the proliferative effect of NPY.

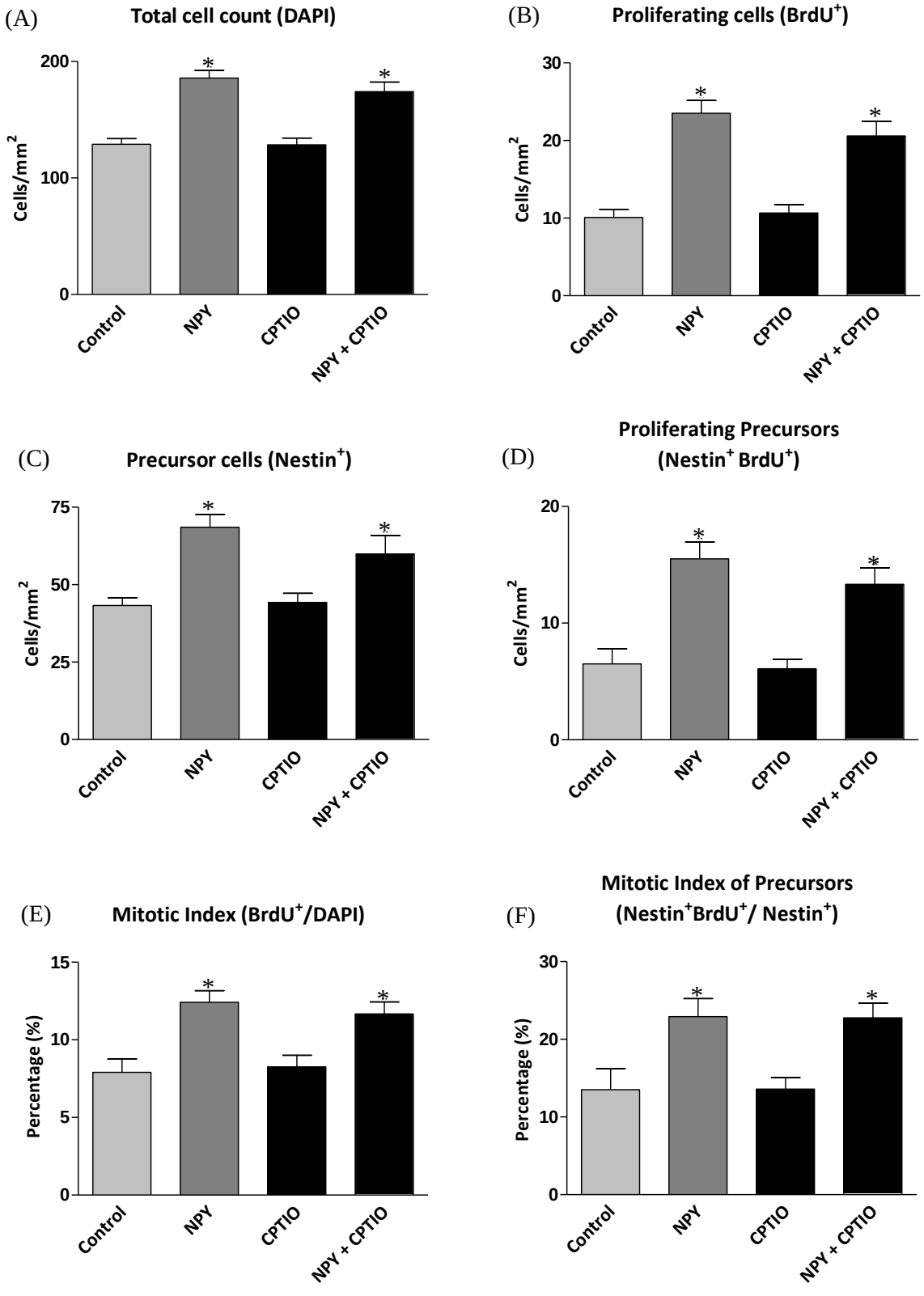


Figure 4.3.9 The proliferative effect of NPY is mediated via an intracellular NO signalling pathway and not by extracellular release and stimulation. Cells were cultured for 3 d under control (NBA-A/B27/Glu), 1 µM NPY and/or 10 µM CPTIO (NO scavenger) conditions, before BrdU was added for the final 6 h. A significant increase was observed in (A) the total cell count, (B) numbers of

$BrdU^+$ cells, (C) $nestin^+$ cells, (D) $nestin^+$ $BrdU^+$ cells, and the mitotic indices of the (E) overall and (F) $nestin^+$ cell population in response to NPY exposure, which was still significantly increased in the presence of CPTIO, suggesting an intracellular, rather than extracellular, signalling pathway in the NPY bound cell. Data represent mean ± SEM based on a sample that represents at least 12 wells per condition from at least three separate experiments. One-way ANOVA with Dunnett's multiple comparison test, compared to control condition. *$p<0.05$.

### 4.3.8 The extracellular application of NO is inhibitory for cell proliferation

If NO is released intracellularly in response to NPY stimulation and mediates proliferative processes, does extracellular NO, as described previously by Luo et al. (2010), exert anti-proliferative effects? To answer this question, hippocampal cells were cultured in the presence of the NO donor, DETA/NONOate (NOC-18), for 3 DIV to determine the effect of extracellular NO on cell proliferation. NOC-18 at concentrations of 50, 100 and 200 µM were investigated to explore the dose-response relationship. NOC-18 at the lowest concentration of 50 µM exerted no effect on cell proliferation. The total cell count ($p>0.05$, $F=0.2692$ and d.f.=44), number of $BrdU^+$ cells ($p>0.05$, $F=46.66$ and d.f.=44), $nestin^+$ cells ($p>0.05$, $F=44.90$ and d.f.=45), $nestin^+$ $BrdU^+$ cells ($p>0.05$, $F=16.19$ and d.f.=45) and the mitotic indices of the overall ($p>0.05$, $F=44.39$ and d.f.=44) and $nestin^+$ cell ($p>0.05$, $F=5.321$ and d.f.=45) population were unchanged from control levels (Fig. 4.3.10A-F). At 100 µM concentration, however, a negative effect on cell proliferation was observed. Although total cell counts in response to 100 µM NOC-18 were unchanged ($p>0.05$, $F=0.2692$ and d.f.=44) (Fig. 4.3.10A), the number of $BrdU^+$ cells ($p<0.05$, $F=46.66$ and d.f.=44) (Fig. 4.3.10B) and the overall mitotic index ($p<0.05$, $F=44.39$ and d.f.=44) (Fig. 4.3.10E) were significantly reduced to below control levels. The number of $nestin^+$ cells ($p<0.05$, $F=44.90$ and d.f.=45) (Fig. 4.3.10C) and $nestin^+$ $BrdU^+$ cells ($p<0.05$, $F=16.19$ and d.f.=45) (Fig. 4.3.10D) were also significantly reduced, however, the mitotic index of $nestin^+$ precursor cells was not different to control levels ($p>0.05$, $F=5.321$ and d.f.=45) (Fig. 4.3.10F). NOC-18 at the highest concentration tested, 200 µM, fully reduced proliferation to well below control levels. The number of $BrdU^+$ cells ($p<0.05$, $F=46.66$ and d.f.=44), $nestin^+$ cells ($p<0.05$, $F=44.90$ and d.f.=45), $nestin^+$ $BrdU^+$ cells ($p<0.05$, $F=16.19$ and d.f.=45) and the mitotic indices of the overall ($p<0.05$, $F=44.39$ and d.f.=44) and $nestin^+$ cell population ($p<0.05$, $F=5.321$ and d.f.=45) were significantly decreased compared to control levels, although the total cell count was also unchanged ($p>0.05$, $F=0.2692$ and d.f.=44) (Fig. 4.3.10A-F). The inhibition of basal cell proliferation, especially of $nestin^+$ precursor cells, increased in response to NOC-18 concentration, with higher concentrations exerting a more prominent inhibitory effect. The negative effect of NOC18 on the numbers of $BrdU^+$ cells (Fig. 4.3.10B), $nestin^+$ cells (Fig. 4.3.10C), $nestin^+$ $BrdU^+$ cells (Fig. 4.3.10D) and the mitotic index (Fig. 4.3.10E) was significantly more pronounced with 100 µM, compared to 50 µM NOC18 (One-way ANOVA with Bonferroni's Multiple Comparison Test comparing 50 µM NOC18 condition to 100 µM NOC condition, $p<0.05$). Similarly, 200 µM NOC18 significantly reduced the numbers of

$BrdU^+$ cells (Fig. 4.3.10B) and $nestin^+$ cells (Fig. 4.3.10C), as well as the mitotic indices of the overall (Fig. 4.3.10E) and $nestin^+$ cell (Fig. 4.3.10F) population, compared to 100 µM NOC18 (One-way ANOVA with Bonferroni's Multiple Comparison Test comparing 100 µM NOC18 condition to 200 µM NOC condition, $p<0.05$). Interestingly, however, there were no significant changes in the total cell count in response to any NOC-18 concentration tested, which could be explained by the fact that the proportion of cells affected were less than 10% of the total cell population and any effects were masked by the noise ratio.

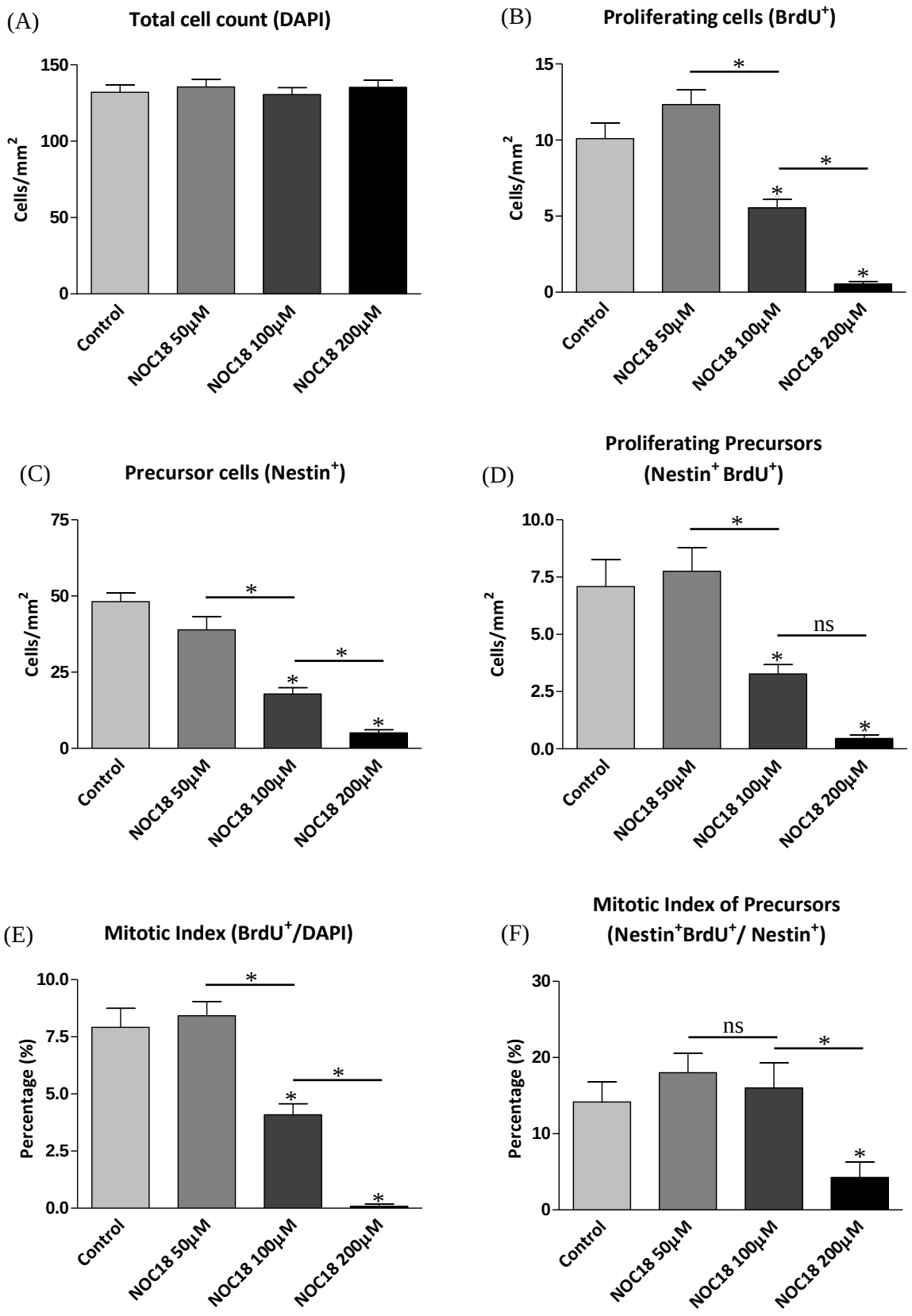


Figure 4.3.10 Extracellular NO exerts a negative effect on basal proliferation rates. Hippocampal cells were cultured under control conditions (NBA-A/B27/glutamine) or 50, 100 or 200 µM DETA/NONOate (NOC-18) for 3 DIV before BrdU was added for the final 6 h. NOC-18 at 50 µM

had no effect on basal proliferation rates (A-F). 100 µM NOC-18 exerted a negative effect on proliferation rates by reducing the number of (B) $BrdU^+$ cells, (C) $nestin^+$ cells, (D) $nestin^+$ $BrdU^+$ cells and (E) the mitotic indices of the overall cell population to below control levels, although it showed no effect on (A) the total cell count or (F) the mitotic index of $nestin^+$ precursor cells. 200 µM NOC-18, on the other hand, exerted an anti-proliferative effect on the number of $BrdU^+$ cells, $nestin^+$ cells, $nestin^+$ $BrdU^+$ cells and the mitotic indices of the overall and $nestin^+$ cell population (B-F), although, similar to the treatment with 100 µM NOC-18, the total cell count was unaffected. Data represent mean ± SEM based on a sample that represents at least 11 wells per condition from three different experiments. One-way ANOVA with Dunnett's and Bonferroni's multiple comparison test, compared to control condition (ns, not significant). *$p < 0.05$.

## 4.4 Discussion

Chapter 3 had identified NOS and NO mechanisms as mediators of the NPY signalling pathway, but how this ultimately results in an increase in cell proliferation was unknown. The aim of this chapter was to decipher the signalling pathway downstream of NOS/NO responsible for mediating the proliferative effect of NPY in postnatal hippocampal cultures.

### 4.4.1 Involvement of sGC and PKG

The most common target of NO, sGC, activates a variety of intracellular kinase pathways through the synthesis of cGMP (Denninger & Marletta, 1999; Derbyshire & Marletta, 2009). A heterodimeric protein, sGC consists of two homologous subunits, α and β, for which two isoforms of each subunit have been identified (α1/α2 and β1/β2) (Harteneck et al., 1991; Yuen et al., 1990). Although this gives rise to a variety of sGC isoforms, only the α1β1 and α2β1 isoforms are active (Russwurm et al., 1998). The α1β1 isoform predominates in all other tissues except for the brain, where levels of α1β1 and α2β1 are comparable (Mergia et al., 2003). The sGC inhibitor, ODQ, which inhibits both sGC isoforms (Nimmegeers et al., 2007), reduced the proliferative effect of NPY, while the cGMP analogue, 8-Br-cGMP, mimicked the proliferative response, supporting the involvement of both sGC and cGMP in mediating the proliferative response of NPY. Combined treatment with NPY and 8-Br-GMP was not accompanied by any further increase in proliferation (as a result of cumulative effects) compared to NPY-only or 8-Br-cGMP-only conditions, possibly due to saturation of the signalling system. The addition of ODQ on its own was found to have an inhibitory effect on basal proliferation, suggesting a role for sGC in maintaining basal proliferation rates, however, ODQ at sufficiently high concentrations (above 10 μM) have been shown to inhibit the proliferation of prostate cell lines, independent of its effects on sGC (Haramis et al., 2008). The inhibitory effect of ODQ in this study may be partly explained by the high 50 μM concentration used, although nevertheless, in the presence of ODQ, NPY was still unable to restore proliferation back to basal rates. On a side note, it would also have been interesting to see whether the decreased proliferation in response to ODQ would have been restored by the addition of 8-Br-cGMP, which would have strengthened the results.

The second messenger of NO, cGMP, exerts its effects through three main cellular targets: the PKGs, cGMP-gated cation channels and cyclic nucleotide phosphodiesterases

(PDEs) (Garthwaite & Boulton, 1995). PKGs are activated on cGMP binding, which results in the phosphorylation of serines and threonines on different cellular protein targets (Francis et al., 2010). This phosphorylation of proteins by PKG changes their activation status, function or subcellular localisation, leading to a range of physiological effects ranging from the regulation of calcium homeostasis and smooth muscle contraction to controlling the expression of select genes or negative feedback back onto the NO pathway (Francis et al., 2010). Two isoforms of PKG exist, PKG-I and PKG-II (Uhler, 1993). Both are individually encoded by distinct genes (Uhler, 1993) and widely expressed within the mammalian brain (Feil et al., 2005). Of the PKG-I isoform, which can be further subdivided into PKG-Iα and PKG-Iβ, Feil et al. (2005) showed that the PKG-Iβ subtype predominates in the hippocampus of the mouse brain. The expression of distinct PKG isoforms/subtypes in specific brain regions contribute to the selective control of PKG activity (Feil et al., 2005). The involvement of PKG in the NPY signalling pathway was confirmed by the addition of KT5823, a selective PKG inhibitor, which significantly reduced the proliferative effects mediated by both NPY and 8-Br-cGMP. This inhibition of both upstream factors suggested that PKG was the next intermediary step after cGMP during the cellular signalling mechanisms of NPY. In addition, like sGC, PKG may have a role in maintaining basal proliferation rates.

The importance of PKG in signalling pathways is evident for the neural cell adhesion molecule (NCAM), which has important roles in regulating neuronal development, synaptic plasticity and regeneration (Ditlevsen et al., 2007). In NCAM-mediated neurite outgrowth and neuroprotection of primary neurons, Ditlevsen et al. (2007) showed that NCAM binding leads to the activation of NOS, which results in NO synthesis and cGMP production through the NO-mediated activation of sGC. In turn, the increased synthesis of cGMP leads to the activation of PKG. In addition, PKG has been shown to activate ERK 1/2 in adult smooth muscle cells by stimulating the activity of MEK (the kinases upstream of ERK 1/2) (Komalavilas et al., 1999).

### 4.4.2 ERK 1/2 mediates the proliferative effect of NPY

The ERK 1/2 have been shown by Hansel et al. (2001), Howell et al. (2005) and Alvaro et al. (2008) to be involved in mediating the effect of NPY in postnatal precursor cells from the olfactory epithelium, hippocampus and retina, respectively. My results also confirm ERK 1/2 involvement, showing a reduction in NPY-mediated proliferation upon ERK 1/2

inhibition. The pharmacological compound U0126 completely reduced the neuroproliferative effects of NPY and 8-Br-cGMP on hippocampal cultures back down to control levels and had no effect on basal proliferation rates on its own. The inhibition of 8-Br-cGMP activity allows us to conclude that ERK 1/2 activation was downstream of both sGC and cGMP, demonstrating interlinks within the pathway which had not been shown previously.

### 4.4.3 NPY activates the ERK pathway through NOS

The phosphorylation (activation) of ERK 1/2 is required for mediating the proliferative effect of NPY (Hansel et al., 2001; Howell et al., 2005). The signalling pathways initiated by the NPY Y receptors are diverse and activation of ERK 1/2 may be possible by acting through NO-independent mechanisms (Mullins et al., 2002). Levels of ERK 1/2 phosphorylation were assessed by Western blotting in response to NOS inhibition to determine the importance of the NO pathway in mediating the proliferative effect of NPY. As expected, ERK phosphorylation was increased in response to NPY treatment, especially in the case of ERK 2 (p42). On the other hand, inhibition of NOS by L-NAME treatment reduced NPY-mediated ERK phosphorylation back down to control levels, confirming the importance of NO in mediating ERK 1/2 activation by NPY. Unexpectedly, the inactive enantiomer D-NAME also had a significant inhibitory effect on ERK phosphorylation levels induced by NPY. Similar to the pharmacological results in the last chapter, this may be explained by the presence of minute amounts of the active enantiomer, L-NAME, in the D-NAME, although it is unlikely that such small amounts would be able to cause such significant inhibition. Indeed, L-NAME or D-NAME treatment alone had no effect on basal levels of ERK phosphorylation. Some studies, however, have reported the chiral conversion of similar L-arginine derivatives (such as nitro-D-arginine (D-NA) into nitro-L-arginine (L-NA; the active enantiomer for inhibiting NOS)) *in vivo* (Wang et al., 1999b), which may be one explanation, as L-NAME/D-NAME are methyl ester prodrugs which are hydrolysed by intracellular esterases into L-NA/D-NA, although it is unknown whether this may also be present in *in vitro* systems. Wang et al. (1999b) also showed that D-NA, although 400 times less potent than L-NA, still caused a dose-dependent inhibition of nNOS *in vitro* at sufficient concentrations ($EC_{50}$ = 200 µM), which may possibly explain the inhibitory effect of 500 µM D-NAME observed in this current study.

Another conclusion drawn from the Western blotting investigations was that the whole signalling cascade from NPY to ERK 1/2 occurs in a matter of seconds to minutes. NPY was able to increase ERK 1/2 phosphorylation in hippocampal cultures in less than 8 minutes (treatment time), while even earlier observations on olfactory cultures by Hansel et al. (2001) demonstrated increased ERK 1/2 phosphorylation 30 seconds after NPY treatment. ERK 1/2 signalling is a key regulator of cell proliferation. After activation, ERK can either regulate targets in the cytosol by phosphorylation or translocate to the nucleus of the cell to regulate gene expression through the phosphorylation of a variety of transcription factors, such as c-Myc and c-Fos, which have important roles in controlling cell proliferation and the cell cycle (Roux & Blenis., 2004). Although the pharmacological profile of NPY in the dentate gyrus, for example, the rate of NPY release from GABAergic interneurons, is unknown, NPY acts quickly to exert its physiological effects.

### 4.4.4 The proliferative effect of NPY is mediated through a NO-cGMP-PKG and ERK 1/2 pathway

From what has been identified so far, the proliferative effect of NPY is mediated via a NO-cGMP-PKG and ERK 1/2 pathway (Fig. 4.4.1). The activation order within this NPY signalling pathway was further reinforced by combined pharmacological investigations with L-arginine, ODQ and U0126. The proliferative effect mediated by L-arginine, which promotes intracellular NO production and the signalling pathway upstream at NOS, was inhibited when the sGC inhibitor, ODQ, or the ERK 1/2 inhibitor, U0126, was present. This addition of ODQ or U0126 blocks the signalling pathway downstream of L-arginine and NO, thus eliminating the proliferative effect.

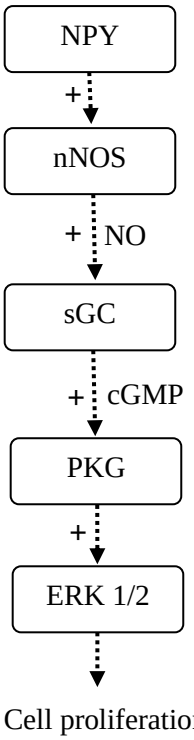


Figure 4.4.1 The proliferative effect of NPY is mediated through a NO signalling cascade. NPY most likely activates neuronal nitric oxide synthase (nNOS) which synthesises NO. NO in turn induces the conversion of GTP into cGMP by soluble guanylate cyclase (sGC), upon which cGMP binds to and activates cGMP-dependent protein kinase (PKG). PKG stimulates a range of protein targets, ultimately resulting in the phosphorylation of the extracellular-regulated kinases (ERK) 1/2 of the mitogen activated protein kinase (MAPK) pathway. ERK 1/2 direct the expression of genes involved in regulating cell proliferation and differentiation.

The NO-cGMP-PKG pathway is a common signalling mechanism utilised by physiological processes (Garthwaite & Boulton, 1995) and the ERK 1/2 mediate intracellular signals which regulate the expression of genes controlling cell proliferation and differentiation (Cano & Mahadevan, 1995). The importance of a NO-cGMP-PKG pathway in mediating the activation of ERK 1/2 was demonstrated previously in rat cerebellar Purkinje cells, where the use of NO donors combined with the simultaneous application of high potassium and glutamate induced ERK 1/2 phosphorylation, which was important in enhancing the declustering of the ionotropic glutamate receptor subunit 2/3 (Endo & Launey, 2003). Declustering of the glutamate receptor is thought to be a preliminary step in glutamate receptor internalisation, an important part of the molecular mechanisms of early-phase long-term depression. The pharmacological inhibitor KT5823 was similarly used to inhibit PKG (Endo & Launey, 2003).

### 4.4.5 The proliferative effect of NPY is probably mediated via intracellular NO signalling

The proliferative effect of NPY was probably mediated via an intracellular NO signalling pathway which involved NO release inside the cell, as the membrane-impermeable NO scavenger, CPTIO, had no effect on NPY action. Although other studies typically use higher levels of CPTIO (~200-300 µM) (Griffiths et al., 2003; Onitsuka et al., 1998; Podda et al., 2004), as CPTIO reacts slowly with NO (rate constant of 1.01 x $10^4$ $M^{-1}s^{-1}$ and 1.6 x $10^4$ $M^{-1}s^{-1}$ at 25°C and 37°C, respectively) (Akaike et al., 1993; Griffiths et al., 2003) and so may not be able to inhibit very local effects, 10 µM CPTIO was used in this study to maintain consistency and allow comparison with Luo et al's (2010) study. Extracellular NO, on the other hand, exerted a negative effect on basal proliferation rates. The addition of the NO donor, DETA/NONOate (NOC-18), induced a dose-dependent decrease in proliferation rates which also inhibited the proliferation of $nestin^+$ precursor cells. Similar to the CPTIO investigation, the same concentrations of DETA/NONOate as Luo et al's study were used to allow comparison of results. The 50 to 200 µM DETA/NONOate concentration was based on the fact that the estimated physiological concentration of NO in the normal brain ranges between 10 and 100 nM (Shibuki, 1990), and that the lowest concentration of DETA/NONOate, 50 µM, was approximately equivalent to physiological levels (Luo et al., 2010). However, as mentioned previously, huge variations in *in vivo* NO concentration have been obtained by different groups (Hall & Garthwaite, 2009), casting doubt over whether the levels of DETA/NONOate used are physiologically relevant. Moreover, a review of independent studies conducted by Hall and Garthwaite (2009) suggests that the physiological concentration of NO is more likely to be 100 pM (or below) up to ~5 nM, much lower than initially thought. If these levels are indeed more representative of endogenous NO levels, then the concentrations of DETA/NONOate used, in not only this but also other studies, may be too high for NO levels to be physiologically representative. In fact, in the study by Covacu et al. (2006), who Luo et al. (2010) based their choice of DETA/NONOate concentrations on, ~500 nM NO was found to be released from 0.1 mM DETA/NONOate at the peak of NO release (~2 h) using a NO-selective microelectrode (NO release was measured over a period of 24 h). If 0.1 mM DETA/NONOate releases ~500 nM NO at its peak, then 50 µM, 100 µM, and 200 µM DETA/NONOate would release ~250 nM, ~500 nM, and ~1 µM NO, respectively (Covacu et al., 2006), far exceeding the physiological concentration of NO proposed by Hall & Garthwaite (2009) of 100 pM (or below) up to ~5 nM. Increased cell death usually

associated with high NO levels (Beckman & Koppenol, 1996), however, was not observed in hippocampal cultures (please refer to Appendix A; page 195), and DETA/NONOate clearly had only an inhibitory effect on the mitotic index, which decreased with an increase in donor concentration, reflective of the results by Luo et al. (2010).

This dual effect of NO, with intracellular NO mediating proliferative effects while extracellular NO exerted anti-proliferative effects, as previously described by Luo et al. (2010), demonstrates a way in which the actions of NO may be regulated. In this case, the source of NO (intracellular or extracellular) dictates the effect of NO on the proliferation of nestin$^{+}$ precursor cells. Although the mechanisms underlying the inhibitory effect of extracellular NO on my own cultures is unknown, the study by Luo et al. (2010) showed that the NO produced by nNOS in neurons deceased the proliferation of neural stem cells by exerting a negative control, possibly through cAMP-dependent protein kinase (PKA), on cAMP response element-binding (CREB) phosphorylation. This in turn inhibited nNOS expression and intracellular NO production in the neural stem cell, resulting in reduced cell proliferation. In fact, the negative role of nNOS in regulating adult neurogenesis *in vivo*, as described previously, could be as a result of the inhibitory effect mediated via the release of, possibly high concentrations, of extracellular NO by nNOS in neurons, which, due to the predominant expression of nNOS in neurons, may have surpassed the proliferative effect of intracellular NO from nNOS in neural stem cells (Luo et al., 2010). Indeed, a transient decrease in the proliferation of neural precursor cells during the early postnatal period is observed in the olfactory epithelium of nNOS knockout mice (Chen et al., 2004), which supports the involvement of nNOS in mediating neural stem/precursor cell proliferation.

### 4.4.6 Conclusions

For the first time, NPY has been shown to exert a neuroproliferative effect on rat hippocampal cells through a NO-cGMP-PKG and ERK 1/2 signalling pathway. This signalling pathway is possibly mediated entirely intracellularly with a localised release of NO. On the contrary, extracellular NO exerted anti-proliferative effects, a clear demonstration of the bifunctional nature of NO.

# Chapter 5

## Chapter 5 - A novel synthetic silica hydrogel for culturing rat hippocampal neuronal cells in three-dimensions

### 5.1 Introduction

Cell culture is an important tool for studying living cells under controlled conditions which would otherwise not be possible in intact tissues *in vivo*. Cell culture is frequently used to produce enriched or homogenous populations of desired cell types for ease of study and to decrease the uncertainty associated with interpreting the cellular target of a variety of experimental conditions or substances (Bottenstein & Sato, 1985). Advantages to cultured cells are that isolated cells allow for simple *in vitro* access for the direct application of pharmacological agents or electrophysiological studies and allows for morphological studies into cellular characteristics because of easy visual access (Brewer, 1997). An *in vitro* environment allows better control and maintenance of variables, producing uniform conditions which allow greater reproducibility to be obtained in physiological measurements and recordings than studies *in vivo* (Bottenstein & Sato, 1985). Although biomedical research is currently dominated by the growth of cells in conventional monolayers, where cells propagate in a two-dimensional (2D) environment on the surface of glass or plastic vessels, whether this is a true representation of the *in vivo* environment is uncertain (Xu et al., 2009). The *in vivo* extracellular environment, the extracellular matrix (ECM), is a dynamic and highly specialised three-dimensional (3D) environment containing diverse structures, molecules and components (Alberts et al., 2002). Specific cellular interactions exist between cells with other cells and their environment, which are important for regulating cell growth, migration and differentiation (Buck & Horwitz, 1987). Studies have shown that removing cells from their natural environment and culturing them in a restrictive 2D environment is linked with unnatural behaviour, as many features and interactions characteristic of their original environment are lost (Cukierman et al., 2002; Tibbitt & Anseth, 2009). Real-time fluorescence imaging, for example, has illustrated distinct differences in the behaviour of lymphocytes under *in vitro* conditions compared to their natural 3D environment of the intact lymph nodes, with lymphocytes showing significantly enhanced cellular movements *in vivo* (Miller et al., 2002). Similarly, Petersen et al. (1992) showed that human breast epithelial cells cultured in 2D developed like tumour cells, while normal growth behaviour was exhibited when cultured in a 3D reconstituted basement membrane. 3D cultures offer many advantages over conventional 2D cultures by allowing the combination of a controllable *in vitro* environment with features more representative of an *in vivo* environment.

I have shown that NOS and NO signalling pathways mediate the neuroproliferative effect of NPY on hippocampal cells cultured in conventional monolayers. It would be intriguing, however, to determine whether hippocampal neuronal cultures would proliferate, differentiate and interact differently to NPY in an environment which was much more comparable to an *in vivo* environment. One of the most common scaffold materials used for creating 3D cultures are hydrogels (Hoffman, 2002). These extremely hydrated hydrophilic polymeric matrices contain abundant amounts of water (typically more than 30% by weight), and in some instances, can absorb up to thousands of times their dry weight in water while still maintaining a stable 3D network (Hoffman, 2002; Kopecek, 2007). Indeed, the proposition that NPY-releasing interneurons in the dentate hilus interact with progenitors within the SGZ by releasing NPY to control their proliferation and adult hippocampal neurogenesis *in vivo* (Gray, 2008), could be investigated *in vitro*, as the unique rheological properties of many hydrogels will allow the assembly of complex 3D cultures incorporating multiple sectors consisting of different cell types i.e. NPY-releasing interneurons and nestin$^{+}$ precursor cells, and/or chemical or biological factors. With this in mind, attempts were made to develop viable 3D cultures of hippocampal cells in hydrogel matrices. 3D cell cultures using conventional hydrogels, such as collagen or polymer-based hydrogels, are frequently used for culturing a myriad of cell types, which made it appealing to try a novel synthetic silica hydrogel known as Laponite as the 3D matrix material.

### 5.1.1 Three-dimensional cell cultures

There are three main types of 3D culture, organ culture, organotypic culture and histotypic culture (Freshney, 1987). In organ culture, small fragments of organ are cultured at an air-fluid interface (to optimise gas and nutrient exchange). These tissues retain a 3D structure and possibly most of their *in vivo* functional features as the relationship and interactions between cells are still intact (Browning & Trier, 1969). This type of culture is often used to study the effect of exogenous stimuli on development, as demonstrated by Lasnitzki & Mizuno (1979), who showed the importance of the mesenchyme tissue in the induction of the rat prostate gland by androgens. Most types of organ culture are developed for the study of fragmented or whole organs and recombined tissues. Organotypic cultures, on the hand, involve the recombination of isolated cells of different lineages to recreate components of a particular organ of study (Freshney, 1987). Previous attempts to regenerate tissue-like architecture from isolated monolayer cell cultures include efforts by

Kruse & Miedema (1965), who showed that perfused monolayers could form dense multi-layers which were more than ten cells deep, whilst, in the presence of endothelial growth factor and tumour cell conditioned medium, Folkman & Haudenschild (1980) showed that capillary tubules formed in vascular endothelial cell cultures. In contrast to organ or organotypic cultures, histotypic cell culture is a technique where isolated cells are reassociated and grown to high density in an artificial 3D matrix to generate an architecture which resembles a tissue of the studied organ (Freshney, 1987). As the focus of this study, the ability to manipulate the 3D scaffold of histotypic cultures allows for unprecedented possibilities for investigating the effect of different environmental parameters on cell response. 3D histotypic cultures tend to show superior physical properties, higher complexity and enhanced cell survival compared to monolayer cultures. Additionally, advantageous aspects typical of traditional 2D cultures are retained in histotypic cultures, including the ability to control the attachment, proliferation, pharmacological and electrophysiological properties of dissociated cells, which may prove difficult under *in vivo* conditions because of the many influencing factors *in situ*.

### 5.1.2 Basic requirements of a 3D histotypic cell culture system

Most cells in conventional 2D culture are anchorage-dependent cells which grow as monolayers on the surface of a vessel, often helped by attachment factors such as poly-L-lysine for adherence (Brewer et al., 1997). In their natural 3D environment, the ECM is present not only as a scaffold to support cells, but is also important for regulating cellular interactions which ultimately determine the survival and development of the cell and tissue as a whole (Buck & Horwitz, 1987). An important requirement of a 3D histotypic culture system is the presence of a matrix which is sufficient to support the cells growing within (Hubbell, 2003). It is hard to mimic the ECM due to its highly complex nature, but attempts have been made to reproduce a similar environment *in vitro* for 3D cell culture. This biomimicry is mainly focused on reproducing the biochemical composition, fibrillar structure and viscoelastic gel-like properties (Hubbell, 2003). This has been achieved through the use of both naturally-derived and or synthetic materials to varying degrees of success.

Gas and nutrient exchange is relatively efficient in 2D cultures due to the organisation of isolated cells into monolayers, although this becomes more complicated in 3D cultures due to the presence of a 3D matrix. Depending on the type of scaffold material used,

gaseous diffusion, metabolite and nutrient exchange may be either sufficient or limited (Amsden, 1998). Gas and nutrient exchange issues have typically affected organ cultures, where large explants show central necrosis due to limited gas diffusion and nutrient exchange (Browning & Trier, 1969), although this would not be an issue in a living organism due to the diffuse vasculature present throughout tissues, which constantly regulate gas and nutrient exchange in metabolising cells (Hoffman, 2002). The ECM is also composed predominantly of hydrophilic glycosaminoglycans (GAGs) or unbranched polysaccharide chains which form a highly hydrated porous gel-like matter which permits the rapid diffusion of gases, nutrients and metabolites (Trowbridge & Gallo, 2002). These GAG gels are able to withstand vast compressive forces and form gels at low concentrations. In this aspect, hydrogels are very similar to the GAG gels making up the ECM.

### 5.1.3 Hydrogels as synthetic extracellular matrices

Hydrogels show properties similar to those of GAG gels in that many form gels at low concentrations, permit the rapid diffusion of gas and nutrients due to its highly hydrated nature, are non-toxic and are able to withstand compressive forces (Kopecek, 2007). In this sense, hydrogels are one of the best candidate materials for replacing the ECM in 3D histotypic cultures. Indeed, hyaluronic acid (HA), the simplest GAG, is used to form naturally-derived hydrogels for a range of applications (Vercruysse et al., 1997). An additional benefit to HA hydrogels is the natural degradation by hyaluronidase in the body, allowing regulation of hydrogel clearance from the body when used as tissue engineering matrices (Drury & Mooney, 2003).

Collagen, a major constituent of the mammalian ECM, is also one of the polymers most frequently used for the synthesis of hydrogels. These collagen hydrogels have been extensively used for the study of cell migration, motility and contraction (Hubbell, 2003). Elsdale & Bard (1972) were one of the first to describe a collagen substrata containing 1% collagen by weight. These 3D hydrated collagen lattices synthesised from polymerised collagen I matrices were similar to tissue matrices and induced morphological changes in fibroblasts (Elsdale & Bard, 1972). Yang et al. (1979, 1980) also demonstrated the sustained growth of primary mouse mammary tumour epithelial cells embedded within collagen hydrogels. These epithelial cells were shown to form duct-like structures which

extended into the matrix (Yang et al., 1979). Although naturally-derived hydrogels have many advantages to their use, they are limited to only a partial reconstitution of the ECM.

### 5.1.4 Mimicking the fibrillary and viscoelastic nature of the ECM

The reconstitution of specific mechanical properties of the ECM through the use of biosynthetic or synthetic materials in the hope to produce 3D matrices which are more representative of the natural ECM have been well attempted (Hubbell, 2003). Fibrillar matrices with fibre diameters in the order of tens of micrometers have been synthesised from synthetic polymers, while the process of electrospinning has been used to generate fibrillar matrices composed of even thinner fibres with diameters which are several microns down to 100 nm or less (Sun et al., 2007). This fabrication process involves the control of polymer fibre deposition through an electric field, which produces fibres with diameters more representative of those in the ECM (Matthews et al., 2002). It is possible to fabricate either random or highly complex and ordered 3D matrices. Classic polymers used for the synthesis of fibrillar matrices include synthetic aliphatic polyesters and even natural materials such as collagen and fibrinogen (Sun et al., 2007; Matthews et al., 2002; Wnek et al., 2003). Matthews at al. (2002) showed that collagen matrices produced from electrospinning promoted cell penetration, integration and growth within the matrix. To replicate the viscoelastic nature of the ECM, naturally elastic hydrogels such as alginate and the temperature-sensitive synthetic polymers poly(ethylene glycol) and poly(propylene glycol) have been extensively investigated (Cellesi et al., 2002).

### 5.1.5 Mimicking the molecular recognition properties of the ECM

In living organisms, there are both bi-directional and dynamic interactions between cells and the ECM. Many of these interactions, such as cell adhesion, influence of bound growth factors and proteolytic sensitivity, are important for normal cellular development (Alberts et al., 2002). In 2D systems these interactions may be considerably reduced, prompting research not only into the biomimicry of the ECM structure but also into the challenge of replicating the molecular recognition properties (Hubbell, 2003).

Many groups have tried to replicate the cell adhesion properties of the ECM, which is important for regulating a range of physiological responses such as cell growth and migration (Cukierman et al., 2002). Schense et al. (2000) used the enzymatic activity of Factor XIIIa to covalently incorporate exogenous bioactive peptides (adhesion domains) from laminin and N-cadherin into fibrin hydrogels. It was shown that neurite extension *in*

*vitro* and the regeneration of severed dorsal root axons in animal models was enhanced (with a maximal improvement of 75% and 85% respectively) in the presence of these peptides (Schense et al., 2000).

The presentation of growth factors is another key function of the ECM. These bound growth factors may partition from the ECM into a soluble phase to regulate an array of cellular processes (Alberts et al., 2002). Efforts to reproduce bound growth factors include the work by Sakiyama-Elbert and Hubbell (2000), in which a heparin-containing fibrin-based cell ingrowth matrix consisting mainly of fibrin, immobilised heparin-binding peptides, heparin and basic fibroblast growth factor (b-FGF) was investigated. The immobilised heparin-binding peptides contained a factor XIIIa substrate which interacts with heparin to immobilise it within the matrix, allowing heparin in turn to interact with b-FGF. This model system showed a slow, controlled local release of b-FGF by passive diffusion or enzymatic factors (e.g. heparinase or plasmin) released from cells, which enhanced neurite extension from dorsal root ganglia by up to 100% relative to neurite extension in fibrin matrices which were not modified. Without this delivery system, neurite extension in fibrin matrices was not enhanced by the presence of free b-FGF (Sakiyama-Elbert & Hubbell, 2000).

Homeostatic regulation *in vivo* may also be lost in an *in vitro* environment. Efforts to replace homeostasis include hormone supplements in the culture medium (Yang et al., 1981). In the context of 3D cultures, studies on the effects of hormones (insulin and cortisol) and growth factors (epidermal growth factor) on primary human mammary epithelial cells in collagen hydrogel culture by Yang et al. (1981) showed that hormone and growth factor supplement sustained growth over the first 2 to 3 weeks which lead to a 10- to 30-fold increase in cell number.

The proteolytic sensitivity of the ECM is important in permitting cell migration. Materials which are sensitive to proteases expressed by migrating cells have been developed, including a synthetic hydrogel system incorporating the ability to present bound growth factors, adhesion peptides and show proteolytic sensitivity (Lutolf et al., 2003). In this system created by Lutolf et al. (2003), multifunctional poly(ethylene glycol) is crosslinked with a di-cysteine peptide containing a proteolytically sensitive sequence through a Michael-type addition reaction to form a synthetic hydrogel network. Adhesion

peptides and growth factors were incorporated through reaction via cysteine residues (adhesion peptides and growth factors) or entrapment (growth factors) and cells incorporated within the synthetic matrix were viable and able to migrate three-dimensionally via proteolytic degradation of the hydrogel (Lutolf et al., 2003).

These materials demonstrate the remarkable ability by which we can now imitate the many properties of the ECM, but by no means are these synthetic imitations complete. Through greater understanding of the biology and mechanisms of the ECM and further development of synthetic or biomaterials, we will ultimately be able to generate 3D matrices which replicate more fully the unique ECM.

### 5.1.6 The aims of this chapter

3D cell culture models truly reflective of *in vivo* environments will be valuable for future biomedical research, however, 3D hydrogel cultures are currently dominated by the use of only a handful of hydrogels (e.g. collagen), although there are a vast range of other hydrogels which may provide far superior properties to those at current. Laponite, a synthetic silica hydrogel, is an attractive alternative because of its appealing rheological properties. Laponite dispersions are thixotropic (Martin, 2002), which means they show time-dependent changes in viscosity. The rheological characteristics and handling properties of the Laponite hydrogels, as well as their potential for creating 3D multi-layered or multi-sectored matrices, were investigated prior to this chapter and covered in detail in Appendix B (pages 199 to 230). Furthermore, in order to optimise the survival of hippocampal cultures in Laponite, thixotropic culture medium-based Laponite hydrogels were also developed (please refer to Appendix B; pages 199 to 230). The aims of this chapter were to determine the viability of hippocampal cells in this novel culture medium-based Laponite hydrogel and the potential for using Laponite hydrogels as a cell culture matrix.

## 5.2 Methods

### 5.2.1 Methodology and experimental aim

Laponite RDS (rapid diffusion sol) is one of a variety of Laponite formulations (Rockwood additives Ltd.). Thixotropic culture medium-based Laponite RDS hydrogels were the key findings of previous investigations (please refer to Appendix B; pages 199 to 230). 16% w/v Laponite RDS produced the optimal culture medium-based hydrogel, which was investigated in the present study for its potential as a cell culture matrix for hippocampal cells. Laponite XLS, the low heavy metal content variation of RDS, was also explored. A range of dyes and staining techniques was used to determine whether Laponite was a biocompatible hydrogel. A brief description of the fluorescent dyes and abbreviations used are listed in Table 5.2.1.

Table 5.2.1 Fluorescent dyes and stains

| Fluorescent Dye | Company | Concentration | Description |
|---|---|---|---|
| Mitotracker green (**MTG**) | Life Technologies, Paisley, UK | 100 nM | Green-fluorescent mitochondrial stain: live cell |
| Mitotracker orange (**MTO**) | Life Technologies, Paisley, UK | 200 nM | Red-fluorescent mitochondrial stain: live cell |
| Vybrant Carbocyanine cell-labelling solution (**CM-DiI**) | Life Technologies, Paisley, UK | 5 µl/ml | Red-fluorescent lipophilic membrane dye: live cell |
| Propidium Iodide (**PI**) (1mg/ml stock) | Sigma Aldrich, UK | 5 µl/ml (7.5 µM) | Red-fluorescent nucleic acid stain: dead cell |
| Sytox green | Life Technologies, Paisley, UK | 50-500 nM | Green-fluorescent nucleic acid stain: dead cell |
| 4',6-diamidino-2-phenylindole (**DAPI**) (1mg/ml stock) | Sigma Aldrich, UK | 20 µl/ml (57 µM) | Blue-fluorescent nucleic acid stain: live and dead cells |

### 5.2.2 Primary hippocampal neuronal culture generation

The generation of primary hippocampal monolayer cultures is provided in Chapter 2.

#### 5.2.2.1 Neurosphere generation

Neurospheres are free-floating non-adherent spherical aggregates of neural stem cells (Bez et al., 2003). 6-well polystyrene multiwell plates were used to cultivate neurospheres. 2

ml/well of cell suspension in NBA-A/B27/Glu at a cell density of 100,000 cells/ml were transferred into non-surface treated 6-well plates (210 cells/$mm^2$). The cell suspension was supplemented with 1% antibiotic/antimycotic, 20 ng/ml EGF and 20 ng/ml bFGF. Cells were incubated under 5% $CO_2$, 95% air (~20% $O_2$), 37°C and 100% humidity conditions.

After 7-10 d, half of the neurosphere growth media was changed. Neurosphere cultures from a 6-well plate (12 ml) were collected into a 15 ml centrifuge tube and centrifuged for 5 min at 200g at room temperature. After centrifugation, half of the medium was carefully aspirated and discarded and replaced with fresh pre-warmed NBA-A/B27/Glu medium supplemented with 1% antibiotic/antimycotic, 20 ng/ml EGF and 20 ng/ml bFGF. The neurospheres were gently triturated back into suspension and re-plated onto a new plate. Thereafter, half of the neurosphere culture medium was changed every 2-3 d.

#### 5.2.2.2 Passaging neurospheres

After 14 d of culture, neurospheres were passaged to expand cultures. Neurosphere cultures from a 6-well plate (12 ml) were collected into a 15 ml tube and centrifuged for 5 min at 200g at room temperature. After centrifugation the supernatant was aspirated, leaving only 1 ml of supernatant and the cell pellet. Using a 1 ml pipette, the cell pellet was broken up with gentle trituration. Trituration was repeated several times to dissociate the neurospheres into single cells until a cloudy suspension was obtained.

To determine the number of viable cells, 30 µl of cell suspension was mixed with 50 µl Trypan blue (Sigma Aldrich, UK), transferred onto a haemocytometer slide and live (dye-excluding) cells counted. The cells were re-plated at 2 ml/well of cell suspension in NBA-A/B27/Glu at a cell density of 100,000 cells/ml (210 cells/$mm^2$). supplemented with 1% antibiotic/antimycotic, 20 ng/ml EGF and 20 ng/ml bFGF.

#### 5.2.2.3 Cryopreservation of neurospheres

Neurosphere cultures from a 6-well plate (12 ml) were collected into a 15 ml centrifuge tube and centrifuged for 5 min at 200g at room temperature. The supernatant was removed and discarded and the cell pellet gently re-suspended in 10 ml NBA-A/B27/Glu serum-free medium containing 15 mM 4-(2-hydroxyethyl)-1-piperazineethanesulfonic acid (HEPES) buffer (Sigma Aldrich, UK) and 15% dimethyl sulfoxide (DMSO) (Sigma Aldrich, UK). The neurosphere suspension was aliquoted into 1.5 ml aliquots per 2 ml capacity polypropylene cryovials and transferred to a -80°C freezer.

#### 5.2.2.4 Monolayer dissociation from multiwell plates using Trypsin-EDTA

The culture medium was carefully aspirated off the plates before addition of 500 µl (24-well plate) or 1 ml (6-well plate) Trypsin-EDTA (ethylenediaminetetraacetic acid) (Sigma Aldrich, UK) to each well. After 5 min, the Trypsin-EDTA was stopped with the addition of 10% FBS (50 µl in a 24 well plate or 100 µl in a 6-well plate) (Sigma Aldrich, UK). The cells were gently rinsed off the plate (3/4 times per well) before transfer to a 15 ml tube. The cell suspension was centrifuged at 1100 rpm for 5 min followed by removal of the supernatant and Trypsin-EDTA. Fresh medium (about 2 ml) was added and the cells released from the pellet by gentle trituration. The cellular density was determined by using a haemocytometer and Trypan blue, diluted as required and used immediately.

### 5.2.3 Laponite RDS and Laponite XLS hydrogel formation - Sterile conditions

Laponite RDS and Laponite XLS (low heavy metal content version of RDS) powder (courtesy of Mr Patrick Jenness, Rockwood Additives Ltd.) was autoclaved before use (autoclaving does not affect hydrogel formation). The balance was wiped down with 70% ethanol, glass weighing boats and spatulas used for measuring out the powder were autoclaved, and all procedures carried out in sterile hoods. All equipment brought into the sterile hoods was disinfected using 70% ethanol spray. To keep the measured Laponite powder sterile during transitions between hoods, measured powder was transferred into sterile 15 ml centrifuge tubes. After the addition of Laponite powder to culture medium (NBA-A/B27/Glu medium supplemented with 1% antibiotic/antimycotic), the sample was quickly vortexed for at least 10 s outside the hood. To ensure sterility during this process, the sample was made up in 15 ml or 50 ml (depending on the amount of hydrogel) centrifuge tubes and the lid tightly screwed onto the top of the tube before transferring the tube out of the sterile hood for vortexing. After vortex, the tube was disinfected with 70% ethanol before transfer back into the sterile hood. The hydrogel setting times differed depending on the concentration (% w/v) and type of Laponite (RDS or XLS).

Different thicknesses of gel could be achieved by using the formula:
$\pi$ x radius$^2$ (mm) x height (mm) = volume required (µl), with details of the well diameter or radius. For example, to create a 2 mm thick hydrogel layer in a 6-well plate which has a diameter of 34.8 mm (17.4 mm radius) the volume required is 3.14 x 17.4$^2$ x 2 mm = 1902.3 µl.

### 5.2.4 pH of Laponite RDS culture medium hydrogels

The pH of Laponite hydrogels was measured using a pH meter (pH 210 advanced microprocessor based bench pH meter, Hanna Instruments, Norway). HEPES buffer ($pK_a$ = 7.55) (Sigma Aldrich, UK), an organic zwitterionic buffer (pH range 7-8) widely used in cell culture, was chosen as the buffering agent for 16% Laponite RDS culture medium hydrogels. To find the optimum concentration of HEPES for buffering, a range of concentrations of HEPES (0, 10, 15, 20, 25, 30, 35, 40, 45 mM final concentration in hydrogel) was prepared. The pH of the culture medium was measured before and after the addition of 16% Laponite RDS at room temperature. The pH probe was calibrated and rinsed carefully between each use and each measurement was repeated 5 times.

### 5.2.5 Laponite RDS culture medium hydrogels

Laponite RDS/XLS culture medium hydrogels were prepared by adding 12-16% Laponite RDS/XLS powder (w/v) to neat culture medium (NBA/B27/Glu) supplemented with 35 mM HEPES, 1% antibiotic/antimycotic and/or growth factors/serum (EGF/FGF/FBS). Although Laponite RDS/XLS preparations below 15% did not form full hydrogels, a range of Laponite RDS/XLS concentrations were investigated to test the biocompatibility of Laponite. The preparations were vortexed to ensure thorough dispersion of Laponite powder before use and transferred via pipettes with cut pipette tips to overcome blockage.

### 5.2.6 Seeding and embedding cells on and in Laponite RDS hydrogels

Cells were seeded onto and embedded within Laponite RDS hydrogels to assess the potential for Laponite as a cell culture material. For cell seeding, 1 to 2 mm thick 16% Laponite RDS culture medium hydrogels were layered in 6- or 24-well multiwell plates and allowed to set. Hippocampal cells obtained through either primary hippocampal culture generation or Trypsin dissociation of existing monolayer cultures were seeded onto the top of Laponite RDS hydrogels at different cell densities (ranging from 100,000 to 300,000 cells/ml) and followed over time.

For cell embedding, 16% Laponite RDS powder (w/v) was added to culture medium containing hippocampal cells (100,000 cells/ml) obtained through either primary hippocampal culture generation or Trypsin dissociation of existing monolayer cultures. The preparation was vortexed for about 5 s to ensure thorough dispersion of Laponite powder before the hydrogel/cells were transferred to 6- or 24-well multiwell plates to

create gels of about 1-2 mm thickness. 500 µl of growth media (NBA/B27/Glu) was transferred on top of the gels to minimise gel desiccation.

All seeded and embedded cultures were maintained at 37ºC, 100% humidity, 5% $CO_2$ and 95% air (~20% $O_2$). A variety of fluorescent dyes were used to help with cell visualisation (Table 3.2.1). Fluorescence cell visualisation was performed on an inverted DM IRB microscope (Leica Microsystems UK Ltd, Milton Keynes, UK) and analysed using Volocity imaging software 4.2.0 (Improvision, Lexington, MA, USA).

### 5.2.7 Laponite hydrogel autofluorescence

Laponite hydrogels were tested for autofluorescence. 5% Laponite RD (rapid diffusion) water-based hydrogels, 16% Laponite RDS Neurobasal A medium hydrogels and 16% Laponite RDS culture medium (NBA/B27/Glu) hydrogels were prepared and layered in a 24-well plate at thicknesses of 1-2 mm. The hydrogels were then exposed to a range of fluorescent excitation wavelengths (456 nm, 520 nm and 640 nm) at different intensities (50 msec to 1 sec exposure) to test for autofluorescence.

### 5.2.8 Staining and embedding neurospheres in hydrogels

Neurosphere cultures were stained with one of two fluorescent dyes, DAPI or CM-DiI. After 40 min incubation time, the neurospheres were transferred to individual 15 ml tubes and allowed to settle. The liquid medium above the settled neurospheres was carefully aspirated and replaced with pre-warmed culture medium (NBA/B27/Glu). After gentle inversion of the tubes to mix the neurospheres, they were allowed to settle before the liquid medium was removed and replaced with fresh media. This rinsing process was repeated 3 times to remove excess dye.

Subsequently, 1% antibiotic/antimycotic and 35 mM HEPES buffer was added to the neurosphere suspension before the addition of 16% Laponite RDS powder (w/v) followed by vortexing for 10 s. The preparation was quickly plated at 1 mm hydrogel thickness in 6-well (1000 µl) and 24-well (200 µl) multiwell plates and covered with 1000 µl or 500 µl culture medium respectively to avoid gel desiccation. Neurosphere in hydrogel cultures were maintained at 37ºC, 100% humidity, 5% $CO_2$ and 95% air (~20% $O_2$). Fluorescence cell visualisation was performed on an inverted Leica DM IRB microscope and analysed using Volocity imaging software.

### 5.2.9 Seeding neurospheres onto semi-set Laponite hydrogels

Neurospheres were stained with DAPI or CM-DiI following the protocol described in section 5.2.8. Laponite RDS culture medium hydrogels with 1% antibiotic/antimycotic were prepared at the concentration and vortex times shown in table 5.2.2. Similarly, a range of Laponite RDS concentrations were used to investigate Laponite biocompatibility regardless of hydrogel formation.

Table 5.2.2 Laponite RDS concentration and vortex times for neurosphere seeding

| Laponite RDS concentration (w/v) | Vortex times |
|---|---|
| - 10% RDS | - 30 s<br>- 2 min |
| - 12% RDS | - 30 s<br>- 2 min |
| - 14% RDS | - 30 s<br>- 2 min |
| - 16% RDS | - 30 s<br>- 2 min |

The prepared hydrogels were plated in 24-well multiwell plates at 200 µl per well (1 mm hydrogel thickness) and, before the hydrogels were set, 100 µl of stained neurospheres were transferred on top. Culture medium with no cells/neurospheres was transferred onto the top of control cultures. All seeded neurosphere cultures were maintained at 37ºC, 100% humidity, 5% $CO_2$ and 95% air (~20% $O_2$). PI and MTG staining was used to investigate cell death and survival. Fluorescence cell visualisation was performed on an inverted Leica DM IRB microscope and analysed using Volocity imaging software.

### 5.2.10 Layering Laponite hydrogels over hippocampal monolayers

Hippocampal monolayer cultures were pre-stained with CM-DiI or MTG. After 40 min incubation, monolayers were rinsed 3 times with fresh medium before all the medium was carefully aspirated and a 1 mm layer of Laponite hydrogel (with 1% antibiotic/antimycotic) transferred over the top. The hydrogel was allowed to set before culture medium was transferred over the top of the hydrogels to prevent gel desiccation. The medium in control cultures were changed with fresh medium but had no hydrogel transferred over the top. A range of conditions was investigated, including:

1. 16% Laponite RDS or XLS culture medium hydrogels
2. Buffered (35 mM HEPES) and non-buffered hydrogels
3. Varying Laponite concentration (2-16% w/v) to investigate biocompatibility.
4. Cultures of different age (1 d to 7 d plus)
5. Incorporation of growth factors (EGF/FGF)
6. Staining cultures before or after hydrogel application or after a period of time (h to d).

All monolayer cultures were maintained at 37ºC, 100% humidity, 5% $CO_2$ and 95% air (~20% $O_2$). Accounting for the hydrogel volume, MTG, Sytox green and PI were used to investigate cell viability and cell death, respectively. Fluorescence cell visualisation was performed on an inverted Leica DM IRB microscope and analysed using Volocity imaging software.

### 5.2.11 PI incorporation into hydrogels to assess cell death in hydrogel-covered monolayers

PI (5 µl/ml) was incorporated into 16% Laponite hydrogels by prior addition to culture medium (NBA/B27/Glu) supplemented with 1% antibiotic/antimycotic, EGF/FGF and 35 mM HEPES buffer before the addition of Laponite powder. The PI containing hydrogels were transferred onto hippocampal monolayer cultures at 1 mm thickness in 24-well multiwell plates. The parameters were as follows:

1. PI incorporated into hydrogel transferred over hippocampal monolayers
2. Control: hydrogel with no PI transferred over hippocampal monolayers
3. Control: PI in culture medium over hippocampal monolayers
4. Control: hippocampal monolayers in culture medium with no hydrogel or PI addition
5. Control: PI incorporated into hydrogel – no cells
6. Control: hydrogel with no PI – no cells

Culture medium (500 µl/well) was transferred over hydrogels after setting and the cultures followed over time. Fluorescence visualisation was performed on an inverted Leica DM IRB microscope and analysed using Volocity imaging software. Plates were imaged: immediately after, 1 h after and every 2 h/d afterwards, as necessary. All

monolayer cultures were maintained at 37ºC, 100% humidity, 5% $CO_2$ and 95% air (~20% $O_2$).

### 5.2.12 Pre-staining monolayers with PI and Sytox green to assess cell death

Hippocampal monolayer cultures were stained with PI (5 µl/ml) and Sytox green (0.01 µl/ml) for 40 min before rinsing 3 times with fresh culture medium. After staining, culture medium was aspirated (400 µl) from each well leaving 100 µl of dye containing medium. 16% Laponite RDS culture medium hydrogels or culture medium were transferred over wells and the cultures maintained at 37ºC, 100% humidity, 5% $CO_2$ and 95% air (~20% $O_2$). The parameters were as follows:

1. PI or Sytox stained monolayers covered with 1 mm 16% RDS culture medium hydrogel
2. Negative control: PI or Sytox stained monolayers with culture medium (no hydrogel)
3. Positive control: PI or Sytox stained monolayer cells killed with 4% PFA (15 min treatment) covered with 1 mm 16% RDS culture medium gel
4. Control: unstained monolayers covered with 1 mm 16% RDS culture medium hydrogel

Cultures were imaged directly after the addition of hydrogel and followed over time. Fluorescence visualisation was performed on an inverted Leica DM IRB microscope and analysed using Volocity imaging software.

### 5.2.13 Insert cultures

Hippocampal monolayers grown on culture inserts allow an alternative access route (from underneath the insert), potentially useful in determining cell viability and hydrogel biocompatibility under gel cover. A range of culture inserts were investigated for optimal cell growth.

1. Millipore polytetrafluoroethene (PTFE) 6-Well Millicell Inserts (0.4 µm pore) – (Millipore, UK)
2. Millipore polyethylene terephthalate (PET) 6-Well Millicell Hanging Inserts (0.4 µm pore) – (Millipore, UK)
3. Greiner Lumox PetriPERM 35 hydrophilic culture dishes (adherent surface) – (Sigma Aldrich, UK)

### 5.2.14 Optimising hippocampal monolayers on inserts

Millipore PTFE well inserts require coating for adherence of hippocampal monolayer cultures. A variety of coating techniques were investigated to find one which produced optimal cell growth. The parameters were as follows:

1. Non-treated Millipore PTFE inserts
2. Millipore PTFE inserts coated with poly-L-lysine for 1 h (500 µl/well)
3. Millipore inserts technical note protocol (see Appendix C, page 233).
4. Sigma laminin technical note protocol (Sigma Aldrich, UK) (see Appendix C, page 233).

Primary hippocampal cell suspensions of 100,000 cells/ml were transferred over coating-treated inserts and maintained in basic growth media (NBA/B27/Glu/1% antibiotic/antimycotic) at 37ºC, 100% humidity, 5% $CO_2$ and 95% air (~20% $O_2$). The confluence of cultures achieved by the different coatings were compared.

### 5.2.15 Layering hydrogels over culture insert hippocampal monolayers

Similar to section 5.2.10, Laponite RDS/XLS culture medium hydrogels supplemented with 1% antibiotic/antimycotic and/or buffer (35 mM HEPES) and growth factors (20 ng/ml EGF/FGF) were transferred over insert monolayer cultures at gel thicknesses of ~1 mm. A variety of fluorescent dyes/stains were used to assess cell viability and death, including MTG, MTO, CM-DiI, PI and Sytox green, by staining the hydrogel from underneath. A range of dye combinations were explored:

1. Hippocampal monolayers were pre-stained with CM-DiI (5 µl/ml) before covered with hydrogel and stained from underneath with Sytox green (0.01 µl/ml).
2. Hippocampal monolayers were covered with hydrogel and stained from underneath with a mixture of MTG (1 µl/ml) and PI (5 µl/ml).
3. Hippocampal monolayers were covered with hydrogel and stained from underneath with a mixture of MTO (200 nM) and Sytox green (0.01-0.1 µl/ml).

Fluorescent dyes were applied at different time points i.e. after different lengths of hydrogel exposure, and cultures were also imaged at different times i.e. immediately or a few h/d after gel cover. Insert controls included hippocampal monolayers with no hydrogel over the top, inserts with no cells with hydrogel over the top, and inserts with no cells or hydrogel. All insert cultures were maintained at 37ºC, 100% humidity, 5% $CO_2$ and 95% air (~20% $O_2$).

### 5.2.16 CM-DiI stained cell seeding and embedding

Hippocampal monolayer cultures were pre-stained with CM-DiI (5 µl/ml) for 40 min, washed well in culture medium and dissociated from plates using Trypsin-EDTA (section 5.2.2.4). Dissociated cells were seeded at 500 µl/well over 1 mm thick Laponite hydrogels plated in 24-well multiwell plates. Parameters investigated included:

1. 12% or 16% Laponite RDS/XLS culture medium hydrogels supplemented with 1% antibiotic/antimycotic, growth factors (EGF/FGF) and/or buffer (35 mM HEPES).
2. 12% or 16% Laponite RDS/XLS culture medium hydrogels supplemented with 1% antibiotic/antimycotic, growth factors (EGF/FGF), and laminin (5 µl/ml) (Sigma Aldrich, UK) and/or buffer (35 mM HEPES).

Cell embedding was also attempted using CM-DiI pre-stained dissociated hippocampal cells. For a gentler incorporation of cells into the Laponite hydrogel, Laponite powder was first made up in half the culture media of the final desired volume, which was subsequently gently mixed using a pipette with the other half of the culture medium containing CM-DiI stained cells. For example, for a 10 ml final volume of 16% Laponite hydrogel, 16% w/v of Laponite powder was added to 5 ml of culture media and thoroughly vortexed to disperse the powder evenly. This gel was then mixed with 5 ml of culture medium containing cells to give a final 10 ml of 16% Laponite hydrogel containing cells.

Culture medium (500 µl/well) containing no cells was transferred over control hydrogel. Cultures were imaged immediately after cell seeding or embedding and followed over time. All seeded or embedded cultures were maintained at 37ºC, 100% humidity, 5% $CO_2$ and 95% air (~20% $O_2$). Fluorescent cell visualisation was performed on an inverted Leica DM IRB microscope and analysed using Volocity imaging software.

### 5.2.17 Osmolarity of Laponite hydrogels

The osmolarity of Laponite RDS culture medium hydrogels (Table 5.2.3) was measured using an osmometer (Advanced Micro Osmometer Model 3300).

Table 5.2.3 Variations of Laponite RDS culture medium hydrogels tested.

| **Non-buffered Laponite RDS culture medium hydrogels** | **Buffered Laponite RDS culture medium hydrogels (35 mM HEPES)** |
|---|---|
| - 10% Laponite RDS<br>- 12% Laponite RDS<br>- 14% Laponite RDS<br>- 16% Laponite RDS<br>- 18% Laponite RDS<br>- 20% Laponite RDS | - 10% Laponite RDS<br>- 12% Laponite RDS<br>- 14% Laponite RDS<br>- 16% Laponite RDS<br>- 18% Laponite RDS<br>- 20% Laponite RDS |

The osmolarity of plain culture medium and of the hydrogels were measured at room temperature. Each measurement was repeated 5 times, with new samples each time.

## 5.3 Results

### 5.3.1 Seeded or embedded hippocampal cells are difficult to visualise without pre-staining

Hippocampal neuronal cells were seeded onto or embedded within 16% Laponite RDS culture medium hydrogels. Determination of cell viability via visualisation under an inverted light transmission microscope (Leica DM IRB) proved inconclusive due to difficulties in cell identification. As can be observed in control Laponite hydrogels (with no cell seeding or embedding), the hydrogel itself was inhomogeneous and contained many natural structures which were quite cell-like in appearance (Fig. 5.3.1). This presented a diverse background which made cellular identification complicated in both seeded and embedded cultures.

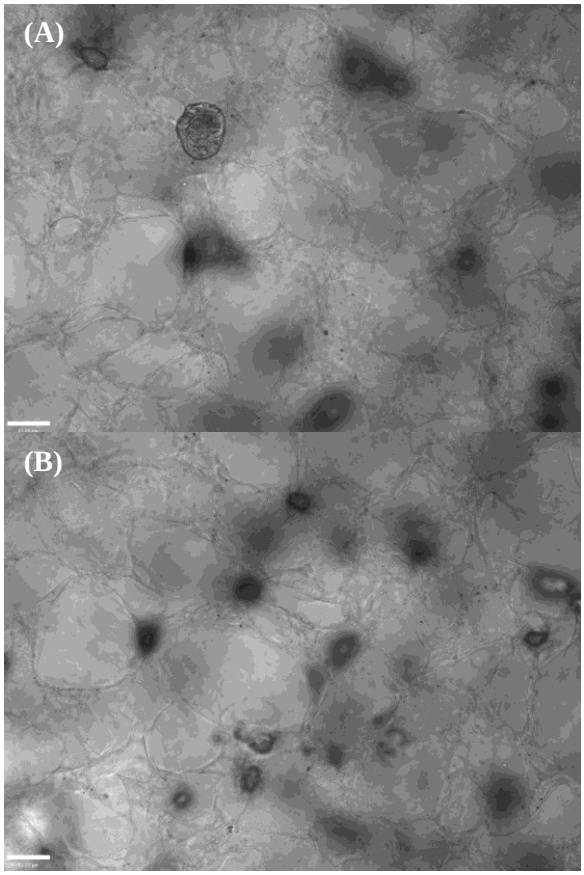


Figure 5.3.1 Seeded hippocampal cells were difficult to visualise without pre-staining. 16% Laponite RDS culture medium hydrogels under light transmission with (A) no hippocampal cells seeded on top (control) and (B) with hippocampal cells in culture medium seeded on top. The natural inhomogeneous structures within Laponite made cell identification difficult. Scale bar, 50 μm.

Viability indicators such as DAPI, MTG, PI and Sytox green were added to aid with cell visualisation. Unfortunately, fluorescent dye addition resulted in dye-gel binding and high background fluorescence, irrespective of the dye used (Fig. 5.3.2).

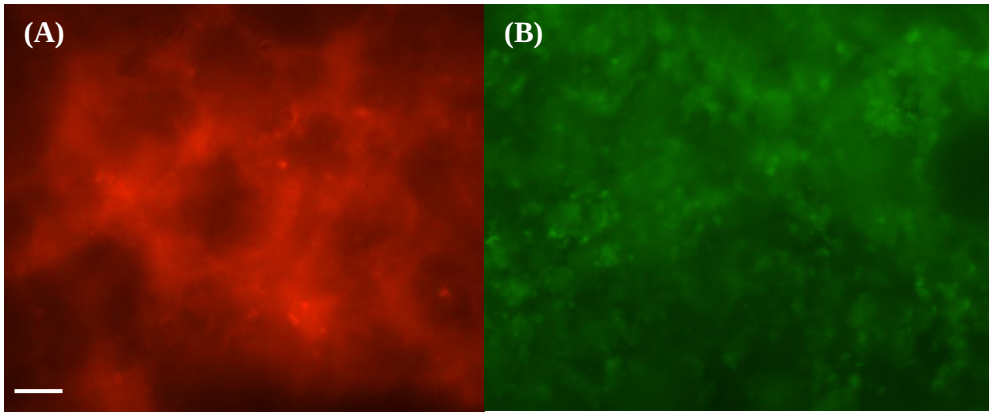


Figure 5.3.2 Laponite RDS culture medium hydrogels under fluorescence microscopy with (A) PI staining and (B) Sytox green staining, which bound and produced high background fluorescence. Scale bar, 50 μm.

### 5.3.2 Laponite hydrogels are not autofluorescent

Autofluorescence is a type of endogenous self-induced fluorescence that has no association with the fluorophore of interest. To rule out the possibility of autofluorescence as a cause of the high background fluorescence observed on fluorescent dye addition, a variety of Laponite hydrogels (5% Laponite RD water-based, 16% Laponite RDS Neurobasal A medium and 16% Laponite RDS culture medium hydrogels) were exposed to a range of fluorescent excitation wavelengths at different intensities. All types of Laponite hydrogel showed zero/minimal autofluorescence at excitation intensities/exposure typically used for fluorescence dye visualisation (100-500 ms) or higher exposures (500 ms to 1 s) (Fig. 5.3.3). This suggested that the high background fluorescence, as observed in Fig. 5.3.2, was caused by bound fluorescent dye.

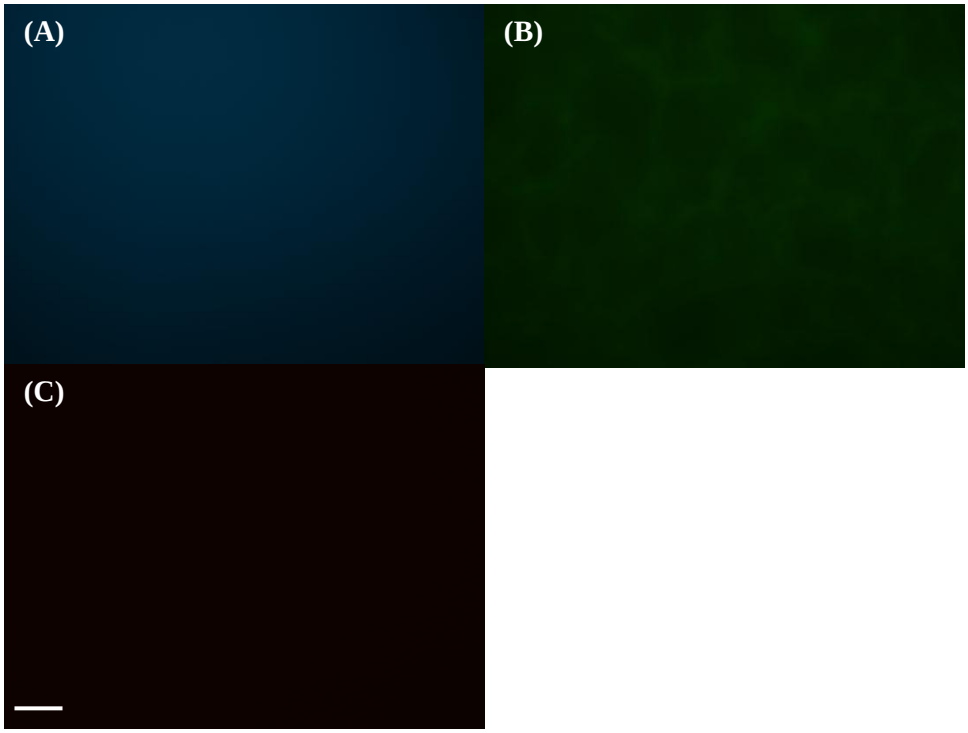


Figure 5.3.3 Laponite RDS culture medium hydrogels under fluorescence microscopy were not autofluorescent. Excitation wavelengths are (A) 456 nm, (B) 520 nm and (C) 640 nm respectively. No significant fluorescent emission was observed in response to excitation. Scale bar, 50 μm.

### 5.3.3 The high pH of Laponite RDS culture medium hydrogels can be corrected through the use of HEPES buffer

The pH indicator phenol red is routinely added to basal growth media as a basic means of monitoring media pH. Phenol red shows a colour variation from yellow to red/pink which corresponds to a gradual increase in pH. 16% Laponite RDS culture medium hydrogels are pink, which indicates a pH above 8. Measurement with a pH meter confirmed the pH of 16% Laponite RDS culture medium hydrogels as pH 8.6, whilst the pH of culture medium (NBA-A/B27/Glu) without Laponite was pH 7.2. As the normal physiological pH range for hippocampal cell viability is around pH 7.2-7.6, the Laponite hydrogels were too alkali. HEPES buffer was chosen to reduce and control the pH of Laponite hydrogels. The buffer was first tested for any effects on Laponite hydrogel formation. The addition of 10 to 45 mM HEPES to 16% Laponite culture medium hydrogels did not affect gel formation and all set within 10 min at room temperature.

An increase in HEPES concentration resulted in a decrease in the pH of 16% Laponite RDS culture medium hydrogels (Fig. 5.3.4). On addition of 25 mM HEPES, the pH of the

hydrogels were reduced to pH 8.0, a pH decrease of 7% compared to non-buffered controls. However, the trend for decreasing pH with increasing HEPES concentration levels off after 30 mM HEPES, where the percentage pH reduction becomes less marked with increasing HEPES. A 35 mM concentration of HEPES was chosen for buffering 16% Laponite culture medium hydrogels as higher concentrations had no more effect on pH reduction. This concentration reduced the pH of the 16% Laponite RDS culture medium hydrogels by 9.3% to pH 7.8.

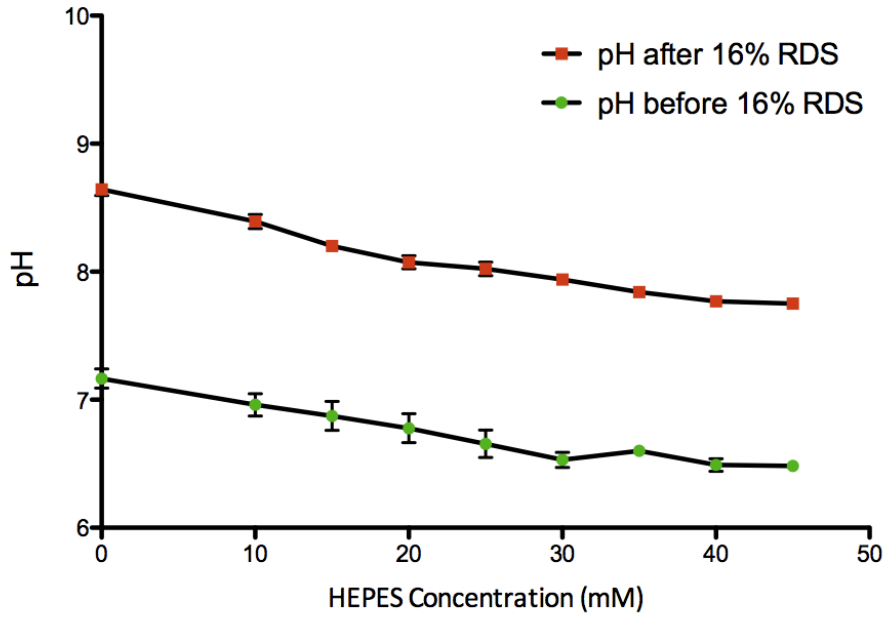


Figure 5.3.4 Effect of HEPES buffer concentration on culture medium pH before and after the addition of 16% Laponite RDS. An increase in HEPES concentration correlates with a decrease in culture medium (green line) and hydrogel (red line) pH. The effect of increasing HEPES concentration on reducing pH starts to plateau at 30 mM HEPES concentration.

### 5.3.4 Neurospheres can be pre-stained and seeded over or embedded within Laponite hydrogels

To overcome the problem of high background fluorescence caused by dye binding to Laponite hydrogel, cells were pre-stained before incorporation. The comparatively large size (100 μm plus) of neurospheres ensured easy cell visualisation and identification. Neurospheres pre-stained with DAPI or CM-DiI were embedded within Laponite RDS culture medium hydrogels (Fig. 5.3.5).

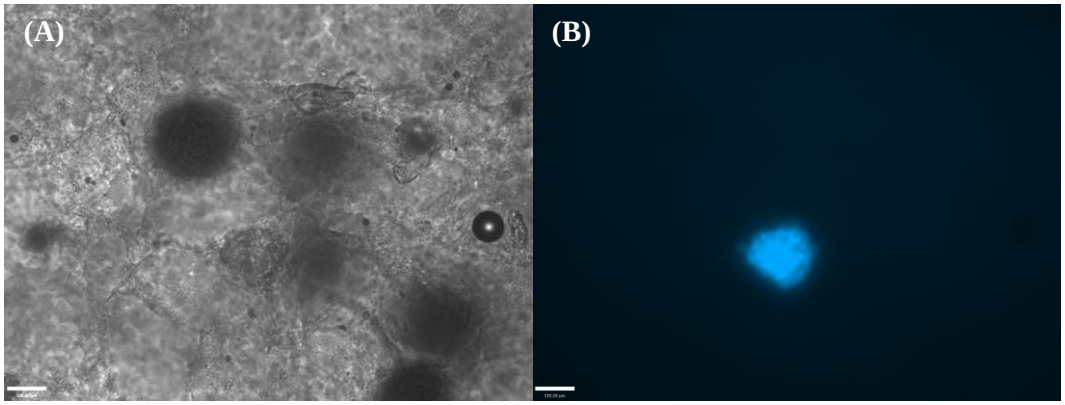


Figure 5.3.5 Laponite hydrogel embedded DAPI pre-stained neurosphere under (A) light transmission and (B) fluorescence microscopy. It would have been difficult to identify the neurosphere if it had not been pre-stained with DAPI. Scale bar, 100 μm.

Neurospheres were also seeded over varying concentrations of Laponite culture medium hydrogel to determine whether hydrogel concentration or vortex time affected neurosphere incorporation (Table 5.2.2). Seeded neurospheres remained adhered to the surface of all Laponite hydrogels, irrespective of gel concentration or vortex time, and did not show any visible integration or movement in the hydrogel over time (Fig. 5.3.6A,B). The fluorescent dyes PI and MTG were used to assess neurosphere survival by direct application and, as expected, bound to the hydrogel and caused high background fluorescence with no convincing staining indicative of viability (Fig. 5.3.6C).

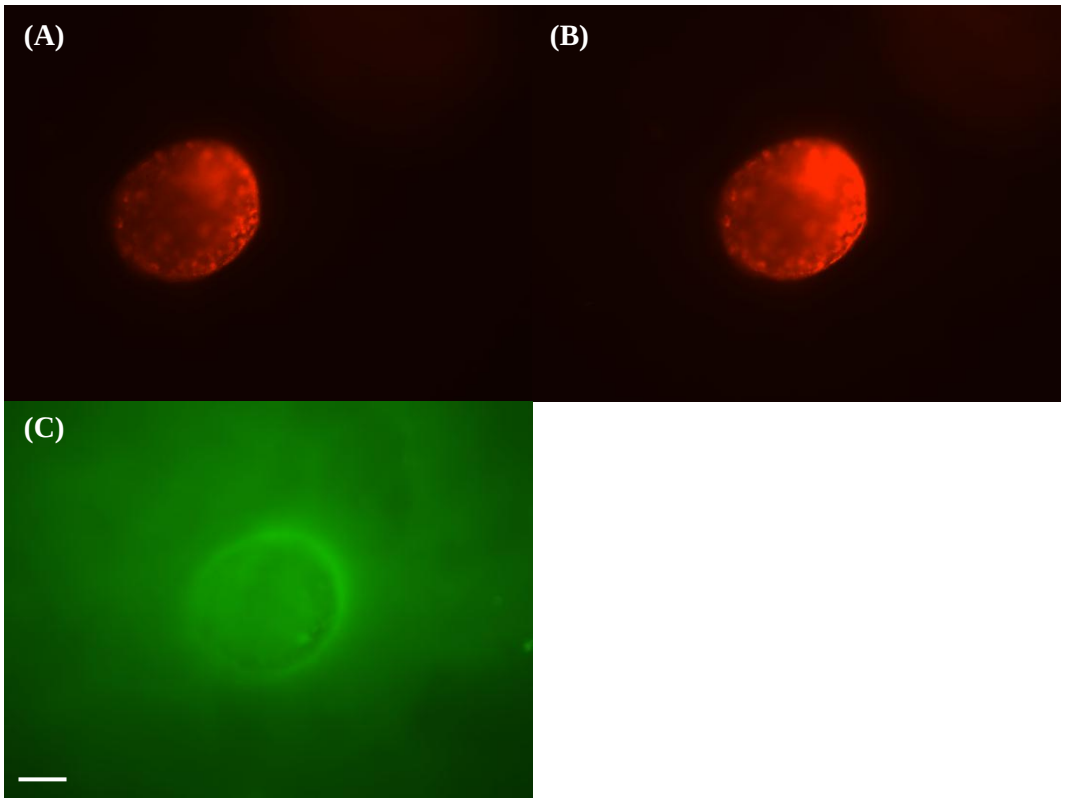


Figure 5.3.6 CM-DiI-stained neurosphere seeded over 10% Laponite RDS culture medium hydrogel after (A) 10 d and (B) 2 wk in culture, under fluorescence microscopy. (B) Direct addition of MTG stain to assess cell survival. There was high background fluorescence due to dye-gel binding and no convincing MTG staining was achieved. Scale bar, 100 μm.

In both embedded and seeded neurosphere cultures, neurospheres were dispersed throughout the Laponite hydrogels or spread across the surface at different gel depths, which proved difficult for following neurospheres over time. It was also hard to follow the response i.e. the movement or cell death of individual cells when focusing on these large cell aggregates. Other methods may prove far more appropriate for investigating cell viability.

### 5.3.5 Hippocampal monolayers can be followed over time under Laponite hydrogels

Given the success of pre-staining neurospheres before hydrogel exposure, a similar method was applied to dissociated cells in monolayer culture. Hippocampal monolayers pre-stained with CM-DiI or MTG were covered by a 1 mm layer of Laponite culture medium hydrogel and followed over time to assess the biocompatibility of the gel. Pre-stained monolayers and individual cells could be observed easily under the hydrogel (Fig. 5.3.7) and a range of influencing factors were investigated (section 5.2.10).

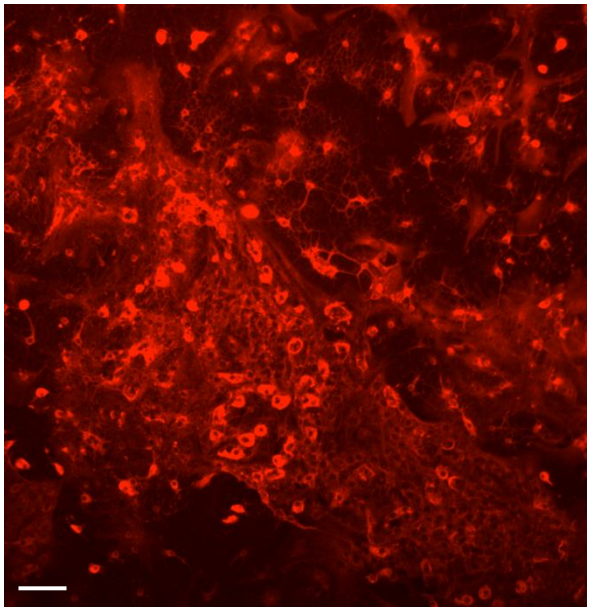

Figure 5.3.7 CM-DiI-stained 7 day old hippocampal monolayer culture covered with 16% Laponite RDS culture medium hydrogel visualised under fluorescence microscopy. Individual cells and small processes could be easily observed. Scale bar, 100 μm.

Initial observations of Laponite gel covered CM-DiI-stained hippocampal monolayers showed no particular differences in appearance to control, however, on careful analysis and comparison of monolayers over time, a disparity was observed. Hippocampal monolayers are dynamic organisations showing continuous spatial and morphological changes over time, such as the migration of cells and extension of neural processes. On close observation of the hydrogel covered cultures, however, the hippocampal monolayers were static in appearance and showed no spatial or morphological changes over the time periods investigated. As well as whole cell structures, even small neural processes remained unchanged over time (Fig. 5.3.8).

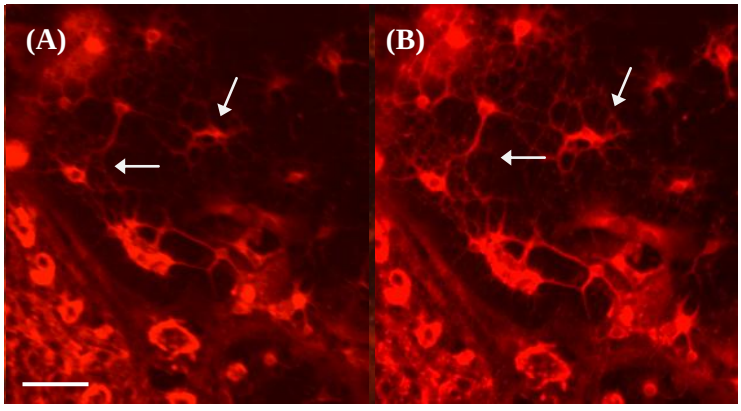


Figure 5.3.8 CM-DiI-stained 7 day old hippocampal monolayers covered with 16% Laponite RDS culture medium hydrogel visualised under fluorescence microscopy on (A) day 1, (B) day 2 and (C) day 3 since hydrogel cover. Hippocampal monolayers, and even the small processes, remained unchanged over time period (arrows). Scale bar, 50 μm.

MTG-stained hippocampal monolayers covered with 16% Laponite RDS culture medium hydrogels also showed similar results. In comparison to CM-DiI-stained cultures, however, MTG proved toxic to control cultures with no hydrogel. Over an investigation period of one week, the majority of MTG-stained (on day 0) control monolayers were dead by day 3 and non-existent by day 7 (Fig. 5.3.9).

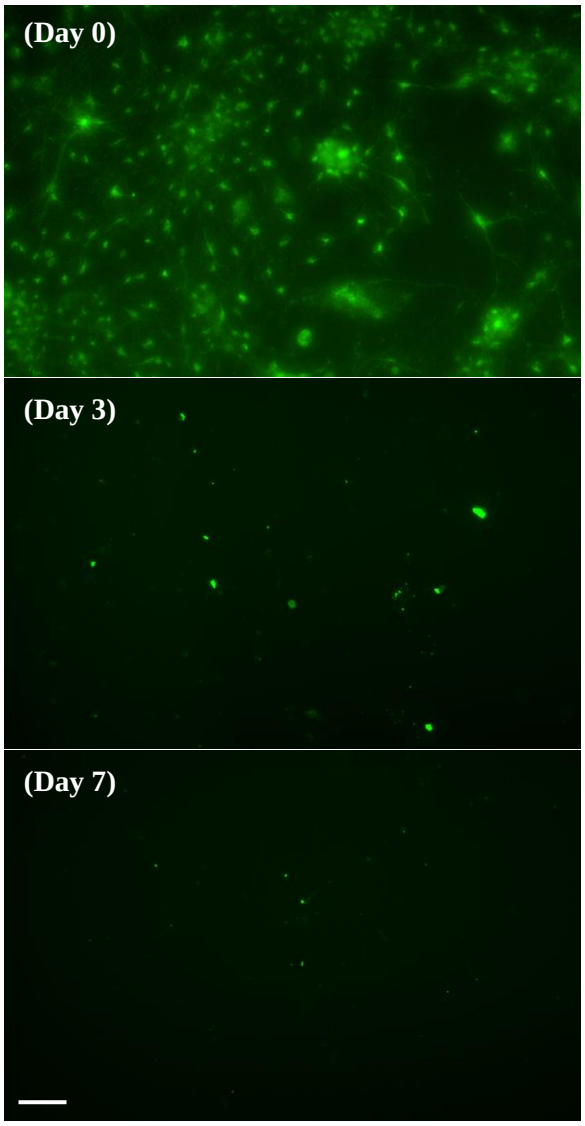


Figure 5.3.9 MTG-stained uncovered 6 day old hippocampal monolayers in culture medium (NBA-A/B27/Glu) visualised under fluorescence microscopy. On day 0, the hippocampal monolayers were stained with MTG, but by day 3, the majority of cells were dead. At 7 days after MTG application all cells are dead. Scale bar, 100 μm.

In direct contrast to these results, MTG-stained hippocampal monolayers covered by 16% Laponite RDS culture medium hydrogels showed no cell death as a result of MTG staining. Similar to the results observed with the hydrogel covered CM-DiI-stained monolayers, MTG-stained monolayers showed no spatial or morphological changes over time (Fig. 5.3.10).

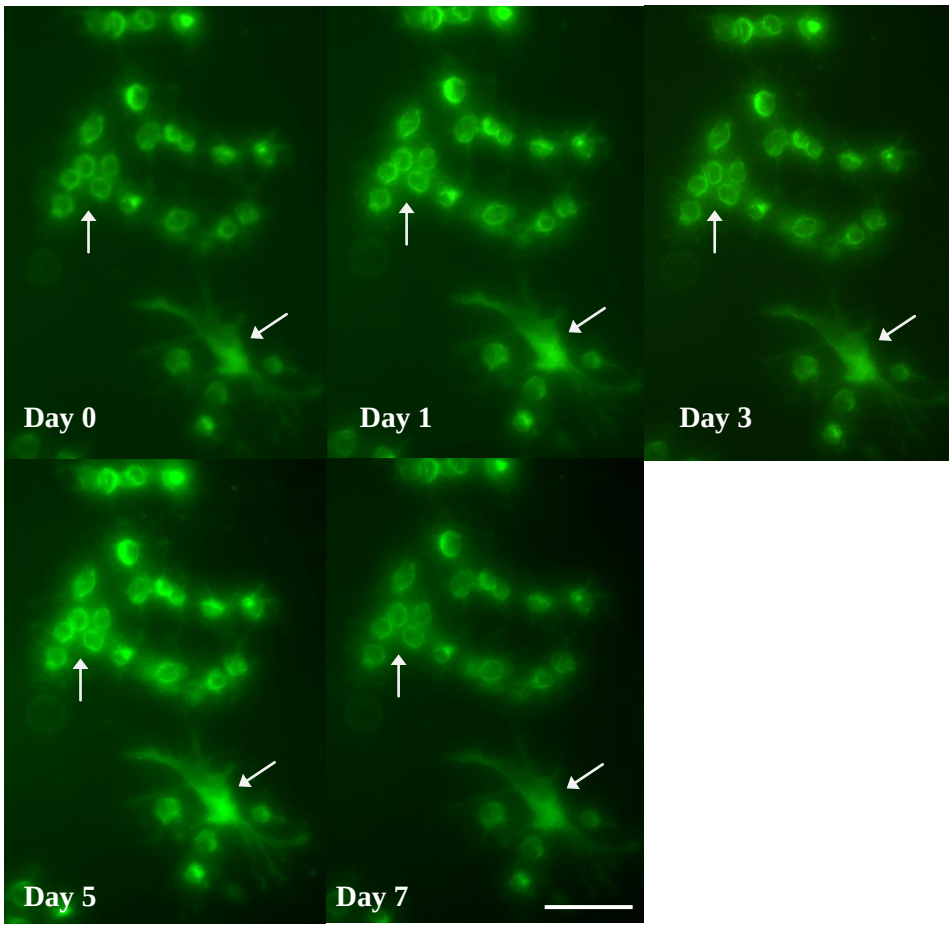


Figure 5.3.10 MTG-stained 6 day old hippocampal monolayer covered by 16% Laponite RDS culture medium hydrogel visualised over a period of 7 days under fluorescence microscopy. Even though MTG showed toxicity in control cultures with no hydrogel cover, hydrogel covered monolayers showed no spatial or morphological changes over time and no cell death (arrows). Scale bar, 50 μm.

Many factors could have contributed to the observations noted above, such as the culture age, pH or Laponite concentration, so with that taken into account, a range of conditions were investigated (section 5.2.10). The same preservation effect, however, was observed under all conditions investigated. The incorporation of growth factors or buffer, variation of Laponite concentration (2-16%) and type (RDS or XLS) or cultures of a different age, all showed the same static appearance, regardless of fluorescent stain used.

Both MTG and CM-DiI are live cell stains. Although the majority of cells were live before hydrogel cover, it was unknown whether the Laponite covered hippocampal monolayers were alive or dead. Even though the initial fluorescent stain (MTG or CM-DiI) remains intact, it is no longer a reliable indicator of cell viability. Attempts at staining

hydrogel covered hippocampal monolayers with MTG, Sytox green or PI to assess cell viability proved futile due to dye absorption and binding to the hydrogel, leading to high background fluorescence and lack of stain diffusion to the monolayers underneath.

### 5.3.6 Assessing cell viability using PI and Sytox green

The cell death markers PI and Sytox green were used to assess the viability of cells underneath Laponite hydrogel. The incorporation of PI into Laponite hydrogels or pre-staining monolayers with PI before gel cover was investigated to determine whether cell death occurred in response to hydrogel exposure. When PI was incorporated into hydrogels, there was a lack of PI staining and no indication of cell death in the underlying monolayer. Instead of staining dead or dying cells, it was likely that PI remained tightly bound to the gel to give high background fluorescence (Fig. 5.3.11).

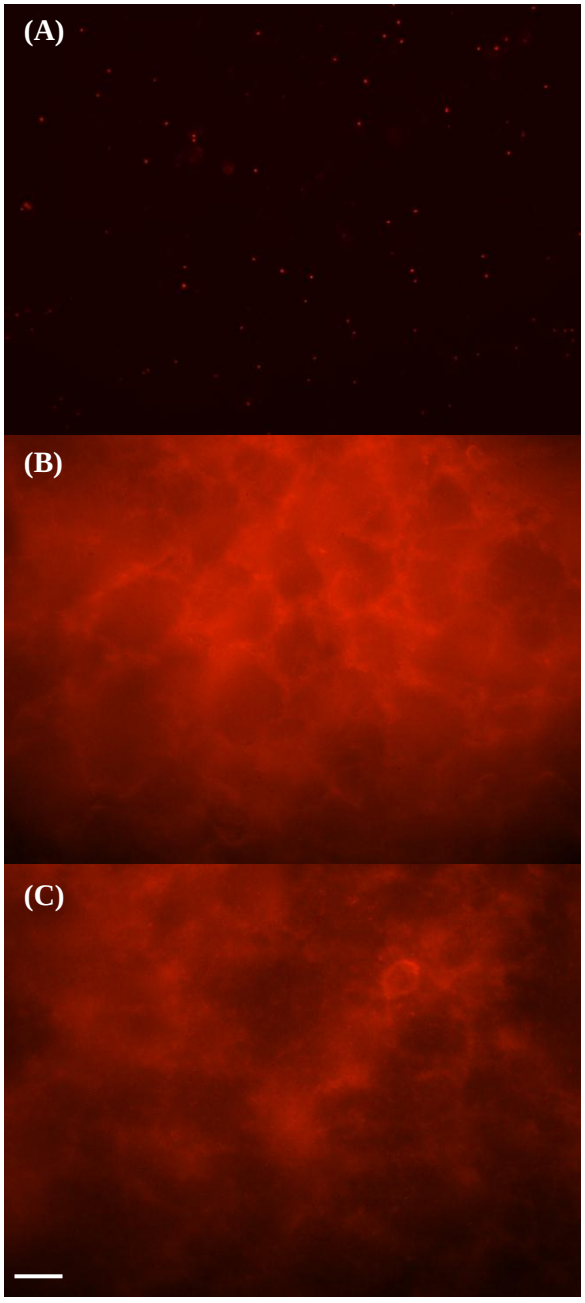


Figure 5.3.11 PI was incorporated into Laponite gels to assess monolayer cell death, visualised one day after hydrogel application. (A) PI staining could be observed in control monolayers with no hydrogel cover. (B) Control with PI incorporated into hydrogel with no cells. (C) PI incorporated into hydrogel over hippocampal monolayer. There was high background staining and no convincing PI staining could be observed. Scale bar, 100 μm.

In a different approach, hippocampal monolayers were pre-stained with PI or Sytox green before gel cover. Although stained monolayers could be visualised under hydrogel, there were no changes in cell death staining over time. Control cultures with no gel cover showed increased PI staining over time, as expected as a result of cell death, but hydrogel-covered monolayers instead showed a static response (Fig. 5.3.12), similar to the hydrogel-covered monolayers described in section 5.3.5.

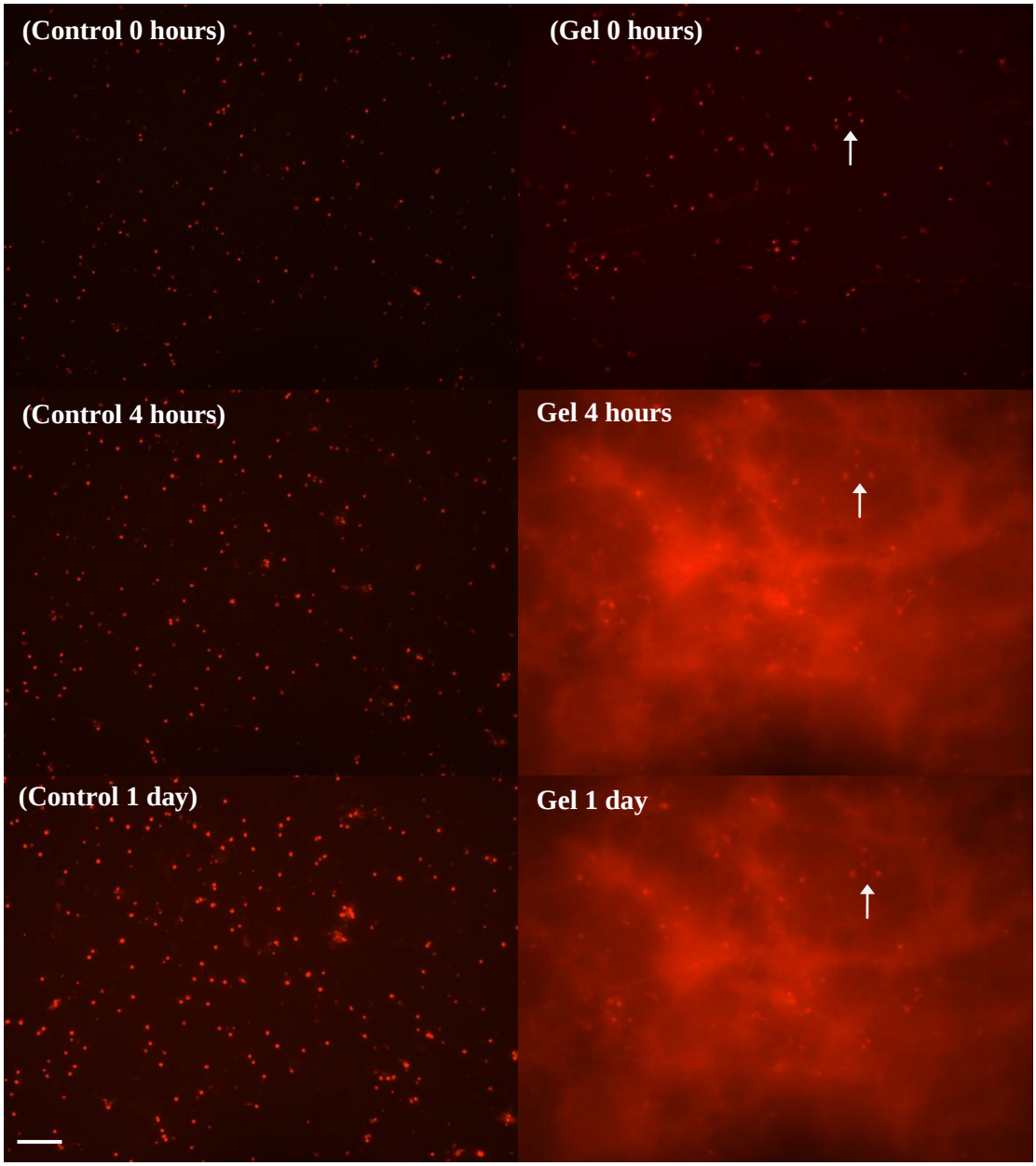


Figure 5.3.12 PI pre-stained hippocampal monolayers. Monolayers with no hydrogel cover (Control) and monolayers covered in 16% Laponite RDS hydrogel (Gel) at time 0 hours (before gel addition), 4 hours (after gel addition), and 1 day (after gel addition). The number of PI stained cells

(cell death) increased under control conditions but showed no change under hydrogel cover (arrows). Scale bar, 100 μm.

### 5.3.7 Hippocampal monolayers grown on inserts could be stained from underneath

Determining the viability of hippocampal monolayers under hydrogel cover was difficult because fluorescents stains could not reach the monolayer due to absorption by the Laponite hydrogel. To overcome this problem hippocampal monolayers were grown on culture inserts with porous membranes, which allowed fluorescent stains to be introduced to hydrogel-covered monolayers from underneath.

#### 5.3.7.1 Optimising hippocampal monolayers on PTFE culture inserts

Confluent hippocampal monolayers were achieved in one week using both the Sigma Aldrich laminin technical note protocol or by pre-coating inserts with a mixture of laminin and poly-L-lysine. Both treatments were applied at least 24 h before and rinsed before cell addition. Insert cultures were supplemented with EGF/FGF/FBS to support cell growth.

#### 5.3.7.2 Staining hydrogel-covered hippocampal insert cultures

A variety of fluorescent dyes (MTG, MTO, CM-DiI, PI and Sytox green) were used to determine the viability of Laponite culture medium hydrogel-covered hippocampal monolayers grown on culture inserts. All dyes except MTG (Fig. 5.3.13) were able to stain uncovered hippocampal monolayers from underneath the inserts, however, none of the hydrogel-covered monolayers were convincingly stained with any fluorescent dye or dye combination (Fig. 5.3.14). Even though the dyes could reach the monolayer from underneath, they still bound to the gel to produce high background fluorescence, which obscured further analysis. Furthermore, it was difficult to obtain MTG staining in both control insert cultures with no gel cover and gel-covered cultures. Unfortunately, the viability of hippocampal cells under hydrogel cover could not be deduced via this method.

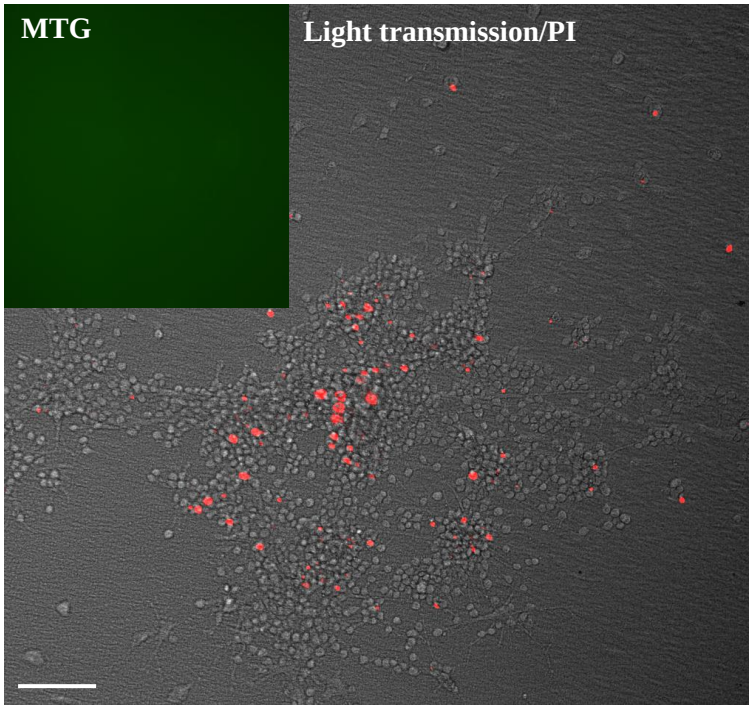


Figure 5.3.13 Culture insert hippocampal monolayer under light transmission microscopy with combined MTG/PI staining. PI (red) stained the dead/dying cells through the porous insert membrane when introduced from underneath the insert, while MTG could not. The respective image of MTG (green) shows no staining, irrespective of insert type. Scale bar, 100 μm.

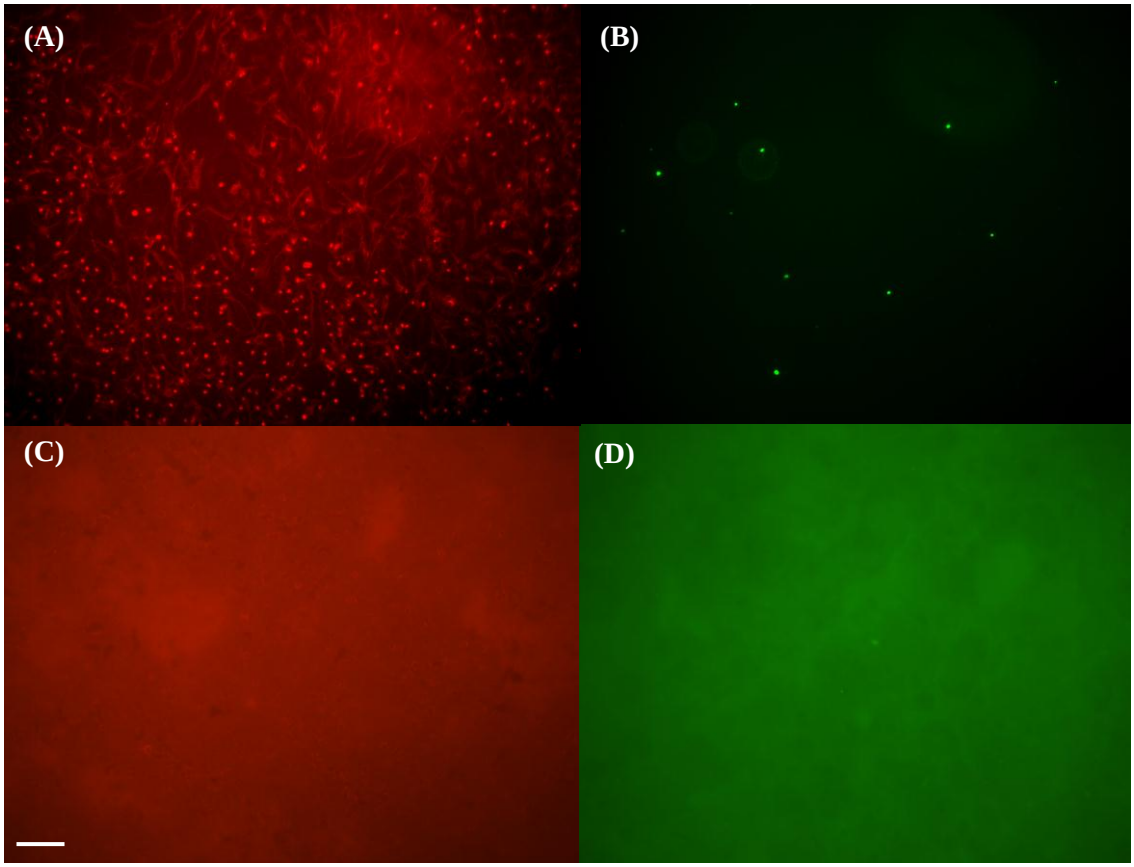


Figure 5.3.14 MTO (red) and Sytox green (green)-stained culture insert hippocampal monolayers visualised under fluorescence microscopy. (A and B), Control (no hydrogel) hippocampal monolayer stained with (A) MTO and (B) Sytox green. (C and D), (C) MTO- and (D) Sytox green-stained cultures covered with 12% Laponite RDS culture medium hydrogel. Under gel cover (C

and D), there was a lack of convincing staining and a lot of unspecific MTO and Sytox binding to the gel which produced high background fluorescence. Scale bar, 100 μm.

### 5.3.8 Seeded hippocampal cells adhere to Laponite XLS culture medium hydrogels

In addition to hydrogel cover, cells were also seeded onto Laponite hydrogels to assess gel biocompatibility. Dissociated CM-DiI pre-stained hippocampal cells were seeded over Laponite RDS and XLS hydrogels. Initial observations showed cells floating freely above the gel, but with time, some cells adhered and possibly integrated into Laponite XLS culture medium hydrogels. A defined adherence pattern was observed on XLS hydrogels and cells remained attached through periods of culture medium change and rinsing (Fig. 5.3.15B,D). This cell behaviour was not observed on Laponite RDS hydrogels, although a minority of cells did adhere but not in a defined manner (Fig. 5.3.15A,C).

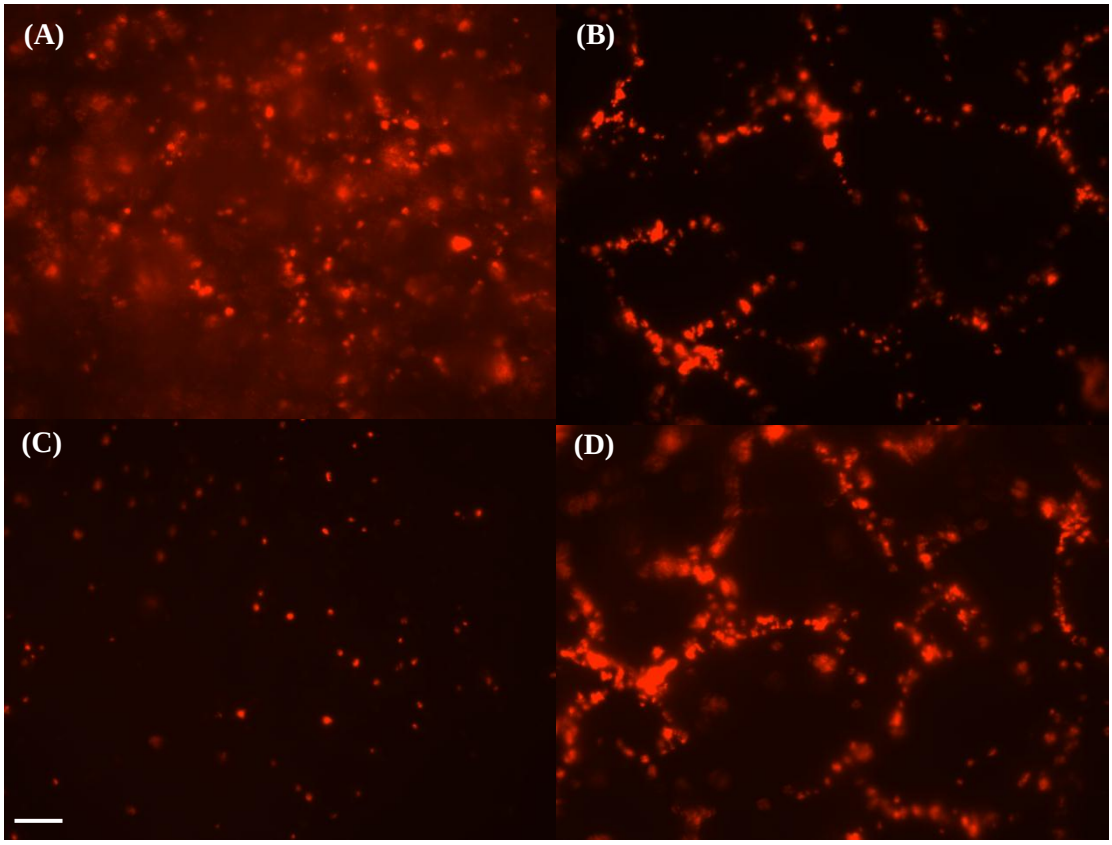


Figure 5.3.15 CM-DiI (red) pre-stained dissociated hippocampal neuronal cells seeded over (A and C) 16% Laponite RDS culture medium hydrogels and (B and D) 16% Laponite XLS culture medium hydrogels, visualised under fluorescence microscopy. (A and B) show the cultures 17 days after seeding, while (C and D) show the Laponite hydrogels after being rinsed with culture medium to remove free-floating cells. The dissociated cells adhered randomly to Laponite RDS hydrogels but were observed to form a distinct adherence pattern over Laponite XLS hydrogels. Scale bar, 50 μm.

Although there was a distinct difference in the cell adherence pattern between RDS and XLS hydrogels, the concentration of Laponite hydrogel (12% or 16%) and addition of laminin (extracellular matrix protein) made no difference to the hydrogel cell adherence preferences observed. In addition, when the cultures were visualised under light transmission and fluorescence microscopy, the adherence pattern of cells to Laponite XLS hydrogels seemed to follow the network structure of the hydrogel (Fig. 5.3.16). Attempts at assessing cell viability using MTG and Sytox green proved unsuccessful as dyes bound to the hydrogel.

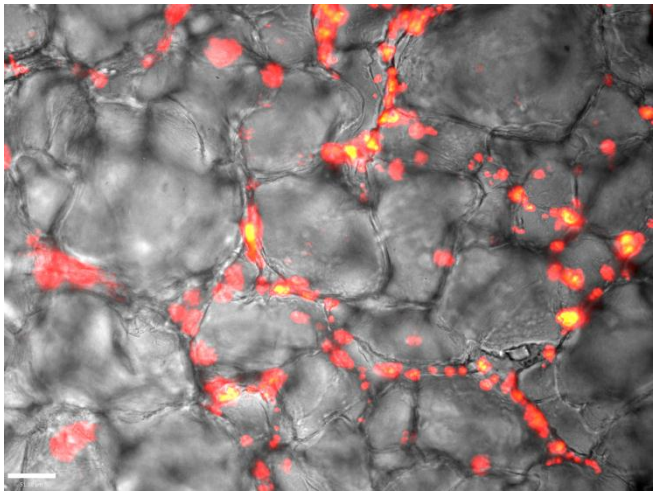

Figure 5.3.16 Overlaid images of fluorescent CM-DiI (red)-stained cells over 16% Laponite XLS culture medium hydrogel under light transmission. Cells were observed to adhere to the porous 3D network structure of Laponite to form a distinct adherence pattern. Scale bar, 50 μm.

### 5.3.9 Laponite culture medium gels have high osmolarity

The osmolarity of gels (buffered and non-buffered) were measured across a range of Laponite concentrations (% w/v) to determine whether this was the cause of the static response of cells to Laponite hydrogel cover. Results showed that the osmolarity of culture medium (NBA-A/B27/Glu) was ~250 mOsm. The addition of Laponite, however, increased the osmolarity significantly, which increased even further with the addition of higher concentrations of Laponite (Linear regression analysis *$p<0.0001$). This trend was observed in both buffered and non-buffered gels (Fig. 5.3.17). On the whole, buffered hydrogels had ~50 mOsm higher osmolarity than non-buffered gels across all Laponite concentrations tested. The addition of 16% Laponite RDS produced a hydrogel with an osmolarity of ~400-450 mOsm, which is high from a physiological perspective.

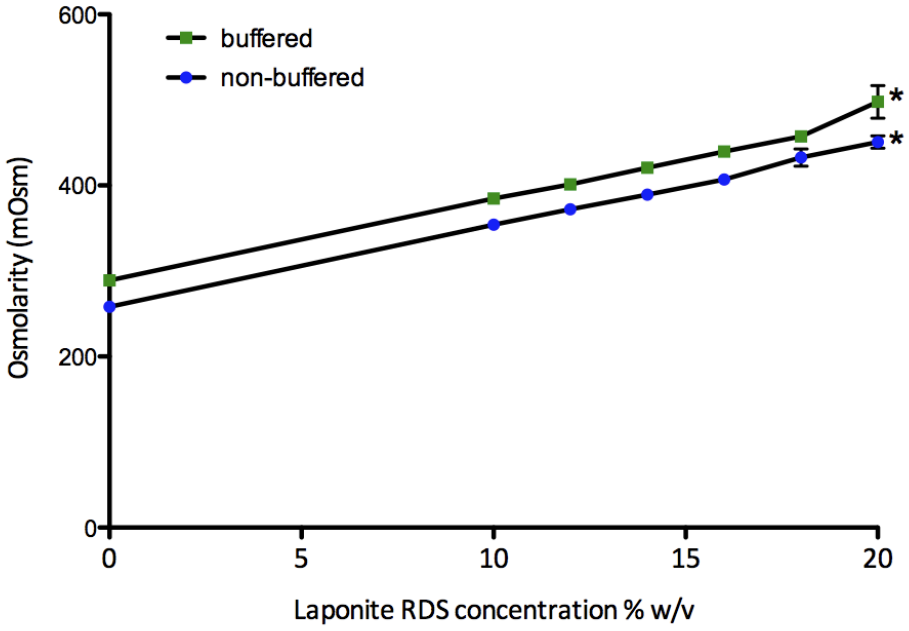


Figure 5.3.17 Osmolarity of non-buffered and buffered (35 mM HEPES) Laponite RDS culture medium hydrogels. There was a corresponding increase in hydrogel osmolarity as the concentration of Laponite increased. Buffered hydrogels had an osmolarity ~50 mOsm higher than those of non-buffered gels.

## 5.4 Discussion

The biocompatibility of Laponite RDS/XLS culture medium hydrogels for postnatal rat hippocampal cells were investigated to explore their potential as synthetic matrices for 3D culture. The response of hippocampal cells to hydrogel exposure was explored and assessed through the use of a range of novel techniques.

### 5.4.1 Hippocampal cells must be pre-stained before hydrogel incorporation

The synthetic hydrophilic clay Laponite has a rich absorptive chemistry which proved problematic for cell visualisation with fluorescent dyes. As described in the attractive theory for Laponite hydrogel formation, Laponite itself is comprised primarily of a network of disk-shaped, nano-sized monomers which are both positively and negatively charged and connected together by weak electrostatic interactions and van der Waals attractions (Martin et al., 2002). The presence of multiple charges attracts molecules, such as dye particles, which in turn remain bound to the hydrogel network structure. Most probably, it is this absorption of dyes which cause the high background fluorescence and deter the determination of cell viability. A simple way to overcome this was to pre-stain cells and neurospheres before hydrogel incorporation.

### 5.4.2 Hippocampal monolayers remain static in response to hydrogel exposure

Cells in culture are dynamic assemblies, showing constant spatial and morphological changes over time as cells grow and differentiate, with hippocampal monolayers proving no exception (Brewer, 1997). In this respect, cells exposed to hydrogel should also be expected to show the same dynamic diversity. Unexpectedly, however, hippocampal monolayers covered by Laponite culture medium hydrogels showed no dynamic changes over time and no spatial or morphological change, although there could be many physiological explanations for the static effect observed.

Over time, as the age of cultures increase, monolayers may become less active as cell growth and differentiation peaks. This issue was investigated by covering cultures of different age under hydrogel, which made no difference to the static effect observed. In addition, even if monolayers became less dynamic, there are ongoing and continual processes, such as cell migration and extension of neural processes, which were not observed in any of the hydrogel-covered monolayers. All cells and cellular processes remained unchanged. The addition of growth factors also made no significant difference, which suggested that the hydrogel itself was the main causative factor. Static hippocampal

cultures in response to cover by a range of Laponite RDS/XLS preparations (2-16%), irrespective of hydrogel formation, supported the fact that it was Laponite itself that was not biocompatible. Further investigations, therefore, were made with regards to two basic properties of the hydrogel which would contribute to cell survival in culture: the pH and osmolarity. The hydrogel pH was initially investigated due to the colour of the phenol red indicator in the media, and was corrected through the use of HEPES buffer to reduce the pH from 8.6 to 7.8 in 16% Laponite RDS culture medium hydrogels. Buffered hydrogels made no difference to the static effect observed in cultures. On the other hand, the osmolarity (osmoles of solute per litre of solution) of the Laponite hydrogels were very high (~400-450 mOsm in 16% Laponite culture medium hydrogel) compared to plain culture medium (~250 mOsm). The hyperosmotic Laponite hydrogel was not physiologically suitable for the survival and cultivation of hippocampal cells, which may partly explain the static behaviour observed, as cells were exposed to hyperosmotic stress. Cells, however, usually shrink in response to a hyperosmotic environment, which was not observed in the hydrogel-covered cultures (Kreisman et al., 1995). The chemical composition of Laponite, which consists of high quantities of chemical compounds such as magnesium oxide (26% dry composition) and sodium oxide (5.6% dry composition), contribute to its high osmolarity and the presence of these ions is central to Laponite hydrogel formation (Mourchid et al., 1995a, 1995b). Although the osmolarity may be manipulated for enhanced cell survival, the consequence of this on hydrogel formation is unknown and provides the basis for further investigation.

The viability of hippocampal cells under hydrogel cover remains elusive due to difficulties in cell viability staining due to dye absorption by the hydrogel. Efforts to overcome this through the incorporation of PI into gels and the culturing of cells on inserts with porous membranes have proved unsuccessful. Further techniques which may allow the determination of cell viability under the hydrogel will need to be explored.

### 5.4.3 Laponite XLS may be a more biocompatible alternative to Laponite RDS

Laponite XLS, the low heavy metal content variation of Laponite RDS, is typically used for cosmetic applications. The basic chemical composition remains largely unchanged except for the regulation of heavy metal content, with particular focus on minimising the contribution from heavy metals such as lead (< 3mg/kg), arsenic (< 1mg/kg), mercury (< 2mg/kg) and nickel (< 2mg/kg) (Laponite technical bulletin, L246/06e). Heavy metals such

as lead and arsenic are well known to be neurotoxic to cells such as hippocampal neurons (Yang et al.; 1999; Yang et al.; 2003), although the concentration of heavy metals in the final Laponite hydrogel is negligible and was unlikely to have had any significant contribution to cell death. Hippocampal cells did not show cell death in response to hydrogel cover, instead, they remained unchanged over time.

The cells which were seeded over Laponite RDS and Laponite XLS culture medium hydrogels showed preferential adherence to XLS hydrogel. This increased adherence may be explained by the decreased heavy metal content and overall purer composition of XLS. This does not explain, however, why the behaviour of hippocampal monolayers remained inactive when Laponite XLS hydrogels were transferred on top. Although Laponite XLS may show better compatibility with cells, Laponite hydrogels, in general, need optimisation for improved cell biocompatibility.

### 5.4.4 Advantages of a 3D culture of hippocampal cells in silica hydrogel

Attempts have been made to create silica-based culture matrices from sodium silicate since the 1930's. With chemically and physically distinct properties to Laponite (sodium magnesium silicate), sodium silicate gel formation requires reaction with hydrogen ions in acid and heating for gel formation. The inorganic nature of sodium silicate is a great advantage, allowing for the free manipulation of nutrients within the gel to control the growth of both autotrophic and heterotrophic bacteria (Sterges, 1942), although there have been no attempts at cultivating hippocampal neurons in such gels.

The culture of rat hippocampal and cortical neurons in 3D hydrogel matrices has been well attempted in other, mainly natural, hydrogels such as collagen (Xu et al. 2009), agarose (O'Connor et al., 2001) and hyaluronic acid (Wei et al., 2010). Xu et al. (2009) cultured rat embryonic hippocampal neurons in three different models of collagen hydrogel culture. Neurons were either cultured as embedded cells evenly distributed within a 3D collagen matrix, at the interface between two layers of collagen called the sandwich model, or seeded on the surface of collagen-coated coverslips as a 2D model. Neurons cultured within the 3D model demonstrated improved survival compared to the 2D model and extended neuronal processes into the surrounding 3D matrix. Older 3D cultures (14 and 21 day old) also exhibited spontaneous postsynaptic currents, presenting evidence for functional synapse formation (Xu et al., 2009). Functional multi-level 3D hippocampal

circuits can be created in collagen hydrogels for applications in neuronal regeneration and repair and brain research.

Commercially available hydrogels which can be used to create 3D matrices of hippocampal cells include BD Matrigel™ basement membrane matrix (BD Biosciences). This heterogeneous protein mixture secreted by mouse tumour cells contains diverse structural and adhesive proteins such as laminin and collagen (natural components of the extracellular matrix) (Kleinman et al., 1982; 1986), as well as growth factors which help to promote neuronal cell growth and differentiation (Biederer & Scheiffele, 2007). In addition to being extremely costly, the complex milieu of proteins present in Matrigel presents difficulties when performing experiments which require an accurate knowledge of constituents (Vukicevic et al., 1992). Although Laponite had not been previously investigated as a cell culture matrix, its relatively low cost, gentle gelling conditions and thixotrophic properties provide advantages over many current hydrogels. In addition, similar to sodium silicate (Sterges, 1942), the inorganic nature of Laponite allows for the fabrication of a highly controlled cell environment, although unlike bacteria, mammalian cells, and especially hippocampal neurons, are much more sensitive to environmental conditions.

### 5.4.5 Conclusions

Although Laponite hydrogels are attractive as 3D culture matrices because of their rheological properties, this will not be possible until they are more biocompatible. The high osmolarity of Laponite culture medium hydrogels seems to be the most obvious issue and remains a difficult obstacle to overcome. Although Laponite XLS hydrogels have proved more promising, other ways of determining cell viability within the hydrogels still need to be investigated. Unfortunately, due to time and physical constraints, Laponite hydrogels could not be further optimised for cell survival, although it remains a potential alternative to many current hydrogels frequently used in cell culture applications.

# Chapter 6

## Chapter 6 - General discussion

### 6.1 Cellular mechanisms underlying NPY-mediated neuroproliferation

It has been proposed that NPY-releasing interneurons in the dentate hilus release NPY onto progenitors within the SGZ to regulate their proliferation and adult hippocampal neurogenesis (Gray, 2008). I have confirmed previous observations (Howell et al., 2003) that NPY exerts a purely proliferative effect on hippocampal cultures, but the question remained as to how NPY mediates this increase in proliferation. Through combining the observations identified so far, the key mediators of this proliferative effect can be organised into a systematic signalling pathway.

The neuroproliferative effect was mediated via the NPY $Y_1$ receptor, whereupon NPY-binding resulted, presumably, in the activation of nNOS, possibly via $G_i/G_o$ G proteins (Limbird, 1988). Indeed, signalling between GPCRs, such as the $Y_1$ receptor, and nNOS may be possible through GPCR-mediated mechanisms. In the cholecystokinin-mediated proliferation of Chinese hamster ovary cells, for example, the cholecystokinin A GPCR activated nNOS via the G-protein βγ subunit and the tyrosine phosphatase SHP-2 (Cordelier et al., 1999). NOS activation converts the amino acid L-arginine into citrulline and NO (Alderton et al., 2001), for which I have shown a significant increase in intracellular $NO/N_2O_3$ production upon NPY addition. This NO mediates further intracellular signalling mechanisms which ultimately results in cell proliferation. Imaging studies using DAF-FM DA showed that, even before a NPY or PBS pulse, hippocampal cells had some endogenous $NO/N_2O_3$ activity. It is unlikely, however, that this background level of NO was involved in mediating basal proliferative processes, as pharmacological analysis using L-NAME showed that it had little effect on basal cell proliferation. On the contrary, both sGC and PKG were associated with maintaining basal proliferation rates, which may be due to NO-independent sGC activation (Ignarro et al., 1982; Stasch et al., 2001) which is less efficient than NO at promoting cGMP synthesis. Moreover, many of the physiological effects of NO are concentration dependent and an increase in endogenous (basal) NO levels, as a result of NPY stimulation or L-arginine supplementation, may initiate proliferative processes which would otherwise not occur if NO levels were low.

The targets immediately downstream of NO were identified as sGC and the second messenger cGMP, which in turn, activated PKG. PKG activation typically leads to the phosphorylation of serine and threonine residues on protein targets which (indirectly)

regulate the activity of downstream targets such as ERK 1/2 (Francis & Corbin, 1999). As well as confirming the involvement of ERK 1/2, I have also shown that ERK 1/2 activation by NPY was solely mediated via NOS/NO mechanisms. ERK 1/2 are involved in mediating further pathways involved in regulating the expression of genes controlling cell proliferation and differentiation (Cano & Mahadevan, 1995; Lopez-Ilasaca, 1998) (Fig. 6.1). The signalling mechanisms downstream of ERK 1/2, such as the activation of transcription factors involved in the regulation of cell proliferation, remains a topic for further investigation.

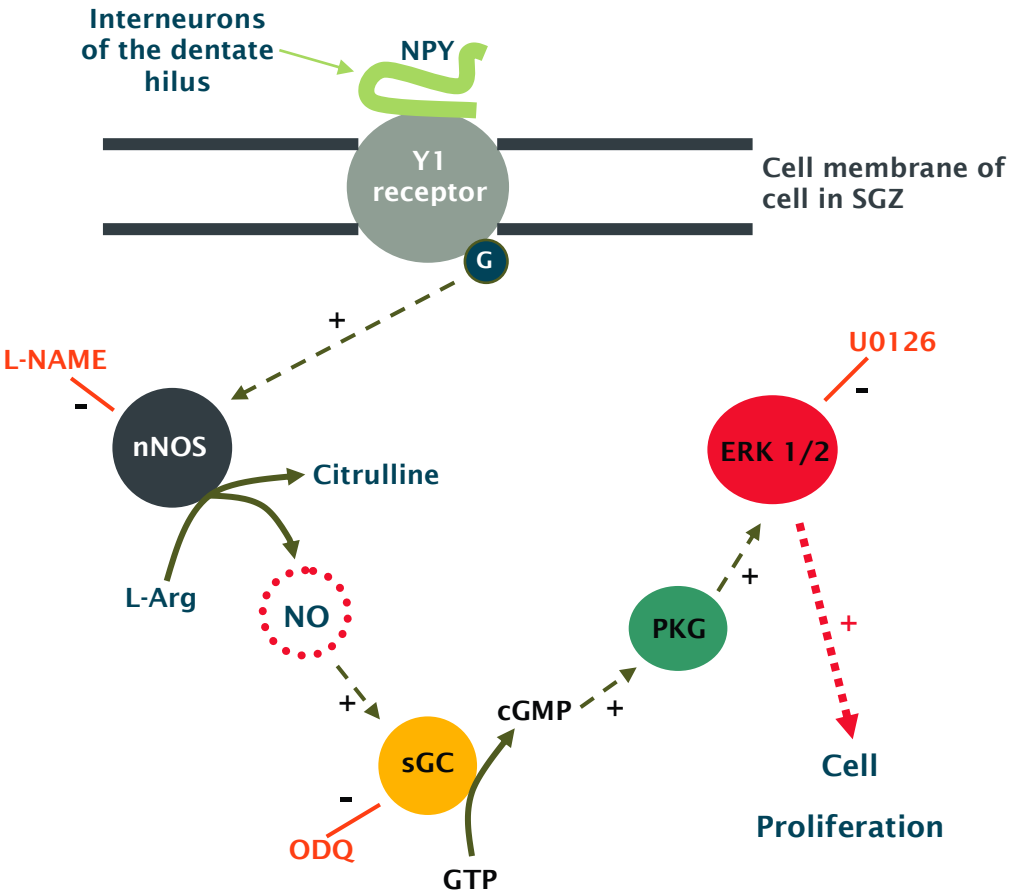


Figure 6.1 Schematic diagram of the intracellular mechanisms underlying NPY-mediated neuroproliferation. NPY released by interneurons of the dentate hilus acts on NPY $Y_1$ receptors in the subgranular zone (SGZ) to initiate a neuroproliferative effect. The $Y_1$ GPCR activates neuronal nitric oxide synthase (nNOS) which synthesises NO from L-arginine. The target of NO is soluble guanylate cyclase (sGC), which converts GTP into cGMP. cGMP activates cGMP-dependent protein kinase (PKG), which in turn leads to the activation of a range of protein targets or kinase pathways, including the extracellular-regulated kinases 1/2 (ERK 1/2). ERK 1/2 are involved in

regulating the expression of genes involved in controlling cell proliferation and differentiation (adapted from Alvaro et al., 2008).

NO synthesised by nNOS in response to NPY was most likely intracellular and mediated its proliferative effect, while extracellular NO was antiproliferative, a finding consistent with the dual role of nNOS-derived NO recently demonstrated by Luo et al. (2010). My study significantly extends these findings by identifying NPY as a possible mediator of intracellular NO-induced proliferation. While high level concentrations and sustained NO release is commonly associated with anti-proliferative effects (Cardenas et al., 2005), a low level and localised release of NO, in response to NPY for example, may be involved in mediating proliferative pathways. This dual role is a common characteristic of NO and may be enforced by the differential subcellular compartmentalisation of nNOS, for example, to the nuclei of neural stem cells or to the cytoplasm of neurons as proposed by Luo et al. (2010), a trend also observed during the nNOS immunostaining of hippocampal cultures in my study (Fig. 3.3.6), or possibly, the existence of the nNOS splice variants such as nNOSα, nNOSβ and nNOSγ (Corso-Diaz & Krukoff, 2010; Alderton et al., 2001). Although the involvement of NO was previously suggested to mediate the proliferative effect of NPY on retinal neural cells by Alvaro et al. (2008), my results are the first to suggest that intracellular NO produced by nNOS signals the complete $Y_1$ receptor-mediated proliferative effect of NPY on hippocampal nestin$^+$ precursor cells, while extracellular NO had the opposite antiproliferative effect.

### 6.2 Levels of NO in *in vitro* culture

There are many influential factors in tissue culture which can affect levels of NO, one of which is the oxygen ($O_2$) concentration. The synthesis of NO by NOS occurs via two monooxygenation reactions and the rate of NO synthesis is related to the concentration of $O_2$. nNOS (*Km* = 350 µM), the most likely mediator of the neuroproliferative effect of NPY, is more sensitive to physiological levels of $O_2$ than iNOS (*Km* = 130 µM) or eNOS (*Km* = 4 µM) (Stuehr et al., 2004). In tissue culture, cell monolayers are cultured under air equilibrated levels of $O_2$ (210 µM $O_2$) (Hall & Garthwaite, 2009), which is about 10-fold higher than levels normally present within the brain *in vivo* (20 µM $O_2$) (Dings et al., 1998). In this hyperoxic environment *in vitro* the production of NO will be significantly increased (Hall & Garthwaite, 2009), and in addition to this, high $O_2$ levels can cause oxidative stress (Coyle & Puttfarcken, 1993). Although increased oxidative stress as a

result of high $O_2$ levels is not likely a major issue in *in vitro* hippocampal cultures, as cells proliferated well under basal conditions and overall cell death was low (~10%), the effect of increased NO production on cultures is unknown. The effect of $O_2$ levels on hippocampal cultures and NO signalling should be addressed in the future, as it has important consequences for a vast number of studies.

Similar to high $O_2$, certain chemical components of culture media have also been demonstrated to react with and influence levels of NO *in vitro*. In aqueous solution, NO can be simply inactivated by an autoxidation reaction with $O_2$ (Ford et al., 1993), however, the study by Keynes et al. (2003) identified HEPES buffer and, under laboratory lighting, the vitamin riboflavin, as NO-consuming components which are present within a variety of culture media. NO produced by the donor, DETA/NONOate, was reduced in the presence of these two components, which probably occurs via the generation of superoxide anions and subsequent interactions with NO (Keynes et al., 2003) (Fig. 6.2).

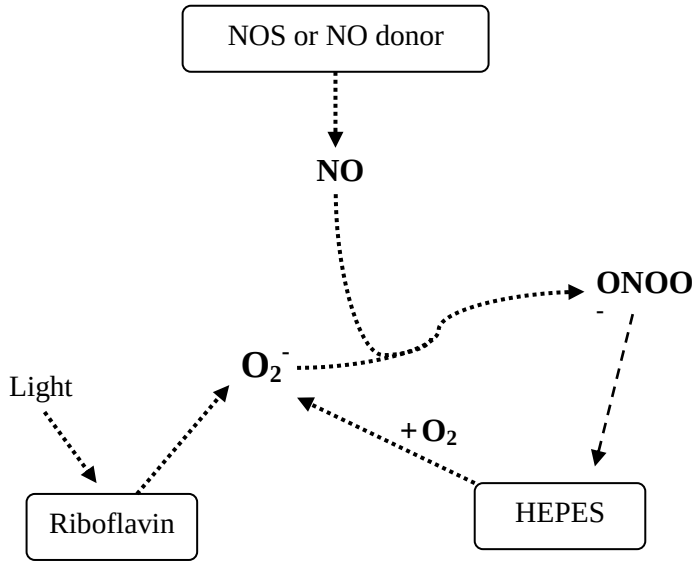


Figure 6.2 Interactions of NO with riboflavin and HEPES in culture media (adapted from Keynes et al., 2003). Superoxide anion ($O_2^-$) generated from riboflavin reacts with NO to form peroxynitrite ($ONOO^-$), which can be cytotoxic. In turn, $ONOO^-$ can oxidise HEPES, which, upon subsequent reaction with molecular oxygen ($O_2$), generates more $O_2^-$.

Neurobasal A, the culture medium used in this study, contains both HEPES (10.92 mM) and riboflavin (0.4 mg/L) (Media Formulation, Life Technologies, UK). Compared to

Keynes et al's (2003) study, where 0.1-0.2 mg/L riboflavin and 12.5-200 mM HEPES significantly reduced the generated NO (~1 μM) from 300 μM DETA/NONOate, the amount of riboflavin present in Neurobasal A media is relatively high and may have acted as a significant NO-consumer when cultures were exposed to laboratory lighting. The influence of these factors limits the reliability of any NO studies conducted *in vitro*, and are issues which were considered during data interpretation.

### 6.3 NPY-mediated neuroproliferation *in vivo*

This study has identified the importance of NO mechanisms in mediating the neuroproliferative effect of NPY on hippocampal cultures *in vitro*. Would these mechanisms, however, still hold true *in vivo*? Although the proliferative effect of NPY for hippocampal neurogenesis has been well demonstrated *in vivo* (Decressac et al., 2011; Howell et al., 2007), no attempts have yet been made to decipher any of the underlying mechanisms. Indeed, the next step in this study would be to confirm my findings *in vivo*. With nNOS identified as a possible mediator of the neuroproliferative effect of NPY, hippocampal precursor cell proliferation in response to exogenous NPY application could be assessed *in vivo* using nNOS knockout mice (Packer et al., 2003). This will be challenging, however, given the highly complex, wide-ranging and bifunctional effects of NO *in vivo* and difficulties in specifically targeting the intracellular nNOS and $Y_1$ receptors of neural stem cells in the hippocampal SGZ. Nevertheless, *in vitro* hippocampal cultures could at least be derived from nNOS knockout mice for further confirming the importance of NO in mediating the effect of NPY. On the other hand, Cre/LoxP-mediated recombination using nestin-Cre transgenic mice (Dubois et al., 2006; Sclafani et al., 2006) is another possibility which could be used for the specific deletion of nNOS in nestin expressing precursor cells, as the NOS subtypes are encoded for by distinct genes (Alderton et al., 2001).

### 6.4 Is NO a common mediator of NPY and the NPY Y receptors?

Of the four NPY receptor subtypes functional in humans ($Y_1$, $Y_2$, $Y_4$ and $Y_5$) (Michel et al., 1998), all four are expressed (albeit at different levels) in the hippocampus (Kopp et al., 2002; Gustafson et al., 1997; Wolak et al., 2003; Dumont et al., 1998). Coupled to G-proteins of the $G_i/G_o$ family (Limbird, 1988), the NPY receptors act through a variety of signalling pathways to exert diverse physiological effects (Michel et al., 1998). Although this and Alvaro et al's study (2008) have been the first to demonstrate the involvement of NO mechanisms in mediating the neuroproliferative effect of NPY, NO has been

implicated in mediating other aspects of NPY action, especially via the NPY $Y_1$ receptor. For instance, NO has been shown to mediate the effect of NPY on neurovascular regulation through the $Y_1$ receptor. In the vascular smooth muscle of peripheral blood vessels, NPY normally acts as a sympathetic neurotransmitter which facilitates adrenaline-evoked vasoconstriction via the $Y_1$ receptor (Wahlestedt, 1990). On the other hand, NPY has also been shown to mediate vasodilatory responses via the $Y_1$ receptor, but this time by acting through NO mechanisms. Nilsson et al. (2000) showed that the NPY-mediated dilation of small human subcutaneous arteries was significantly inhibited by the presence of the $Y_1$ receptor antagonist BIBP3226 and the NOS inhibitor L-NAME, supporting the involvement of NO in mediating NPY $Y_1$-mediated vasodilation. Similarly, noradrenalin and NPY binding to the $\alpha_2$ adrenoreceptor and $Y_1$ receptor on endothelial cells stimulates eNOS and NO production which promotes the vasodilator response (Hodges et al., 2009; Vanhoutte & Miller, 1989). Heat-induced vasodilation, for example, is abolished with both the presynaptic sympathetic blockade of cutaneous vasoconstrictor nerves with bretylium tosylate and/or L-NAME application, further supporting the requirement for NO production in mediating the neurovascular effects of NPY (Hodges et al., 2008). In fact, the release of catecholamines from NPY-stimulated adrenal chromaffin cells has been shown to occur via the $Y_1$ receptor and involves the activation of NOS/NO mechanisms (Rosmaninho-Salgado et al., 2007). In addition to the $Y_1$ receptor, NO processes have also been shown to mediate the vasodilatory effect of NPY in cerebral vessels by acting through the $Y_2$ receptor (You et al., 2001).

NPY has been shown to induce angiogenesis in ischemic tissues via NO-dependent pathways (Zukowska et al., 2003). NPY itself exerts a proliferative effect on vascular smooth muscle cells (VSMC) (Pons et al., 2003; Zukowska-Grojec et al., 1998a) and endothelial cells (Zukowska-Grojec et al., 1998b), which, during hindlimb ischemia (due to vessel occlusion), is released from perivascular sympathetic nerves and endothelial cells (Zukowska-Grojec & Wahlestedt, 1993; Zukowska et al., 2003). Ischemia upregulates the expression of the $Y_2/Y_5$ receptors (Zukowska-Grojec et al., 1998a; Lee et al., 2003) and dipeptidyl-peptidase IV (DPPIV), a peptidase which forms the $Y_2/Y_5$ agonist, NPY 3-36 (Mentlein et al., 1993; Ghersi et al., 2001). The failure of NPY-mediated aortic sprouting in mice null for eNOS (Lee et al., 2003) has led to the hypothesis that stimulation of the $Y_2/Y_5$ receptors results in eNOS activation and the production of NO, which mediates the

angiogenic effects of NPY (Zukowska et al., 2003). In fact, NO itself has also been shown to exhibit angiogenic effects of its own (Ziche & Morbidelli, 2000).

In the CNS, the NPY $Y_1$ receptor has been shown to modulate NO levels during stroke in rats (Chen et al., 2002). Using a middle cerebral artery occlusion (MCAO) stroke model, Chen et al. (2002) showed that the intracerebroventricular injection of NPY or a $Y_1$ agonist increased the infarct volume, a $Y_2$ agonist had no effect, and the $Y_1$ receptor antagonist BIBP3226 reduced the infarct volume. Using electron paramagnetic resonance spectroscopy to measure NO levels, MCAO was found to increase the relative brain NO concentration to 131.94 ± 7.99%, while NPY treatment increased this further to 250.94 ± 50.48%. BIBP3226, however, significantly reduced the relative brain NO concentration to 69.63 ± 8.84% (Chen et al., 2002). This study suggests that $Y_1$-mediated NO generation during cerebral ischemia mediates ischemic damage via NO overproduction (Malinski et al., 1993; Matsui et al., 1999). To the contrary, however, ischemic injury has also been associated with increased adult neurogenesis (Lichtenwalner & Parent, 2006). The first to describe this effect was Liu et al. (1998a), who observed a 12-fold increase in the number of $BrdU^+$ cells in the dentate SGZ after transient global ischemia in the adult gerbil. The proliferative effect of ischemia on adult hippocampal neurogenesis has also been demonstrated in rats (Jin et al., 2001) and mice (Takagi et al., 1999), occurs after a latent period of about 1-2 weeks and is transient in its effects (Liu et al., 1998a; Lichtenwalner & Parent, 2006). Indeed, contrary to the role of NO in mediating ischemic damage, Zhang et al. (2001) have shown that the administration of the NO donor DETA/NONOate increased cell proliferation and neurogenesis in the dentate gyrus of rats under both basal and ischemic conditions. Cortical levels of cGMP were significantly increased and the administration of DETA/NONOate considerably improved the neurological outcome during recovery from ischemic damage mediated via MCAO (Zhang et al., 2001). Although the mechanisms underlying these processes are complex, this illustrates again the dual role of NO and how a single molecule of NO can be controlled to exert a range of diverse physiological effects. In this instance, the NOS subtype producing NO and the levels of NO are probably the main determinators. nNOS probably mediates the NO injury in response to ischemia by producing high levels of NO, since as described previously, nNOS knockout mice show reduced infarct size in response to transient focal cerebral ischemia (Sun et al., 2005). eNOS and iNOS, on the other hand, have been shown to be important in mediating basal (Reif et al., 2004) and ischemia-induced (Zhu et al., 2003)

neurogenesis, respectively. As well as ischemia, a significant increase in NO production is also associated with epileptic seizures (Bashkatova et al., 2000; Kaneko et al., 2002) and Jiang et al. (2004) have shown that administration of the relatively non-selective nNOS inhibitor, 7-nitroindazole, significantly reduced the number of $BrdU^+$ cells in the dentate gyrus 3, 7 and 14 days after pentylenetrazol-induced seizures in rats. This possible involvement of nNOS in initiating hippocampal neurogenesis after seizures (Jiang et al., 2004) and the fact that NPY itself is necessary for seizure-induced hippocampal precursor cell proliferation (Howell et al., 2007) suggests that nNOS-derived NO may potentially mediate the proliferative effect of NPY in response to seizure activity *in vivo*, although further verification of this is required. Nevertheless, the conclusion from these studies is that NO may be a more common mediator of the effects of NPY than first thought.

### 6.5 The NO-cGMP-PKG pathway and synaptic plasticity

NO mediates a broad variety of physiological processes in the CNS (Garthwaite & Boulton, 1995) which, due to practical reasons, cannot be fully covered in this discussion. However, the NO-cGMP-PKG pathway, which was found to mediate the neuroproliferative effect of NPY in this study, is involved in regulating some key neurological processes such as synaptic plasticity. Synaptic plasticity, a process whereby the strength of connections between neurons is manipulated in response to various factors, seems to be necessary for learning and memory (Martin et al., 2000). In a study by Ota et al. (2008), the NO-cGMP-PKG signalling pathway was found to be involved in the regulation of synaptic plasticity and fear memory consolidation in the lateral amygdala (LA) of the rat (Ota et al., 2008). The intra-LA infusion of a PKG inhibitor or PKG activator, impaired or enhanced, respectively, fear memory consolidation in behavioural experiments, while slice electrophysiology experiments showed that the application of 8-Br-cGMP or the sGC activator YC-1 enhanced long-term potentiation (LTP), a form of synaptic plasticity whereby synaptic transmission efficacy is enhanced in the long-term, at thalamic inputs to the LA (Ota et al., 2008). As well as the involvement of NO mechanisms, the inhibition of the YC-1-induced LTP enhancement in the LA by U0126 suggested the involvement of ERK 1/2 mechanisms (Ota et al., 2008). In fact, the NO-cGMP-PKG pathway promotes fear memory consolidation, in part, by mediating ERK 1/2-driven gene transcription (Ota et al., 2010). Similarly, NO plays an important role in LTP in the hippocampus (Bohme et al., 1991; Doyle et al., 1996), which some studies have shown is mediated via cGMP-PKG processes (Boulton et al., 1995). Zhuo et al. (1994)

showed that the induction of LTP in the CA1 region of hippocampal slices was blocked by the inhibition of sGC or PKG, while cGMP analogues or PKG activators produced activity-dependent long-lasting enhancement of the excitatory postsynaptic potential. Likewise, Monfort et al. (2004) showed that the activation of sGC, PKG and cGMP-degrading phosphodiesterase was essential for the proper induction of NMDA receptor-dependent LTP in the CA1 region of the hippocampus. In summary, cGMP and PKG are major mediators of NO in fundamental processes of the CNS.

### 6.6 Considerations on the dual nature of NO

At a cellular level, the NO-cGMP-PKG pathway has been implicated in the regulation of apoptosis and survival in neural cells (Fiscus, 2002). As briefly mentioned previously, the cell type, cell source, duration of exposure, timing of synthesis and the concentration of NO are major factors contributing to its seemingly dual role (Cardenas et al., 2005). Indeed, with regards to cell survival, NO can also have both an apoptotic/necrotic (toxic) effect, or antiapoptotic (protective) effect depending on the circumstances (Beckman & Koppenol, 1996; Fiscus, 2002). NO at relatively low (submicromolar) concentrations is usually correlated with mediating its protective effects and the activation of sGC leading to cGMP synthesis (Bobba et al., 2007; Fiscus, 2002). On the other hand, excess NO production, such as in response to ischemia, is neurotoxic and can lead to cellular damage by inducing oxidative stress (Bobba et al., 2007). The oxidative stress and damage initiated by, for example, peroxynitrite, a reactive species formed as result of NO reaction with superoxide anion, can ultimately result in cell apoptosis or necrosis (Beckman & Koppenol, 1996; Estévez et al., 1998a). Although the cGMP-PKG pathway contributes to the proapoptotic actions of NO in certain cell types, such as vascular smooth muscle cells (Pollman et al., 1996) and vascular endothelial cells (Suenobu et al., 1999), cGMP has been shown to mediate the neuroprotective or antiapoptotic effects of NO in mammalian neural cells such as motor neurons (Estévez et al., 1998b), dorsal root ganglion neurons (Thippeswamy & Morris, 1997) and cerebellar granule neurons (Bobba et al., 2007). Indeed, the addition of extracellular NO (through the application of NO donors) protected serum-deprived PC12 cells (Kim et al., 1999), as well as nerve growth factor-deprived sympathetic neurons (Farinelli et al., 1996), from cell death *in vitro*. Of particular significance, however, is that the neuroprotective effects of the NO donors (sodium nitroprusside or SNAP) were only observed with low concentrations (below 100 µM) of the donor (Farinelli et al., 1996; Kim et al., 1999). It is possible that low concentrations of

NO activate sGC and cGMP production, which contributes to its neuroprotective effects, while higher concentrations of NO may elicit toxic effects through the formation of reactive species (Fiscus, 2002). These findings support my observations regarding the dual role of NO in regulating the proliferation of hippocampal cells, especially of the nestin$^{+}$ precursor cell population. I have shown that intracellular NO probably mediates the proliferative effect of NPY, which was perhaps low level and short-lived, while the long-term application of extracellular NO through the use of the NO donor DETA/NONOate, which has a half-life of around 22 h (Keefer et al., 1996), was antiproliferative. Similarly, inhibition of cell proliferation occurred at higher concentrations (100 µM) of DETA/NONOate, and showed further inhibition with increased donor concentration (200 µM). In fact, Carreira et al. (2010) had previously reported a dual effect of DETA/NONOate, depending on the concentration, on the proliferation of neural stem cell cultures derived from the mouse SVZ. While a low concentration of DETA/NONOate (10 µM) increased cell proliferation, higher concentrations (100 µM) inhibited cell proliferation (Carreira et al., 2010). This increased cell proliferation in response to low levels of NO donor was blocked by inhibiting the MAPK pathway with U0126 (Carreira et al., 2010), supporting the involvement of ERK 1/2 in mediating the proliferative aspect of NO identified in my own investigations. Indeed, as mentioned previously, DETA/NONOate was used at quite high concentrations within my own investigations and exerted a negative effect on neural proliferation. In reality, a biphasic effect of extracellular NO may have been observed if the concentration range I examined was not so limited. Lower concentrations of DETA/NONOate may have exerted proliferative effects similar to that of the intracellular NO pathway identified, and remains a topic for further investigation. As well as neural proliferation, low doses of DETA/NONOate (0.1 and 0.4 µM) have also been shown to promote (Chen et al., 2006), while high doses (50 µM) inhibited (Luo et al., 2010), neuronal differentiation and neurite outgrowth. Although the context may be slightly different i.e. cell proliferation compared to cell survival, the ability to manipulate the effects of NO through regulating its properties (i.e. concentration) and the positive effects of the NO-cGMP-PKG pathway are well demonstrated in both cases.

### 6.7 Is the neuroproliferative effect of NPY on the SVZ mediated via NO?

As in the SGZ, NPY exerts a neuroproliferative effect on SVZ cells which has been shown to be mediated via the NPY $Y_1$ receptor and the ERK 1/2 pathway in mice (Agasse et al., 2008). As well as enhancing neurogenesis, NPY has also been shown to increase the

chemokinetic activity of cells in the rat SVZ (Thiriet et al., 2011). Unlike the SGZ, however, the stress-activated protein kinase/c-Jun $NH_2$-terminal kinase (SAPK/JNK) pathway has also been implicated in mediating the action of NPY in the SVZ (Agasse et al., 2008). Like the ERK 1/2 pathway, the SAPK/JNKs are MAPKs involved in mediating neural proliferation and differentiation (Agasse et al., 2008). Other than the involvement of the MAPKs, no other mechanisms underlying the neuroproliferative effect of NPY on SVZ cells is known, which raises the question over whether NO mechanisms may also be involved. Indeed, the localisation of nNOS to the SVZ, olfactory and rostral migratory stream of adult male mice was demonstrated previously by Moreno-Lopez et al. (2000), however, nNOS was never found co-localised to, only intermingled with, PSA-$NCAM^+$ precursor cells (neuroblasts). Although this might suggest against the direct involvement of intracellular NO in mediating the effects of NPY on SVZ precursor cells, the anatomical proximity of the $nNOS^+$ neurons nevertheless supports the findings that NO, regardless of NPY, influences adult neurogenesis in the SVZ (Moreno-Lopez et al., 2000). On the other hand, contradictory to the findings by Moreno-Lopez et al., Torroglosa et al. (2007) have shown the expression of both nNOS and eNOS, as well as the intracellular production of NO, in neurosphere cultures derived from the SVZ of adult mice. Further immunocytochemical studies confirming these findings would prove beneficial, as well as exploring the nNOS expression by other cell types and looking at the expression of the other NOS subtypes in the SVZ. The question of whether NO is involved in mediating the effect of NPY on SVZ precursor cells, and if it is, how, remains a topic for further investigation.

### 6.8 Pathological relevance

The potential in furthering our understanding of the mechanisms by which the proliferation of endogenous neural stem/precursor cells are controlled lies with the prospect for manipulating these cells for therapeutic purposes. Of particular relevance are disorders afflicting the hippocampus, including stress and depression, and neurodegenerative diseases such as Alzheimer's disease (AD) and temporal lobe epilepsy (TLE). Progressive neuronal degeneration and cell death, for example, is associated with AD, as well as a disruption of neurogenesis in the SVZ and hippocampus of mouse models of AD by the main constituent of amyloid plaques, β-amyloid peptide (Aβ) (Haughey et al., 2002). In human AD sufferers, however, Jin et al. (2004) have shown that there is enhanced neurogenesis in the hippocampus, as demonstrated by an increase in the expression of

neurogenic markers and the number of expressing cells. Much like the enhanced neurogenesis observed in response to ischemia (Liu et al., 1998a), these observations suggest the presence of an intrinsic mechanism whereby the brain attempts to restore function to areas of neuronal damage or loss. This enhanced neurogenesis in response to AD, however, is insufficient in restoring function and is still associated with ongoing cell loss (Jin et al., 2004). Similarly, the loss of hilar and hippocampal interneurons, including NPY-immunoreactive interneurons (de Lanerolle et al., 1989; Chan-Palay et al., 1986), is a common feature of TLE, all of which contribute to cognitive decline (Gray, 2008). Much like the response to AD and ischemia, an increase in hippocampal neurogenesis is observed in response to seizure activity (Parent et al., 1997) and in experimental TLE (Parent et al., 2006). The loss of hippocampal volume and neuronal cell death is also associated with the pathogenesis of stress and depression, although in this case there is decreased neurogenesis (Lee et al., 2002; Lucassen et al., 2006; Gould & Tanapat, 1999; Malberg et al., 2000). In retrospect, the prominent cell loss associated with the progression of these hippocampal disorders suggest the possibility of replacing or protecting the deteriorating neuronal population through the control of neural stem/precursor cells.

The therapeutic potential of neural stem/precursor cells could be harnessed in a number of ways as a means to ameliorate or rescue damaged areas of the hippocampus. The transplantation of neural stem/precursor cells into injured areas of the brain, for example, is one therapeutic strategy, which could also potentially be combined with gene therapy to generate genetically manipulated stem cells *in vitro* which will express therapeutic gene products when transplanted *in vivo* (Shihabuddin et al., 1999). In a transgenic mouse model of AD, for example, Blurton-Jones et al. (2009) found that the transplantation of hippocampal neural stem cells improved cognition by rescuing spatial learning and memory deficits. Alternatively, a different strategy relies on the endogenous ability for neurogenesis in the adult brain. The possibility of isolating multipotent stem cells from both neurogenic and non-neurogenic regions of the adult mammalian CNS suggests that in non-neurogenic regions, adult neurogenesis may be suppressed by a lack of permissiveness in the surrounding environment and/or a deficiency in factors which support differentiation (Shihabuddin et al., 2000). In fact, adult spinal cord stem cells have been shown to generate neurons after being transplanted into the adult dentate gyrus (Shihabuddin et al., 2000). The existence of these endogenous stem/precursor cells could be recruited as an *in situ* source for replacing cells lost during pathological events by manipulating the factors in

their surrounding environment (Shihabuddin et al., 1999). To harness this limitless potential to full effect, however, the events underlying the control of neural stem/precursor cell proliferation and differentiation must be fully understood and appreciated. In this respect, NPY is particularly relevant. Decreased levels of NPY have been detected in the CSF of AD (Nilsson et al., 2001) and depressed (Widerlöv et al., 1988) patients, while the effect of NPY on increasing hippocampal neurogenesis has been implicated in the action of antidepressants (Malberg et al., 2000; Redrobe et al., 2002a). Similarly, NPY is important in mediating the increase in precursor cell proliferation and neurogenesis in the hippocampus in response to seizure activity (Howell et al., 2007). Understanding the central role in which NPY plays in mediating the proliferation of neural stem/precursor cells and in modulating levels of adult hippocampal neurogenesis will prove invaluable for the development of pharmacological mediators of repair or for ameliorating damage in response to a variety of pathological conditions.

Adult neurogenesis, however, is a tightly regulated process which can be influenced by a multitude of factors and increased hippocampal neurogenesis does not necessarily equate to functional repair. The increased hippocampal neurogenesis in response to seizure activity in adult rats, for example, is accompanied by abnormal network re-organisation and the formation of aberrant neural connections by the new granule cells (Parent et al., 1997). Likewise, pathological conditions which result in cell loss and reduced neurogenesis also change the structure and connectivity of the dentate gyrus, and thus have impacts on its physiological function (Gould & Tanapat, 1999). The correct mechanisms must be in place in order for adult neurogenesis to occur functionally. It is only through studying these processes in depth may we be able to direct the correct desired effect. Indeed, I have demonstrated not only the proliferative effect of NO mechanisms in mediating the effect of NPY, but also its antiproliferative effect, on neural precursor cells from the hippocampus. The Janus-faced role of NO in mediating both neuroproliferative or neuroinhibitory, and neurodegenerative or neuroprotective, effects serves not only to illustrate the complexity by which physiological and pathophysiological processes are regulated, but also highlights the conflicting factors which must be considered when developing potential therapeutic treatments.

### 6.9 3D hydrogel stem cell cultures

Attempts were made to develop 3D cultures of hippocampal cells in a novel synthetic silica hydrogel in an effort to explore the response and interaction of cultures to NPY in an *in vitro* environment which was more representative of *in vivo* conditions. Studying the proliferative response of neural precursor cells to external factors in 3D hydrogel cultures will not only further expand our understanding of the processes controlling this effect, but forms a means by which neural stem/precursor cells may be transplanted into injured areas of the CNS and their proliferation or differentiation manipulated for therapeutic effect. Indeed, although Laponite hydrogels still require further optimisation for improving its biocompatibility, much interest on the use of hydrogels in 3D cultures has been on the cultivation of stem cells. Stem cells are promising candidates in regenerative medicine and tissue engineering due to their potential to differentiate into a variety of specialised cell types to replace existing tissues (Shihabuddin et al., 1999). In order to fulfil this potential, however, there must be more efficient ways of handling, manipulating and controlling the differentiation of these stem cells *in vitro*, and most importantly, *in vivo* (i.e. inside the stem cell recipient). In this aspect, hydrogels are superior candidates for much the same reasons that they make ideal 3D matrices for cell culture. In fact, hydrogels may even help stem cells to renew and differentiate by mimicking the natural ECM.

Li et al. (2006) demonstrated the short-term self-renewal of human embryonic stem cells (hESCs) in a completely synthetic hydrogel ECM composed of a semi-interpenetrating polymer network. In this polymer hydrogel, cell adhesion ligand density and matrix stiffness was independently manipulated. hESCs adhered to the hydrogel surface, retained viability and morphological aspects and expressed markers representative of undifferentiated hESCs in the short term (Li et al., 2006). The large scale expansion of undifferentiated hESCs is a challenge and major drawback for the use of stem cells in regenerative medicine. The advantages of growing hESCs on artificial extracellular matrices, in comparison to more conventional cell-based feeder systems for the large scale expansion of undifferentiated stem cells, is the ease of scale up and reduced pathogen transmission risk (Li et al., 2006). Similarly, bioactive hydrogel scaffolds have been created to control the vascular differentiation of hESCs. Ferreira et al. (2007) developed a new methodology for enhancing the differentiation of hESCs into the vascular lineage via encapsulation in a bioactive dextran-based hydrogel matrix with either insoluble (Arg-Gly-Asp sequences) or soluble factors (vascular endothelial growth factor) for promoting

vascular differentiation. After 10 days, fluorescence activated cell sorting (FACS) and techniques in immunostaining were used to determine the percentage expression of vascular markers such as KDR/flk-1 (VEGF receptor). These dextran-based hydrogels were shown to support hESC differentiation, with a 22-fold increase in VEGF receptor KDR/flk-1 expression compared to spontaneously differentiated embryoid bodies (cell culture used for assessing stem cell differentiation potential) (Ferreira et al., 2007). Through the use of different 3D hydrogel matrices incorporating specific bioactive molecules, a primitive control of stem cell differentiation may be achieved (Nisbet et al., 2008).

As well as hESCs, neural stem cells (NSCs) have also been incorporated into 3D hydrogel matrices. Watanabe et al. (2007) established a 3D culture of NSCs in a collagen type-1 gel. The focus of their study was to produce a hydrogel scaffold for the transplantation of NSCs into injured spinal cord to promote functional recovery. This required a scaffold which was biocompatible, entrap NSCs within a cavity and act as a support for neurite extension. NSCs derived from embryonic rat striatum were grown in a 3D collagen hydrogel and subjected to a viability and migration assay to determine the optimal cell density and collagen concentration. The viability rate increased with an increase in NSC density and a decrease in collagen concentration. Under these optimal 3D collagen hydrogel conditions, the NSCs differentiated into neurons (40.1%), astrocytes (53.1%) and oligodendrocytes (5.3%) (Watanabe et al., 2007). Similarly, in a different strategy to develop a hydrogel scaffold for the repair of spinal cord injury by Nisbet et al. (2009), mouse NSCs and primary cortical neurons were cultured in a 3D thermoresponsive xyloglucan hydrogel which was optimised to provide similar mechanical characteristics to spinal cord and functionalised through immobilising poly-D-lysine to promote neural adhesion and neurite outgrowth. As well as supporting neuronal growth and differentiation, this functionalisation enabled the cell diameter, migration, neurite density and growth direction to be manipulated (Nisbet et al., 2009). Leipzig et al. (2011) also directed the neuronal differentiation of adult mouse NSCs encapsulated in a 3D methacrylamide chitosan hydrogel through the immobilisation of proliferative factors (pro-neural rat interferon-γ). As well as conventional methods such as cell entrapment, a novel method for controlling NSC differentiation by Ilkhanizadeh et al. (2007) involved using the inkjet printing of macromolecules on hydrogels to steer NSC differentiation. Biologically active molecules fibroblast growth factor-2 (FGF2), fetal bovine serum (FBS) and ciliary

neurotrophic factor (CNTF) were printed onto polyacrylamide-based hydrogels using an inkjet printer and seeded with primary fetal NSCs. While NSCs seeded onto FGF2 printed hydrogel remained undifferentiated, NSCs on FBS and CNTF printed areas displayed markers for smooth muscle or astrocytic differentiation, respectively. These results were coherent with the known effects of FGF2, CNTF and FBS on NSCs (Ilkhanizadeh et al., 2007). The use of hydrogels as 3D scaffolds for stem cells lie not only in its clinical applications but also as tools for studying the mechanisms underlying stem cell renewal and differentiation.

### 6.10 Conclusion

The ubiquitous neuropeptide, NPY, exerts a neuroproliferative effect on postnatal rat hippocampal cultures which was most likely mediated via intracellular NO production and signalled via a nNOS-cGMP-PKG and ERK 1/2 signalling pathway. The bifunctional nature of NO was demonstrated by its conflicting effects on neural precursor cell proliferation. While the literature on the effects of NO signalling on adult neurogenesis *in vivo* is complex and conflicting, the NPY $Y_1$ receptor has been identified as a key target to selectively promote NO-mediated neural stem/precursor cell proliferation as a possible therapeutic intervention for promoting hippocampal neurogenesis. Notably, this study has united two significant modulators of adult hippocampal neurogenesis into a common signalling framework.

# Appendix A

## Appendix A

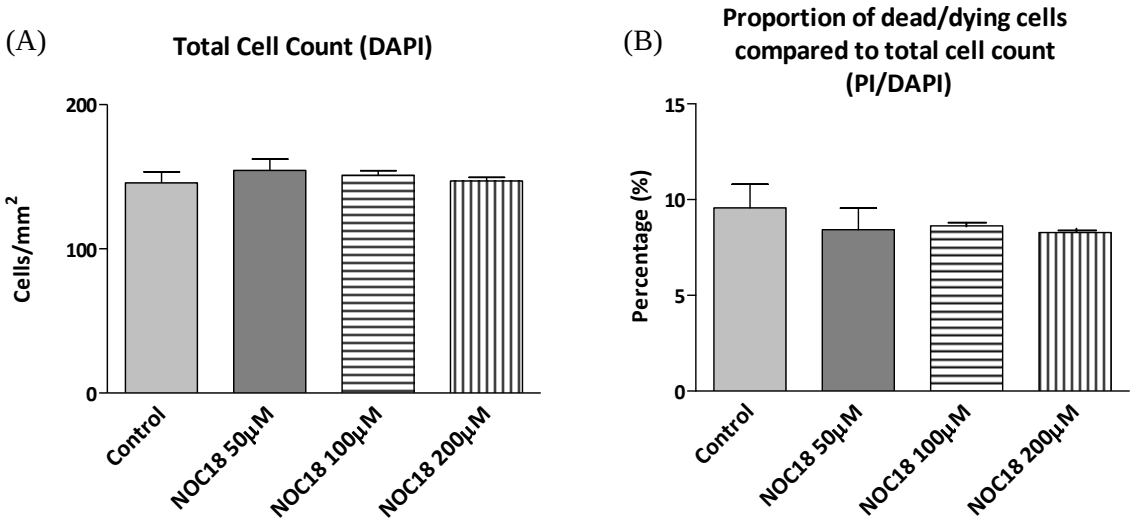


Figure A.1The NO donor, DETA/NONOate (NOC18) had no effect on cell death in hippocampal cultures. Hippocampal cells were cultured under control conditions (NBA-A/B27/glutamine) or 50, 100 or 200 µM DETA/NONOate for 3 DIV before cell death was assessed by PI and DAPI staining. The (A) total cell counts and (B) percentage of dead/dying cells were unchanged in the presence of DETA/NONOate, regardless of the concentration. Data represent mean ± SEM based on a sample that represents at least 7 wells per condition from two different experiments. One-way ANOVA with Dunnett's multiple comparison test, compared to control condition. *$p < 0.05$. None of the test conditions were significantly different from control.

# Appendix B

## Appendix B - Laponite: A synthetic silica hydrogel

### B.1 Introduction

The rheological and handling properties of Laponite, a thixotropic hydrogel, was investigated in order to determine, and optimise, its potential as a 3D cell culture matrix.

#### B.1.1 Hydrogels

Hydrogels were one of the first biomaterials developed for use in the human body (Kopecek, 2007). Hydroxyethyl methacrylate (HEMA), a hydrogel first described by Wichterle and Lim (1960), was later used for constructing contact lenses. A range of natural, synthetic and semi-synthetic hydrogels have been explored for use as the scaffold material in 3D cultures. The vast range of available hydrogels and their extensive physical properties are promising for creating highly adapted 3D cell cultures for an array of applications.

#### B.1.2 Types of hydrogel

Hydrogels fall into three main classes depending on the nature of the polymer used for synthesis: synthetic, natural or semi-synthetic combination hydrogels (Hoffman, 2002; Drury & Mooney, 2003). A select few from each class is listed in table B.1.1.

Table B.1.1 Polymers used to synthesise hydrogels (Drury & Mooney, 2003; Lee & Mooney, 2001).

| Natural polymers and derivatives: |
|---|
| - Anionic polymers: alginic acid, pectin, chondroitin sulphate.<br>- Cationic polymers: chitosan, polylysine<br>- Amphipathic polymers: collagen, fibrin<br>- Neutral polymers: dextran, agarose |
| Synthetic polymers: |
| - Polyesters: PEG-PLA-PEG, PLA-PEG-PLA (PEG: poly(ethylene glycol), PLA: poly(lactic acid)), PEO (poly(ethylene oxide)<br>- Other polymers: PEG-bis-(PLA-acrylate), P(biscarboxy-phenoxy-phosphazene)<br>- Silica hydrogels: Laponite RD |
| Synthetic and natural combination polymers: |
| - P(PEG-co-peptides), collagen-acrylate, alginate-acrylate |

Depending on the nature of the hydrogel network, hydrogels can be further classified into two groups, physical/reversible hydrogels and chemical/permanent hydrogels. Physical or reversible hydrogel networks are held together by molecular entanglements

and/or secondary forces such as H-bonding, ionic or hydrophobic forces (Hoffman, 2002). These hydrogels are not chemically stable and transient network defects can occur in response to changes in temperature, pH, ionic strength, shear stress or specific solutes, lending to their reversible nature. Depending on the specific hydrogel, response to different factors may lead to network disruption and hydrogel breakdown, or network formation and hydrogel formation. One such physical hydrogel is calcium alginate, where a multivalent ion of opposite charge is combined with a polyelectrolyte for hydrogel formation (Kikuchi et al., 1997). Conversely, chemical or permanent hydrogels contain covalently-crosslinked polymer networks which are much stronger and resilient to breakage (Hoffman, 2002). These hydrogels reach an equilibrium swelling level in aqueous solution which is determined by the crosslink density. Hyaluronic acid is a chemical hydrogel formed by crosslinking hyaluronic acid with any of a variety of hydrazide derivatives such as adipic dihydrazide (ADH) (Lee & Mooney, 2001; Prestwich, 1998).

### B.1.3 Methods for synthesising hydrogels

There are many varieties of hydrogel, and as such, are synthesised via a range of methods. With regards to physical gels, changes in physical factors such as temperature or pH can lead to hydrogel formation. PEO-PPO-PEO (PEO: poly(ethylene oxide), PPO: poly(propylene oxide)) triblock copolymers form hydrogels through an increase in temperature (Fusco et al., 2006), while on the contrary, agarose gels require cooling for gel formation (Thompson et al., 1985). Meanwhile, PEO and PAAc (polyacrylic acid) form H-bonded gels in aqueous solution after a reduction in pH (Nho et al., 2004). In contrast, chemical gels require cross-linking of polymers. These polymers can be cross-linked in the solid state or in solution with chemical crosslinkers, multi-functional reactive compounds or radiation. Monomers can also be copolymerised with chemical crosslinkers or multifunctional macromers (Drury & Mooney 2003; Lee & Mooney, 2001).

### B.1.4 Hydrogel applications

Hydrogels are promising materials currently used in a range of biomedical applications due to their diverse chemical and physical properties (Fig. B.1.1).

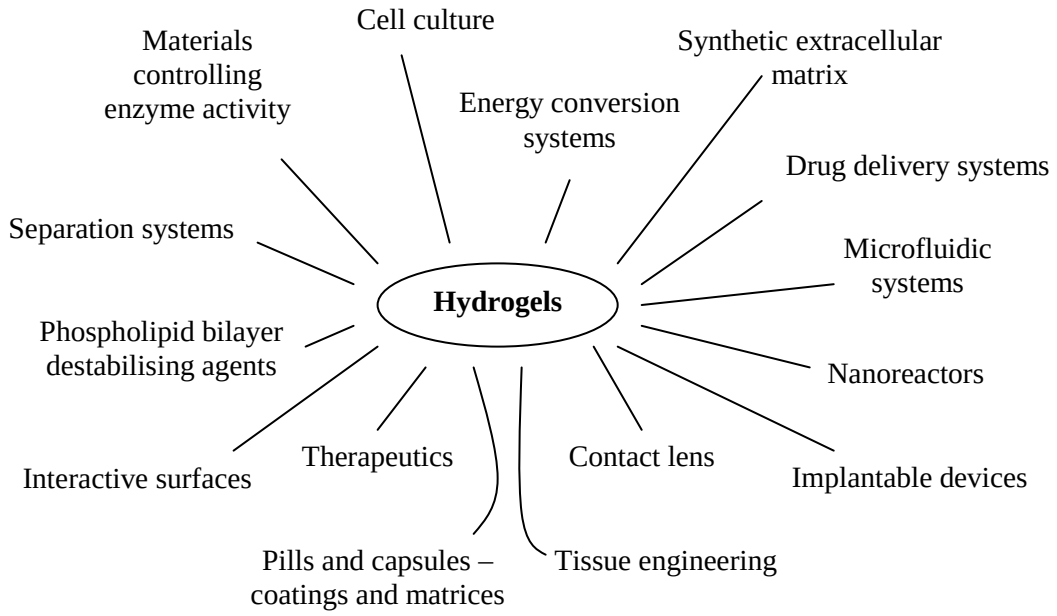


Figure B.1.1 Current and potential applications of hydrogels (adapted from Kopecek, 2007).

3D hydrogel matrices which are highly hydrated and provide cells with a place for adherence, proliferation and differentiation are highly appealing, especially as scaffolds for cell delivery or the possibility of creating transplantable 'bioartificial' organs or tissues (Khademhosseini & Langer, 2007). When considering the use of either synthetic or natural hydrogels, however, both classes have their merits and drawbacks. Synthetic hydrogels have more controllable and reproducible properties than natural hydrogels, but may be less biologically compatible. For example, PLG (poly(lactide-co-glycolide)), a Food and Drug Administration (FDA) approved scaffold material, is mechanically strong and hydrolytically degradable, but the hydrophobic nature and synthesis methods makes it hard to produce matrices containing viable cells (Gunatillake & Adhikari, 2003). On the other hand, natural hydrogels are usually favoured over their synthetic counterparts because of their biocompatibility. Natural hydrogels are often composed of molecules derived from and/or have macromolecular properties which are similar to the natural ECM and so usually interact more favourably *in vivo* than synthetic hydrogels. For instance, collagen, an abundant structural protein in the mammalian ECM (Alberts et al., 2002), is one of the most widely used hydrogels for 3D matrices. Naturally existing metalloproteases (especially collagenase) and serine proteases degrade collagen, allowing for local control of degradation by cells in the engineered tissue (Drury & Mooney, 2003).

### B.1.5 Laponite

Laponite, or hydrous sodium magnesium silicate, is a colloidal synthetic layered silicate (Avery & Ramsey, 1986) often used as a speciality additive which improves the performance of a wide range of industrial and household products through controlling viscosity and flow properties (Cummins, 2007; Rockwood Clay Additives Ltd.). While Laponite dispersions are capable of forming gels which can suspend solid particles, it is also sensitive to shear stress. It is a thixotropic physical hydrogel which changes its rheological properties in response to shear stress, exhibiting high viscosity at low shear rates, low viscosity at high shear rates and progressive restructuring after shear (Willenbacher, 1996; Martin et al., 2002). This thixotropic behaviour underlies the many applications of Laponite.

The dispersed primary particle of Laponite is a disk-like clay particle with a thickness of 0.92 nm and diameter of 25 nm (Fig. B.1.2) (Avery & Ramsey, 1986; Thompson & Butterworth, 1992). The particle disk is ionised in aqueous solution with the disk face possessing a negative charge, typically of about 50-55 mmol.100g-1, while the disk rim may be negatively or positively charged depending on pH, but is typically positively charged due to the absorption of hydroxyl groups (Kroon et al., 1998; Mongondry et al., 2005). The typical positive charge of the disk rim is 4-5 mmol.100g-1 (Tawari et al., 2001).

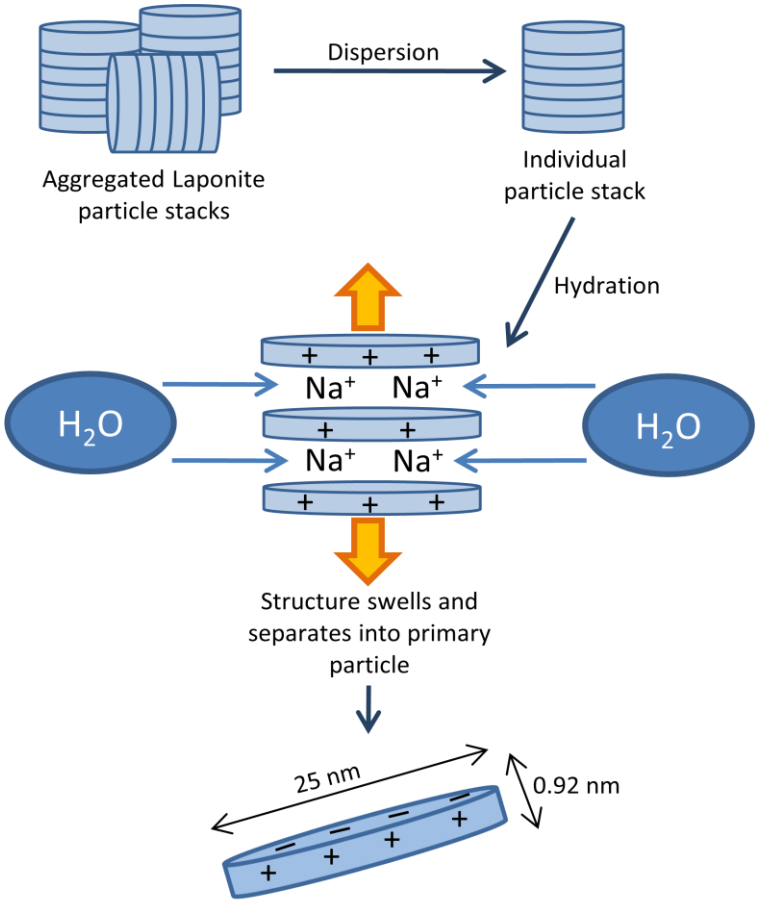


Figure B.1.2 Laponite addition to water. Laponite powder added to aqueous solution initially form aggregated particle stacks, followed by dispersal into individual stacks. The sodium ions between each Laponite layer are hydrated by water, which results in a swelling of the stack structure and separation into primary particle disks (redrawn from Rockwood Clay Additives Ltd.).

When dispersed, a narrow band of solubilised sodium ions are held between Laponite disks. Through electrostatic interactions, the solubilised sodium ions are drawn towards the Laponite crystal surface; while on the other hand, osmotic pressure from the surrounding aqueous solution pulls the sodium ions away. This forms an equilibrium where sodium ions are retained in a diffuse region on both sides of the Laponite particle disks, known as electrical double layers (Tawari et al., 2001) (Fig. B.1.3). Thus, when two Laponite particle disks approach, they repel each other due to mutual positive charge resulting in low dispersion viscosity (Kutter et al., 2000).

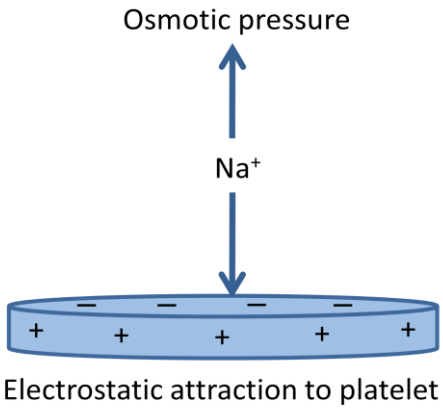


Figure B.1.3 Dispersed Laponite primary particle disk. The electrostatic attraction from the negative charge on the surface of the Laponite platelet forms an equilibrium with the osmotic pressure drawing the sodium ion away from the platelet, forming a diffuse region where sodium ions are held (redrawn from Rockwood Clay Additives Ltd.).

If polar compounds (such as salts and surfactants) are added during Laponite dispersion, the osmotic pressure drawing the sodium ions away from the particle surface is reduced, which in turn causes a reduction in the electrical double layer. Weaker positive charges localised on the Laponite crystal edges can then interact with the negative surface of adjacent Laponite crystals. These interactions between Laponite crystals can result in the formation of a connected hydrogel network (Mongondry et al., 2005; Mourchid et al., 1995a; Nicolai & Cocard, 2001).

### B.1.6 Laponite Phase diagram

The phase diagram first proposed by Mourchid et al. in 1995 illustrates the transition of Laponite dispersions from a sol to gel phase as a function of the salt and Laponite concentration (Fig. B.1.4) (Mourchid et al., 1995a; Mourchid et al., 1995b; Mourchid et al., 1998).

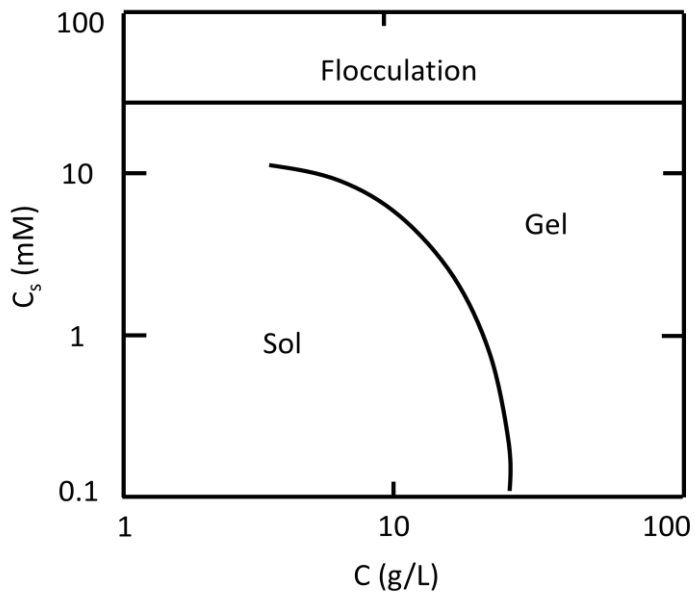


Figure B.1.4 State diagram of Laponite dispersions. The x-axis represents the solid fraction or concentration of Laponite (g/L) while the y-axis represents the salt concentration (mM). The sol to gel transition line in the middle divides the two states of Laponite dispersions. Flocculation of Laponite dispersions occur at high salt concentrations ($C_s$ > 20 mM) (redrawn from Mongondry et al., 2005).

If Laponite dispersions showed a measurable storage shear modulus or viscoelastic solid-like behaviour, the dispersions are considered in gel state. Gel-like behaviour develops slowly and is time-dependent (Mongondry et al., 2005). The time it takes for Laponite dispersions to reach gel-like behaviour increases strongly with decreasing Laponite and salt concentration. An increase in salt concentration (ionic strength), however, shifts the transition and allows for lower Laponite concentrations to reach a gel-like state (Mourchid et al., 1995a). Gel fragility increases with a decrease in Laponite concentration and increase in ionic strength (Nicolai & Cocard, 2001). The mechanisms dictating the transition from sol to gel are not fully understood.

### B.1.7 Laponite hydrogel formation – The attractive and repulsive theories

Two opposing theories exist for the mechanism of Laponite hydrogel formation, the attractive theory and repulsive theory. The attractive theory suggests that attractive interactions between Laponite particles result in aggregation and the formation of a connected network or 'house of cards' structure (Fig. B.1.5) (van Olphen, 1962). In the 'house of cards' theory, attractive interactions between the negatively charged face and positively charged rim of Laponite particles result in a gathering of particles in

microdomains which associate to form large fractal superaggregated structures held together by weak electrostatic forces and weak van der Waals attractions. When the connection network is macroscopic, a gel state is obtained (Martin et al., 2002). A gel state is a colloidal system described as a porous network of interconnected nanoparticles spanning a liquid medium. Instead of a homogenous distribution of particles, hydrogels usually contain areas of high density dispersed within a low density hydrogel network (Ramsay & Lindner, 1993; Willenbacher, 1996).

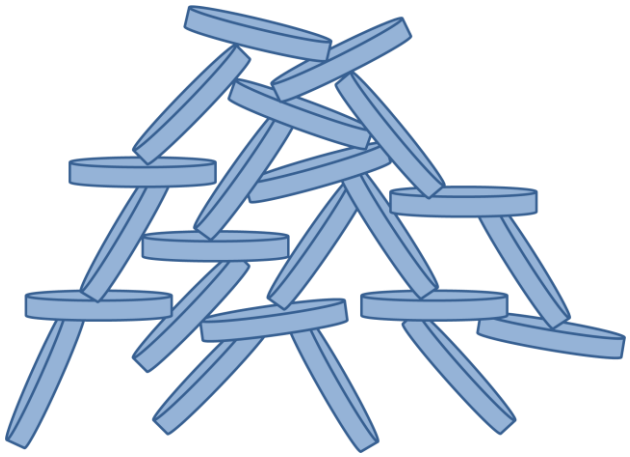

Figure B.1.5 House of cards structure. Individual Laponite particles interact through the negatively charged faces and positively charged edges to form a macroscopic gel network (redrawn from Rockwood Clay Additives Ltd.).

Several aspects of the rheology of Laponite support the attractive gel formation theory. As the bonds holding the structure together are ionic, temperature does not affect the viscosity of the hydrogel, instead, the ‘house of cards’ structure is easily disrupted under application of shear stress which breaks the weak ionic and van der Waal interactions, lending to the hydrogel's reversible characteristics (Mourchid et al., 1995a). In addition, restructuring after stress requires time as the particles must reorientate and interact with other particles (Ramsay & Lindner, 1993). Dynamic light scattering studies on Laponite particle aggregation have shown an increase in aggregation rates with increasing electrolyte concentration due to the screening of electrostatic repulsion between particles and a decrease in the energy barrier (Mongondry et al., 2005). On the other hand, an increase in pH, which favours deprotonation and reduces the positive charge of the disk rim, causes an overall decrease in particle aggregation (Tawari et al., 2001). In a separate study using time- and ensemble-averaged light scattering, gel formation was shown to be

preceded by aggregation (Nicolai & Cocard, 2000). Laponite particles were shown to form fractal clusters through aggregation which grow in size until they sediment at low concentrations (since they are too weak to resist gravity) or fill up the space and form a gel with increasing viscosity at higher concentrations through the growth of aggregates until the network spans the whole volume (Nicolai & Cocard, 2000). This slow aggregation process is induced by electrostatic repulsion screening. Although concentration and ionic strength do not determine aggregate structure, the aggregation rate increases significantly with increasing ionic strength due to a reduction in electrostatic repulsion (Nicolai & Cocard, 2000). Dynamic light scattering studies on large aggregates show that these aggregates are not rigid. The angle between the positive edge of one particle and negative face of another, which may be close to 90°, fluctuates (Mongondry et al., 2005).

Other studies have shown that the attractive interactions can be weakened by the addition of peptisers (salts) which bind to the positively charged disk rim and obstruct their interaction with the negatively charged disk face. When peptisers (such as tetrasodium diphosphate) are present, the Laponite network forms slowly and restructuring after shear is much delayed with an extended fluid state (Martin et al., 2002). The presence of these positive charges on the edge of Laponite disks seem to be necessary for inducing aggregation and gelation (Mongondry et al., 2005). By delicately manipulating the balance between repulsive and attractive interactions, the behaviour of Laponite dispersions can be controlled, which form the basis for diverse formulations of Laponite with unique properties. The theory of attractive interaction, aggregation and the formation of a ‘house of cards’ structure is favoured by biomaterial scientists.

In contrast to the attractive theory, the repulsive or glass formation theory suggests that interparticle repulsive interactions lead to a glassy state (a disordered solid phase) instead of a gel state (presence of an ordered network) and aggregation does not occur except at high ionic strength (salt concentration > 10mM) (Kroon et al., 1998; Bonn et al., 1999). In this case, the lack of free volume means that each particle is unable to move because every location surrounding it is already occupied. These long-range electrostatic repulsions between double layers were originally suggested by Norrish (1954). During light and x-ray scattering studies, even though the reorientation of charged Laponite particles were observed during gelation, the formation of hydrogel did not occur via aggregation to form larger clusters (Kroon et al., 1998). Static light scattering and rheometric studies also show

no evidence of an organisation of colloidal particles with increased viscosity (Bonn et al., 1995). Gel-like behaviour, however, occurs even at low Laponite concentrations and occurs more rapidly when salt is added, which contradicts the presence of strong repulsive interactions supported by the glass formation theory (Levitz et al., 2000).

Both mechanisms may have equally important roles in Laponite gelation, depending on factors such as ionic strength and Laponite concentration. At low ionic strengths the electrostatic interactions are long-range type, possibly interparticle repulsions, while at moderate ionic strengths the electrostatic interactions are short range, typical of attractive interactions. Particles tend to aggregate spontaneously under these circumstances and possibly form microdomains which may become interconnected (Nicolai & Cocard, 2001). Concentrated dispersions would form hydrogels relatively quickly or successfully compared to less concentrated dispersions (Martin et al., 2002). On the whole, the precise mechanism of Laponite solid phase formation and network structure is still undefined and many studies are continually conducted into the two theories. One possible reason for this may be due to the sensitivity of Laponite to sample preparation procedures, which makes result comparison difficult between separate groups (Cummins, 2007).

### B.1.8 The aims of this chapter

Laponite hydrogels were assessed in its ability to form distinct hydrogel layers and sectors, which would have been important for constructing multilayered or multi-sectored 3D cultures, as well as optimisation for supporting cell growth by exploring its response to dispersion in culture media.

## B.2 Methods

### B.2.1 Methodology and experimental aim

A variety of different Laponite formulations exist, some of which are listed in table B.2.1. The aim of this chapter was to explore the properties of the Laponite hydrogel, focusing initially on the conventional Laponite formulation, Laponite RD (rapid diffusion). After determination of a suitable working concentration of Laponite RD, its handling and manipulation as a potential 3D cell culture material was explored before it was optimised for supporting cell survival. All investigations were carried out at room temperature (20-25°C).

Table B.2.1 Formulations of Laponite (from Southern Clay Products, inc., Rockwood Additives Ltd.)

| Laponite formulation | Description |
|---|---|
| Laponite RD (rapid diffusion) | Highly thixotropic hydrogels produced at concentrations of 2% or greater in water |
| Laponite RDS (rapid diffusion sol) | At 10% concentration in water, these will remain free flowing for 24 hours. On addition of small quantities of electrolyte, highly thixotropic hydrogels are formed rapidly. |
| Laponite XLG | Low heavy metals content version of RD |
| Laponite XLS | Low heavy metals content version of RDS |
| Laponite JS | At 18% concentration in water, these will remain free flowing for at least 1 month. |
| Laponite B | Highly thixotropic hydrogels produced at concentrations of 2% or greater in water |

### B.2.2 Laponite RDS and Laponite XLS hydrogel formation - Non-sterile conditions

The Laponite RDS/XLS powder (courtesy of Mr Patrick Jenness, Rockwood Additives Ltd.) was added to water or solution (i.e. NBA-A/B27/Glu medium) and quickly vortexed for at least 10 s to ensure thorough powder dispersion. Depending on the concentration (percentage weight/volume or % w/v) and type of Laponite (RD or XLG), setting times differed remarkably. The hydrogels were considered set if they remained undisturbed by physical inversion.

In accordance with the manufacturer's instructions, a 2% dispersion of Laponite RD in water was the minimum concentration required to produce a thixotropic hydrogel. A Laponite RD hydrogel concentration of 5% dispersion in water was used for handling and

manipulation studies as the hydrogels produced set quickly and were less fragile than 2% Laponite dispersions.

Gel thixotrophy (in response to shear stress) was determined by passing the hydrogel through a syringe fitted with a 0.8 x 40 mm hypodermic needle and observing its response. In response to the high shear stress from enforcement through the needle, the viscosity of the gel is reduced and the gel flows. After removal of shear stress, the hydrogel slowly reforms and becomes more viscous over time, eventually returning to its original gelled state.

### B.2.3 Handling and Manipulation of Laponite hydrogels – Layering

The layering of hydrogels ultimately provides a platform upon which a complex 3D cell culture system consisting of different niches could be created. Laponite RD preparations at 5% concentration dispersion in water were pre-stained with one of a range of dyes for better visualisation, including Phenolphthalein (anionic) (Sigma Aldrich, UK), Litmus (Sigma Aldrich, UK), Rhodamine 6G (cationic) (Sigma Aldrich, UK) and Eosin Y (anionic) (Sigma Aldrich, UK) or not stained (clear). Prepared hydrogels were transferred via pipette to a cuvette where the gels were layered. The hydrogels were allowed to set completely before the addition of another layer and layered gels were centrifuged to determine whether the layers remained separated.

### B.2.4 Layering hydrogels in multiwell plates

6-, 12- and 24-well multiwell plates are frequently used for conventional cell culture and would be a good foundation for the formation of multilayered 3D cultures. In order to form these multilayered complexes, however, Laponite hydrogels must first be able to form distinct layers within these plates. A range of Laponite RD (% w/v) preparations were pre-stained with one of a range of dyes (1-2 drops) including Phenolphthalein (anionic), Litmus, Rhodamine 6G (cationic) and Eosin Y (anionic) or not stained (clear). Hydrogels were transferred via pipette to multiwell (6-well, 12-well and 24-well) plates where the hydrogels were layered. Thicknesses of the hydrogel were calculated using the formula: $\pi$ x radius$^2$ (mm) x height (mm) = volume required (µl), and details of the well diameter or radius.

Attempts at layering hydrogels in multiwell plates, however, proved difficult because of the formation of a meniscus inside each well and the inability to obtain flat gel layers. Flat gel layers were important for generating a distinct multi-tiered 3D cell culture system. Attempts at obtaining flat hydrogels and to reduce meniscus formation included centrifugation, modifying the percentage Laponite RD, and the use of non surface-treated hydrophobic plates.

#### B.2.4.1 Centrifugation to obtain flat hydrogel layers

A range of concentrations of Laponite RD (% w/v) preparations were pre-stained with one of a range of dyes and transferred via pipette to multiwell (6-well, 12-well and 24-well) plates where the hydrogels were layered. The plates were then centrifuged (5177 Sorvall Legend RT Centrifuge) at 4600rpm (3760g) for 10 min with the aid of plate adaptors.

#### B.2.4.2 Modifying the percentage of Laponite RD to obtain flat hydrogel layers

The Laponite concentration of hydrogel may affect meniscus formation. A range of concentrations of Laponite RD (1%, 2%, 3%, 4%, 5% and 6% w/v) preparations in water were pre-stained with Phenolphthalein, gels transferred via pipette to multiwell (6-well, 12-well and 24-well) plates, and layers created to determine the effect of Laponite RD percentage (w/v) on the size of the meniscus.

#### B.2.4.3 Non surface-treated hydrophobic (polystyrene) multiwell plates to reduce meniscus formation

A range of concentrations of Laponite RD (% w/v) preparations were pre-stained with one of a range of dyes and transferred via pipette to non surface-treated hydrophobic multiwell (6-well and 24-well) plates where the hydrogels were layered.

### B.2.5 Hydrogel Injection

The ability to form structures other than layers were investigated by injecting Laponite RD hydrogels into layered gels. 5% Laponite RD (w/v) dispersions in water were pre-stained with Rhodamine 6G or not stained (clear). Unset stained hydrogels were quickly transferred to 10 ml syringes and allowed to set, while clear gels were layered in 6-well plates. Stained Laponite hydrogels were injected into set and semi-set clear Laponite hydrogels.

### B.2.6 Hydrogel transfer

3D cultures may need to be removed from multiwell culture plates for further investigations. To test this idea, Polytetrafluoroethylene (PTFE) or Teflon membrane (Millipore, UK) was cut to size and layered on the bottom of petri-dishes and multiwell plates. 5% Laponite RD (w/v) dispersions in water were pre-stained with Rhodamine 6G or not stained (clear) and transferred to the PTFE-layered petri-dishes or multiwell plates. After setting, PTFE coated instruments (i.e. scalpel and tweezers) could be used to remove the hydrogel slabs from the plates and dishes.

### B.2.7 Laponite culture medium hydrogels

In order to optimise Laponite hydrogels for cell growth, culture medium must be incorporated. The culture medium for hippocampal cells consists of Neurobasal A medium (Life Technologies, UK) supplemented with 2% B27 (Life Technologies, UK) and 0.5 mM Glutamine (Sigma Aldrich, UK).

#### B.2.7.1 Laponite RD culture medium hydrogels

In order to obtain a better idea of the hydrogel formation dynamics in culture medium, a range of Laponite RD dispersions (% w/v) were made up with varying concentrations of culture medium diluted in distilled water (table B.2.2) in glass vials (for gel visualisation). The vial lids were screwed on tightly to prevent gel desiccation and hydrogel formation was assessed.

Table B.2.2 Laponite dispersions in varying concentrations of culture medium diluted in distilled water.

| Culture medium dilution (in distilled water) | Laponite RD (w/v) | | | |
|---|---|---|---|---|
| 25% | 5% | 10% | 15% | 20% |
| 30% | | | | |
| 40% | | | | |
| 50% | | | | |
| 75% | | | | |
| 100% | | | | |

The possibility of developing 100% (neat) culture medium Laponite RD hydrogels was explored to maximise the chances cell survival. Laponite RD at a range of concentrations (10%, 15%, 16%, 17%, 18%, 19%, 20%, 25%) was dispersed in neat culture medium to assess hydrogel formation. Setting times were recorded and thixotropic properties investigated by passing through a syringe.

### B.2.8 Laponite RDS, JS and B hydrogels

Other formulations of Laponite, such as RDS (rapid diffusion sol), JS and B (courtesy of Mr Patrick Jenness, Rockwood Additives Ltd.), were tested for hydrogel formation in distilled water and culture medium. The Laponite RDS/JS/B powder was added to water or medium (NBA-A/B27/Glu medium) at varying concentrations (% w/v) and vortexed for at least 10 s to ensure thorough powder dispersion.

### B.2.9 Laponite RDS culture medium hydrogels

A range of Laponite RDS concentrations (2.5%, 5%, 10%, 15% and 20% w/v) were dispersed in 100% culture medium and hydrogel formation assessed. Setting times were recorded and thixotropic properties investigated by passing through a syringe.

#### B.2.9.1 Layering Laponite RDS culture medium hydrogels in multiwell plates

16% Laponite RDS preparations in 100% culture medium were prepared and layered in non surface-treated 6- and 24-well multiwell plates to verify that handling properties were similar to water-based Laponite hydrogels.

## B.3 Results

### B.3.1 Hydrogel setting time decreased with increased Laponite concentration

In an inverse relationship, an increase in Laponite RD concentration (% w/v) was directly linked to a decrease in setting time. The setting time for Laponite dispersions at 2%, the minimum required for hydrogel formation, was around 2 h, however, Laponite dispersions above 5% all set within 10 min. The higher the percentage of Laponite the quicker the hydrogel set (Fig. B.3.1). This increase in Laponite concentration was also associated with an observed increase in hydrogel opacity (Fig. B.3.2).

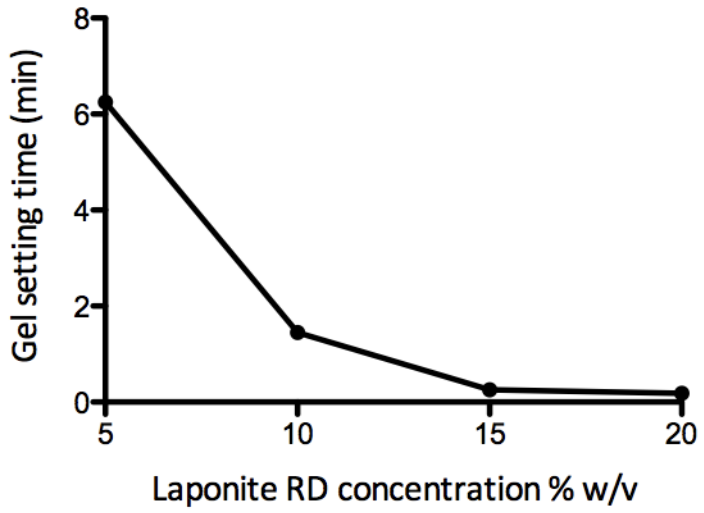


Figure B.3.1 An increase in Laponite RD concentration was directly linked to a decrease in setting time.

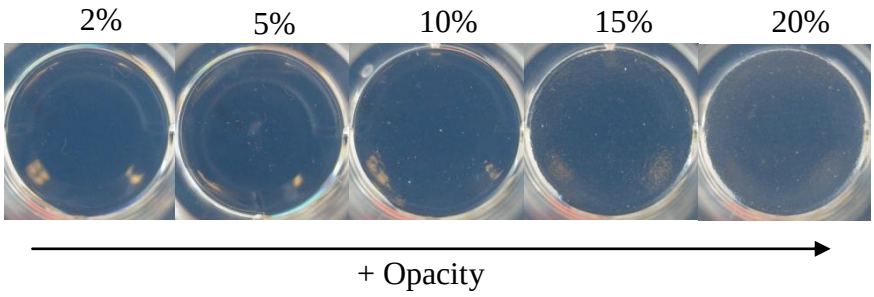


Figure B.3.2 Hydrogel opacity increased with an increase in Laponite RD concentration.

### B.3.2 Thixotropic Laponite hydrogels

Laponite hydrogels were passed through a syringe to determine its thixotropic properties in response to shear stress. While low concentrations of Laponite (5%) demonstrated a thixotropic response, higher concentrations of Laponite (15%) were not thixotropic. The 5% Laponite hydrogel had a low, almost fluid, viscosity when enforced through the needle, before returning to its gel state once the stress was removed (Fig. B.3.3A and B). In contrast, the viscosity of the 15% Laponite hydrogel remained unchanged when exposed to shear stress (Fig. B.3.3 C and D).

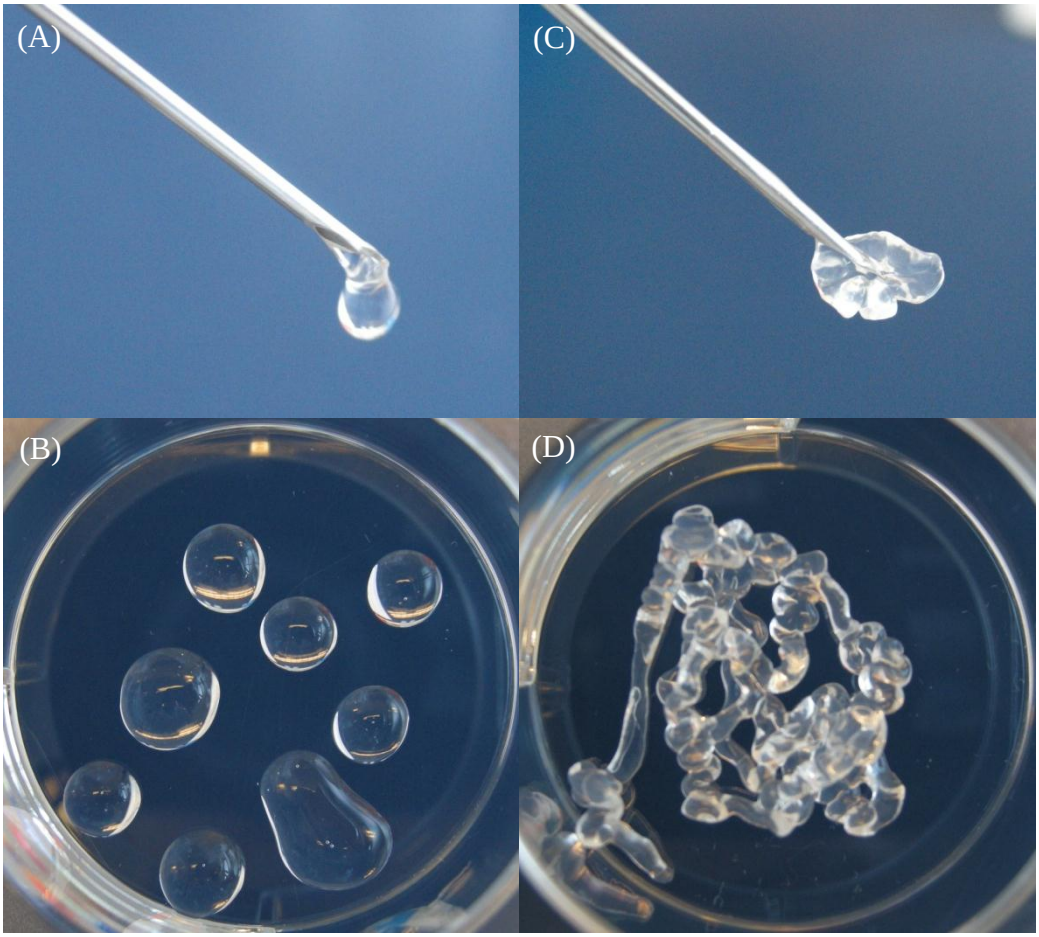


Figure B.3.3 Laponite hydrogels were passed through a syringe to determine its thixotropic response to shear stress. 5% Laponite hydrogels exhibited a thixotropic response, as demonstrated by (A) a decrease in viscosity and (B) reformation of a gel state over time. 15% Laponite hydrogels, on the other hand, were (C) not thixotropic and (D) showed no changes in gel viscosity.

### B.3.3 Laponite hydrogels could be manipulated by layering

The ability to layer Laponite hydrogels would permit the formation of complex multi-layered or -sectored 3D cultures. To determine whether Laponite hydrogels could be layered on top of one another, alternating layers of stained and non-stained Laponite hydrogel layers were created in clear plastic cuvettes (Fig. B.3.4). It was possible to manipulate the layer thicknesses (1 mm to 1 cm) by changing the volume of gel and the layers remained distinct from each other.

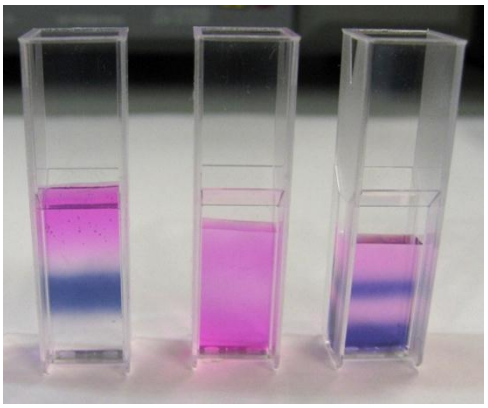

Figure B.3.4 Laponite hydrogels layered in plastic cuvettes stained with either phenolphthalein (pink), litmus (purple) or unstained.

### B.3.4 Hydrogel layering in multiwell plates was hindered by meniscus formation

As a vessel for creating 3D cultures, hydrogel layering was attempted in multiwell plates. Layer formation, however, was hindered by meniscus formation (1.9 - 2 mm size meniscus) (Fig. B.3.5) and the inability to obtain flat gel layers, which were essential for creating multilayered 3D hydrogel culture constructs. Attempts to obtain flat gel layers and reduce meniscus formation included centrifugation, modifying the percentage Laponite RD, and non surface-treated hydrophobic plates.

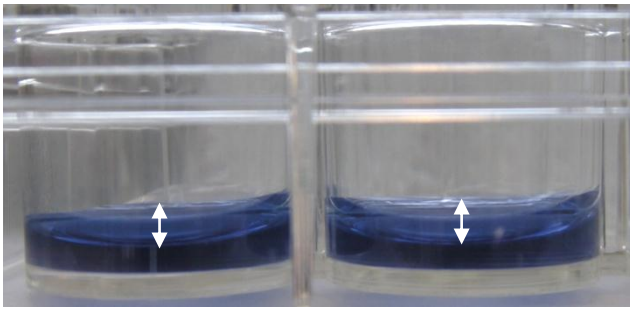

Figure B.3.5 The formation of flat Laponite hydrogel layers were hindered by the presence of a meniscus (arrows).

#### B.3.4.1 Flat gel layers could be obtained by centrifugation but layers were slanted

With the use of plate adaptors, plated Laponite hydrogels were centrifuged at 4600 rpm for 10 min in an attempt to flatten the layers using centrifugal force. Although flat gel layers

were achieved after centrifugation, layers were slanted at an angle and not horizontal, most likely due to the centrifugal force the hydrogel was exposed to (Fig. B.3.6).

Figure B.3.6 Slanted phenolphthalein-stained Laponite hydrogels after centrifugation. Gels are flat but slanted at an angle (dotted lines) due to centrifugal force.

The angle of the hydrogels increased as they became further away from the centre of the multiwell plate, following the shape of the centrifugal force it was exposed to (Fig. B.3.7).

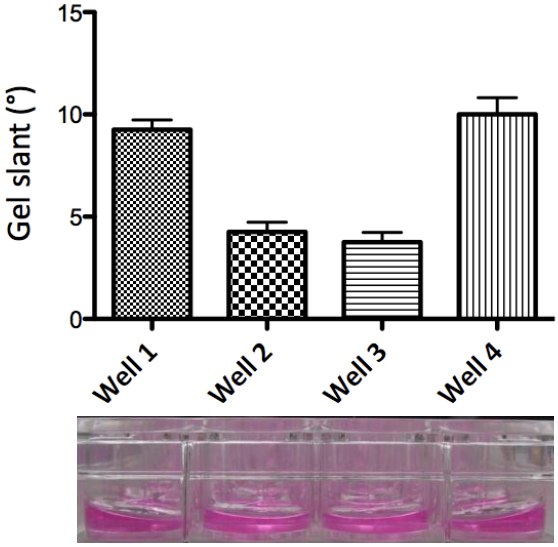


Figure B.3.7 The angle of the hydrogel layers (°) increased the further they were away from the centre of the plate. Wells 1 and 4 are situated on the outside of the plate, while wells 2 and 3 are in the centre.

### B.3.4.2 The meniscus decreased with an increase in Laponite concentration

In a different approach to minimising the meniscus of hydrogel layers, a range of Laponite RD concentrations (1%, 2%, 3%, 4%, 5% and 6% w/v) were investigated for any potential effects on meniscus size. An increase in Laponite concentration was associated with a

visual decrease in the meniscus height (Fig. B.3.8), which was quantified by directly measuring the size of the meniscus. There was, on average, about a 0.2 mm reduction with every 1% increase in Laponite RD concentration, and a significant decrease in the meniscus size was observed with higher Laponite concentrations (4-6%) when compared to 1% dispersions (One-way ANOVA with Dunnett's post-hoc test, $p<0.05$, $F=80.78$ and d.f.=17) (Fig. B.3.9).

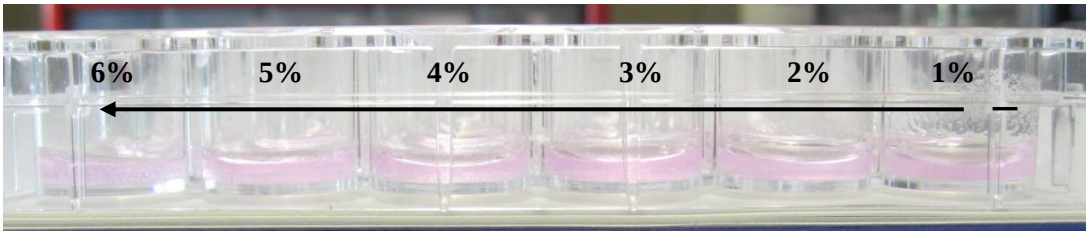


Figure B.3.8. 1% to 6% (w/v) Laponite RD concentration hydrogels layered in a multiwell plate. The meniscus was reduced with increasing Laponite concentration (arrow).

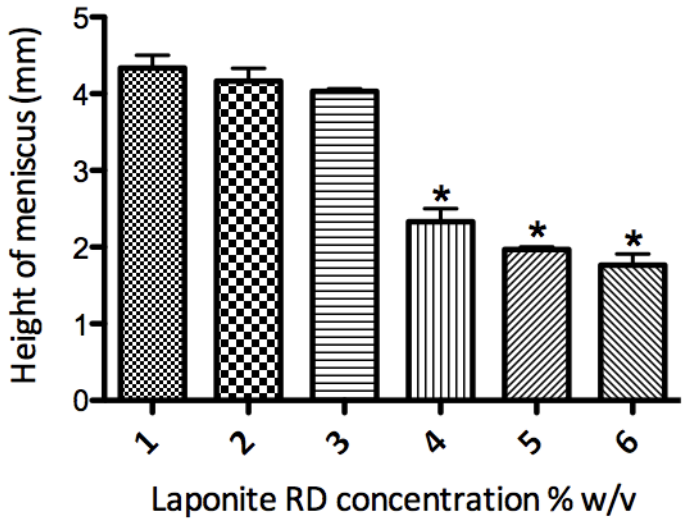


Figure B.3.9 The meniscus height of hydrogel layers decreased with an increase in Laponite RD concentration. Data represent mean ± SEM based on a sample from three separate experiments. One-way ANOVA with Dunnett's multiple comparison test, compared to 1% Laponite RD dispersion. *$p < 0.05$.

### B.3.4.3 Flat hydrogel layers could be achieved by layering in non surface-treated hydrophobic multiwell plates

To overcome the formation of a meniscus, Laponite hydrogels were layered in non surface-treated (polystyrene) multiwell plates. While tissue culture-treated multiwell plates (i.e. with a cell-attractive coating) are hydrophilic, thus attracting water, non surface-treated

multiwell plates are hydrophobic and repel water. In these hydrophobic plates Laponite hydrogel meniscus formation was significantly reduced (Fig. B.3.10), allowing the formation of flat gel layers.

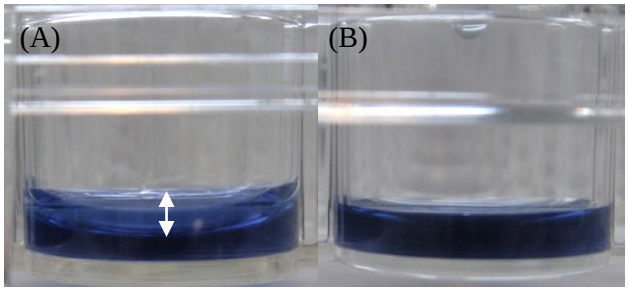


Figure B.3.10 Flat Laponite hydrogel layers could be formed in hydrophobic multiwell plates. (A) Hydrogel layer in surface-treated (hydrophilic) well with prominent meniscus (arrow) and (B) hydrogel layer in non surface-treated (hydrophobic) well with minimal meniscus formation.

From a meniscus size of about 1.9-2.0 mm in surface-treated (hydrophilic) plates, the meniscus was reduced to below 0.5 mm in non surface-treated (hydrophobic) plates. After resolving the meniscus problem and being able to achieve flat gel layers, alternating layers of stained and non-stained Laponite hydrogel layers could be created in 6- and 24-well non surface-treated hydrophobic multiwell plates (Fig. B.3.11). A range of hydrogel layer thicknesses could be achieved (0.5 mm to 1 cm) and the bands remained distinct from each other.

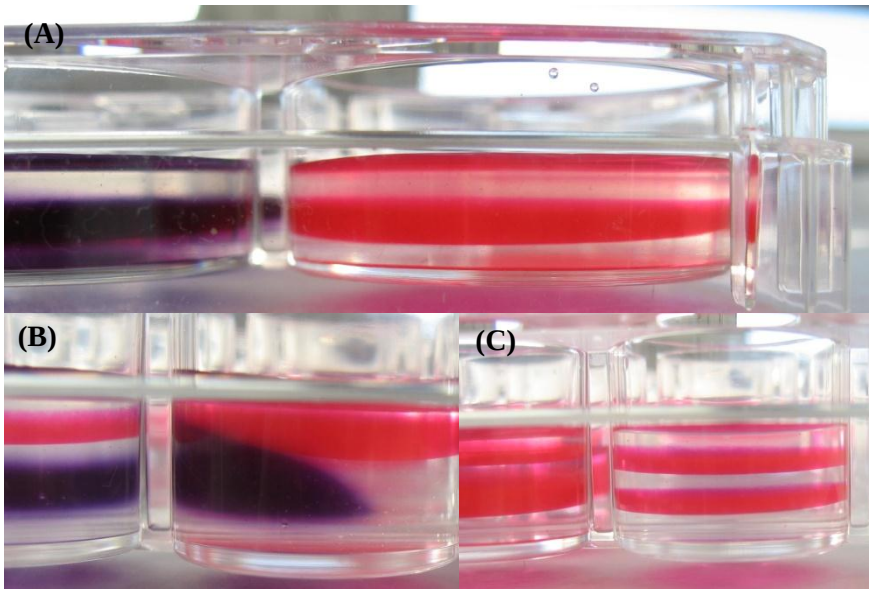


Figure B.3.11 Laponite hydrogel layering in multiwell plates. (A) 2 mm thick Laponite hydrogel layers in a 6-well multiwell plate. (B) Hydrogels could be layered at an angle which occupies half a well. C) 1 mm thick Laponite hydrogel layers in a 24-well multiwell plate.

### B.3.5 Laponite gels could be injected into semi-set Laponite hydrogels

In order to create a multi-sectored 3D culture, other ways of handling Laponite hydrogels were explored. As Laponite hydrogels are thixotropic when exposed to shear stress, gels could easily be injected through a needle into other hydrogel preparations, but only when the preparations were semi-set, as gel injection into set hydrogels resulted in gel displacement and cracked surfaces. Injected Laponite hydrogel capsules retained their form and many diverse shapes and structures could be created (Fig. B.3.12).

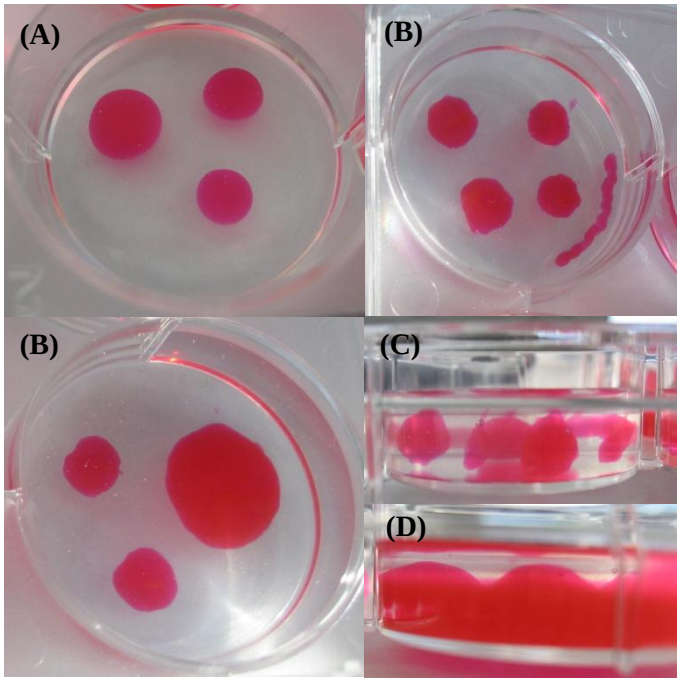


Figure B.3.12 Laponite injection. (A) Gels could be injected as capsules directly onto plates before covered with gel or (B) gels could be injected directly into semi-set gels. (C) Side view of injected capsules. (D) Side view of stained gel layers with gel capsules on top and covered with clear gel.

### B.3.6 Laponite hydrogels could be transferred out of plates

In case 3D hydrogel culture removal from multiwell plates was required for further investigations, the possibility of transferring whole gel constructs out of wells was explored. Hydrogels could be successfully transferred out of multiwell plates and petri-dishes if the bottom of the wells/dishes were pre-layered with PTFE/Teflon membranes before hydrogel addition (Fig. B.3.13).


Figure B.3.13 Clear Laponite hydrogel block transferred out of a petri-dish and inverted.

### B.3.6 Laponite RD-based culture medium hydrogels are not suitable for use as cell culture matrices

As Laponite hydrogels will ultimately be used for the culture of hippocampal cells *in vitro*, culture medium-based hydrogels needed to be developed. The gel formation dynamics in culture medium were first investigated. Laponite RD was added at different concentrations (% w/v) to varying dilutions of culture medium. On addition, Laponite RD either dispersed and formed a hydrogel, or flocculated (solute comes out of solution and aggregates) to varying degrees to form a pellet at the bottom of the vial. The presence of culture medium directed this flocculation effect as the higher the ratio of culture medium to water, the more likely Laponite was to flocculate (Fig. B.3.14). The flocculated pellet also became progressively more compact with an increase in the amount of culture medium.

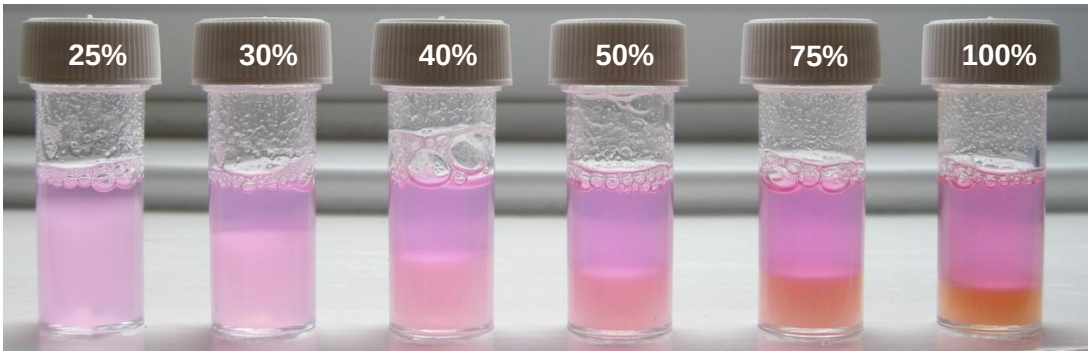


Figure B.3.14 Laponite flocculation increased with increasing culture medium concentration. Laponite (5% w/v) was added to a range of culture medium dilutions (25%, 30%, 40%, 50% and 75% culture medium diluted in water, to 100% culture medium neat, noted on vial caps). There was partial gel formation in 25% culture medium, but as the concentration of culture medium increased, gel flocculation became more pronounced (pellet).

Flocculation at higher culture medium concentrations could be overcome, to a certain extent, by further increasing the concentration of Laponite (Fig. B.3.15).

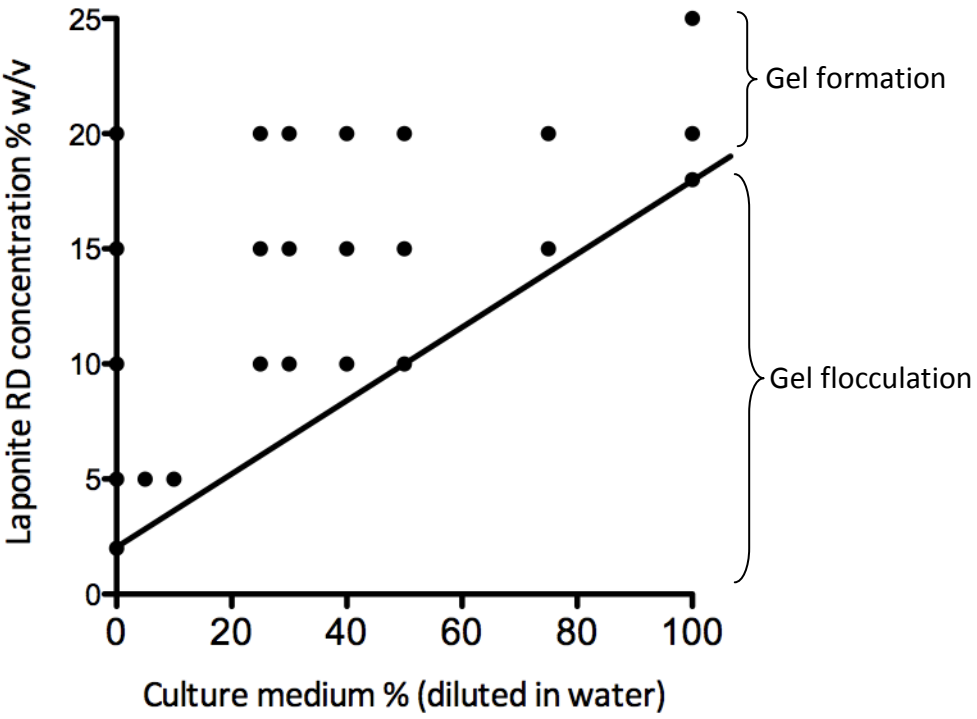


Figure B.3.15 Larger amounts of Laponite RD were required for hydrogel formation as the concentration of the culture medium increased. Laponite RD dispersions in culture media resulted in either hydrogel formation (●) or flocculation. The black line represents the boundary between hydrogel formation and flocculation.

After exploring the gel formation dynamics, the formation of culture medium-based Laponite hydrogels were investigated. As a means to maximise the chances of cell survival, hydrogels were developed by dispersing Laponite RD in 100% culture medium. The aim was create a thixotropic Laponite hydrogel using the lowest possible concentration of Laponite dispersed in 100% culture medium. From the gel formation dynamics graph above (Fig. B.3.15), a Laponite concentration of around 18% would be sufficient for hydrogel formation in 100% culture medium, which was explored along with a range of other Laponite concentrations. Indeed, 18% Laponite RD was the minimum concentration required for hydrogel formation in 100% culture medium. These 18% Laponite RD dispersions typically set in 5 minutes, while significant flocculation was observed with concentrations below 18% (Fig. B.3.16).

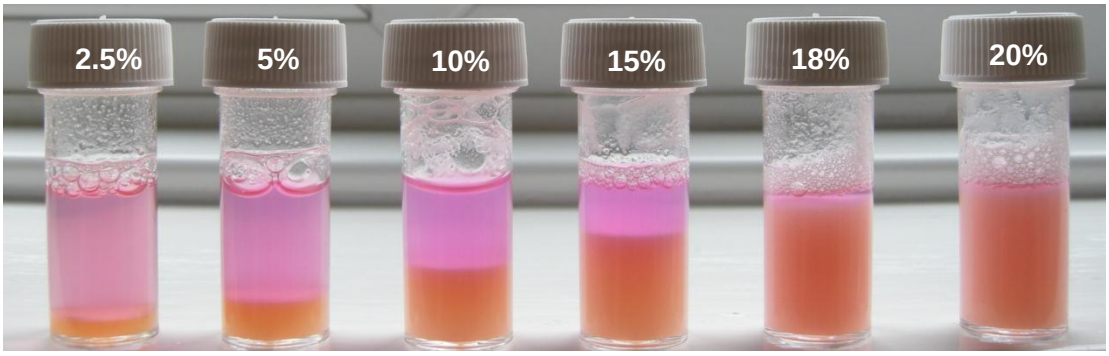


Figure B.3.16 Laponite RD hydrogel formation in 100% culture medium. A range of Laponite RD concentrations (2.5%, 5%, 10%, 15%, 18% and 20%, noted on vial caps) were dispersed in 100% culture medium. 18% Laponite RD was the minimum concentration required for hydrogel formation. Any Laponite concentrations below 18% resulted in gel flocculation.

The 18% Laponite RD culture medium hydrogels, however, had a gritty texture and were not thixotropic (Fig. B.3.17), most likely due to the high concentrations of Laponite required for hydrogel formation in 100% culture medium. The 18% Laponite RD dispersion in 100% culture medium may have been, in fact, a large flocculated pellet.

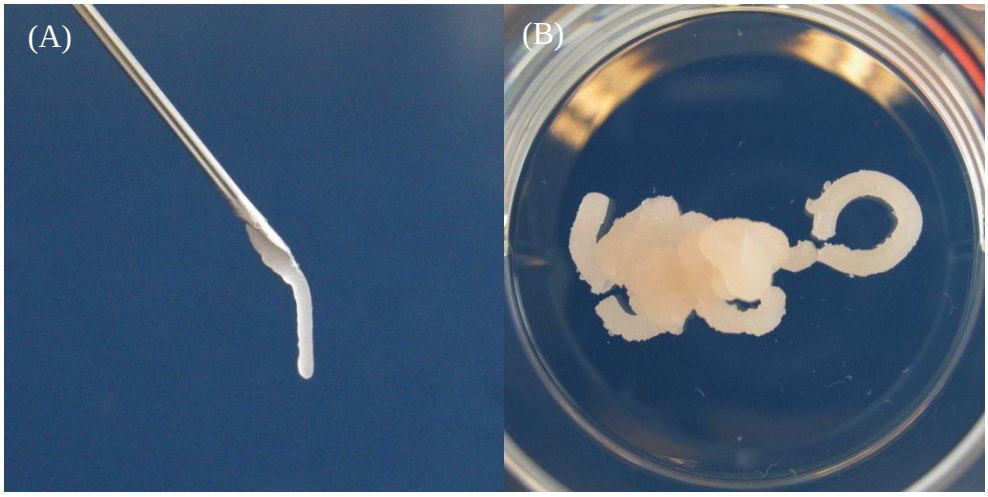


Figure B.3.17 18% Laponite RD culture medium hydrogels were not thixotropic in response to application of shear stress. (A) 18% Laponite RD culture medium hydrogels did not exhibit decreased viscosity in response to shear stress application and (B) hydrogels were of a gritty texture.

The properties of 18% Laponite RD culture medium hydrogels were not desirable for creating 3D cultures and so other Laponite formulations were explored.

### B.3.7 Laponite RDS, JS and B hydrogels

Other Laponite formulations were explored for their potential in forming thixotropic hydrogels in 100% culture medium. Their properties were first confirmed by dispersion in water before adding to culture medium. Laponite RDS, JS and B formulations were dispersed at 5% concentration in distilled water. As expected, Laponite RDS and JS did not form hydrogels and remained as sols (stable dispersion of solid in liquid), while Laponite B formed hydrogels. On addition to 100% culture medium, however, 15% Laponite RDS formed clear hydrogels while Laponite JS and B flocculated from solution. These results support Laponite RDS as a potential alternative to Laponite RD in the development of culture medium-based hydrogels for 3D cultures.

### B.3.8 Laponite RDS-based culture medium hydrogels have greater potential as 3D cell culture matrices

The lowest Laponite RDS concentration (% w/v) required for forming culture medium-based Laponite RDS hydrogels was investigated by dispersing varying concentrations (2.5%, 5%, 10%, 15% and 20%) of Laponite RDS in 100% culture medium and assessing gel formation. While Laponite RDS concentrations below 15% flocculated from solution and did not gel, concentrations above 15% formed clear hydrogels. 16%, instead of 15%, Laponite RDS was determined as the minimum concentration required for 100% hydrogel formation as, on closer inspection, 15% dispersions had a thin layer of culture medium on top and were not 100% set (Fig. B.3.18). 16% Laponite RDS dispersions set within 5 minutes of preparation and setting times decreased as the concentration of Laponite RDS increased. 20% dispersions, for example, set within a minute of preparation.

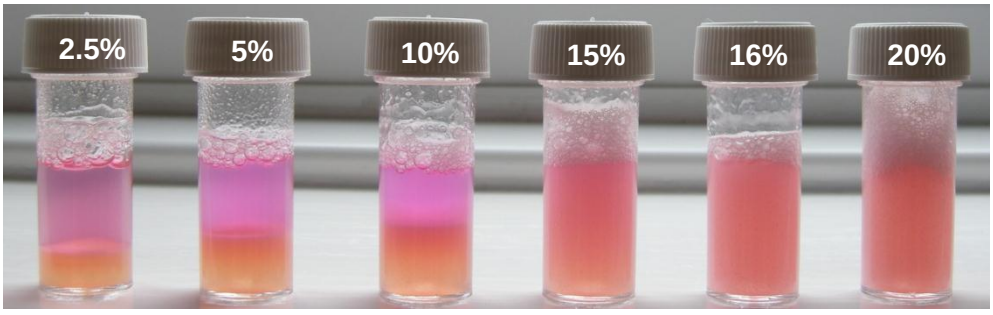


Figure B.3.18 Laponite RDS dispersions in 100% culture medium. A range of Laponite RD concentrations (2.5%, 5%, 10%, 15%, 16% and 20%, noted on vial caps) were dispersed in 100% culture medium. 16% Laponite RDS was the minimum concentration required for 100% hydrogel formation. Any Laponite concentrations below 16% resulted in either flocculation or incomplete hydrogel formation.

16% Laponite RDS produced clear, thixotropic culture medium hydrogels which exhibited low viscosity in response to shear stress (from passing through a 0.8 mm needle) (Fig. B.3.19A) and progressive restructuring after shear (Fig. B.3.19B). Similarly, 16% Laponite XLS, the low heavy metal content formulation of RDS, was also able to produce thixotropic culture medium hydrogels (Fig. B.3.19C). 16% Laponite RDS/XLS culture medium hydrogels are viscous enough to be able to hold their shape and support any cells which may be embedded within (Fig. B.3.19D).

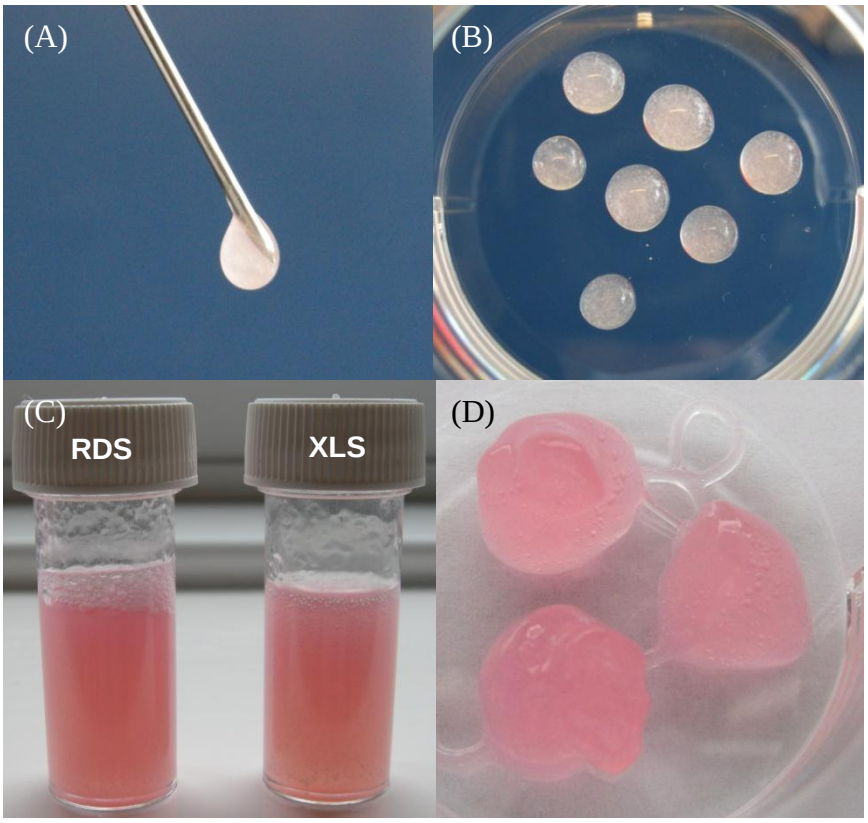


Figure B.3.19 16% Laponite RDS/XLS culture medium hydrogels. (A) 16% Laponite RDS culture medium hydrogels were thixotropic when passed through a needle, exhibiting decreased viscosity on application of shear stress and (B) reformation of a gel of high viscosity once the shear stress was removed. (C) 16% Laponite RDS and XLS culture medium hydrogels are the same except for the low heavy metal content of XLS. (D) 16% Laponite RDS culture medium hydrogel in a 6-well plate.

### B.3.9 Laponite RDS culture medium hydrogels can be layered in multiwell plates

The handling properties of 16% Laponite RDS culture medium hydrogels were investigated by layering in multiwell plates. Hydrogels formed flat layers which remained intact when covered with culture medium to prevent gel desiccation (Fig. B.3.20).

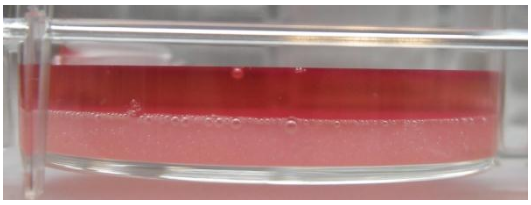

Figure B.3.20 16% Laponite RDS culture medium hydrogels layered in multiwell plates remained intact when covered with culture medium to prevent gel desiccation.

## B.4 Discussion

Much current emphasis in research on novel 3D culture matrices is focused primarily on a select few hydrogels, such as the natural collagen and fibrin hydrogels and the synthetic poly(ethylene glycol) and poly(propylene glycol) block copolymers (Drury & Mooney, 2003). Laponite has not been previously described as a cell culture matrix but it's intriguing rheological properties, such as thixotrophy (Martin et al., 2002), allow for the creation of complex multilayered 3D constructs. The key finding of this work has been the development of thixotropic culture medium-based Laponite hydrogels.

### B.4.1 Multilayered 3D hydrogel complexes can be created with Laponite

In an effort to mimic the complex 3D structural organisation of cells in the ECM in *in vitro* cultures, hydrogels prove superior to other biomaterials because their properties are very similar to the natural ECM (Tibbitt & Anseth, 2009). The aqueous environment allows for the efficient diffusion of molecules, while the ability to withstand compressive forces is representative of the mechanical aspects of the ECM. In fact, due to the vast range of hydrogels currently available, many aspects of the natural ECM, whether it is the structural, mechanical or molecular recognition properties, can be imitated in some form or another to varying degrees of success (Hubbell, 2003). It is these adaptable characteristics of hydrogels which allow for the creation of a variety of specialised 3D cultures. In particular, the thixotropic characteristic of Laponite hydrogels allow for the construction of complex multilayered hydrogel matrices which are highly advantageous in 3D cultures.

Initial attempts at creating multilayered Laponite hydrogel complexes was hindered by the formation of a meniscus, which obstructed the formation of flat hydrogel layers. The solution to this problem was the use of non surface-treated polystyrene culture plates. Conventional polystyrene culture plates treated for tissue culture use have a hydrophilic well coating for promoting cell adhesion; however, the Laponite hydrogels themselves were also hydrophilic in nature. This presentation of hydrophilic forces led to an attraction between the well surface and the hydrogel, leading to the formation of a meniscus. On the other hand, non surface-treated polystyrene plates have a well surface which is hydrophobic in nature. The hydrophilic Laponite hydrogel was not attracted to the hydrophobic well surface, allowing the formation of a flat hydrogel layer. Subsequently, multilayered Laponite hydrogels consisting of distinct multiple layers (1-2mm thick) could be constructed. Once the first gel layer was set, additional layers could be easily transferred

on top, with the new layer of hydrogel binding to the previous layer (Fig. B.3.11). As well as multilayering, Laponite hydrogel injection could be utilised to create distinct zones of hydrogel of any shape or volume during structural design (Fig. B.3.12).

The clear advantage of being able to construct multilayered/sectored hydrogel matrices lies within the possibility of varying the composition of each layer. By incorporating varying cell types (co-cultures) and/or pharmacological reagents i.e. growth factors or drugs, specific cell interactions and pharmacological responses could be easily investigated. The presence of a boundary between layers/zones allows for investigations into the effect of environmental changes on cell response (Liebmann et al., 2007).

In fact, the ability to control the three-dimensional structure of hydrogel matrices could be used to mimic the natural structure of *in vivo* tissues, especially those characterised by defined cell and tissue organisation, such as the skin, liver and kidney. The defined organisation of cells is often necessary for cellular communication during cell differentiation and tissue formation. Once such attempt was the construction of a multilayered culture of human skin fibroblasts and keratinocytes by Lee et al. (2009), which aimed at mirroring skin layers. A 3D freeform fabrication technique, which involved using a robotic platform to print collagen hydrogel precursor and cells, was used to engineer the biomimetic multilayered culture (Lee et al., 2009). Each printed layer of collagen hydrogel precursor was suspended with cells, which was subsequently cross-linked to form a hydrogel before the next layer was printed. This printing process was repeated to construct distinct layers of inner fibroblasts and outer keratinocytes, which demonstrated high viability within the layers. This type of tissue-reconstruction using collagen hydrogel has potential applications in skin wound repair as skin grafts or as artificial tissue assays in pharmacological studies (Lee et al.. 2009). By being able to co-culture different cell types in a structurally organised 3D *in vitro* environment, more realistically representative cell-cell interactions and motility may be studied (Elisseeff, 2008).

### B.4.2 Laponite RDS culture medium hydrogels have greater potential as cell culture matrices

To determine the suitability of Laponite hydrogels as a cell culture matrix, cells will eventually be cultured within the hydrogels. Hippocampal neuronal cells, however, cannot

be cultured in water-based Laponite hydrogels alone, which prompted the development of culture medium-based Laponite hydrogels. The growth media conventionally used for culturing hippocampal neurons is Neurobasal A medium supplemented with the growth supplement B27 and glutamine (Brewer et al., 1993), which made this the media of choice for developing culture medium-based Laponite hydrogels.

Laponite is a material with highly sensitive chemical properties which influence the rheological response. Especially well described is the relationship between the Laponite concentration and the concentration of added salt (ionic strength), as illustrated in the Laponite phase diagram (Fig. B.1.4; Mourchid et al., 1995a, 1995b). Laponite flocculates out of solution when the dispersion media has an ionic strength surpassing the upper limit of 20 mM salt concentration, irrespective of Laponite concentration (Mourchid et al., 1995a, 1995b). Indeed, this sensitivity of Laponite has led to the development of a wide range of Laponite formulations with diverse properties.

The standard Laponite formulation, Laponite RD (rapid diffusion), was used for the layering and handling studies as described above. Laponite RD easily forms highly thixotropic hydrogels in water at 2% (w/v) concentrations or above and was first investigated for hydrogel formation in culture media. Preliminary attempts at Laponite RD hydrogel formation, however, were obstructed by gel flocculation. The increased ionic strength of culture media compared to water is the most likely explanation for Laponite flocculation. A solution of high ionic strength will dramatically reduce the electrical double layers and electrostatic repulsion between Laponite particle disks. This, coupled with dominating van der Waals attractions, promotes particle aggregation (Bonn et al., 1999). An increase in the ionic strength of the dispersion media will result in an increase in fractal aggregate size until they sediment due to the effect of gravity. Differences in the size of the flocculation pellet, which became smaller and denser with an increase in culture media concentration, may be due to a reduction in steric hindrance due to the tighter compaction of aggregates (Nicolai & Cocard, 2001). This flocculation and compaction may explain the unexpected consistency of 18% Laponite RD 100% culture medium hydrogels, which exhibited a gritty texture and no thixotrophy. The high ionic strength of full media may have caused much of the Laponite to flocculate, aggregate and grow in size within the hydrogel to produce the consistency observed.

Other Laponite formulations were investigated for hydrogel forming potential in culture medium. Only Laponite RDS (rapid diffusion sol) and its low heavy metal content formulation (XLS), was successful at forming clear, thixotropic hydrogels in 100% culture medium. Laponite RDS dispersions in 100% culture medium produced clear thixotropic hydrogels at 16%, which could also be layered like water-based Laponite RD hydrogels. Unlike Laponite RD culture medium hydrogels, however, Laponite RDS dispersions showed no flocculation at 18% concentration in full media. This difference in property is most likely due to the addition of inorganic polyphosphate peptisers to Laponite RDS (Rockwood Additives Ltd.; Martin et al., 2002). These peptisers are attracted to and bind to the positive charge on the rim of Laponite disks, which interferes with the establishment of electrostatic interactions during hydrogel formation. Thus, Laponite RDS dispersions in water remain as free-flowing sols (dispersions of low viscosity), until the addition of small quantities of electrolyte, which result in the rapid formation of thixotropic hydrogels. In effect, referring back to the Laponite phase diagram (Mourchid et al., 1995a, 1995b), the upper limit of ionic strength where flocculation occurs is effectively raised. The ionic threshold for Laponite RDS flocculation was higher compared to that of Laponite RD, which allowed for its free flowing sol state at 10% concentration in water and the ability to form hydrogels in solutions of high ionic strength such as culture media.

### B.4.3 Conclusions

Laponite is a novel hydrogel with appealing rheological and handling properties which underpin its use in a range of applications. Laponite has not been previously investigated as a cell culture matrix, however, its relatively low cost, gentle gelling conditions and thixotropic properties may prove advantageous over many other conventional hydrogels. The ability to construct multilayered/zoned 3D matrices with Laponite hydrogels is promising for creating *in vitro* cultures more representative of *in vivo* environments, whilst the capacity for hydrogel formation in full culture media would be essential for supporting cell survival. In conclusion, Laponite shows potential as a novel alternative to existing hydrogels used in 3D culture and further investigations are necessary to determine the viability of hippocampal neuronal cells within this hydrogel.

# Appendix C

## Appendix C

### A) Laminin Coating (amended from TN2004EN00 Millipore Technical Guide, Millipore)

1. Dilute the laminin 1:10 in NBA-A medium and vortex until the laminin is solubilised.
2. Place the 30 mm inserts into a 6-well cell culture plate.
3. Using a sterile pipette, add 700 µl of laminin/NBA-A mixture to each of the 30 mm inserts.
4. Gently shake the cell culture plate to coat.
5. Air-dry inserts overnight in a laminar flow hood. Leave the cell culture plate cover ajar to allow airflow and prevent condensation.
6. Seed Millicell-CM insert with appropriate cell density (100,000 cells/ml or 260 cells/$mm^2$).

### B) Laminin Coating (amended from Sigma Aldrich product L2020 Product Information Guide)

1. Slowly thaw the laminin solution at 2-8 °C to avoid the formation of a gel.
2. Place the 30 mm inserts into a 6-well cell culture plate.
3. Dilute laminin in sterile water (5 µl/ml) and coat culture surface with a minimal volume (500 µl/well).
4. Incubate at 37 °C for at least 24 h.
5. Seed Millicell-CM insert with appropriate cell density (100,000 cells/ml or 260 cells/$mm^2$).

# References

Abbosh C, Lawkowski A, Zaben M, Gray WP (2011) GalR2/3 mediates proliferative and trophic effects of galanin on postnatal hippocampal precursors. *J Neurochem* **117**:425-436.

Abrous DN, Koehl M, Le Moal M (2005) Adult neurogenesis: from precursors to network and physiology. *Physiol Rev* **85**:523-569.

Adak S, Santolini J, Tikunova S, Wang Q, Johnson JD, Stuehr DJ (2001) Neuronal nitric-oxide synthase mutant (Ser-1412 3 Asp) demonstrates surprising connections between heme reduction, NO complex formation, and catalysis. *J Biol Chem* **276**:1244 –1252.

Agasse F, Bernardino L, Kristiansen H, Christiansen SH, Ferreira R, Silva B, Grade S, Woldbye DP, Malva JO (2008) Neuropeptide Y Promotes Neurogenesis in Murine Subventricular Zone. *Stem Cells* **26**:1636 -1645.

Akaike T, Yoshida M, Miyamoto Y, Sato K, Kohno M, Sasamoto K, Miyazaki K, Ueda S, Maeda H (1993) Antagonistic action of imidazolineoxyl *N*-oxides against endothelium-derived relaxing factor/.NO through a radical reaction. *Biochemistry* **32:** 827–831, 1993.

Albers HE, Ferris CF (1984) Neuropeptide Y: role in light-dark cycle entrainment of hamster circadian rhythms. *Neurosci Lett* **50:**163-168.

Alberts B, Johnson A, Lewis J, Raff M, Roberts K, Walter P (2002) Molecular Biology of the Cell. 4th edn. *New York: Garland Science, Taylor & Francis Group*.

Alderton WK, Cooper CE, Knowles RG (2001) Nitric oxide synthases: structure, function and inhibition. *Biochem J* **357**:593-615.

Allen YS, Adrian TE, Allen JM, Tatemoto K, Crow TJ, Bloom SR, Polak JM (1983) Neuropeptide Y distribution in the rat brain. *Science* **221**:877-9.

Altman J (1962) Are new neurons formed in the brains of adult mammals? *Science* **135**(3509):1127-1128.

Altman J, Das GD (1965) Autoradiographic and histological evidence of postnatal hippocampal neurogenesis in rats. *J Comp Neurol* **124**:319–335.

Altman J (1969) Autoradiographic and histological studies of postnatal neurogenesis. IV. Cell proliferation and migration in the anterior forebrain, with special reference to persisting neurogenesis in the olfactory bulb. *J Comp Neurol* **137**(4):433–457.

Altman J, Bayer SA (1990) Mosaic organization of the hippocampal neuroepithelium and the multiple germinal sources of dentate granule cells. *J Comp Neurol* **301**:325-342.

Alvaro AR, Martins J, Araújo IM, Rosmaninho-Salgado J, Ambrósio AF, Cavadas C (2008) Neuropeptide Y stimulates retinal neural cell proliferation - involvement of nitric oxide. *J Neurochem* **105**:2501-2510.

Amsden B (1998) Solute diffusion within hydrogels. Mechanisms and models. *Macromolecules* **31**:8382-8395.

Andersen P, Morris R, Amaral D, Bliss T, O'Keefe J (2007) The Hippocampus Book. *Oxford University Press, Inc*.

Arbonés ML, Ribera J, Agulló L, Baltrons MA, Casanovas A, Riveros-Moreno V, García A (1996) Characteristics of nitric oxide synthase type I of rat cerebellar astrocytes. *Glia* **18**:224-232.

Avery RG, Ramsey JDF (1986) Colloidal Properties of Synthetic Hectorite Clay Dispersions. 2. Light and Small-Angle Neutron-Scattering. *J Colloid Interface Sci* **109**:448-454.

Bashkatova V, Vitskova G, Narkevich V, Vanin A, Mikoyan V, Rayevsky K (2000) Nitric oxide content measured by ESR-spectroscopy in the rat brain is increased during pentylenetetrazole-induced seizures. *J Mol Neurosci* **14**:183–190.

Beckman JS, Koppenol WH (1996) Nitric oxide, superoxide and peroxynitrite: The good, the bad, and the ugly. *Am J Physiol* **271**:C1424-C1437.

Bengzon J, Kokaia Z, Elmer E, Nanobashvili A, Kokaia M, Lindvall O (1997) Apoptosis and proliferation of dentate gyrus neurons after single and intermittent limbic seizures. *Proc Natl Acad Sci USA* **94**:10432–10437.

Bez A, Corsini E, Curti D, Biggiogera M, Colombo A, Nicosia RF, Pagano SF, Parati EA (2003) Neurosphere and neurosphere-forming cells: morphological and ultrastructural characterization. *Brain Res* **993**:18-29.

Biebl M, Cooper CM, Winkler J, Kuhn HG (2000) Analysis of neurogenesis and programmed cell death reveals a self-renewing capacity in the adult rat brain. *Neurosci Lett* **291**:17–20.

Biederer T, Scheiffele P (2007) Mixed-culture assays for analyzing neuronal synapse formation. *Nat Protoc* **2**:670-676.

Bland-Ward PA, Pitcher A, Wallace P, Gaffen Z, Babbedge RG, Moore PK (1994) Isoform selectivity of indazole-based nitric oxide synthase inhibitors. *Br J Pharmacol* **112**:351P.

Bland-Ward PA, Moore PK (1995) 7-Nitroindazole derivatives are potent inhibitors of brain, endothelium and inducible isoforms of nitric oxide synthase. *Life Sci* **57**:131-135.

Blurton-Jones M, Kitazawa M, Martinez-Coria H, Castello NA, Müller FJ, Loring JF, Yamasaki TR, Poon WW, Green KN, LaFerla FM (2009) Neural stem cells improve cognition via BDNF in a transgenic model of Alzheimer disease. *Proc Natl Acad Sci USA* **106**:13594-13599.

Bobba A, Atlante A, Moro L, Calissano P, Marra E (2007) Nitric oxide has dual opposite roles during early and late phases of apoptosis in cerebellar granule neurons. *Apoptosis* **12**:1597-1610.

Böhme GA, Bon C, Stutzmann JM, Doble A, Blanchard JC (1991) Possible involvement of nitric oxide in long-term potentiation. *Eur J Pharmacol* **199**:379–381.

Boldrini M, Underwood MD, Hen R, Rosoklija GB, Dwork AJ, John Mann J, Arango V (2009) Antidepressants increase neural progenitor cells in the human hippocampus. *Neuropsychopharmacology* **34**:2376-2389.

Bonn D, Kellay H, Tanaka H, Wegdam G, Meunier J (1999) Laponite: What is the difference between a Gel and a Glass? *Langmuir* **15**:7534-7536.

Bottenstein JE, Sato GH (1985) Cell Culture in the Neurosciences. *New York: Plenum Press*.

Boulton CL, Southam E, Garthwaite J (1995) Nitric oxide-dependent long-term potentiation is blocked by a specific inhibitor of soluble guanylyl cyclase. *Neuroscience* **69**:699–703.

Brandt MD, Jessberger S, Steiner B, Kronenberg G, Reuter Km Bick-Sander A, von der Behrens W, Kempermann G (2003) Transient calretinin-expression defines early postmitotic step of

neuronal differentiation in adult hippocampal neurogenesis of mice. *Mol Cell Neurosci* **24**:603–613.

Bredt DS, Snyder SH (1990) Isolation of nitric oxide synthase, a calmodulin-requiring enzyme. *Proc Natl Acad Sci USA* **87**:682-685.

Bredt DS, Hwang PM, Snyder SH (1990) Localization of nitric oxide synthase indicating a neural role for nitric oxide. *Nature* **347**:768-770.

Brewer GJ, Torricelli JR, Evege EK, Price PJ (1993) Optimized survival of hippocampal neurons in B27-supplemented Neurobasal, a new serum-free medium combination. *J Neurosci Res* **35**:567-576.

Brewer GJ (1997) Isolation and culture of adult rat hippocampal neurons. *J Neurosci Methods* **71**:143-155.

Briand R, Yamaguchi N, Gagne J, Nadeau R, De Champlain J (1990) Alpha2-adrenoceptor modulation of catecholamine and neuropeptide Y responses during haemorrhagic hypotension in anaesthetized dogs. *J Auton Nerv Syst* **30**:111-112.

Broillet, MC, Randin, O, Chatton, JY (2001) Photoactivation and calcium sensitivity of the fluorescent NO indicator 4,5-diaminofluorescein (DAF-2): implications for cellular NO imaging. *FEBS Lett* **491**:227-232.

Brown JP, Couillard-Després S, Cooper-Kuhn CM, Winkler J, Aigner L, Kuhn HG (2003) Transient expression of doublecortin during adult neurogenesis. *J Comp Neurol* **467**:1-10.

Browning TH, Trier JS (1969) Organ culture of mucosal biopsies of human small intestine. *J Clin Invest* **48**:1423-1432.

Buck CA, Horwitz AF (1987) Cell surface receptors for extracellular matrix molecules. *Ann Rev Cell Biol* **3**:179-205.

Burnett AL, Lowenstein CJ, Bredt DS, Chang TS, Snyder SH (1992) Nitric oxide: a physiologic mediator of penile erection. *Science* **257**:401-403.

Burnette WN (1981) "Western blotting": electrophoretic transfer of proteins from sodium dodecyl sulfate-polyacrylamide gels to unmodified nitrocellulose and radiographic detection with antibody and radioiodinated protein A. *Anal Biochem* **112**:195-203.

Caberlotto L, Fuxe K, Overstreet DH, Gerrard P, Hurd YL (1998) Alterations in neuropeptide Y and Y1 receptor mRNA expression in brains from an animal model of depression: region specific adaptation after fluoxetine treatment. *Mol Brain Res.* **59**:58-65.

Cameron HA, Hazel TG, McKay RD (1998) Regulation of neurogenesis by growth factors and neurotransmitters. *J Neurobiol* **36**(2):287-306.

Cameron HA, McKay RD (2001) Adult neurogenesis produces a large pool of new granule cells in the dentate gyrus. *J Comp Neurol.* **435**:406-17.

Cano E, Mahadevan LC (1995) Parallel signal processing among mammalian MAPKs. *Trends Biochem Sci.* **20**:117-22.

Cárdenas A, Moro MA, Hurtado O, Leza JC, Lizasoain I (2005) Dual role of nitric oxide in adult neurogenesis. *Brain Res Rev* **50**:1-6.

Carreira BP, Morte MI, Inácio A, Costa G, Rosmaninho-Salgado J, Agasse F, Carmo A, Couceiro P, Brundin P, Ambrósio AF, Carvalho CM, Araújo IM (2010) Nitric oxide stimulates the proliferation of neural stem cells bypassing the epidermal growth factor receptor. *Stem Cells* **28**:1219-1230.

Cellesi F, Tirelli N, Hubbell JA (2002) Materials for cell encapsulation via a new tandem approach combining reverse thermal gelation and covalent crosslinking. *Macromol Chem Phys* **203**:1466-1472.

Chan-Palay V, Lang W, Haesler U, Köhler C, Yasargil G (1986) Distribution of altered hippocampal neurons and axons immunoreactive with antisera against neuropeptide Y in Alzheimer's-type dementia. *J Comp Neurol* **248**:376-394.

Chen J, Tu Y, Moon C, Matarazzo V, Ronnett GV (2004) The localization of neuronal nitric oxide synthase may influence its role in neuronal precursor proliferation and synaptic maintenance. *Dev Biol* **269**:165-182.

Chen J, Zacharek A, Li Y, Li A, Wang L, Katakowski M, Roberts C, Lu M, Chopp M (2006) N-cadherin mediates nitric oxide-induced neurogenesis in young and retired breeder neurospheres. *Neuroscience* **140**:377-388.

Chen SH, Fung PC, Cheung RT (2002) Neuropeptide Y-Y1 receptor modulates nitric oxide level during stroke in the rat. *Free Radic Biol Med* **32**:776-784.

Cholet N, Bonvento G, Seylaz, J (1996) Effect of neuronal NO synthase inhibition on the cerebral vasodilatory response to somatosensory stimulation. *Brain Res* **708**:197-200.

Chronwall BM, DiMaggio DA, Massari VJ, Pickel VM, Ruggiero DA, O'Donohue TL (1985) The anatomy of neuropeptide-Y-containing neurons in rat brain. *Neuroscience* **15**:1159-1181.

Conner EM, Brand SJ, Davis JM, Kang DY, Grisham MB (1996) Role of reactive metabolites of oxygen and nitrogen in inflammatory bowel disease: toxins, mediators, and modulators of gene expression. *Inflamm Bowel Dis* **2**:133-147.

Consolo S, Uboldi MC, Caltavuturo C, Bartfai T (1998) Galanin stimulates the N-methyl-D-aspartate receptor/nitric oxide/cyclic GMP pathway in vivo in the rat ventral hippocampus. *Neuroscience* **85**:819-826.

Contestabile A, Ciani E (2004) Role of nitric oxide in the regulation of neuronal proliferation, survival and differentiation. *Neurochem. Int.* **45**:903-914.

Cordelier P, Estève JP, Rivard N, Marletta M, Vaysse N, Susini C, Buscail L (1999) The activation of neuronal NO synthase is mediated by G-protein betagamma subunit and the tyrosine phosphatase SHP-2. *FASEB J* **13:**2037-2050.

Corso-Diaz X, Krukoff TL (2010) nNOS alpha and nNOS beta localization to aggresome-like inclusions is dependent on HSP90 activity. *J Neurochem* **114**:864-872.

Covacu R, Danilov AI, Rasmussen BS, Hallén K, Moe MC, Lobell A, Johansson CB, Svensson MA, Olsson T, Brundin L (2006) Nitric oxide exposure diverts stem cell fate from neurogenesis towards astrogliogenesis. *Stem Cells* **24**:2792-2800.

Coyle JT, Puttfarcken P (1993) Oxidative stress, glutamate, and neurodegenerative disorders. *Science* **262**:689-695.

Cukierman E, Pankov R, Yamada KM (2002) Cell interactions with three-dimensional matrices. *Curr Opin Cell Biol* **14**:633-639.

Cummins HZ (2007) Liquid, glass, gel: The phases of colloidal Laponite. *J Non-Cryst Solids* **353**:3891-3905.

Daniel H, Levenes C, Crepel F (1998) Cellular mechanisms of cerebellar LTD. *Trends Neurosci* **21**:401–407.

Dash PK, Mach SA, Moore AN (2001) Enhanced neurogenesis in the rodent hippocampus following traumatic brain injury. *J Neurosci Res* **63**:313–319.

de Lanerolle NC, Kim JH, Robbins RJ, Spencer DD (1989) Hippocampal interneuron loss and plasticity in human temporal lobe epilepsy. *Brain Res* **495**:387-395.

Decressac M, Wright B, David B, Tyers P, Jaber M, Barker RA, Gaillard A (2011) Exogenous neuropeptide Y promotes in vivo hippocampal neurogenesis. *Hippocampus* **21**:233-238.

Denninger JW, Marletta MA (1999) Guanylate cyclase and the NO/cGMP signaling pathway. *Biochim Biophys Acta* **1411**:334-350.

Derbyshire ER, Marletta MA (2009) Biochemistry of soluble guanylate cyclase. *Handb Exp Pharmacol* **191**:17-31.

Dimmeler S, Fleming I, Fisslthaler B, Hermann C, Busse R, Zeiher AM (1999) Activation of nitric oxide synthase in endothelial cells by Akt-dependent phosphorylation. *Nature* **399**:601-605.

Dinerman JL, Dawson TM, Schell MJ, Snowman A, Snyder SH (1994) Endothelial nitric oxide synthase localized to hippocampal pyramidal cells: implications for synaptic plasticity. *Proc Natl Acad Sci USA* **91**:4214-4218.

Dings J, Meixensberger J, Jager A, Roosen K (1998) Clinical experience with 118 brain tissue oxygen partial pressure catheter probes. *Neurosurgery* **43**:1082-1095.

Ditlevsen DK, Køhler LB, Berezin V, Bock E (2007) Cyclic guanosine monophosphate signalling pathway plays a role in neural cell adhesion molecule-mediated neurite outgrowth and survival. *J Neurosci Res* **85**:703-711.

Doyle C, Hölscher C, Rowan MJ, Anwyl R (1996) The selective neuronal NO synthase inhibitor 7-nitroindazole blocks both long-term potentiation and depotentiation of field EPSPs in rat hippocampal CA1 in vivo. *J Neurosci* **16**:418–424.

Dreyer J, Schleicher M, Tappe A, Schilling K, Kuner T, Kusumawidijaja G, Müller-Esterl W, Oess S, Kuner R (2004) Nitric oxide synthase (NOS)-interacting protein interacts with neuronal NOS and regulates its distribution and activity. *J Neurosci* **24**:10454-10465.

Drury JL, Mooney DJ (2003) Hydrogels for tissue engineering: scaffold design variables and applications. *Biomaterials* **24**:4337-4351.

Du M, Islam MM, Lin L, Ohmura Y, Moriyama Y, Fujimura S (1997) Promotion of proliferation of murine BALB/C3T3 fibroblasts mediated by nitric oxide at lower concentrations. *Biochem Mol Biol Int* **41**:625-631.

Dubois NC, Hofmann D, Kaloulis K, Bishop JM, Trumpp A (2006) Nestin-Cre transgenic mouse line Nes-Cre1 mediates highly efficient Cre/loxP mediated recombination in the nervous system, kidney, and somite-derived tissues. *Genesis* **44**:355-360.

Duman RS (2004) Depression: a case of neuronal life and death? *Biol Psychiatry* **56**:140-145.

Dumont Y, Jacques D, Bouchard P, Quirion R (1998) Species differences in the expression and distribution of the neuropeptide Y Y1, Y2, Y4, and Y5 receptors in rodents, guinea pig, and primates brains. *J Com Neurol* **402**:372-84.

Ehninger D, Kempermann G (2008) Neurogenesis in the adult hippocampus. *Cell Tissue Res* **331**:243-250.

El Mabrouk M, Singh A, Touyz RM, Schiffrin EL (2000) Antiproliferative effect of L-NAME on rat vascular smooth muscle cells. *Life Sci* **67**:1613-1623.

Elisseeff J (2008) Hydrogels: structure starts to gel. *Nat Mater* **7**:271-273.

Elsdale T, Bard J (1972) Collagen substrata for studies on cell behaviour. *J Cell Biol* **54**:626-637.

Endo S, Launey T (2003) Nitric oxide activates extracellular signal-regulated kinase 1/2 and enhances declustering of ionotropic glutamate receptor subunit 2/3 in rat cerebellar Purkinje cells. *Neurosci Lett* **350**:122-126.

Erickson JC, Clegg KE, Palmiter RD (1996) Sensitivity to leptin and susceptibility to seizures of mice lacking neuropeptide Y. *Nature* **381**:415-421.

Eriksson PS, Perfilieva E, Bjork-Eriksson T, Alborn AM, Nordborg C, Peterson DA, Gage FH (1998) Neurogenesis in the adult human hippocampus. *Nat Med* **4**:1313-1317.

Espey MG, Miranda KM, Thomas DD, Wink DA (2001) Distinction between nitrosating mechanisms within human cells and aqueous solution. *J Biol Chem* **276**:30085–30091.

Estévez AG, Spear N, Manuel SM, Barbeito L, Radi R, Beckman JS (1998a) Role of endogenous nitric oxide and peroxynitrite formation in the survival and death of motor neurons in culture. *Prog Brain Res* **118**:269-280.

Estévez AG, Spear N, Thompson JA, Cornwell TL, Radi R, Barbeito L, Beckman JS (1998b) Nitric oxide-dependent production of cGMP supports the survival of rat embryonic motor neurons cultured with brain-derived neurotrophic factor. *J Neurosci* **18**:3708–3714.

Everitt BJ, Hökfelt T (1989) The coexistence of neuropeptide Y with other peptides and amines in the central nervous system. *Raven Press, New York,* pp 61–72.

Farinelli SE, Park DS, Greene LA (1996) Nitric oxide delays the death of trophic factor-deprived PC12 cells and sympathetic neurons by a cGMP-mediated mechanism. *J Neurosci* **16**:2325–2334.

Feil S, Zimmermann P, Knorn A, Brummer S, Schlossmann J, Hofmann F, Feil R (2005) Distribution of cGMP-dependent protein kinase type I and its isoforms in the mouse brain and retina. *Neuroscience* **135**:863-868.

Ferreira LS, Gerecht S, Fuller J, Shieh HF, Vunjak-Novakovic G, Langer R (2007) Bioactive hydrogel scaffolds for controllable vascular differentiation of human embryonic stem cells. *Biomaterials* **28**:2706-2717.

Filippov V, Kronenberg G, Pivneva T, Reuter K, Steiner B, Wang LP, Yamaguchi M, Kettenmann H, Kempermann G (2003) Subpopulation of nestin-expressing progenitor cells in the adult murine hippocampus shows electrophysiological and morphological characteristics of astrocytes. *Mol. Cell. Neurosci.* **23**:373–382.

Fiscus RR, Rapoport RM, Murad F (1983) Endothelium-dependent and nitrovasodilator-induced activation of cyclic GMP-dependent protein kinase in rat aorta. *J Cyclic Nucleotide Protein Phosphor Res* **9**:415–425.

Fiscus RR (2002) Involvement of cyclic GMP and protein kinase G in the regulation of apoptosis and survival in neural cells. *Neurosignals* **11**:175-190.

Flood JF, Hernandez EN, Morley JE (1987) Modulation of memory processing by neuropeptide Y. *Brain Res* **421**:280-290.

Flood JF, Morley JE (1989) Dissociation of the effects of neuropeptide Y on feeding and memory: evidence for pre- and postsynaptic mediation. *Peptides* **10**:963-966.

Francis SH, Corbin JD (1999) Cyclic nucleotide-dependent protein kinases: intracellular receptors for cAMP and cGMP action. *Crit Rev Clin Lab Sci.* **36**:275-328.

Francis SH, Busch JL, Corbin JD, Sibley D (2010) cGMP-dependent proteins kinases and cGMP phosphodiesterases in nitric oxide and cGMP action. *Pharmacol Rev* **62**:525-563.

Freshney RI (1987) Culture of animal cells: A manual of basic technique. 2nd edn. *New York: Liss, A.R, Inc.*

Freund TF, Buzsaki G (1996) Interneurons of the hippocampus. *Hippocampus* **6**:347-470.

Folkman J, Haudenschild C (1980) Angiogenesis *in vitro. Nature* **288**:551-556.

Ford PC, Wink DA, Stanbury DM (1993) Autoxidation kinetics of aqueous nitric oxide. *FEBS Lett* **326**:1-3.

Fukuda S, Kato F, Tozuka Y, Yamaguchi M, Miyamoto Y, Hisatsune T (2003) Two distinct subpopulations of nestin-positive cells in adult mouse dentate gyrus. *J Neurosci* **23**:9357-9366.

Furchgott RF, Zawadzki JV (1980) The obligatory role of endothelial cells in the relaxation of arterial smooth muscle by acetylcholine. *Nature.* **288**:373-6.

Fusco S, Borzacchiello A, Netti PA (2006) Perspectives on: PEO-PPO-PEO triblock copolymers and their biomedical applications. *J Bioact Compat Polymers* **21**:149-164.

Gachhui R, Abu-Soud HM, Ghosha DK, Presta A, Blazing MA, Mayer B, George SE, Stuehr DJ (1998) Neuronal nitric-oxide synthase interaction with calmodulin-troponin C chimeras. *J Biol Chem* **273**(10):5451–5454.

Garcia-Cardena G, Fan R, Shah V, Sorrentino R, Cirino G, Papapetropoulos A, Sessa WC (1998) Dynamic activation of endothelial nitric oxide synthase by Hsp90. *Nature* **392**:821-824.

Garcin ED, Arvai AS, Rosenfeld RJ, Kroeger MD, Crane BR, Andersson G, Andrews G, Hamley PJ, Mallinder PR, Nicholls DJ, St-Gallay SA, Tinker AC, Gensmantel NP, Mete A, Cheshire DR, Connolly S, Stuehr DJ, Åberg A, Wallace AV, Tainer JA, Getzoff ED (2008) Anchored plasticity opens doors for selective inhibitor design in nitric oxide synthase. *Nat Chem Biol* **4**:700-707.

Garg UC, Hassid A (1989) Nitric oxide generating vasodilators and 8-bromo-cyclic guanosine monophosphate inhibit mitogenesis and proliferation of cultured rat vascular smooth muscle cells. *J Clin Invest* **83**:1774-1777.

Garthwaite J, Charles SL, Chess-Williams R (1988) Endothelium-derived relacing factor release on activation of NMDA receptors suggests role as intercellular messenger in the brain. *Nature* **336**:385-388.

Garthwaite J (1991) Glutamate, nitric oxide and cell cell signalling in the nervous system. *Trends Neurosci* **14**:60–67.

Garthwaite J, Boulton CL (1995) Nitric oxide signaling in the central nervous system. *Annu Rev Physiol* **57**:683–706.

Gehlert DR (2004) Introduction to the reviews on neuropeptide Y. *Neuropeptides* **38**:135-140.

Ghersi G, Chen W, Lee EW, Zukowska Z (2001) Critical role of dipeptidyl peptidase IV in neuropeptide Y-mediated endothelial cell migration in response to wounding. *Peptides* **22**:453–458.

Ghosh DK, Stuehr DJ (1995) Macrophage NO synthase: characterization of isolated oxygenase and reductase domains reveals a head-to-head subunit interaction. *Biochemistry* **34**:801-807.

Gilman AG (1987) G Proteins: Transducers of Receptor-Generated Signals. *Annu Rev Biochem* **56**:615-649.

Gould E, McEwen BS, Tanapat P, Galea LA, Fuchs E (1997) Neurogenesis in the dentate gyrus of the adult tree shrew is regulated by psychosocial stress and NMDA receptor activation. *J Neurosci.* **17**:2492-2498.

Gould E, Beylin A, Tanapat P, Reeves A, Shors TJ (1999) Learning enhances adult neurogenesis in the hippocampal formation. *Nat. Neurosci.* **2**:260–265.

Gould E, Tanapat P (1999) Stress and hippocampal neurogenesis. *Biol Psychiatry* **46**:1472-1479.

Gould E, Tanapat P, Rydel T, Hastings N (2000) Regulation of hippocampal neurogenesis in adulthood. *Biol Psychiatry* **48**(8):715-720.

Gray WP, Sundstrom LE (1998) Kainic acid increases the proliferation of granule cell progenitors in the dentate gyrus of the adult rat. *Brain Res* **790**:52–59.

Gray WP (2008) Neuropeptide Y signalling on hippocampal stem cells in health and disease. *Mol. Cell. Endocrinol.* **288**:52-62.

Griffiths C, Wykes V, Bellamy TC, Garthwaite J (2003) A new and simple method for delivering clamped nitric oxide concentrations in the physiological range: application to activation of guanylyl cyclase-coupled nitric oxide receptors. *Mol Pharmacol* **64**:1349-1356.

Gunatillake PA, Adhikari R (2003) Biodegradable synthetic polymers for tissue engineering. *Eur Cell Mater* **5**:1-16.

Gustafson EL, Smith KE, Durkin MM, Walker MW, Gerald C, Weinshank R, Branchek TA (1997) Distribution of the neuropeptide Y Y2 receptor mRNA in rat central nervous system. *Mol Brain Res* **46**:223–235.

Gutkind JS (1998) The pathways connecting G protein-coupled receptors to the nucleus through divergent mitogen-activated protein kinase cascades. *J Biol Chem* **273**:1839-1842.

Hah JM, Roman LJ, Martásek P, Silverman RB (2001) Reduced amide bond peptidomimetics. (4S)-N-(4-amino-5-[aminoakyl]aminopentyl)-N'-nitroguanidines, potent and highly selective inhibitors of neuronal nitric oxide synthase. *J Med Chem* **44**:2667-2670.

Hall CN & Garthwaite J (2006) Inactivation of nitric oxide by rat cerebellar slices. *J Physiol* **577**:549–567.

Hall CN & Attwell D (2008) Assessing the physiological concentration and targets of nitric oxide in brain tissue. *J Physiol* **586**:3597–3615.

Hall CN, Garthwaite J (2009) What is the real physiological NO concentration *in vivo*? *Nitric Oxide* **21**:92-103.

Hansel DE, Eipper BA, Ronnett GV (2001) Neuropeptide Y functions as a neuroproliferative factor. *Nature* **410**:940-944.

Haramis G, Zhou Z, Pyriochou A, Koutsilieris M, Roussos C, Papapetropoulos A (2008) cGMP-independent anti-tumour actions of the inhibitor of soluble guanylyl cyclase, ODQ, in prostate cancer cell lines. *Br J Pharmacol* **155**:804-813.

Harteneck C, Wedel B, Koesling D, Malkewitz J, Bohme E, Schultz G (1991) Molecular cloning and expression of a new alpha-subunit of soluble guanylyl cyclase. Interchangeability of the alpha-subunits of the enzyme. *FEBS Lett* **292**:217-222.

Haughey N J, Nath A, Chan SL, Borchard AC, Rao MS, Mattson MP (2002) Disruption of neurogenesis by amyloid β-peptide, and perturbed neural progenitor cell homeostasis, in models of Alzheimer's disease. *J Neurochem* **83**:1509–1524.

Hawes JJ, Narasimhaiah R, Picciotto MR (2006) Galanin and galanin-like peptide modulate neurite outgrowth via protein kinase C-mediated activation of extracellular signal-related kinase. *Eur J Neurosci* **23**:2937-2946.

Hawkins RD, Son H, Arancio O (1998) Nitric oxide as a retrograde messenger during long-term potentiation in hippocampus. *Prog Brain Res* **118**:155–172.

Hayes NL, Nowakowski RS (2000) Exploiting the dynamics of S-phase tracers in developing brain: interkinetic nuclear migration for cells entering versus leaving the S-phase. *Dev Neurosci* **22**:44-55.

Heilig M (2004) The NPY system in stress, anxiety and depression. *Neuropeptides* **38:**213-224.

Herzog H, Hort YJ, Ball HJ, Hayes G, Shine J, Selbie LA (1992) Cloned human neuropeptide Y receptor couples to two different second messenger systems. *Proc Natl Acad Sci USA* **89**:5794-5798.

Hibbs JB Jr, Taintor RR, Vavrin Z, Rachlin EM (1988) Nitric oxide: a cytotoxic activated macrophage effector molecule. *Biochem Biophys Res Commun* **157**:87-94.

Hobson SA, Bacon A, Elliot-Hunt CR, Holmes FE, Kerr NC, Pope R, Vanderplank P, Wynick D (2008) Galanin acts as a trophic factor to the central and peripheral nervous systems. *Cell Mol Life Sci* **65**:1806-1812.

Hodges GJ, Kosiba WA, Zhao K, Johnson JM (2008) The involvement of norepinephrine, neuropeptide Y, and nitric oxide in the cutaneous vasodilator response to local heating in humans. *J Appl Physiol* **105**:233–240.

Hodges GJ, Jackson DN, Mattar L, Johnson JM, Shoemaker JK (2009) Neuropeptide Y and neurovascular control in skeletal muscle and skin. *Am J Physiol Regul Integr Comp Physiol* **297**:R546-555.

Hoffman AS (2002) Hydrogels for biomedical applications. *Adv Drug Deliv Rev* **43**:3-12.

Hökfelt T, Lundberg JM, Tatemoto K, Mutt V, Terenius L, Polak J, Bloom S, Sasek C, Elde R, Goldstein M (1983) Neuropeptide Y (NPY)- and FMRFamide neuropeptide-like immunoreactivities in catecholamine neurons of the rat medulla oblongata. *Acta Physiol Scand* **117**:315-318.

Howell OW, Scharfman HE, Herzog H, Sundstrom LE, Beck-Sickinger A, Gray WP (2003) Neuropeptide Y is neuroproliferative for post-natal hippocampal precursor cells. *J Neurochem* **86**:646-659.

Howell OW, Doyle K, Goodman JH, Scharfman HE, Herzog H, Pringle A, Beck-Sickinger AG, Gray WP (2005) Neuropeptide Y stimulates neuronal precursor proliferation in the post-natal and adult dentate gyrus. *J Neurochem* **93**:560-570.

Howell OW, Silva S, Scharfman HE, Sosunov AA, Zaben M, Shatya A, McKhann G 2nd, Herzog H, Laskowski A, Gray WP (2007) Neuropeptide Y is important for basal and seizure-induced precursor cell proliferation in the hippocampus. *Neurobiol Dis.* **26**:174-88.

Hua Y, Huang XY, Zhou L, Zhou QG, Hu Y, Luo CX, Li F, Zhu DY (2008) DETA/NONOate, a nitric oxide donor, produces antidepressant effects by promoting hippocampal neurogenesis. *Psychopharmacology* **200**:231-242.

Hubbell JA (2003) Materials as morphogenetic guides in tissue engineering. *Curr Opin Biotechnol* **14**:551-558.

Husum H, Mikkelsen JD, Hogg S, Mathé AA, Mørk A (2000) Involvement of hippocampal neuropeptide Y in mediating the chronic actions of lithium, electroconvulsive stimulation and citalopram. *Neuropharmacology*. **39**:1463-73.

Ignarro LJ, Wood KS, Wolin MS (1982) Activation of purified soluble guanylate cyclase by protoporphyrin IX. *Proc Natl Acad Sci USA* **79**:2870-2873.

Ignarro LJ, Byrns RE, Buga GM, Wood KS (1987) Endothelium-derived relaxing factor from pulmonary artery and vein possesses pharmacological and chemical properties that are identical to those for nitric oxide radical. *Circ Res* **61**:866-879.

Ignarro LJ (1990) Nitric oxide. A novel signal transduction mechanism for transcellular communication. *Hypertension* **16**(5):477-483.

Ilkhanizadeh S, Teixeira AI, Hermanson O (2007) Inkjet printing of macromolecules on hydrogels to steer neural stem cell differentiation. *Biomaterials* **28**:3936-3943.

Islam AT, Kuraoka A, Kawabuchi M (2003) Morphological basis of nitric oxide production and its correlation with the polysialylated precursor cells in the dentate gyrus of the adult guinea pig hippocampus. *Anat Sci Int* **78**:98-103.

Jaffrey SR, Snyder SH (1996) PIN: an associated protein inhibitor of neuronal nitric oxide synthase. *Science* **274**:774-777.

Jessberger S, Kempermann G (2003) Adult-born hippocampal neurons mature into activity-dependent responsiveness. *Eur J Neurosci* **18**:2707–2712.

Jiang W, Xiao L, Wang JC, Huang YG, Zhang X (2004) Effects of nitric oxide on dentate gyrus cell proliferation after seizures induced by pentylenetrazol in the adult rat brain. *Neurosci Lett* **367**:344-348.

Jin K, Minami M, Lan JQ, Mao XO, Batteur S, Simon RP, Greenberg DA (2001) Neurogenesis in dentate subgranular zone and rostral subventricular zone after focal cerebral ischemia in the rat. *Proc Natl Acad Sci USA* **98**:4710–4715.

Jin K, Peel AL, Mao XO, Xie L, Cottrell BA, Henshall DC, Greenberg DA (2004) Increased hippocampal neurogenesis in Alzheimer's disease. *Proc Natl Acad Sci USA* **101**:343-347.

Kaneko K, Itoh K, Berliner LJ, Miyasaka K, Fujii H (2002) Consequences of nitric oxide generation in epileptic-seizure rodent models as studied by in vivo EPR. *Magn Reson Med* **48**:1051–1056.

Keefer LK, Nims RW, Davies KM, Wink DA (1996) "NONOates" (1-substituted diazen-1-ium-1,2-diolates) as nitric oxide donors: convenient nitric oxide dosage forms. *Methods Enzymol* **268**:281–293.

Kelly RA, Balligand JL, Smith TW (1996) Nitric oxide and cardiac function. *Circ Res* **79**:363-380.

Kempermann G, Gast D, Kronenberg G, Yamaguchi M, Gage FH (2003) Early determination and long-term persistence of adult-generated new neurons in the hippocampus of mice. *Development* **130**:391-9.

Kempermann G, Jessberger S, Steiner B, Kronenberg G (2004) Milestones of neuronal development in the adult hippocampus. *Trends Neurosci* **8**:447-452.

Keynes RG, Griffiths C, Garthwaite J (2003) Superoxide-dependent consumption of nitric oxide in biological media may confound in vitro experiments. *Biochem J* **369**:399-406.

Khademhosseini A, Langer R (2007) Microengineered hydrogels for tissue engineering. *Biomaterials* **28**:5087-5092.

Kikuchi A, Kawabuchi M, Sugihara M, Sakurai Y, Okano T (1997) Pulsed dextran release from calcium-alginate gel beads. *J Control Release* **47**:21-29.

Kim YM, Chung HT, Kim SS, Han JA, Yoo YM, Kim KM, Lee GH, Yun HY, Green A, Li J, Simmons RL, Billiar TR (1999) Nitric oxide protects PC12 cells from serum deprivation-induced apoptosis by cGMP-dependent inhibition of caspase signaling. *J Neurosci* **19**:6740-6747.

Kissner R, Nauser T, Bugnon P, Lye PG, Koppenol WH (1997) Formation and properties of peroxynitrite as studied by laser flash photolysis, high-pressure stopped-flow technique, and pulse radiolysis. *Chem Res Toxicol* **10**:1285–1292.

Kleinman HK, McGarvey ML, Liotta LA, Robey PG, Tryggvason K, Martin GR (1982) Isolation and characterization of type IV procollagen, laminin, and heparan sulfate proteoglycan from the EHS sarcoma. *Biochemistry* **21**:6188-6193.

Kleinman HK, McGarvey ML, Hassell JR, Star VL, Cannon FB, Laurie GW, Martin GR (1986) Basement membrane complexes with biological activity. *Biochemistry* **25**:312-318.

Knoth R, Singec I, Ditter M, Pantazis G, Capetian P, Meyer RP, Horvat V, Volk B, Kempermann G (2010) Murine features of neurogenesis in the human hippocampus across the lifespan from 0 to 100 years. *PloS One* **5**:e8809.

Knowles RG, Palacios M, Palmer RM, Moncada S (1989) Formation of nitric oxide from L-arginine in the central nervous system: A transduction mechanism for stimulation of the soluble guanylate cyclase. *Proc Natl Acad Sci USA* **86**:5159-5162.

Knowles RG, Palacios M, Palmer RM, Moncada S (1990) Kinetic characteristics of nitric oxide synthase from rat brain. *Biochem J* **269**:207-210.

Knowles RG, Moncada S (1994) Nitric oxide synthases in mammals. *Biochem J* **298**:249-258.

Knowles WD, Schwartzkroin PA (1981) Local circuit synaptic interactions in hippocampal brain slices. *J Neurosci* **1**:318-322.

Kohler C, Eriksson L, Davies S, Chan-Palay V (1986) Neuropeptide Y innervation of the hippocampal region in the rat and monkey brain. *J Comp Neurol* **244**:384-400.

Kojima H, Nakatsubo N, Kikuchi K, Kawahara S, Kirino Y, Nagoshi H, Hirata Y, Nagano T (1998a) Detection and imaging of nitric oxide with novel fluorescent indicators: diaminofluoresceins. *Anal Chem* **70**:2446-2453.

Kojima H, Nakatsubo N, Kikuchi K, Urano Y, Higuchi T, Tanaka J, Kudo Y, Nagano T (1998b) Direct evidence of NO production in rat hippocampus and cortex using a new fluorescent indicator: DAF-2 DA. *Neuroreport* **9**:3345-3348.

Komalavilas P, Shah PK, Jo H, Lincoln TM (1999) Activation of mitogen activated protein kinase pathways by cyclic GMP and cyclic GMP-dependent protein kinase in contractile vascular smooth muscle cells. *J Biol Chem* **274**:34301–34309.

Komeima K, Hayashi Y, Naito Y, Watanabe Y (2000) Inhibition of neuronal nitric-oxide synthase by calcium/calmodulin-dependent protein kinase IIalpha through Ser847 phosphorylation in NG108±NG115 neuronal cells. *J Biol Chem* **275**:28139-28143.

Kopecek J (2007) Hydrogel biomaterials: a smart future? *Biomaterials* **28**:5185-5192.

Kopp J, Xu ZQ, Zhang X, Pedrazzini T, Herzog H, Kresse A, Wong H, Walsh JH, Hökfelt T (2002) Expression of the neuropeptide Y Y1 receptor in the CNS of rat and of wild-type and Y1 receptor knock-out mice. Focus on immunohistochemical localization. *Neuroscience.* **111**:443-532.

Kreisman NR, LaManna JC, Liao SC, Yeh ER, Alcala JR (1995) Light transmittance as an index of cell volume in hippocampal slices: optical differences of interfaced and submerged positions. *Brain Res* **693**:179-186.

Kronenberg G, Reuter K, Steiner B, Brandt MD, Jessberger S, Yamaguchi M, Kempermann G (2003) Subpopulations of proliferating cells of the adult hippocampus respond differently to physiologic neurogenic stimuli. *J Comp Neurol* **467**(4):455-463.

Kroon M, Vos WL, Wegdam GH (1998) Structure and formation of a gel of colloidal disks. *Phys Rev E* **57**:1962-1970.

Kruse PF, Miedema E (1965) Production and characterization of multiple layered populations of animal cells. *J Cell Biol* **27**:273-279.

Kuhn H G, Dickinson-Anson H, Gage FH (1996) Neurogenesis in the dentate gyrus of the adult rat: age-related decrease of neuronal progenitor proliferation. *J Neurosci.* **16**:2027–2033.

Kutter S, Hansen JP, Sprik M, Boek E (2000) Structure and Phase Behaviour of a Model Clay Dispersion: A Molecular Dynamics Investigation. *J Chem Phys* **112**:311-322.

Lancaster JR Jr (1997) A tutorial on the diffusibility and reactivity of free nitric oxide. *Nitric Oxide* **1**(1):18-30.

Lasnitzki I, Mizuno T (1979) Role of the mesenchyme in the induction of the rat prostate gland by androgens in organ culture. *J Endocrinol* **82**:171-178.

Lee AL, Ogle WO, Sapolsky RM (2002) Stress and depression: possible links to neuron death in the hippocampus. *Bipolar Disord* **4**:117-128.

Lee EW, Grant DS, Movafagh S, Zukowska Z (2003) Impaired angiogenesis in neuropeptide Y (NPY)-Y2 receptor knockout mice. *Peptides* **24**:99-106.

Lee KY, Mooney DJ (2001) Hydrogels for Tissue Engineering. *Chem Rev* **101**:1869-1879.

Lee W, Debasitis JC, Lee VK, Lee JH, Fischer K, Edminster K, Park JK, Yoo SS (2009) Multi-layered culture of human skin fibroblasts and keratinocytes through three-dimensional freeform fabrication. *Biomaterials* **30**:1587-1595.

Leipzig ND, Wylie RG, Kim H, Shoichet MS (2011) Differentiation of neural stem cells in three-dimensional growth factor-immobilized chitosan hydrogel scaffolds. *Biomaterials* **32**:57-64.

Levitz P, Lecolier E, Mourchid A, Delville A, Lyonnard S (2000) Liquid-solid transition of Laponite suspensions at very low ionic strength: Long-range electrostatic stabilisation of anisotropic colloids. *Europhys Lett* **49**:672-677.

Li YJ, Chung EH, Rodriguez RT, Firpo MT, Healy KE (2006) Hydrogels as artificial matrices for human embryonic stem cell self-renewal. *J Biomed Mater Res A* **79**:1-5.

Lichtenwalner RJ, Parent JM (2006) Adult neurogenesis and the ischemic forebrain. *J Cereb Blood Flow Metab* **26**:1-20.

Liebmann T, Rydholm S, Akpe V, Brismar H (2007) Self-assembling Fmoc dipeptide hydrogel for *in situ* 3D cell culturing. *BMC Biotechnol* **7:**88.

Limbird LE (1988) Receptors linked to inhibition of adenylate cyclase: Additional signaling mechanisms. FASEB J **2**:2686-2695.

Liu J, Solway K, Messing RO, Sharp FR (1998a) Increased neurogenesis in the dentate gyrus after transient global ischemia in gerbils. *J Neurosci* **18**:7768–7778.

Liu P, Smith PF, Appleton I, Darlington CL, Bilkey DK (2003) Regional variations and age-related changes in nitric oxide synthase and arginase in the sub-regions of the hippocampus. *Neuroscience* **119**: 679-687.

Liu X, Miller MJ, Joshi MS, Sadowska-Krowicka H, Clark DA, Lancaster JR (1998b) Diffusion-limited reaction of free nitric oxide with erythrocytes. *J Biol Chem* **273**:18709–18713.

Lopez-Ilasaca M (1998) Signaling from G-protein-coupled receptors to mitogen-activated protein (MAP)-kinase cascades. *Biochem Pharmacol.* **56**:269-77.

Lucassen PJ, Heine VM, Muller MB, van der Beek EM, Wiegant VM, De Kloet ER, Joels M, Fuchs E, Swaab DF, Czeh B (2006) Stress, depression and hippocampal apoptosis. *CNS Neurol Disord Drug Targets* **5**:531-546.

Lundberg JM, Terenius L, Hökfelt T, Martling CR, Tatemoto K, Mutt V, Polak J, Bloom S, Goldstein M (1982) Neuropeptide Y (NPY)-like immunoreactivity in peripheral noradrenergic neurons and effect of NPY on sympathetic function. *Acta Physiol Scand* **116**:477–480.

Lundberg JM, Terenius L, Hökfelt T, Tatemoto K (1984a) Comparative immunohistochemical and biochemical analysis of pancreatic polypeptide-like peptides with special reference to presence of neuropeptide Y in central and peripheral neurons. *J Neurosci* **4**:2376–2386.

Lundberg JM, Saria A, Anggard A, Hokfelt T, Terenius L (1984b) Neuropeptide Y and noradrenaline interaction in peripheral cardiovascular control. *Clin Expl Theory Pract* **6**:1961–1972.

Lundberg JM, Torssell L, Sollevi A, Pernow J, Theodorsson Norheim E, Anggard A, Hamberger B (1985) Neuropeptide Y and sympathetic vascular control in man. *Regul. Pept.* **13**:41–52.

Lundberg JM, Hemsen A, Larsson O, Rudehill A, Saria A, Fredholm BB (1988) Neuropeptide Y receptor in pig spleen: binding characteristics, reduction of cyclic AMP formation and calcium antagonist inhibition of vasoconstriction. *Eur J Pharmac* **145**:21–29.

Lundberg JM, FrancoCereceda A, Hemsen A, Lacroix JS, Pernow J (1990) Pharmacology of noradrenaline and neuropeptide tyrosine (NPY)-mediated sympathetic cotransmission. *Fund. Clin. Pharmacol.* **4**:373–391.

Lundström L, Elmquist A, Bartfai T, Langel U (2005) Galanin and its receptors in neurological disorders. *Neuromol Med* **7**:157–180.

Luo CX, Jin X, Cao CC, Zhu MM, Wang B, Chang L, Zhou QG, Wu HY, Zhu DY (2010) Bidirectional regulation of neurogenesis by neuronal nitric oxide synthase derived from neurons and neural stem cells. *Stem Cells* **28**:2041-2052.

Lutolf MP, Raeber G, Zisch AH, Tirelli N, Hubbell JA (2003) Cell-responsive synthetic hydrogels. *Adv. Mater.* **15**:888-892.

Malberg JE, Eisch AJ, Nestler EJ, Duman RS (2000) Chronic antidepressant treatment increases neurogenesis in adult rat hippocampus. *J Neurosci.* **20**:9104–9110.

Malinski T, Bailey F, Zhang ZG, Chopp M (1993) Nitric oxide measured by a porphyrinic microsensor in rat brain after transient middle cerebral artery occlusion. *J Cereb Blood Flow Metab* **13:**355–358.

Marksteiner J, Sperk G, Mass D (1989) Differential increases in brain levels of neuropeptide Y and vasoactive intestinal polypeptide after kainic acid-induced seizures in the rat. *Naunyn-Schmiedeberg's Archives of Pharmacology* **339**:173-177.

Martin C, Pignon F, Piau JM, Magnin A, Lindner P, Cabane B (2002) Dissociation of thixotropic clay gels. *Phys Rev E* **66**:021401.

Martin SJ, Grimwood PD, Morris RG (2000) Synaptic plasticity and memory: an evaluation of the hypothesis. *Annu Rev Neurosci* **23**:649-711.

Massion PB, Feron O, Dessy C, Balligand JL (2003) Nitric oxide and cardiac function. *Circ Res* **93**:388-398.

Matarredona ER, Murillo-Carretero M, Moreno-López B, Estrada C (2005) Role of nitric oxide in subventricular zone neurogenesis. *Brain Res Rev* **49**:355-366.

Matsui T, Nagafuji T, Kumanishi T, Asano T (1999) Role of nitric oxide in pathogenesis underlying ischemic cerebral damage. *Cell Mol Neurobiol* **19:**177–189.

Matthews JA, Wnek GE, Simpson DG, Bowlin GL (2002) Electrospinning of collagen nanofibers. *Biomacromolecules* **3**:232-238.

Mentlein R, Dahms P, Grandt D, Kruger R (1993) Proteolytic processing of neuropeptide Y and peptide YY by dipeptidyl peptidase IV. *Regul Pept* **49**:133–144.

Mergia E, Russwurm M, Zoidl G, Koesling D (2003) Major occurrence of the new α2β1 isoform of NO-sensitive guanylyl cyclase in brain. *Cell Signal* **15**:189–195.

Michel MC, Beck-Sickinger A, Cox H, Doods HN, Larhammar D, Quirion R, Schwartz T, Westfall T (1998) XVI International Union of Pharmacology recommendations for the nomenclature of neuropeptide Y, peptide YY, and pancreatic polypeptide receptors. Pharmacol Rev **50**:143–150.

Miettinen R, Freund TF (1992) Neuropeptide Y-containing interneurons in the hippocampys receive synaptic input from median raphe and Gabaergic septal afferents. *Neuropeptides* **22**:185-193.

Milenkovic I, Weick M, Wiedemann P, Reichenbach A, Bringmann A (2004) Neuropeptide Y-evoked proliferation of retinal glial (Muller) cells. *Graefes Arch Clin Exp Ophthalmol.* **242**:944-50.

Miller MJ, Wei SH, Parker I, Cahalan MD (2002) Two-photon imaging of lymphocyte motility and antigen response in intact lymph node. *Science* **296**:1869-1873.

Moncada S, Higgs A (1993) The L-arginine-nitric oxide pathway. *N Engl J Med* **329**:2002-2012.

Monfort P, Muñoz MD, Kosenko E, Llansola M, Sánchez-Pérez A, Cauli O, Felipo V (2004) Sequential activation of soluble guanylate cyclase, protein kinase G and cGMP-degrading phosphodiesterase is necessary for proper induction of long-term potentiation in CA1 of hippocampus. Alterations in hyperammonemia. *Neurochem Int* **45**:895-901.

Mongondry P, Tassin JF, Nicolai T (2005) Revised state diagram of Laponite dispersions. *J Colloid Interface Sci* **283**:397-405.

Moore PK, Wallace P, Gaffen Z, Hart SL, Babbedge RC (1993) Characterisation of the novel nitric oxide synthase inhibitor 7-nitroindazole and related indazoles: Antinociceptive and cardiovascular effects. *Br J Pharmacol* **110**:219-224.

Moore PK, Handy RLC (1997) Selective inhibitors of neuronal nitric oxide synthase is no NOS really good NOS for the nervous system. *Trend Pharmacol Sci* **18**:204-211.

Moreno-López B, Noval JA, González-Bonet LG, Estrada C (2000) Morphological bases for a role of nitric oxide in adult neurogenesis. *Brain Res* **869**:244-250

Moreno-López B, Romero-Grimaldi C, Noval JA, Murillo-Carretero M, Matarredona ER, Estrada C (2004) Nitric Oxide Is a Physiological Inhibitor of Neurogenesis in the Adult Mouse Subventricular Zone and Olfactory Bulb. *J Neurosci* **24**(1):85-95.

Morley JE, Flood JF (1991) Evidence that nitric oxide modulates food intake in mice. *Life Sci* **49**:707.

Morley JE, Alshaher MM, Farr SA, Flood JF, Kumar VB (1999) Leptin and neuropeptide Y (NPY) modulate nitric oxide synthase: further evidence for a role of nitric in feeding. *Peptides* **20**:595-600.

Mourchid A, Delville A, Levitz P (1995a) Sol-Gel Transition of Colloidal Suspensions of Anisotropic Particles of Laponite. *Faraday Discuss.* **101**:275-285.

Mourchid A, Delville A, Lambard J, LeColier E, Levitz P (1995b) Phase Diagram of Colloidal Dispersions of Anisotropic Charged Particles: Equilibrium Properties, Structure, and Rheology of Laponite Suspensions. *Langmuir* **11**:1942-1950.

Mourchid A, Lecolier E, Van Damme H, Levitz P (1998) On viscoelastic, birefringent, and swelling properties of Laponite clay suspensions: Revisited phase diagram. *Langmuir* **14**:4718-4723.

Movafagh S, Hobson JP, Spiegel S, Kleinman HK, Zukowska Z (2006) Neuropeptide Y induces migration, proliferation, and tube formation of endothelial cells bimodally via Y1, Y2, and Y5 receptors. *FASEB J* **20**:1924–1926.

Mullins DE, Zhang XP, Hawes BE (2002) Activation of extracellular signal regulated protein kinase by neuropeptide Y and pancreatic polypeptide in CHO cells expressing the NPY $Y_1$, $Y_2$, $Y_4$ and $Y_5$ receptor subtypes. *Regul Pept* **105**:65-73.

Myers AK, Farhat MY, Vaz CA, Keiser HR, Zukowska-Grojec Z (1988) Release of immunoreactive-neuropeptide by rat platelets. *Biochem Biophys Res Commun* **155**:118-122.

Nakamura K, Habano W, Kojo T, Komagiri Y, Kubota T, Kubokawa M (2006) Involvement of endogenous nitric oxide in the regulation of $K^+$ channel activity in cultured human proximal tubule cells. *J Physiol Sci* **56**:407-413.

Nakane M, Klinghofer V, Kuk JE, Donnelly JL, Budzik GP, Pollock JS, Basha F, Carter GW (1995) Novel potent and selective inhibitors of inducible nitric oxide synthase. *Mol Pharmacol* **47**:831-834.

Nam SY, Kratzsch J, Kim KW, Kim KR, Lim SK, Marcus C (2001) Cerebrospinal fluid and plasma concentrations of leptin, NPY, and alpha-MSH in obese women and their relationship to negative energy balance. *J Clin Endocrinol Metab* **86**:4849-4853.

Nathan C (1992) Nitric oxide as a secretory product of mammalian cells. *FASEB J* **6**:3051-64.

Nho YC, Lim YM, Lee YM (2004) Preparation, properties and biological applications of pH-sensitive poly(ethylene oxide) (PEO) hydrogels grafted with acrylic acid (AAc) using gamma-ray irradiation. *Radiat Phys Chem* **71**:239-242.

Nicolai T, Cocard S (2000) Light scattering study of the dispersion of Laponite. *Langmuir* **16**:8189-8193.

Nicolai T, Cocard S (2001) Structure of gels and aggregates of disk-like colloids. *Eur Phys J E* **5**:221-227.

Nie M, Selbie LA (1998) Neuropeptide Y Y1 and Y2 receptor-mediated stimulation of mitogen-activated protein kinase activity. *Regul Pept* **75/76**:207-213.

Nilsson CL, Brinkmalm A, Minthon L, Blennow K, Ekman R (2001) Processing of neuropeptide Y, galanin, and somatostatin in the cerebrospinal fluid of patients with Alzheimer's disease and frontotemporal dementia. *Peptides* **22**:2105-2112.

Nilsson T, Lind H, Brunkvall J, Edvinsson L (2000) Vasodilation in human subcutaneous arteries induced by neuropeptide Y is mediated by neuropeptide Y $Y_1$ receptors and is nitric oxide dependent. *Can J Physiol Pharmacol* **78**:251-255.

Nimmegeers S, Sips P, Buys E, Brouckaert P, Van de Voorde J (2007) Functional role of the soluble guanylyl cyclase alpha(1) subunit in vascular smooth muscle relaxation. *Cardiovasc Res* **76**:149-159.

Nisbet DR, Crompton KE, Horne MK, Finkelstein DI, Forsythe JS (2008) Neural Tissue Engineering of the CNS Using Hydrogels. *J Biomed Mater Res B Appl Biomater* **87**:251-263.

Nisbet DR, Moses D, Gengenbach TR, Forsythe JS, Finkelstein DI, Horne MK (2009) Enhancing neurite outgrowth from primary neurons and neural stem cells using thermoresponsive hydrogel scaffolds for the repair of spinal cord injury. *J Biomed Mater Res A* **89**:24-35.

Norrish K (1954) The swelling of montmorillonite. *Disc Farad Soc* **18:**120-134.

O'Connor SM, Stenger DA, Shaffer KM, Ma W (2001) Survival and neurite outgrowth of rat cortical neurons in three-dimensional agarose and collagen gel matrices. *Neurosci Lett* **304**:189-193.

Onitsuka M, Mihara S, Yamamoto S, Shigemori M, Higashi H (1998) Nitric oxide contributes to irreversible membrane dysfunction caused by experimental ischemia in rat hippocampal CA1 neurons. *Neurosci Res* **30**:7-12.

Ota KT, Pierre VJ, Ploski JE, Queen K, Schafe GE (2008) The NO-cGMP-PKG signaling pathway regulates synaptic plasticity and fear memory consolidation in the lateral amygdala via activation of ERK/MAP kinase. *Learn Mem* **15**:792-805.

Ota KT, Monsey MS, Wu MS, Young GJ, Schafe GE (2010) Synaptic plasticity and NO-cGMP-PKG signaling coordinately regulate ERK-driven gene expression in the lateral amygdala and in the auditory thalamus following Pavlovian fear conditioning. *Learn Mem* **17**:221-235.

Packer MA, Stasiv Y, Benraiss A, Chmielnicki E, Grinberg A, Westphal H, Goldman SA, Enikolopov G (2003) Nitric oxide negatively regulates mammalian adult neurogenesis. *Proc Natl Acad Sci U S A* **100**:9566–9571.

Padmaja S & Huie RE (1993) The reaction of nitric oxide with organic peroxyl radicals. *Biochem Biophys Res Commun* **195**:539–544.

Palmer RMJ, Ferrige AG, Moncada S (1987) Nitric oxide release accounts for the biological activity of endothelium-derived relaxing factor. *Nature* **327**:524-526.

Parent JM, Yu TW, Leibowitz RT, Geschwind DH, Sloviter RS, Lowenstein DH (1997) Dentate granule cell neurogenesis is increased by seizures and contributes to aberrant network reorganization in the adult rat hippocampus. *J Neurosci.* **17**:3727–3738.

Parent JM, Valentin VV, Lowenstein DH (2002) Prolonged seizures increase proliferating neuroblasts in the adult rat subventricular zone-olfactory bulb pathway. *J Neurosci.* **22**:3174-88.

Parent JM, Elliott RC, Pleasure SJ, Barbaro NM, Lowenstein DH (2006) Aberrant seizure-induced neurogenesis in experimental temporal lobe epilepsy. *Ann Neurol* **59**:81-91.

Park C, Sohn Y, Shin KS, Kim J, Ahn H, Huh Y (2003) The chronic inhibition of nitric oxide synthase enhances cell proliferation in the adult rat hippocampus. *Neurosci Lett* **339**:9–12.

Pernow J, Lundberg JM, Kaiiser L, Hjemdahl P, Theodorsson-Norheim E, Martinsson A, Pernow B (1986) Plasma neuropeptide Y-like immunoreactivity and catecholamines during various degrees of sympathetic activation in man. *Clin Physiol* **6**:561-578.

Petersen OW, Ronnov-Jessen L, Howlett AR, Bissell MJ (1992) Interaction with basement membrane serves to rapidly distinguish growth and differentiation pattern of normal and malignant human breast epithelial cells. *Proc Natl Acad Sci USA* **89**:9064-9068.

Pheng LH, Dumont Y, Fournier A, Chabot JG, Beaudet A, Quirion R (2003) Agonist- and antagonist-induced sequestration/internalization of neuropeptide Y $Y_1$ receptors in HEK293 cells. *Br J Pharmacol.* **139**:695-704.

Philippides A, Husbands P, O'Shea M (2000) Four-dimensional neuronal signaling by nitric oxide: a computational analysis. *J Neurosci* **20**:1199-1207.

Podda MV, Marcocci ME, Oggiano L, D'Ascenzo M, Tolu E, Palamara AT, Azzena GB, Grassi C (2004) Nitric oxide increases the spontaneous firing rate of rat medial vestibular nucleus neurons in vitro via a cyclic GMP-mediated PKG-independent mechanism. *Eur J Neurosci* **20**:2124–2132.

Pollman MJ, Yamada T, Horiuchi M, Gibbons GH (1996) Vasoactive substances regulate vascular smooth muscle cell apoptosis. Countervailing influences of nitric oxide and angiotensin II. *Circ Res* **79**:748–756.

Pollock JS, Förstermann U, Mitchell JA, Warner TD, Schmidt HH, Nakane M, Murad F (1991) Purification and characterization of particulate endothelium-derived relaxing factor synthase from cultured and native bovine aortic endothelial cells. *Proc. Natl. Acad. Sci. U. S. A.* **88:**10480-10484.

Pons J, Kitlinska J, Ji H, Lee EW, Zukowska Z (2003) Neuropeptide Y and vascular growth: role of Y1 and Y5 receptors and adrenergic activation. *Can J Phys Pharm* **81**:177-85.

Pons J, Kitlinska J, Jacques D, Perreault C, Nader M, Everhart L, Zhang Y, Zukowska Z (2008) Interactions of multiple signaling pathways in neuropeptide Y-mediated bimodal vascular smooth muscle cell growth. *Can J Physiol Pharmacol* **86**:438-448.

Prestwich GD, Marecak DM, Marecek JF, Vercruysse KP, Ziebell MR (1998) Controlled chemical modification of hyaluronic acid: synthesis, applications, and biodegradation of hydrazide derivatives. *J Control Release* **53**:93-103.

Rameau GA, Chiu LY, Ziff EB (2004) Bidirectional regulation of neuronal nitric-oxide synthase phosphorylation at serine 847 by the N-methyl-D-aspartate receptor. J Biol Chem **279**:14307–14314.

Ramon y Cajal S (1928) Degeneration and regeneration of the nervous system. Volume 2. *Haffner Publishing Co. New York.* p. 750.

Ramsay JDF, Lindner P (1993) Small-angle Neutron Scattering Investigations of the Structure of Thixotropic Dispersions of Smectite Clay Colloids. *J Chem Soc Faraday Trans* **89**:4207-4214.

RayChaudhury A, Frischer H, Malik AB (1996) Inhibition of endothelial cell proliferation and bFGF induced phenotypic modulation by nitric oxide. *J Cell Biochem* **63**:125-134.

Raza A, Ucar K, Bhayana R, Kempski M, Preisler HD (1985) Utility and sensitivity of anti-BrdU antibodies in assessing S-phase cells compared to autoradiography. *Cell Biochem Funct* **3**:149-153.

Redrobe JP, Dumont Y, St-Pierre JA, Quirion R (1999) Multiple receptors for neuropeptide Y in the hippocampus: putative roles in seizures and cognition. *Brain Res*. **848**:153-166.

Redrobe JP, Dumont Y, Fournier A, Quirion R (2002a) The Neuropeptide Y (NPY) Y1 Receptor Subtype Mediates NPY-induced Antidepressant-like Activity in the Mouse Forced Swimming Test. *Neuropsychopharmacology* **26**:615-624.

Redrobe JP, Dumont, Y, Quirion R (2002b) Neuropeptide Y (NPY) and depression: from animal studies to the human condition. *Life Sci.* **71**:2921-37.

Redrobe JP, Dumont Y, Herzog H, Quirion R (2004) Characterization of neuropeptide Y, $Y_2$ receptor knockout mice in two animal models of learning and memory processing. *J Mol Neurosci* **22**:159-166.

Reif A, Schmitt A, Fritzen S, Chourbaji S, Bartsch C, Urani A, Wycislo M, Mössner R, Sommer C, Gass P, Lesch KP (2004) Differential effect of endothelial nitric oxide synthase (NOS-III) on the regulation of adult neurogenesis and behaviour. *Eur J Neurosci* **20**:885-895.

Reiner A, Zagvazdin Y (1998) On the selectivity of 7-nitroindazole as an inhibitor of neuronal nitric oxide synthase. *Trends Pharmacol Sci* **19**:348-350.

Reyes-Harde M, Potter BV, Galione A, Stanton PK (1999) Induction of hippocampal LTD requires nitric-oxide-stimulated PKG activity and Ca2+ release from cyclic ADP-ribose-sensitive stores. J *Neurophysiol* **82**:1569-1576.

Robbins RA, Grisham MB (1997) Nitric Oxide. *Int J Biochem Cell Biol* **29**:857-860.

Rodríguez J, Specian V, Maloney R, Jourd'heuil D, Feelisch M (2005) Performance of diamino fluorophores for the localization of sources and targets of nitric oxide. *Free Radic Biol Med* **38**:356–368.

Rosmaninho-Salgado J, Araújo IM, Alvaro AR, Duarte EP, Cavadas C (2007) Intracellular signaling mechanisms mediating catecholamine release upon activation of NPY $Y_1$ receptors in mouse chromaffin cells. *J Neurochem* **103**:896-903.

Roux PP, Blenis J (2004) ERK and p38 MAPK-activated protein kinases: a family of protein kinases with diverse biological functions. *Microbiol Mol Biol Rev* **68**:320–344.

Ruscica M, Dozio E, Boghossian S, Bovo G, Martos Riano V, Motta M, Magni P (2006) Activation of the Y1 receptor by neuropeptide Y regulates the growth of prostate cancer cells. *Endocrinology* **147**:1466–1473.

Russwurm M, Behrends S, Harteneck C, Koesling D (1998) Functional properties of a naturally occurring isoform of soluble guanylyl cyclase. *Biochem J* **335**:125-130.

Sakiyama-Elbert SE, Hubbell JA (2000) Development of fibrin derivatives for controlled release of heparin-binding growth factors. *J Control Release* **65**:389-402.

Santarelli L, Saxe M, Gross C, Surget A, Battaglia F, Dulawa S, Weisstaub N, Lee J, Duman R, Arancio O, Belzung C, Hen R (2003) Requirement of hippocampal neurogenesis for the behavioral effects of antidepressants. *Science* **301**:805-809.

Santolini J, Adak S, Curran CM, Stuehr DJ (2001) A kinetic simulation model that describes catalysis and regulation in nitric-oxide synthase. *J Biol Chem* **276**:1233-1243.

Seidel B, Stanarius A, Wolf G (1997) Differential expression of neuronal and endothelial nitric oxide synthase in blood vessels of the rat brain. *Neurosci Lett* **239**:109-112.

Seki T, Arai Y (1995) Age-related production of new granule cells in the adult dentate gyrus. *Neuroreport* **6**:2479–2482.

Schense JC, Bloch J, Aebischer P, Hubbell JA (2000) Enzymatic incorporation of bioactive peptides into fibrin matrices enhances neurite extension. *Nat Biotech* **18**:415-419.

Schuppe H, Cuttle M, Chad JE, Newland PL (2002) 4,5-diaminofluorescein imaging of nitric oxide synthesis in crayfish terminal ganglia. *J Neurobiol* **53**:361-369.

Sclafani AM, Skidmore JM, Ramaprakash H, Trumpp A, Gage PJ, Martin DM (2006) Nestin-Cre mediated deletion of Pitx2 in the mouse. *Genesis* **44**:336-344.

Shen PJ, Yuan CG, Ma J, Cheng S, Yao M, Turnley AM, Gundlach AL (2005) Galanin in neuro(glio)genesis: expression of galanin and receptors by progenitor cells in vivo and in vitro and effects of galanin on neurosphere proliferation. *Neuropeptides* **39**:201-205.

Sheta EA, McMillan K, Masters BS (1994) Evidence for a bidomain structure of constitutive cerebellar nitric oxide synthase. *J Biol Chem* **269**:15147-15153.

Shibuki K (1990) An electrochemical microprobe for detecting nitric oxide release in brain tissue. *Neurosci Res* **9**:69-76.

Shihabuddin LS, Palmer TD, Gage FH (1999) The search for neural progenitor cells: prospects for the therapy of neurodegenerative disease. *Mol Med Today* **5**:474-480.

Shihabuddin LS, Horner PJ, Ray J, Gage FH (2000) Adult spinal cord stem cells generate neurons after transplantation in the adult dentate gyrus. *J Neurosci* **20**:8727–8735.

Shors TJ, Miesegaes G, Beylin A, Zhao M, Rydel T, Gould E (2001) Neurogenesis in the adult is involved in the formation of trace memories. *Nature* **410**:372-6.

Shors TJ, Townsend DA, Zhao M, Kozorovitskiy Y, Gould E (2002) Neurogenesis may relate to some but not all types of hippocampal-dependent learning. *Hippocampus* **12**:578-84.

Silva AP, Kaufmann JE, Vivancos C, Fakan S, Cavadas C, Shaw P, Brunner HR, Vischer U, Grouzmann E (2005) Neuropeptide Y expression, localization and cellular transducing effects in HUVEC. *Biol Cell.* **97**:457-67.

Snyder JS, Kee N, Wojtowicz JM (2001) Effects of adult neurogenesis on synaptic plasticity in the rat dentate gyrus. *J Neurophysiol* **85**:2423-31.

Snyder SH (1993) Janus faces of nitric oxide. *Nature* **364**:577.

Sperk G, Hamilton T, Colmers WF (2007) Neuropeptide Y in the dentate gyrus. *Prog Brain Res* **163**:285-297.

Squire LR, Cave CB (1991) The hippocampus, memory, and space. *Hippocampus* **1**:269-271.

Stasch JP, Becker EM, Alonso-Alija C, Apeler H, Dembowsky K, Feurer A, Gerzer R, Minuth T, Perzborn E, Pleiss U, Schroder H, Schroeder W, Stahl E, Steinke W, Straub A, Schramm M (2001) NO-independent regulatory site on soluble guanylate cyclase. *Nature* **410**:212-215.

Steiner B, Kronenberg G, Jessberger S, Brandt MD, Reuter K, Kempermann G (2004) Differential regulation of gliogenesis in the context of adult hippocampal neurogenesis in mice. *Glia* **46**:41–52.

Stenfors C, Mathé AA, Theodorsson E (1995) Chromatographic and immunochemical characterization of rat brain neuropeptide Y-like immunoreactivity (NPY-LI) following repeated electroconvulsive stimuli. *J Neurosci Res*. **41**:206-12.

Sterges AJ (1942) Adaptability of silica gel as a culture medium. *J Bacteriol* **43**:317-327.

Stuehr DJ, Griffith OW (1992) Mammalian nitric oxide synthases. *Adv Enzymol, Relat Areas Mol Biol* **65**:287-346.

Stuehr DJ, Santolini J, Wang ZQ, Wei CC, Adak S (2004) Update on mechanism and catalytic regulation in the NO synthases. *J Biol Chem* **279**:36167-36170.

Suenobu N, Shichiri M, Iwashina M, Marumo F, Hirata Y (1999) Natriuretic peptides and nitric oxide induce endothelial apoptosis via a cGMP-dependent mechanism. *Arterioscler Thomb Vasc Biol* **19**:140–146.

Sun T, Norton D, McKean RJ, Haycock JW, Ryan AJ, MacNeil S (2007) Development of a 3D cell culture system for investigating cell interactions with electrospun fibers. *Biotechnol Bioeng* **97**:1318-1328.

Sun Y, Jin K, Childs JT, Xie L, Mao XO, Greenberg DA (2005) Neuronal nitric oxide synthase and ischemia-induced neurogenesis. *J Cereb Blood Flow Metab* **25**:485-492.

Takagi Y, Nozaki K, Takahashi J, Yodoi J, Ishikawa M, Hashimoto N (1999) Proliferation of neuronal precursor cells in the dentate gyrus is accelerated after transient forebrain ischemia in mice. *Brain Res* **831**:283–287.

Tatemoto K (1982) Neuropeptide Y: complete amino acid sequence of the brain peptide. *Proc Natl Acad Sci U S A* **79**:5485–5489.

Tatemoto K, Carlquist M, Mutt V (1982) Neuropeptide Y- a novel brain peptide with structural similarities to peptide YY and pancreatic polypeptide. *Nature* **296:**659-660.

Tawari SL, Koch DL, Cohen C (2001) Electrical Double-Layer Effects on the Brownian Diffusivity and Aggregation Rate of Laponite Clay Particles. *J Colloid Interface Sci* **240**:54-66.

Thippeswamy T, Morris R (1997) Cyclic guanosine 3',5'-monophosphate-mediated neuroprotection by nitric oxide in dissociated cultures of rat dorsal root ganglion neurons. *Brain Res* **774**:116–122.

Thiriet N, Agasse F, Nicoleau C, Guégan C, Vallette F, Cadet JL, Jaber M, Malva JO, Coronas V (2011) NPY promotes chemokinesis and neurogenesis in the rat subventricular zone. *J Neurochem* **116**:1018-1027.

Thompson A, Boekhoorn K, van Dam AM, Lucassen PJ (2008) Changes in adult neurogenesis in neurodegenerative diseases: cause or consequence? *Genes Brain Behav* **7**:28-42.

Thompson AY, Piez KA, Seyedin SM (1985) Chondrogenesis in agarose gel culture. A model for chondrogenic induction, proliferation and differentiation. *Exp Cell Res* **157**:483-494.

Thompson DW, Butterworth JT (1992) The nature of Laponite and its aqueous dispersions. *J Colloid Interface Sci* **151:**236-243.

Thorsell A, Michalkiewicz M, Dumont Y, Quirion R, Caberlotto L, Rimondini R, Mathé AA, Heilig M (2000) Behavioral insensitivity to restraint stress, absent fear suppression of behavior and impaired spatial learning in transgenic rats with hippocampal neuropeptide Y overexpression. *Proc Natl Acad Sci USA* **97**:12852–12857.

Tibbitt MW, Anseth KS (2009) Hydrogels as extracellular matrix mimics for 3D cell culture. *Biotechinol Bioeng* **103**:655-663.

Todoroki S, Goto S, Urata Y, Komatsu K, Sumikawa K, Ogura T, Matsuda I, Kondo T (1998) High concentration of L-arginine suppresses nitric oxide synthase activity and produces reactive oxygen species in NB9 human neuroblastoma cells. *Mol Med* **4**:515-524.

Torroglosa A, Murillo-Carretero M, Romero-Grimaldi C, Matarredona ER, Campos-Caro A, Estrada C (2007) Nitric oxide decreases subventricular zone stem cell proliferation by inhibition of epidermal growth factor receptor and phosphoinositide-3-kinase/Akt pathway. *Stem Cells* **25**:88–97.

Troger J, Sellemond S, Kieselbach G, Kralinger M, Schmid E, Teuchner B, Nguyen QA, Schretter-Irschick E, Göttinger W (2003) Inhibitory effect of certain neuropeptides on the proliferation of human retinal pigment epithelial cells. *Br. J. Ophthalmol.* **87**:1403-1408.

Trowbridge JM, Gallo RL (2002) Dermatan sulfate: new functions from an old glycosaminoglycan. *Glycobiology* **12**:117R-125R.

Tsoukias NM (2008) Nitric oxide bioavailability in the microcirculation: insights from mathematical models. *Microcirculation* **15**:813–834.

Uhler MD (1993) Cloning and expression of a novel cyclic GMP-dependent protein kinase from mouse brain. *J Biol Chem* **268**:13586-13591.

Ulibarri JA, Mozdziak PE, Schultz E, Cook C, Best TM (1999) Nitric oxide donors, sodium nitroprusside and S-nitro-N-acetylpencillamine, stimulate myoblast proliferation in vitro. *In Vitro Cell Dev Biol Anim* **35**:215-218.

van Olphen H (1962) Unit layer interaction in hydrous montmorillonite systems. *J Colloid Interface Sci* **17**:660-667.

van Praag H, Kempermann G, Gage FH (1999) Running increases cell proliferation and neurogenesis in the adult mouse dentate gyrus. *Nat Neurosci.* **2**:266–270.

van Praag H, Schinder AF, Christie BR, Toni N, Palmer TD, Gage FH (2002) Functional neurogenesis in the adult hippocampus. Nature 415:1030-1034.

Vanhoutte PM, Miller VM (1989) Alpha 2-adrenoceptors and endothelium derived relaxing factor. *Am J Med* **87**:1S-5S.

Vercruysse KP, Marecak DM, Marecek JF, Prestwich GD (1997) Synthesis and in vitro degradation of new polyvalent hydrazide cross-linked hydrogels of hyaluronic acid. *Bioconjugate Chem* **8**:686-694.

Vezzani A, Sperk G, Colmers WF (1999) Neuropeptide Y: emerging evidence for a functional role in seizure modulation. *Trends Neurosci* **22**:25-30.

Villalobo A (2006) Nitric oxide and cell proliferation. *FEBS J.* **273**:2329-44.

Volke A, Wegener G, Vasar E, Volke V (2006) High-performance liquid chromatography method with radiochemical detection for measurement of nitric oxide synthase, arginase, and arginine decarboxylase activities. Methods Find *Exp Clin Pharmacol* **28**: 3-6.

von Hörsten S, Hoffman T, Alfalah M, Wrann CD, Karl T, Pabst R, Bedoui S (2004) PP, PYY and NPY: Synthesis, Storage, Release and Degradation. *Handb Exp Pharmacol* **162**:23-44.

Vukicevic S, Kleinman HK, Luyten FP, Roberts AB, Roche NS, Reddi AH (1992) Identification of multiple active growth factors in basement membrane Matrigel suggests caution in interpretation of cellular activity related to extracellular activity related to extracellular matrix components. *Exp Cell Res* **202**:1-8.

Wahlestedt C, Håkanson R, Vaz CA, Zukowska-Grojec Z (1990) Norepinephrine and neuropeptide Y: vasoconstrictor cooperation in vivo and in vitro. *Am J Physiol* **258**:R736-42.

Waldman SA, Murad F (1988) Biochemical mechanisms underlying vascular smooth muscle relaxation: the guanylate cyclase-cyclic GMP system. *J Cardiovasc Pharmacol* **12**:S115-8.

Wang Q, Cwik M, Wright CJ, Cunningham F, Pelligrino DA (1999b) The in vivo unidirectional conversion of nitro-D-arginine to nitro-L-arginine. *J Pharmacol Exp Ther* **288**:270-273.

Wang S, Hashemi T, Fried S, Clemmons AL, Hawes BE (1998) Differential intracellular signaling of the GalR1 and GalR2 galanin receptor subtypes. *Biochemistry* **37**:6711-6717.

Wang T, FitzGerald TJ, Haregewoin A (1999a) Differential expression of nitric oxide synthase in EGF-responsive mouse neural precursor cells. *Cell Tissue Res* **296**:489-497.

Wardman P (2007) Fluorescent and luminescent probes for measurement of oxidative and nitrosative species in cells and tissues: progress, pitfalls, and prospects. *Free Radic Biol Med* **43**:995-1022.

Watanabe K, Nakamura M, Okano H, Toyama Y (2007) Establishment of three-dimensional culture of neural stem/progenitor cells in collagen Type-1 Gel. *Restor Neurol Neurosci* **25**:109-117.

Wei YT, He Y, Xu CL, Wang Y, Liu BF, Wang XM, Sun XD, Cui FZ, Xu QY (2010) Hyaluronic acid hydrogel modified with nogo-66 receptor antibody and poly-L-lysine to promote axon regrowth after spinal cord injury. *J Biomed Mater Res B Appl Biomater* **95**:110-117.

Wettschureck N, Offermanns S (2005) Mammalian G proteins and their cell type specific functions. *Physiol Rev* **85**:1159-1204.

Wichterle O, Lim D (1960) Hydrophilic gels for biological use. *Nature* **185**:117–118.

Widerlöv E, Lindström LH, Wahlestedt C, Ekman R (1988) Neuropeptide Y and peptide YY as possible cerebrospinal fluid markers for major depression and schizophrenia, respectively. *J Psychiatr Res* **22**:69-79.

Willenbacher N (1996) Unusual thixotropic properties of aqueous dispersions of Laponite RD. *J Colloid Interface Sci* **182:**501-510.

Wnek GE, Carr ME, Simpson DG, Bowlin GL (2003) Electrospinning of nanofiber fibrinogen structures. *Nano Letters* **3**:213-216.

Wolak ML, DeJoseph MR, Cator AD, Mokashi AS, Brownfield MS, Urban JH (2003) Comparative distribution of neuropeptide Y Y1 and Y5 receptors in the rat brain by using immunohistochemistry. *J Comp Neurol* **464**:285–311.

Wood J, Garthwaite J (1994) Models of the diffusional spread of nitric oxide: Implications for neural nitric oxide signalling and its pharmacological properties. *Neuropharmacology* **33**:1235-1244.

Wood KC, Batchelor AM, Bartus K, Harris KL, Garthwaite G, Vernon J, Garthwaite J (2011) Picomolar nitric oxide signals from central neurons recorded using ultrasensitive detector cells. *J Biol Chem* **286**:43172-43181.

Xu T, Molnar P, Gregory C, Das M, Boland T, Hickman JJ (2009) Electrophysiological characterization of embryonic hippocampal neurons in a 3D collagen hydrogel. *Biomaterials* **30**:4377-4383.

Yang D, Liang C, Jin Y, Wang D (2003) Effect of arsenic toxicity on morphology and viability of enzyme in primary culture of rat hippocampal neurons. *Wei Sheng Yan Jiu* **32**:309-312.

Yang J, Richards J, Bowman P, Guzman R, Enami J, McCormick K, Hamamoto S, Pitelka D, Nandi S (1979) Sustained growth and three-dimensional organization of primary mammary tumor epithelial cells embedded in collagen gels. *Proc Natl Acad Sci USA* **76**:3401-3405.

Yang J, Richards J, Guzman R, Imagawa W, Nandi S (1980) Sustained growth in primary culture of normal mammary epithelial cells embedded in collagen gels. *Proc Natl Acad Sci USA* **77**:2088-2092.

Yang J, Elias JJ, Petrakis NL, Wellings SR, Nandi S (1981) Effects of hormones and growth factors on human mammary epithelial cells in collagen gel culture. *Cancer Res* **41**:1021-1027.

Yang SH, Shin DH, Baek WK (1999) Apoptosis of Neuronal Cells Induced by Lead. *Korean J Occup Environ Med.* **11**:254-263.

Yau KW, Baylor DA (1989) Cyclic GMP-activated conductance of retinal photoreceptor cells. *Annu. Rev. Neurosci.* **12**:289 327.

Ye XY, Rubakhin SS, Sweedler JV (2008) Detection of nitric oxide in single cells. *Analyst* **133**:423-433.

You J, Edvinsson L, Bryan RM Jr (2001) Neuropeptide Y-mediated constriction and dilation in rat middle cerebral arteries. *J Cereb Blood Flow Metab* **21**:77-84.

Yuen PS, Potter LR, Garbers DL (1990) A new form of guanylyl cyclase is preferentially expressed in rat kidney. *Biochemistry* **29**:10872–10878.

Yui Y, Hattori R, Kosuga K, Eizawa H, Hiki K, Kawai C (1991) Purification of nitric oxide synthase from rat macrophages. *J Biol Chem* **266**:12544-12547.

Zagvazdin Y, Sancesario G, Wang YX, Share L, Fitzgerald MEC, Reiner A (1996) Evidence from its cardiovascular effects that 7-nitroindazole may inhibit endothelial nitric oxide synthase in vivo. *Eur J Pharmacol* **303**:61-69.

Zhang R, Zhang L, Zhang Z, Wang Y, Lu M, Lapointe M, Chopp M (2001) A nitric oxide donor induces neurogenesis and reduces functional deficits after stroke in rats. *Ann Neurol* **50**:602-611.

Zhang X, Kim WS, Hatchers N, Potgieter K, Moroz LL, Gillette R, Sweedler JV (2002) Interfering with nitric oxide measurements. 4,5-Diaminofluorescein reacts with dehydroascorbic acid and ascorbic acid. *J Biol Chem* **277**:48472-48478.

Zhou L, Zhu DY (2009) Neuronal nitric oxide synthase: structure, subcellular localization, regulation, and clinical implications. *Nitric Oxide* **20**:223–230.

Zhou QG, Hu Y, Hua Y, Hu M, Luo CX, Han X, Zhu XJ, Wang B, Xu JS, Zhu DY (2007) Neuronal nitric oxide synthase contributes to chronic stress-induced depression by suppressing hippocampal neurogenesis. *J Neurochem* **103**:1843-1854.

Zhu DY, Liu SH, Sun HS, Lu YM (2003) Expression of inducible nitric oxide synthase after focal cerebral ischemia stimulates neurogenesis in the adult rodent dentate gyrus. *J Neurosci* **23**:223-229.

Zhuo M, Hu Y, Schultz C, Kandel ER, Hawkins RD (1994) Role of guanylyl cyclase and cGMP-dependent protein kinase in long-term potentiation. *Nature* **368**:635–639.

Ziche M, Morbidelli L (2000) Nitric oxide and angiogenesis. *J Neurooncol* **50**:139–148.

Zufall F, Firestein S, Shepherd GM (1994) Cyclic nucleotide gated ion channels and sensory transduction in olfactory receptor neurons. *Annu Rev Biophys Biomol Struct* **23**:577-607.

Zukowska-Grojec Z, Wahlestedt C (1993) Origin and actions of neuropeptide Y in the cardiovascular system. *In* Colmers WF, Wahlestedt C, eds. The Biology of Neuropeptide Y and Related Peptides. *Totowa, NJ, Humana Press*, pp 315–388.

Zukowska-Grojec Z, Karwatowska-Prokopczuk E, Fisher TA, Ji H (1998a) Mechanisms of vascular growth-promoting effects of neuropeptide Y: role of its inducible receptors. *Regul Pept* **75–76**:231-238.

Zukowska-Grojec Z, Karwatowska-Prokopczuk E, Rose W, Rone J, Movafagh S, Ji H, Yeh Y, Chen WT, Kleinman HK, Grouzmann E, Grant DS (1998b) Neuropeptide Y: a novel angiogenic factor from the sympathetic nerves and endothelium. *Circ Res* **83**:187-195.

Zukowska Z, Grant DS, Lee EW (2003) Neuropeptide Y: a novel mechanism for ischemic angiogenesis. *Trends Cardiovasc Med* **13**:86-92.